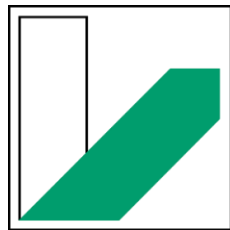


Solubilization of Phosphorus, Silicon, and Calcium and Abundance of Phosphorus-solubilizing Bacteria in Temperate Forest Soils



**UNIVERSITÄT
BAYREUTH**

Dissertation

To obtain the academic degree of Doctor of Natural Science
(Dr. rer. nat)

Submitted to
Faculty of Biology, Chemistry and Earth sciences
University of Bayreuth

Presented by

GIOVANNI PASTORE

born
in San Giovanni Rotondo (Italy)

Bayreuth 2020

This doctoral thesis was prepared at Bayreuth Center of Ecology and Environmental Research (BayCEER), Department of Soil Ecology at the University of Bayreuth from January 2017 until December 2020 and was supervised by Prof. Dr. Marie Spohn.

This is a full reprint of the dissertation submitted to obtain the academic degree of Doctor of Natural Sciences (Dr. rer. nat.) and approved by the Faculty of Biology, Chemistry and Geosciences of the University of Bayreuth.

Date of submission: 09.12.2020

Date of defense: 06.05.2021

Acting dean: Prof. Dr. Matthias Breuning

Doctoral committee:

Prof. Dr. Marie Spohn (reviewers)

Prof. Dr. Eva Lehndorff (reviewers)

Prof. Dr. Martin Obst (chairman)

Prof. Dr. Britta Planer-Friedrich

Summary

This thesis focuses on the question of how microbes from temperate forest soils influence phosphorus (P), silicon (Si), and calcium (Ca) solubilization from minerals and weathered parental materials as well as to which extent P-solubilizing bacteria contribute to the overall solubilization rates. Despite the increasing awareness of the role of microorganisms in plant nutrition, the potential of microbial communities to release phosphate from mineral phases has not been explored with detail, so far. Moreover, the research on the solubilization of siliceous and calcareous parent materials from forest soils is quite fragmented, regardless of the fact that most experiments have been performed with cultured microorganisms and high doses of organic acids addition. A total of seven deciduous temperate forest soils and two soil depth increments from the mineral horizon were chosen to evaluate how, and to which extent, the microbial communities of different depths affect P solubilization. In the first incubation experiment, microbial net P solubilization rates were determined from primary (hydroxyapatite) and secondary (P-loaded goethite) P-minerals after addition of glucose to five acidic soil extracts (ranging from P-rich to P-poor conditions). Net P solubilization rates were derived from the increase of P concentrations in soil extracts incubated with hydroxyapatite and P-loaded goethite over 14 days. In the second and third incubation experiments, net Si and Ca solubilization rates were determined from four siliceous and two calcareous weathered parent materials, respectively. The net Si and Ca solubilization rates were calculated from the difference between the amounts of Si and Ca measured at the end and at the beginning of the experiment over 14 days. In all incubation experiments, the temporal changes in pH and the concentrations of four organic acids (citric, oxalic, 2-keto-D-gluconic and D-gluconic) were determined in soil extracts, while lactic acid was added to the analyses in extracts from the calcareous soils. Gross P solubilization rates were determined at four acidic and two alkaline forest soils developed on siliceous and calcareous bedrocks. Moreover, the abundance and the taxonomic diversity of P-solubilizing bacteria were carried out from acidic and alkaline soils through a physiological assay in combination with 16s rRNA gene sequencing. The microbial net P solubilization rates were higher in incubations of soil extracts with

hydroxyapatite than P-loaded goethite, except one case. The relationship between the pH of soil extracts and microbial net P solubilization rates was negative in incubations with hydroxyapatite and positive in incubations with P-loaded goethite and depended on the different release of protons and organic acids by microbes. In the incubation of goethite, microbes likely downregulated the production of organic acids to prevent acidification, and thus, strong sorption of phosphate ions. Further, the production of monocarboxylic acids coincided significantly with high P release from hydroxyapatite. Altogether, microbial net P solubilization rates from primary and secondary P-minerals increased with the addition of glucose. When weathered siliceous and calcareous parent materials were used, no net P solubilization rates were found as an effect of microbial P immobilization. However, from the net Si and Ca solubilization rates we determined the gross P solubilization rates based on the stoichiometric ratios they had with the P content of bedrocks. The microbial gross P solubilization rates were significantly higher in the incubations of the soil extracts with calcareous than siliceous bedrocks (on average +61%). Carbonates had higher gross P solubilization rates as result of an overall higher microbial activity, as suggested by the amounts of organic acids (up to 4.5 times higher) and microbial biomass (up to 19.1 times higher) in comparison to silicates. This trend was particularly noticeable in the upper soil depth of calcareous soils. Regarding the abundance of P-solubilizing bacteria, our data show that this was significantly higher in calcareous soils than in siliceous soils (on average +46.6%). Also, nonmetric multi-dimensional scaling analyses (nMDS) revealed that the P-solubilizing bacteria in calcareous soils were significantly different from those found in silicate soils. *Bacillales* and *Burkholderiales* dominated at the silicate sites, whereas *Pseudomonadales* and to a much lesser extent *Enterobacteriales* were the dominant orders at the calcareous sites. In conclusion, P-solubilizing bacteria were more abundant in P-poor soils than in P-rich soils, while solubilization rates were influenced by the mineral chemistry of the bedrocks. In future studies, the extent to which P is released from weathered parent materials may be also “attempted” by determining the net solubilization of the major constituent of the bedrock in relation to the stoichiometric ratio of that element with P, considering that the specific release rates of P are often extremely difficult to measure. Not only is more research on net P solubilization from

coniferous and Mediterranean forest soils needed, but also the net P solubilization driven by fungal communities in forest soils warrants further investigation.

Zusammenfassung

Diese Dissertation befasst sich mit der Frage, wie Mikroorganismen in temperaten Waldböden die Solubilisierung von Phosphor (P), Silizium (Si) und Calcium (Ca) aus Mineralien und verwitterten Ausgangsmaterialien beeinflussen sowie in welchem Ausmaß die P-solubilisierenden Bakterien insgesamt zu den Solubilisierungsraten beitragen. Ungeachtet des zunehmenden Bewusstseins über die Rolle der Mikroorganismen in der Pflanzenernährung wurde das Potenzial mikrobieller Gemeinschaften, Phosphat aus Mineralphasen freizusetzen, bisher nicht im Detail untersucht. Darüber hinaus ist die Forschung zur Solubilisierung von silikathaltigen und kalkreichen Ausgangsmaterialien in Waldböden ziemlich lückenhaft, ungeachtet der Tatsache, dass die meisten Experimente mit kultivierten Mikroorganismen und unter Zugabe großer Mengen an organischen Säuren durchgeführt wurden.

Insgesamt wurden für diese Arbeit zwei Bodentiefen im Mineralhorizont von sieben temperaten Laubwäldern ausgewählt, um zu bewerten, wie und in welchem Ausmaß die mikrobiellen Gemeinschaften aus unterschiedlichen Bodentiefen die P-Solubilisierung beeinflussen. Im ersten Inkubationsexperiment wurden die mikrobiellen Netto-P-Solubilisierungsraten von primären (Hydroxylapatit) und sekundären (P-beladener Goethit) P-Mineralien nach Zugabe von Glukose zu fünf sauren Bodenextrakten (unter P-reichen bis P-armen Bedingungen) ermittelt. Die Netto-P-Solubilisierungsraten konnten aus dem Anstieg der P-Konzentrationen in den Bodenextrakten abgeleitet werden, welche für 14 Tage mit Hydroxylapatit oder mit P-beladenem Goethit inkubiert wurden. Im zweiten und dritten Inkubationsexperiment erfolgte die Bestimmung der Netto-Solubilisierungsraten von Si und Ca aus vier silikathaltigen und zwei kalkreichen verwitterten Ausgangsmaterialien. Die Netto-Solubilisierungsraten von Si und Ca konnten aus der Differenz zwischen den am Ende und am Beginn des Experiments über 14 Tage gemessenen Mengen an Si und Ca berechnet werden. In allen Inkubationsexperimenten erfolgte eine Bestimmung der zeitlichen Änderungen des pH-Wertes sowie der Konzentrationen von vier verschiedenen organischen Säuren (Zitronensäure, Oxalsäure, 2-Keto-D-Gluconsäure und D-Gluconsäure) in den Bodenextrakten. Zusätzlich wurde auch Milchsäure (2-Hydroxypropansäure) in die Analyse der Bodenextrakte aus kalkreichen

Ausgangsmaterialien miteinbezogen. Die Berechnung der Brutto-P-Solubilisierungsraten erfolgte für vier saure und zwei alkalische Waldböden, welche sich aus silikathaltigen bzw. kalkreichen Ausgangsmaterialien entwickelten. Darüber hinaus erfolgte die Bestimmung der Abundanz und taxonomische Diversität der P-solubilisierenden Bakterien für die sauren und alkalischen Böden mittels eines physiologischen Assays in Kombination mit der 16S rRNA-Gensequenzierung.

Die mikrobiellen Netto-P-Solubilisierungsraten in den Bodenextrakten waren bei Inkubation mit Hydroxylapatit höher als bei Inkubation mit P-beladenem Goethit, mit Ausnahme eines Falles. Das Verhältnis zwischen dem pH-Wert der Bodenextrakte und den mikrobiellen Netto-P-Solubilisierungsraten war negativ für die Inkubationen mit Hydroxylapatit sowie positiv für die Inkubationen mit P-beladenem Goethit und abhängig von der unterschiedlichen Freisetzung von Protonen und organischen Säuren durch die Mikroorganismen. Bei der Inkubation mit P-beladenem Goethit regulierten die Mikroorganismen vermutlich die Produktion von organischen Säuren herunter, um einer Versauerung der Bodenextrakte und einer damit einhergehenden starken Sorption von Phosphationen vorzubeugen. Zusätzlich fiel die Produktion von Monocarbonsäuren signifikant mit einer hohen P-Freisetzung aus Hydroxylapatit zusammen. Insgesamt nahmen die mikrobiellen Netto-P-Solubilisierungsraten von primären und sekundären P-Mineralien mit der Zugabe von Glukose zu.

Bei Inkubation der Bodenextrakte mit verwitterten silikathaltigen und kalkreichen Ausgangsmaterialien wurden keine Netto-P-Solubilisierungsraten aufgrund einer mikrobiellen P-Immobilisierung gefunden. Jedoch konnten anhand der Netto-Solubilisierungsraten von Si und Ca die Brutto-P-Solubilisierungsraten, basierend auf den stöchiometrischen Verhältnissen dieser drei Elemente in den Ausgangsmaterialien, nachträglich berechnet werden. Die mikrobiellen Brutto-P-Solubilisierungsraten waren in den Bodenextrakten, inkubiert mit kalkreichen Ausgangsmaterialien, signifikant höher als in den Inkubationen mit silikathaltigen Ausgangsmaterialien (im Durchschnitt +61%). Diese höheren Brutto-P-Solubilisierungsraten in den Bodenextrakten nach Inkubation mit kalkreichen Ausgangsmaterialien resultierten aus einer insgesamt höheren mikrobiellen Aktivität, welche durch die Menge an organischen Säuren (bis zu 4,5-mal höher) und der mikrobiellen Biomasse (bis zu 19,1-mal höher) nahegelegt

wurde. Dieser Trend war insbesondere in der oberen Bodentiefe der kalkhaltigen Böden zu beobachten.

Die Abundanzen an P-solubilisierenden Bakterien waren in kalkreichen Böden signifikant höher als in silikathaltigen Böden (im Durchschnitt +46.6%). Ebenso zeigte die Analyse der Daten mittels nicht-metrischer multidimensionaler Skalierung, dass sich die P-solubilisierenden Bakterien in kalkhaltigen Böden signifikant von denen in silikathaltigen Böden unterschieden. Die Ordnungen *Bacillales* und *Burkholderiales* dominierten auf den silikathaltigen Standorten, während *Pseudomonadales* und in viel geringerem Maße *Enterobacteriales* die dominanten Ordnungen auf den kalkreichen Standorten repräsentierten.

Zusammenfassend betrachtet kamen P-solubilisierende Bakterien in P-armen Böden häufiger vor als in P-reichen Böden, wobei die Solubilisierungsraten von P, Si und Ca durch die Mineralchemie der Ausgangsgesteine beeinflusst wurden. In zukünftigen Studien mag „versucht“ werden, das Ausmaß der P-Freisetzung aus verwitterten Ausgangsmaterialien auch über die Netto-Solubilisierung des Hauptbestandteils des Ausgangsmaterials, mit Beachtung des stöchiometrischen Verhältnisses dieses Elements zu P, zu bestimmen. Diese Herangehensweise erscheint insbesondere bedeutsam in Anbetracht dessen, dass die spezifischen Freisetzungsraten von P in den meisten natürlichen Systemen extrem schwierig zu messen sind. Des Weiteren ist nicht nur mehr Forschung zur Netto-P-Solubilisierung in Nadel- und mediterranen Waldböden notwendig, auch die Netto-P-Solubilisierung, angetrieben durch die Pilzgemeinschaften in Waldböden, erfordert weitere Untersuchungen.

Table of contents

Summary	i
Zusammenfassung	iv
Table of contents	viii
List of Figures	x
List of Tables	xii
Statement of original authorship	xiii
Synopsis	1
1. General introduction.....	2
1.1 Introduction	2
1.2 Phosphorus in soils and minerals.....	2
1.3 Silicon and calcium in soils and rocks	4
1.4 P cycling: processes.....	5
1.5 Role of microorganisms in mineral solubilization	9
1.6 Role of organic acids and siderophores in mineral solubilization.....	10
1.7 Ecosystem dynamics in relation to P stocks and rock types	11
1.8 SPP-1685 (Phase II) - project research objectives and hypotheses	12
2. Materials and Methods.....	14
2.1 Study sites	14
2.2 Soil sampling and sample preparation.....	17
2.3 Soil and parent material characteristics	17
2.4 Mineral phases.....	18
2.5 Soil microbial C.....	18
2.6 Solubilization experiments.....	19
2.7 Organic acids and siderophores	22
2.8 Abundance and sequencing of P-solubilizing bacteria	23
2.9 Statistical analysis	24
3. Results and discussion of key findings	25
3.1 Microbial P solubilization from primary and secondary P-minerals and weathered parent materials	25
3.2 The role of pH on net P solubilization from primary and secondary P-minerals	32

3.3 The role of organic acids on net P solubilization from primary and secondary P-minerals.....	35
3.4 The role of pH and organic acids on solubilization of weathered siliceous and calcareous parent materials.....	36
3.5 Relative abundance and community composition of PSB from silicates and calcareous sites	40
4. Conclusion and Outlook.....	46
5. References.....	49
Manuscripts	63
6. Manuscripts.....	63
6.1 Microbial release of apatite- and goethite-bound phosphate in acidic forest soils.....	65
6.2 Microbial solubilization of silicon and phosphorus from bedrock in relation to abundance of phosphorus-solubilizing bacteria in temperate forest soils.....	77
6.3 Weathering of calcareous bedrocks is strongly affected by the activity of soil microorganisms	90
Contribution to the included manuscripts	101
Acknowledgements	102
Publications	104
Versicherungen und Erklärungen (Declarations)	105

List of Figures

Figure 1: Net P solubilization rates for hydroxyapatite incubated with glucose in solutions extracted from different soils collected at two different depths at five forest sites. The bars show means, and error bars indicate standard deviations ($n = 3$). Different letters indicate significant differences, tested separately for the two soil depths by one-way ANOVA, followed by post-hoc Tukey HDS ($p < 0.05$). Stars indicate significant differences between the two depths of each soil, tested by t-test followed by post-hoc Tukey HDS ($p < 0.05$).....25

Figure 2: Net P desorption rates for P-loaded goethite incubated with glucose in solutions extracted from different soils collected at two different depths at five forest sites. Mean values and standard deviations from triplicate experiments are shown. Different letters indicate significant differences, tested separately for the two soil depths by one-way ANOVA followed by post-hoc Tukey HDS ($p < 0.05$). Note that the rates at site BBR site (65-70 cm depth) were not missing but equivalent to zero26

Figure 3: Net Si solubilization rates for silicate parent materials incubated with glucose in aqueous extracts obtained from the four forest soils. The rates were calculated per specific surface area and over 14 days of incubation. The samples were taken at two soil depths (30–35 and 65–70 cm). Bars show means, and error bars indicate standard deviations ($n = 3$). Different letters indicate significant differences tested separately for the two soil depths by one-way ANOVA followed by post-hoc Tukey HDS ($P < 0.05$). Stars indicate significant differences between the two depths of each soil, tested by t-test followed by post-hoc Tukey HDS ($P < 0.05$)28

Figure 4: Net Ca solubilization rates from calcareous rocks incubated in soil extracts from two forest soils with glucose. The rates were normalized according to the specific surface area of the rocks and computed over 14 days of incubation. Soils and rocks were sampled at two different depths of two forest soils developed on dolomite (mineral topsoil: 4-9 cm and mineral subsoil: 22-37 cm) or on limestone (mineral topsoil: 11-18 cm and mineral subsoil: 42-60 cm). Bars show means and error bars indicate standard deviations ($n=3$). Different letters indicate significant differences tested separately for the two soil depths by one-way ANOVA followed by post-hoc Tukey HDS ($P<0.05$). Stars indicate significant differences between the two depths of each soil, tested by t-test followed by post-hoc Tukey HDS ($P<0.05$).....29

Figure 5: Stoichiometrically-derived gross P solubilization rates in two soil depth increments incubated with the respective bedrocks (silicates, $n=5$ and carbonates, $n=2$). Panel (a) shows the gross P solubilization rates based on the measured P content of the rocks, whereas panel (b) shows the weighted rates considering the same content of P. Mean values and standard deviations are shown ($n=3$). Uppercase and lowercase letters show significant differences tested separately for the two soil depths by one-way ANOVA. Because of the unequal sample sizes, the parametric Holm-Sidak post hoc test was chosen ($P<0.05$). T-test was used to indicate significant differences between the two depths of each soil and represented with a star ($P<0.05$).....31

Figure 6: Relationship between the pH and the log₁₀-transformed amounts of carboxyl groups released into solutions extracted from different soils incubated with hydroxyapatite and glucose. Two points in time are shown using respectively black and white dots (panel a) and black and white triangles (panel b). For all panels, the lines represent the best-fit regression line. Short-dashed and dotted lines depict associations after seven and fourteen days, tested separately for the two soil depths, respectively.....36

Figure 7: Total amounts of the organic acids in two soil depth increments incubated with contrasting bedrocks (silicates, n=5 and carbonates, n=2). Bars represent means, and error bars indicate standard deviations. Different uppercase and lowercase letters indicate significant differences between sites tested separately for each soil depth using one-way ANOVA. Because of the unequal sample sizes, the parametric Holm-Sidak post hoc test was chosen (P<0.05). T-test was used to indicate significant differences between the two depths of each soil and represented with a star (P<0.05)40

Figure 8: Relative abundance of different OTUs of P-solubilizing bacteria (PSB) from four forest soils developed on siliceous parent materials. Two panels are shown respectively for the two soil depths: (a) 30–35 cm and (b) 60–65 cm. Isolates identified as PSB were grouped into operational taxonomic units (OTU) at 98% cut-off similarity. Taxonomic classification of isolates is shown at the order level41

Figure 9: Relative abundance of different OTUs of P-solubilizing bacteria (PSB) from two forest soils developed on dolomite and limestone in the topsoil (a) and in the subsoil (b). Isolates identified as PSB were grouped into operational taxonomic units (OTU) at 98% cut-off similarity. Taxonomic classification of isolates is shown at the order level..... 42

Figure 10: Relative abundance of P-solubilizing bacteria (PSB) in two soils and two soils depth increments incubated with contrasting bedrocks (silicates, n=5 and carbonates, n=2). Bars represent means, and error bars indicate standard deviations. Different uppercase and lowercase letters indicate significant differences between soils tested separately for each soil depth using one-way ANOVA. Because of the unequal sample sizes, the parametric Holm-Sidak post hoc test was chosen (P<0.05). T-test was used to indicate significant differences between the two depths of each soil and represented with a star (P<0.05)44

Figure 11: Nonmetric multi-dimensional scaling (nMDS) plot where each point represents the P-solubilizing bacteria (PSB) of a sample (stress = 0.01, non-metric R² = 0.927). Color and shape indicate different parent materials (blue siliceous rocks and red calcareous rocks). Manhattan distances were chosen for computing the dissimilarity between each pair of observations. Bacterial community structures differed significantly between carbonate and silicate sites (P< 0.05).....45

List of Tables

Table 1: Schematic representation of the research plan.....	14
Table 2: Site characteristics of five acidic and two alkaline forest soils in Germany. The acidic forest soils are Bad Brückenau (BBR), Mitterfels (MIT), Vessertal (VES), Conventwald (CON) and Lüss (LUE). The alkaline forest soils are Tuttlingen (TUT) and Mangfall (MAN). The soils represent a geosequence covering a wide range of total P stocks and rock parent materials (silicates and carbonates)	15
Table 3: Soil chemical properties of five acidic and two alkaline forest soils in Germany. Two soil depths were sampled in the mineral layer of the acidic soils (30-35 cm and 65-70 cm). In the alkaline soil developed on limestone two soil depths in the mineral layer were sampled respectively at 11-18 cm and 42-60 cm. In the alkaline soil developed on dolomite, two soil depths in the mineral layer were sampled respectively at 4-9 cm and 22-37 cm	16
Table 4: Average net P solubilization rates from primary (hydroxyapatite) and secondary (P-loaded goethite) P-minerals. The net P solubilization rates from hydroxyapatite from five temperate forest soils (Pastore et al., 2020) were compared with those obtained from soils of the Coastal Cordillera of Chile (Brucker et al., 2020).....	27
Table 5: Results of simple and multiple regression analyses for the variables pH (at day 7 or day 14), low molecular weight organic acids (at day 7 and day 14), DOC (at the beginning of the incubations) and net P solubilization rates across all test sites, calculated separately for the two soil depths (30–35 and 65–70 cm). Given are the coefficients of regression (R^2 for simple regression or adjusted R^2 for multiple linear regression) as well as the p-values (highlighted in bold when statistically significant). For significant relationships, the negative (–) or positive (+) correlation was provided within parenthesis.....	34
Table 6: Relative contribution (%) of organic acids to the hydrogen ion concentration (H^+) of soil extracts incubated with hydroxyapatite (Study I), siliceous parent materials (Study II) and calcareous parent materials (Study III) on the 7 th day after the start of experiments	38

Statement of original authorship

I hereby certify that the submitted work is my own work, was completed while registered as a candidate for the degree stated on the title page, and I have not obtained a degree elsewhere on the basis of the research presented in this submitted work.

Print: Giovanni Pastore

Date: 09 December 2020

1. Synopsis

1. General Introduction

1.1 Introduction

Phosphorus (P) is essential for all living organisms and, after nitrogen (N), is the second most limiting macronutrient in both aquatic and terrestrial ecosystems (Elser et al., 2007; Turner et al., 2018). While N derives from a large, and potentially infinite, atmospheric pool (78% of total gases in Earth's atmosphere), P is found mainly in phosphate rocks, which are a non-renewable resource. Previous studies have shown that temperate and boreal regions are mainly limited by N, whereas tropical regions are severely limited by P (Turner et al., 2007; Menge et al., 2012; Darcy et al., 2018). Yet, increases in atmospheric N depositions can significantly impact the biogeochemical cycle of P (Dirnböck et al., 2017; Remy et al., 2017; Heuck et al., 2018). As a result, it is expected that temperate forests may shift from N to NP co-limitation or even P limitation (Peñuelas et al., 2013). Besides, projections on future climate change suggest that N and P cycling will be affected by increasing temperatures as many regions are likely to become drier than they are today (IPCC, 2008). Soil bacteria and mycorrhizal fungi can increase availability of P by mobilizing it from organic and inorganic sources (Jacoby et al., 2017). However, the specific processes underlying the release of P from mineral phases, and their contribution to forest P nutrition, are far from being well understood, and thus, warrant a detailed and extensive investigation (Cordell et al., 2009).

1.2 Phosphorus in soils and minerals

Soils contain between 200 mg P kg⁻¹ and 3000 mg P kg⁻¹ (Fardeau, 1996). Despite this, P concentrations in the soil solution are relatively low and generally in the order of $\leq 0.1\%$ of total P (Zhu et al., 2011). Phosphorus cycling in soils is greatly affected by numerous environmental factors such as moisture content, temperature, soil chemistry (e.g., pH, ionic strength, redox potential), nature of the solid phases and biological activity (Rosling et al., 2016). Forest ecosystems maintain their productivity, despite low soil P availability, because microbes can enrich this pool by decomposing P-rich organic

matter and by solubilizing P-rich minerals (Jones and Oburger, 2011; Heuck and Spohn, 2016). Phosphorus in soils is present in a variety of organic and inorganic compounds and the distribution of P within these pools changes with time and soil development (Walker and Syers, 1976). The first step of P cycling in terrestrial ecosystems occurs via solubilization of P-rich minerals that form the rock (Filippelli, 2002). In literature, it is common to refer to inorganic P forms when orthophosphate ions are bound to cations present in the crystal lattice of the rock or adsorbed onto mineral surfaces (Hinsinger, 2001). Plant roots and soil microorganisms are able to solubilize insoluble inorganic P forms by either dissolving the mineral phases or desorbing sorbed P species through the release of low-molecular-weight organic acids (LMWOAs), protons (H^+), siderophores and exopolysaccharides (Yi et al., 2008; Frey et al., 2010; Ordoñez et al., 2016). Once released in the soil solution, P can be taken up by organisms solely in the form of orthophosphate ions.

In soils with high pH, calcium phosphates (Ca-P) predominate. However, this does not mean that Ca-P do not exist in soils with low pH (Curtin and Syers, 2001; Prietzel et al., 2016). Hydroxyapatite (HAP; $Ca_5(PO_4)_3(OH)$) is the principal Ca-P mineral occurring in nature (Nezat et al., 2008). In acidic soils, orthophosphate ions mostly precipitate with aluminium (Al) and iron (Fe) (Penn and Camberato, 2019). Variscite ($AlPO_4 \cdot 2H_2O$) and strengite ($FePO_4 \cdot 2H_2O$) are the most important Al and Fe phosphates, although the crystalline form of the latter is quite rare in nature. Beside precipitation, orthophosphates can strongly adsorb to Al and Fe oxyhydroxides (Lindsay, 1979). Orthophosphate ions are preferentially adsorbed to Al and Fe oxyhydroxides through the formation of bidentate bonds (Geelhoed et al., 1998). However, the formation of monodentate bonds have also been reported in literature (Schwertmann, 1991). In nature, goethite ($\alpha-FeO(OH)$) is the most common Fe oxyhydroxide (Cornell and Schwertmann, 2003) and is often used in model experiments addressing basic mechanistic features of hydrous Fe oxides.

Beside inorganic P, the other pool of P is constituted by organic P which, in soils, can be as high as 30–65% of total P (Condrón et al., 2005). On average, organic P values reach a peak to then decrease with increasing soil age and depth (Walker and Syers, 1976). Organic P forms include inositol phosphates, phosphodiesteres, phospholipids,

polyphosphates and nucleic acids (Rodríguez and Fraga, 1999). Plants and microorganisms are capable of mineralizing organically bound P through the release of phosphatase enzymes that catalyze the hydrolysis of the organic P, thus releasing orthophosphate ions. This process is known as P mineralization (Spohn and Kuzyakov, 2013). The production of phosphatase enzymes depends on many soil variables but in particular on N availability (Sinsabaugh et al., 2008; Margalef et al., 2017).

1.3 Silicon and calcium in soils and rocks

Very few studies on silicate and carbonate mineral solubilization have been conducted in forest soils, so far (Williams et al., 2007; Sverdrup et al., 2019). Silicates and carbonates can have very different P concentrations depending on the amount of apatite grains they contain (White, 2003; Porder and Ramachandran, 2012). Although most soil P largely derives from apatite dissolution, other nutrients (Fe, Mg, Ca, Na, K) become mostly available from silicate and carbonate solubilization (Harley and Gilkes, 2000). Silicates compose more than 90% of the Earth's crust and are found in most igneous, sedimentary and metamorphic rocks (for a review see White and Brantley, 1995). Igneous rocks contain on average a higher proportion of apatite than metamorphic and sedimentary rocks, thus, one would expect a higher release of P from rocks having a higher content of apatite-P. The crystallographic arrangement of silicate minerals is centered around the silicon–oxygen tetrahedron group (SiO_4^{4-}). Silica tetrahedra contains void spaces that are occupied by various metal cations to maintain electrical neutrality. Contrary to P, silicon (Si) is not considered essential for plant growth, although several studies have proven its favorable effects on growth and disease resistance in many crops (Guntzer et al., 2012). In soils, the content of bioavailable Si varies from 0.003 to 0.45 g Si kg^{-1} , whereas bioavailable P varies from 0.02 to 0.1 g P kg^{-1} (Yang and Post, 2011). Silicate solubilization can be caused by the same mechanisms as apatite solubilization (Brucker et al., 2020). In addition, the Si concentrations in soil are affected by Si sorption/desorption (Haynes and Zhou, 2020). Some authors (Dessert et al., 2003; Wolff-Boenisch et al., 2006) indicated that basalts have larger solubilization rates than other silicates. In contrast, Newman (1995) found that there are no consistent differences in solubilization rates between major

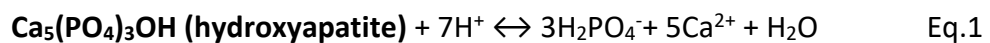
aluminosilicate rock types. Microbes, including soil PSB, are known to also solubilize Si (Brucker et al., 2020). However, the extent to which soil PSB, and more in general microorganisms, impact the solubilization rates of silicate minerals is far from being completely understood.

Carbonates constitute up to 15% of the sedimentary rocks of the Earth's crust (Fairbridge et al., 1967) and occur along various climatic zones mainly in the form of minerals such as limestone [CaCO_3] and dolomite [$\text{CaMg}(\text{CO}_3)_2$]. Younger carbonates are predominantly limestones (rich in calcite) that when exposed to acidic environments release Ca and carbon dioxide (CO_2). Over time, limestones can recrystallize and convert to dolomite following a process called dolomitization (Deelman, 2008). Dolomites react to acids more slowly than limestones, and therefore, their dissolution generally takes longer to occur (Liu et al., 2005). One possible reason for this is that dolomite may contain significant amounts of detrital silicate minerals which are scantily soluble in water (Taylor et al., 2019). Both limestones and dolomites may contain high P concentrations, ranging from 1.5 to 2.8 g kg^{-1} due to the apatite minerals they contain (Porder and Ramachandran, 2012). While the abiotic dissolution of carbonates has been intensively studied, less is known about the biological contribution to this process. Soil microorganisms can accelerate the dissolution of carbonate rocks and apatite minerals as well as increase the desorption of P and Ca, but it is currently unknown to what extent microorganisms affect the Ca and P solubilization of calcareous parent materials in temperate forest soils (Banfield et al., 1999; Hinsinger, 2001).

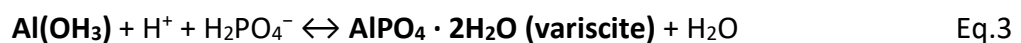
1.4 P cycling: processes

Traditionally, processes involved in soil P cycling can be summarized into four principal categories: (i) dissolution-precipitation, (ii) sorption-desorption, (iii) mineralisation and (iv) immobilization. Dissolution, desorption and mineralization increase P concentrations in the soil solution, while precipitation, sorption and immobilization cause their decrease. Points (i) and (ii) represent a central topic of the work presented in this thesis, and thus, will be treated with due detail below.

With the term “P dissolution” we refer to the effect of pH on the dissolution of phosphate rocks which contains high amounts of phosphate minerals (mainly the group of apatites, having general formula: $\text{Ca}_5(\text{PO}_4)_3(\text{F},\text{Cl},\text{OH})$). Phosphate minerals have variable solubility (Lindsay, 1979). Many studies found that Ca phosphates dissolution increases when the pH decreases (proton-promoted dissolution). The rate of dissolution of Ca phosphates is determined by the concentration of protons (H^+) and the concentration of the reaction products, namely Ca and H_2PO_4^- , which are liberated in the solution (Bolan and Hedley, 1990; Hinsinger, 2001). As the mineral dissolves, the solution becomes progressively closer to equilibrium. At equilibrium, the net dissolution rate of the mineral is zero because the rate of dissolution equals exactly the rate of precipitation (Drever and Stillings, 1997). Since the net rate must be zero at equilibrium, over time, dissolution of the mineral decreases. As an example of Ca phosphates dissolution, it might be worth considering the following reaction (Eq.1):

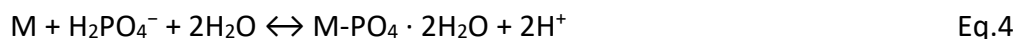


The equation written above shows that hydroxyapatite dissolution can be enhanced if H^+ are supplied or if the reaction products (Ca and H_2PO_4^-) are removed from the soil solution. P ions and metal cations like Ca can be “removed” from the soil solution through (1) adsorption of P ions by soil constituents, (2) by complexation of metal cations by organic ligands (i.e., ligand-promoted dissolution) or (3) by plant and microbial uptake (Hoberg et al., 2005). If points (1), (2) and/or (3) occur, the dissolution reaction can continue to take place. In contrast, Fe and Al phosphates are insoluble at low pH and their dissolution increases when also the pH increases (Penn and Camberato, 2019). The reason for this can be explained if we consider the following examples (Eq.2 and Eq.3):



In bold are reported the solid phases. The equations written above show that if protons are supplied the reaction proceed from left to right (i.e., precipitation of ferric and aluminium phosphates).

Precipitation is a complex phenomenon that, depending on the different physico-chemical conditions, occurs when the soil solution is saturated with the reactants. In alkaline soils, orthophosphate ions bind to metal cations like Ca and precipitation of Ca-P minerals can occur (Penn and Camberato, 2019). In contrast, in acidic soils orthophosphate ions precipitate with Fe and Al cations (Hinsinger, 2001). Precipitation follows the following simplified general reaction (Eq.4):



Where with “M” we indicate any metal cation such as Fe, Al, Ca.

The sorption of phosphate on metal (hydr)oxides influences the availability of this element in terrestrial ecosystems (Geelhoed et al., 1998). With the term “P sorption” we refer to the attraction of an anion (in this case a phosphate anion) on Fe and Al oxides/hydroxides surfaces (Hinsinger, 2001). Previous studies have shown that the adsorption of P onto synthetic Fe and Al oxides/hydroxides occurs through the formation of monodentate complexes followed by bidentate complexes (Sposito, 1986; Torrent, 1997; Geelhoed et al., 1998). In addition, He et al. (1994) suggested that in conditions of low saturation the bidentate complex dominate, while with increasing saturation the equilibrium shifts towards the prevalence of monodentate complexes. Overall, P adsorption involves the formation of stable inner-sphere surface complexes with metal ions and is influenced by many parameters such as pH, competition with other anions and by the degree of crystallinity of Fe and Al oxides/hydroxides (Beebout and Loeppert, 2006). For example, it was shown that decreasing the pH of the solution was accompanied by an increased adsorption of orthophosphate ions onto Fe and Al oxides/hydroxides (Hinsinger, 2001). One of the reasons for this is that with decreasing pH of the solution, variable charge-minerals like goethite become increasingly positively charged due to protonation which favors phosphate sorption, and thus, causes net removal of phosphate from the soil solution (Beebout and Loeppert, 2006). On the contrary, P adsorption decreases with increasing solution pH because at high pH

phosphate anions compete with OH⁻ groups for sorption on mineral surfaces (Ahmed et al., 2020). Also, Geelhoed et al. (1998) showed that the simultaneous addition of citrate and phosphate to goethite resulted in a decrease in the adsorption of both phosphate (especially below pH 7.0) and citrate (over the whole pH range), indicating that they compete for adsorption sites on the goethite.

The relative importance of precipitation vs. sorption is still a matter of debate, but is generally accepted that precipitation is more relevant under high P concentrations, whereas, sorption is more relevant at low P concentrations (Tunesi et al., 1999). In addition, it is important to mention that P precipitation can also occur before the saturation of all P adsorption sites is completed (Li and Stanforth, 2000).

Sorbed P is difficult to desorb by simple ion exchange process. However, several studies showed that a proportion of the sorbed P on the surfaces of metal (hydr)oxides is still available to plants as P can be exchanged by competing ligands such as hydroxyl, organic acids and/or bicarbonate (He et al., 1994; Geelhoed et al., 1998; Beebout and Loeppert, 2006). This process is known as ligand exchange and occurs when a ligand exchanges for inorganic P sorbed onto a mineral surface, thus releasing P in the soil solution. In the case of organic acids released by roots and microorganisms, the effectiveness by which phosphate is desorbed from metal (hydr)oxides depends on the number of carboxyl groups of the acid. Also, Beebout and Loeppert (2006) suggested a second process of desorption called “ligand-enhanced dissolution of metal (hydr)oxides”. This process occurs when the organic ligand is adsorbed at the surface of Fe sites, resulting in the slow dissolution of the Fe-oxide and consequent release of sorbed P in the soil solution. He et al. (1994) found that P desorption from montmorillonite was very rapid and the maximum “desorbability” (the percentage of desorbed P with regard to the total adsorbed P) could reach up to 90% within three days. On the other hand, P desorption from goethite was comparably small and, on average, less than 2% of the sorbed P was desorbed after three-week of incubation. This finding suggests that montmorillonite-P supplies P to the soil solution rapidly but within a short time period, while goethite-P supplies P slowly but likely over a longer period. Taken together, in this thesis, we refer to the term “P solubilization” as the resultant of two processes: “dissolution of P-containing minerals” and “desorption of adsorbed P” (for a review see also Goldstein, 2003). Previous dissolution experiments demonstrated

that some microbial strains are effective in releasing orthophosphate from Ca-P minerals, while the desorption of orthophosphate from Fe hydrous oxides is somehow less effective (Hinsinger, 2001; Hoberg et al., 2005).

1.5 Role of microorganisms in mineral solubilization

Phosphorus cycling in forest ecosystems is largely driven by plants and soil microbes. If one excludes agrochemical fertilizers, the only way to increase the concentrations of orthophosphate ions are through the mineralization of organic P-rich compounds and the dissolution of P-bearing minerals and desorption of phosphate adsorbed to minerals (Alori et al., 2017). Microorganisms that have the potential to solubilize insoluble P forms to soluble forms (orthophosphate) are referred to as P-solubilizing microorganisms (PSM) which consist of P-solubilizing bacteria (PSB) and P-solubilizing fungi (PSF). The two main soil bacteria genera that have been reported to strongly solubilize insoluble P-rich minerals are *Pseudomonas* and *Bacillus* (Browne et al., 2009; Sharma et al., 2013; Thakur et al., 2014). Other efficient PSB include various strains of *Burkholderia*, *Caballeronia*, *Enterobacter*, *Erwinia*, *Flavobacterium*, *Klebsiella*, *Paenibacillus*, *Rhodococcus* and *Serratia* (Chung et al., 2005; Chen et al., 2006; Beneduzi et al., 2013). The two main fungal genera able to solubilize P are *Aspergillus* and *Penicillium* (Asea et al., 1988; Wahid and Mehana, 2000; Zhang et al., 2018). Other fungal strains relevant in P solubilization include *Fusarium*, *Glomus*, *Trichoderma*, *Geomyces*, *Paecilomyces* and *Alternaria* (Jones et al., 1991; Lima-Rivera et al., 2016; Bononi et al., 2020). When considering the culturable soil microflora, about 1–53% of bacteria and 0.1–0.5% of fungi have been reported to contribute to P solubilization (Wakelin et al., 2004). However, in nature, the abundance of PSM can be highly influenced by soil pH. Several studies pointed out that acid soils exhibit a much lower ectomycorrhizal fungal richness than calcareous soils and that the ectomycorrhizal mycelium can host very efficient apatite weathering PSB (Leberecht et al., 2016; Fontaine et al., 2016). Thus, considering the ecology of fungal communities, i.e., higher growth rate at low soil pH (Rousk et al., 2009) and higher capacity to explore large soil volumes than bacteria (Winkelmann, 2007), it seems plausible that the role and the abundance of PSF *in situ* and in alkaline soils could be higher than what has been

reported from laboratory experiments. Yet, culture-dependent methods, though able to provide a practical, direct and relatively cheap estimate of P-solubilizers from a given soil, also have some limitations especially for screening P-solubilizing fungi. Taken together, the mechanisms used by PSM to increase P availability consist of the lowering of the soil pH and the release of low-molecular weight organic acids (LMWOAs), siderophores and exopolysaccharides. These compounds cause the release of orthophosphate ions either via complexation of metal cations (i.e., Ca, Mg, Al, Fe) or by acidifying the soil solution. Beside enhancing P solubilization, soil PSM have been proven to increase the growth, yields and resistance in many plants (Adnan et al., 2017; Alori et al., 2017; Köhl et al., 2019). Also, soil PSM can boost biological N fixation which, in turn, stimulates a high enzymatic activity (i.e., phosphatase enzymes) in soils and help to overcome P-limitation (Batterman et al., 2018). Some soil PSM have also been reported to be able to produce phytohormones that can improve nutrient acquisition and provide resistance to various biotic and abiotic stresses (Rodriguez and Fraga, 1999; Numan et al., 2018; Egamberdieva et al., 2017).

1.6 Role of organic acids and siderophores in mineral solubilization

Organic acids are low-molecular weight compounds which can be released by plants and microbes to access unavailable P bound to minerals. Monocarboxylic LMWOAs are mainly produced by bacteria in the periplasmic space via the direct oxidation pathway (Goldstein, 1995). Di- and tri-carboxylic LMWOAs are instead the resultants of the tricarboxylic acid cycle (Krebs cycle) and the glyoxylate cycle, a variation of the Krebs cycle. Independent of their structure, LMWOAs are usually released as organic anions from cells as the cytosolic cell pH is around 7 (Oburger et al., 2011). Citrate, malate, oxalate, gluconate, 2-keto-gluconate and lactate are among the most important LMWOAs that have been shown to play significant roles in mineral weathering (Illmer and Schinner, 1992; Rodriguez and Fraga, 1999). In plants, the energy required for organic acids synthesis is derived from photosynthetic CO₂ fixation (with differences between C₃, CAM and C₄ plants) and CO₂ fixation in the root. Microbes usually obtain the energy required for organic acids synthesis from root exudates, such as glucose, or through the decomposition of organic matter. Several studies showed that some plants

are able to release large amounts of organic acids in the rhizosphere as a response to P deficiency, whereas other species do not appear to express some of the genes encoding enzymes for organic acids production (for a review see Jones, 1998; Pavinato et al., 2008). Likewise, LMWOAs production is not ubiquitous among the microbial population and their release can be significantly affected by soil depth and the pH of the surrounding environment (for a review see Adeleke et al., 2017; Marra et al., 2015). As mentioned, LMWOAs can carry from one to three carboxylic groups with varying negative charges, thereby allowing the complexation of positively charged metal cations (Ca, Al, Fe) and the consequent displacement of orthophosphate ions in the soil solution. By complexing metal cations, the soil solution becomes undersaturated, thus favouring the weathering of the mineral. Thus, the presence of organic acids decreases the concentration and activity of metal cations by shifting the equilibrium according to Le Chatelier's principle. LMWOAs can also lower the pH which results in an increase of the proton concentration in the soil solution.

Siderophores are low-molecular weight chelators having strong affinities for divalent and trivalent metals, especially Fe. Siderophores are distinguished on the basis of the moieties involved in Fe chelation and are grouped into four main types: catecholates, phenolates, hydroxamates and carboxylates (Matzanke, 2011). Six important microbial siderophores are reported in literature and are reputed to play a significant role in mineral weathering: protochelin, enterobactin, desferrioxamine B, ferricrocin, aerobactin and rhizobactin (Hider and Kong, 2010). Under Fe deficiency, plant roots and microbes are able to secrete high amounts of siderophores which increase the solubilization of Fe oxyhydroxides (Marschner et al., 2011). Also, because silicates are a source of numerous elements, including Fe and Al, siderophores are reputed to play an important role in silicate solubilization and in acidic soils (Liermann et al., 2000). On the contrary, Masalha et al. (2000) suggested that siderophores might be more relevant in calcareous soils, where Fe limitation is a serious problem, and therefore, their contribution to Fe dissolution in acidic soils might be overrated.

1.7 Ecosystem dynamics in relation to P stocks and rock types

Most research on P release from mineral phases has focused on single microorganisms cultured in isolation, but little is known about how microbial communities affect the release of P from minerals. In addition, the influence of rocks and soils on the composition of the microbial communities has been addressed only in very few papers (see also Gleeson et al., 2006; Uroz et al., 2015).

Lang et al. (2016) hypothesized that plants and microbes at sites rich in mineral-bound P introduce P from primary minerals into the P cycle (acquiring systems). In contrast, ecosystems poor in mineral-bound P rapidly cycle P between soil organic matter and plants (recycling systems). The latter strategy makes up most of the annual P flux in the soil-plant system (Jones and Oburger, 2011). However, in extremely P-limiting environments, the first strategy might play a bigger role. For example, in soils with very low P availability, the occurrence and the activity of PSM might be more relevant due to environmental pressures favouring organisms that strongly mobilize P from minerals and rocks (Jones and Oburger, 2011; Nicolitch et al., 2016). On the contrary, in soils with high P availability, the abundance and effectiveness of PSM might be lower since microbes would have no reason to invest much energy into LMWOAs and enzymes production when nutrients are “easily” available. As mentioned earlier, microbes do not have the same potential to solubilize insoluble P forms. Microbial communities are effective in mobilizing orthophosphate from primary mineral phases, such as apatites, but less effective in desorbing orthophosphate sorbed to secondary hydrous oxide phases, such as goethite. Also, Spohn et al. (2020) found that P solubilization was higher in moderately-weathered than in strongly-weathered saprolite and that the abundance of PSB was increased in the strongly-weathered saprolite. This finding is in accordance with other studies showing that the occurrence of PSB differs among soils (Browne et al., 2009 and references therein).

1.8 SPP-1685 (Phase II) - project research objectives and hypotheses

The work in this thesis was conducted as part of the SPP-1685 project (Phase II) with the objective of evaluating the potential of microbial communities in soil extracts from five temperate forest soils along a gradient of P availability to release phosphate from one

typical primary mineral source, namely hydroxyapatite, and desorb phosphate bound to secondary minerals, represented by goethite (study I). A second aim of this thesis was to examine microbial solubilization of Si and P from different silicate parent materials (i.e., basalt, andesite and paragneiss) in four beech forest soils differing in total P stocks and to explore the relationship between the abundance and the community composition of soil PSB and the Si and P solubilization rates (study II). A third objective of this thesis was to determine Ca and P solubilization rates from two alkaline soils developed on different calcareous parent materials (limestone and dolomite) and to assess to which extent the abundance and the taxonomy of PSB from calcareous forest soils is related to the Ca and P solubilization rates from calcareous parent materials (study III). Also, study III aimed at evaluating how PSB communities differed between siliceous and calcareous soils.

The main hypotheses of these studies were:

- (1) the net microbial P solubilization from hydroxyapatite results from acidification of the soil solution, whereas the desorption of orthophosphate from goethite is not promoted by acidification.
- (2) glucose stimulates microbial production of LMWOAs and metal-complexing compounds, which cause increased orthophosphate release from minerals.
- (3) the solubilization rates from siliceous and calcareous parent materials are correlated with the concentrations of LMWOAs and protons released by microorganisms.
- (4) stoichiometrically-derived gross P solubilization rates from calcareous parent materials are higher compared to siliceous parent materials.
- (5) the abundance of PSB increases with decreasing P stocks of the soils.
- (6) the abundance and the diversity of PSB is higher at the silicate soils than at the carbonate soils.

2. Materials and Methods

2.1 Study sites

Solubilization rates were examined in three studies (Table 1). P-solubilizing bacteria (PSB) communities were examined in two sets of study sites, one from the acidic forest soils and the other from the alkaline forest soils. The five acidic forest sites represented a geosequence of P stocks decreasing in the order Bad Brückenau > Mitterfels > Vessertal > Conventwald > Lüss (Lang et al., 2017). The main soil type of all sites was Cambisol. The two alkaline forest sites represented a geosequence of P stocks decreasing in the order Tuttlingen > Mangfall (Prietzl and Ammer, 2008). The main soil type of both sites was Leptosol. Except for the site Lüss which is located in northern lowlands, the remaining sites are all situated at intermediate heights within central and southern German mountain ranges (Table 2).

Table 1 Schematic representation of the research plan.

Incubations	Study I	Study II	Study III
	Acidic forest soils		Alkaline forest soils
Hydroxyapatite and P-loaded goethite	•		
Weathered siliceous parent materials		•	
Weathered calcareous parent materials			•
P-solubilizing bacteria		•	•

Table 2 Site characteristics of five acidic and two alkaline forest soils in Germany. The acidic forest soils are Bad Brückenau (BBR), Mitterfels (MIT), Vessertal (VES), Conventwald (CON) and Lüss (LUE). The alkaline forest soils are Tuttlingen (TUT) and Mangfall (MAN). The soils represent a geosequence covering a wide range of total P stocks and rock parent materials (silicates and carbonates).

Site	Gauss-Krüger coordinates	Altitude (m a.s.l.)	MAT (°C)	MAP (mm)	Soil Type (WRB 2015)	Parent material	Total soil P stocks (g m ⁻²)
Bad Brückenau (BBR)	50° 21' N, 009° 55' E	809	5.8	1031	Dystric skeletal cambisol	Basalt	904
Mitterfels (MIT)	48° 58' N, 12° 52' E	1023	4.5	1299	Hyperdystric chromic folic cambisol	Paragneiss	678
Vessertal (VES)	50° 36' N, 10° 46' E	810	6.0	1200	Hyperdystric skeletal chromic cambisol	Trachyandesite	464
Conventwald (CON)	48° 01' N, 007° 57' E	840	6.8	1749	Hyperdystric skeletal folic cambisol	Paragneiss	231
Lüss (LUE)	52° 50' N, 10° 16' E	115	8.0	779	Hyperdystric folic cambisol	Sandy till	164
Tuttlingen (TUT)	47° 59' N, 8° 45' E	820	6.6	855	Rendzic Leptosol	Limestone	209
Mangfall (MAN)	47° 39' N, 11° 56' E	1190	5.5	1863	Haplic Leptosol	Dolomite	47

Table 3 Soil chemical properties of five acidic and two alkaline forest soils in Germany. Two soil depths were sampled in the mineral layer of the acidic soils (30-35 cm and 65-70 cm). In the alkaline soil developed on limestone two soil depths in the mineral layer were sampled respectively at 11-18 cm and 42-60 cm. In the alkaline soil developed on dolomite, two soil depths in the mineral layer were sampled respectively at 4-9 cm and 22-37 cm.

Site	Soil depth (cm)	Soil pH (in H ₂ O)	Total C (g kg ⁻¹)	Total N (g kg ⁻¹)	Total P (g kg ⁻¹)	Microbial C (mg g ⁻¹)
Bad Brückenau (BBR)	30-35	5.1	42.0	3.2	2.5	0.17
	65-70	5.6	26.2	1.9	2.0	0.11
Mitterfels (MIT)	30-35	4.7	31.4	1.7	0.9	0.22
	65-70	4.7	26.8	1.4	0.9	0.14
Vessertal (VES)	30-35	4.9	37.7	2.3	1.0	0.11
	65-70	4.9	12.8	0.8	0.9	0.03
Conventwald (CON)	30-35	4.5	45.7	2.0	0.6	0.13
	65-70	4.7	7.7	0.6	0.4	0.18
Löss (LUE)	30-35	4.8	10.1	0.5	0.1	0.20
	65-70	4.9	7.0	0.4	0.2	0.11
Tuttlingen (TUT)	11-18	7.2	46.5	3.8	1.0	2.90
	42-60	8.6	39.5	-	0.7	0.14
Mangfall (MAN)	4-9	7.3	92.2	6.2	0.6	2.61
	22-37	7.6	48.5	2.0	0.3	1.44

missing values were below the detection limit (0.5 g kg⁻¹)

2.2 Soil sampling and sample preparation

For Study I, mineral soil samples from two different depths were collected in mid-April 2017 at each of the five forest sites in Germany (Table 2). For study II, we collected the weathered siliceous parent materials at the two different depths from which the mineral soil was formed from four of the five forest sites. The two different soil depths were sampled by combining material taken from five randomly selected spots per depth using a small stainless-steel spatula. The mineral soil was chosen because mineral solubilization is most relevant in horizons poor in organic P. For study III, mineral soil samples from two different depths and the respective weathered calcareous parent materials were sampled and collected in September 2018 from two calcareous forests in Germany. Field-moist samples were sieved in the laboratory (< 2 mm) and all debris were removed. From each soil sample (a) an aliquot was air-dried for chemical analysis. The remaining soil (b) was stored at 5 °C for the incubation experiments or (c) frozen at -20 °C for microbial analysis. Parent materials were crushed in the laboratory using a jaw crusher. Each crushed sample was initially sieved through a 0.63 mm sieve. The resulting size fraction was further sieved through a 0.2 mm sieve. The material that did not pass the latter was used for the incubation experiments.

2.3 Soil and parent material characteristics

Soil pH values were determined with a gel electrode (WTW) in deionized water using a soil-to-water ratio of 1:5 and an equilibration time of 3 h. For the analysis of total C, N and P, subsamples of mineral soils were dried at 60 °C for 24 h. Aliquots of oven-dried samples were finely ground in a ball mill. Soil C and N concentrations were measured with an elemental analyzer (Vario MAX CN, Elementar, Germany) while soil P concentrations were determined with inductively coupled plasma-optical emission spectroscopy (ICP-OES, Vista-Pro radial, Varian) after pressure digestion in concentrated nitric acid (Table 3). In order to analyze the contents of total P (TP), total Ca (TCa) and total Si (TSi) from the different weathered parent materials, crushed subsamples were digested using a combination of nitric acid (65% HNO₃),

hydrofluoric acid (40% HF), and hydrochloric acid (37% HCl) according to Sandroni and Smith (2002) by ICP-OES (Vista-Pro radial, Varian). The specific absorption of radiation for P, Ca, and Si was 190 nm, 356 nm and 253 nm, respectively. The reference material used for the analysis consisted of SPS-WW2 waste water 2 for P, borosilicate glass (SiO₂ 53.98%) for Si and SPS-SW2 surface water 2 for Ca (LGC Standards, France).

2.4 Mineral phases

Hydroxyapatite (Ca₅(PO₄)₃(OH)) was purchased from Sigma-Aldrich (purity ≥ 95%), while Goethite (α-FeO(OH)) was produced according to the method of Atkinson et al. (1967) by neutralising 1 M FeCl₃ solution with NaOH and ageing the precipitate at 55 °C for 3 days. Orthophosphate loading was done by equilibrating 20 g of goethite with 1000 ml KH₂PO₄ solution containing 1000 mg P l⁻¹ on a horizontal shaker at 60 motions min⁻¹ for 16 h at 20 °C. The suspension was centrifuged at 4500×g for 45 min, and the supernatant decanted. The settled goethite was re-suspended in 1000 ml ultrapure water (pH 6) to remove excess orthophosphate, centrifuged at 4500×g for 45 min, and then, the supernatant decanted. After rinsing, P-loaded goethite was freeze dried. Drying usually causes bonds between P and oxide surfaces to become stronger. The specific surface areas (SSA) of weathered parent materials were determined by N₂ adsorption with an automatic analyzer. Similarly, the SSA of hydroxyapatite and P-loaded goethite were determined by N₂ adsorption and were equal to 100 m² g⁻¹ and 58 m² g⁻¹, respectively.

2.5 Soil microbial C

Soil microbial biomass C concentrations were determined from all soils and depths with the chloroform-fumigation extraction method (Table 3; see also Brookes et al., 1982; Vance et al., 1987). For microbial C, one aliquot of soil was extracted with 0.5 M K₂SO₄ with a soil: solution ratio of 1:5 (w/v) and used as control. A second aliquot of soil was fumigated with CHCl₃ for 24 h and extracted similarly. Microbial C were

calculated as the difference of C concentrations in the extracts of fumigated and control soil. The differences were then corrected by 2.22 which is the conversion factor for microbial C (Jenkinson et al., 2004).

2.6 Solubilization experiments

All soil extracts used for incubations were obtained by placing 100 g of each soil sample in polyethylene PE bottles and shaken with 1 l of distilled water at room temperature for 2 h using an overhead shaker. The extracts were filtered through cellulose filters with a particle retention range of 5-8 μm and pores such as to enable the passage of soil microorganisms and small particles of organic matter. To determine the net microbial P release from mineral phases (hydroxyapatite and P-loaded goethite) and weathered parent materials (silicates and carbonates) two different sets of incubation experiments were conducted, using soil extracts, either with or without addition of glucose to test for possible carbon (C) and energy limitations. More details about the handling of soil extracts, the setup of the experiments and the relative chemical analyses can be found in the "Methods" section of each study and, here, will be treated only briefly.

In the first study (hydroxyapatite and P-loaded goethite) the two sets of experiments were carried out in identical manner, except for the use of anion exchange membranes (AEMs) in the soil extracts incubated with P-loaded goethite in order to prevent re-adsorption of phosphate to the mineral. The AEMs were utilized following the protocol described by Saggar et al. (1990) for extracting phosphate. Membranes were withdrawn at defined time intervals and substituted with fresh ones.

The total P released from the mineral phases was determined by placing 99 ml of the soil extracts and 1 ml of glucose (3.33 mM) solution to either 100 mg of hydroxyapatite or 1000 mg of P-loaded goethite. The large amount of goethite was necessary to ensure detectable effects. Solutions were vacuum-filtered at defined time intervals through 0.45- μm cellulose acetate membrane filters (Sartorius Biotech, Germany) and analysed for pH and phosphate. Phosphate was determined according to the molybdenum-blue assay (Murphy and Riley, 1962).

Further, we quantified the mineralization of P from dissolved organic matter by performing two control experiments without addition of hydroxyapatite or P-loaded goethite. For this purpose, 99 ml of sterile water were added to 1 ml of glucose (3.33 mM) solution. In addition, sterile control experiments were conducted to determine the effect of the soil extracts and the AEMs on P release. For this purpose, 99 ml of sterile soil solutions and 1 ml of glucose (3.33 mM) solution were added to either 100 mg of hydroxyapatite or 1000 mg of P-loaded goethite.

In each of the experiments above, the P release rates were derived from the increase of P concentrations in soil extracts incubated with hydroxyapatite and P-loaded goethite over 14 days. Therefore, the net P release from hydroxyapatite and P-loaded goethite were determined as the difference between the respective total P release rates, the corresponding P mineralization rates and the total P release rates in sterile control (Eq.5):

$$\begin{aligned}
 & \text{Net P release rate } (\mu\text{mol d}^{-1}) \\
 & = \text{total P release rate } (\mu\text{mol d}^{-1}) - \text{total P release rate in sterile water } (\mu\text{mol d}^{-1}) \\
 & - \text{P mineralization rate } (\mu\text{mol d}^{-1}) \qquad \qquad \qquad \text{Eq. 5}
 \end{aligned}$$

Finally, the net P release rates were divided by the corresponding amount of hydroxyapatite and goethite utilized, as well as by their respective specific surface areas ($\text{m}^2 \text{g}^{-1}$), to give the rate in $\mu\text{mol m}^{-2} \text{d}^{-1}$.

In study II and III, to determine the net Si and P solubilization rates from silicate parent materials as well as the net Ca and P solubilization rates from calcareous parent materials, incubation experiments were conducted using soil extracts as described earlier. The total Si and P mobilization rates from siliceous parent material as well as the total Ca and P mobilization rates from calcareous parent material were determined by placing 1 g of each parent material with 99 ml of the respective soil extract and 1 ml of glucose (3.33 mM).

Dissolved Si and Ca were analysed at defined time intervals by ICP-OES (Vista-Pro radial, Varian, USA). Phosphate was determined according to the molybdenum-blue assay (Murphy and Riley, 1962). In addition, we performed control experiments without the addition of silicate and calcareous parent materials in order to quantify

the mineralization of P from dissolved organic matter. Further, sterile control incubations were conducted to determine the effect of the soil extracts on solubilization rates. For this purpose, 99 ml of each sterile soil solutions and 1 ml of glucose (3.33 mM) was added to 1 g of each parent material (siliceous or calcareous). In each of the experiments above, the Si release rates were derived from the increase of Si concentrations in soil extracts incubated with siliceous parent materials over 14 days. The net Si solubilization rate from each parent material was estimated as the difference between the total Si mobilization rate and the release rate determined in the sterile experiment (Eq. 6):

$$\begin{aligned}
 & \text{Net Si solubilization rate (nmol d}^{-1}\text{)} \\
 & = \text{total Si mobilization rate (nmol d}^{-1}\text{)} \\
 & - \text{Si release rate from sterile control (nmol d}^{-1}\text{)} \qquad \qquad \qquad \text{Eq. 6}
 \end{aligned}$$

We consider this a net rate because we did not correct for microbial Si uptake. Also, we estimated the solubilization of P from silicate parent materials based on the Si and P content of the parent materials and the Si solubilization rates using the equation below (Eq. 7):

$$\text{Gross P solubilization rate (nmol d}^{-1}\text{)} = \frac{\text{Net Si solubilization rate [nmol d}^{-1}\text{]} * \text{P content [g Kg}^{-1}\text{]}}{\text{Si content [g kg}^{-1}\text{]}} \quad \text{Eq. 7}$$

Similarly, the Ca release rates were derived from the increase of Ca concentrations in soil extracts incubated with calcareous parent materials over 14 days. The net Ca solubilization rate from each parent material was estimated as the difference between the total Ca mobilization rate and the release rate determined in the sterile experiment (Eq. 8):

$$\begin{aligned}
 & \text{Net Ca solubilization rate (nmol d}^{-1}\text{)} \\
 & = \text{total Ca mobilization rate (nmol d}^{-1}\text{)} \\
 & - \text{Ca release rate in sterile control (nmol d}^{-1}\text{)} \qquad \qquad \qquad \text{Eq. 8}
 \end{aligned}$$

We consider this a net rate because we did not correct for microbial Ca uptake. In addition, we determined the gross P solubilization rates from calcareous parent

materials based on the Ca and P content of the parent materials and the net Ca solubilization rates, as follows (Eq. 9):

$$\text{Gross P solubilization rate (nmol d}^{-1}\text{)} = \frac{\text{Net Ca solubilization rate [nmol d}^{-1}\text{]} * \text{P content [g Kg}^{-1}\text{]}}{\text{Ca content [g kg}^{-1}\text{]}} \quad \text{Eq. 9}$$

The net Si solubilization rates (Eq.6), the net Ca solubilization rates (Eq.8) and the gross P solubilization rates (Eq.7 and Eq.9) were divided by the corresponding amount of siliceous and calcareous parent material as well as by the respective surface area of the weathered parent material ($\text{m}^2 \text{g}^{-1}$) to result in a rate expressed as $\text{nmol m}^{-2} \text{d}^{-1}$.

2.7 Organic acids and siderophores

The amounts of four organic acids relevant in P solubilization mechanisms (citric, oxalic, 2-keto-D-gluconic, D-gluconic) were determined in each soil extract 7 and 14 days after the beginning of experiments (Study I, II and III). In the soil extracts from the calcareous sites, together with the four organic acids mentioned above, we also determined the amounts of lactic acid (Study III). Sub aliquots of 0.45 μm -filtered solutions were analysed by high-performance liquid chromatography (HPLC) coupled to a diode-array detector (DAD) and an electrospray ionization mass spectrometer (ESI-MS). Separation of organic acids was performed with a hydro-reversed-phase column in combination with a guard column. Quantification was carried out by calibration with external standards. The amounts of each organic acid were calculated by multiplying the respective concentration (mg l^{-1}) released into the soil extracts with the exact volume (l) present in the flask at day 7 and day 14, and subsequently expressed in μmol . Furthermore, we calculated the concentrations of the carboxyl groups ($-\text{COOH}$) based on the concentrations of organic acids and the number of carboxyl groups of each organic acid. Moreover, within the soil extracts incubated with P-loaded goethite (Study I), the concentrations of six siderophores (protochelin, enterobactin, desferrioxamine B, ferricrocin, aerobactin, rhizobactin) were investigated by means of a Q-Exactive hybrid quadrupole orbitrap (Dionex

Ultimate 3000, Thermo Fisher Scientific, Germany) coupled to a UHPLC-ESI-HRMS platform. Siderophores have a high affinity to form stable complexes with Fe and therefore could play a significant role in the weathering of iron oxides. Details about the composition of the mobile phase and the acquisition of mass spectra can be found in the “Materials and Methods” section of manuscript 1.

2.8 Abundance and sequencing of P-solubilizing bacteria

For Study II and III, the relative abundance of P-solubilizing bacteria (PSB) was assessed by suspending 0.5 g of fresh soil in 49.5 ml of sterile water and shaking it for 1 h. Serial dilutions from each soil suspension were tested to identify the appropriate cell density. Subsequently, from each suspension, an aliquot of 100 µl was aseptically spread on Pikovskaya’s agar medium (PVK) amended with hydroxyapatite as a sole P source. One-hundred colony-forming units (CFUs) from each soil sample were screened. If a bacterial colony dissolves hydroxyapatite, a halo (clear zone) becomes visible in the otherwise milky medium. Bacterial colonies identified as PSB were collected from the PVK agar plates using sterile toothpicks and aseptically transferred into buffer solutions for DNA extraction. Detailed procedure describing the amplification of 16S rRNA genes and processing of sequences data can be found in manuscripts II and III. Sequence similarity searches for high-quality regions larger than 514 bp were conducted against NCBI’s nucleotide database and against the 16S section of NCBI’s RefSeq Targeted Loci Project (max e-value 1e-10). Sequences with a 98% cut-off similarity were clustered into operational taxonomic units (OTUs). To this end, the name of the lowest common rank in the taxonomy was chosen. Only the non-redundant top hits were selected for taxonomic annotation. For this purpose, each 16S sequence was compared with all other sequences and sequences sharing identity above 98% identity were assigned to one taxon. The abundance matrix of the 16S sequence types was uploaded in PRIMER 7 (PRIMER-E Ltd., United Kingdom), standardized and cumulated at the genus level. A resemblance matrix was calculated from the abundance matrix of bacterial fragments before nonmetric multi-dimensional scaling (nMDS) was performed (using a stress test = 0.01) using Manhattan distance. Subsequently, analyses of similarities (ANOSIM) based on the

number of OTUs grouped by taxon were conducted using 999 permutations to determine whether the P-solubilizing bacterial communities were significantly different among the tested soils. All phylogenetic trees were reconstructed and edited in MEGAX (v. 10.1.5) based on the neighbor-joining method with 1000 bootstrap replicates. The maximum composite likelihood method was the chosen distance method.

2.9 Statistical analysis

All data sets were tested for normality (Shapiro-Wilk) as well as for equality of variance, using the Brown-Forsythe test. Not normally distributed data sets underwent the test for homoscedasticity. When variances were not significantly different between groups, analysis of variance (one-way ANOVA) was applied to test for differences between soil chemical properties, net Ca solubilization rates, net Si solubilization rates and P solubilization rates. For equal sample sizes and equal variance, the Tukey's honest significance test (Tukey's HDS) was performed as a post-hoc test following ANOVA. For unequal sample sizes but with equal variance, the parametric Holm-Sidak post hoc test was preferred. Differences in net solubilization rates and the relative abundance of PSB between the two soil depths of each forest site were analysed by t-test for related samples, followed by post-hoc Tukey HDS ($p < 0.05$). The non-parametric Kruskal-Wallis H test was used with a pairwise Wilcoxon test when assumptions were not met. Simple and multiple linear regressions for solubilization rates and soil chemical variables of soil extracts were also performed. All data analysis was carried out using SigmaPlot (version 13.0, Systat Software, San Jose, California, USA). For a more detailed description of the statistical analyses the reader can consult the "Statistics" section of each study.

3. Results and discussion of key findings

3.1 Microbial P solubilization from primary and secondary P-minerals and weathered parent materials

In absence of glucose, we did not observe any net P solubilization from hydroxyapatite as well as no net P desorption from P-loaded goethite during the incubations but rather microbial P immobilization (data not shown), as indicated by decreases in dissolved phosphate in the extracts. When glucose was added, net P solubilization rates from hydroxyapatite ranged between 0.001 and 0.54 $\mu\text{mol m}^{-2} \text{d}^{-1}$ (Figure 1). The net P solubilization rates from hydroxyapatite were significantly larger in the extracts of the upper soil (30–35 cm) than of the lower soil depth (65–70 cm) in three out of five cases, namely BBR (+55.1%), CON (+49.3%), and LUE (+96.1%).

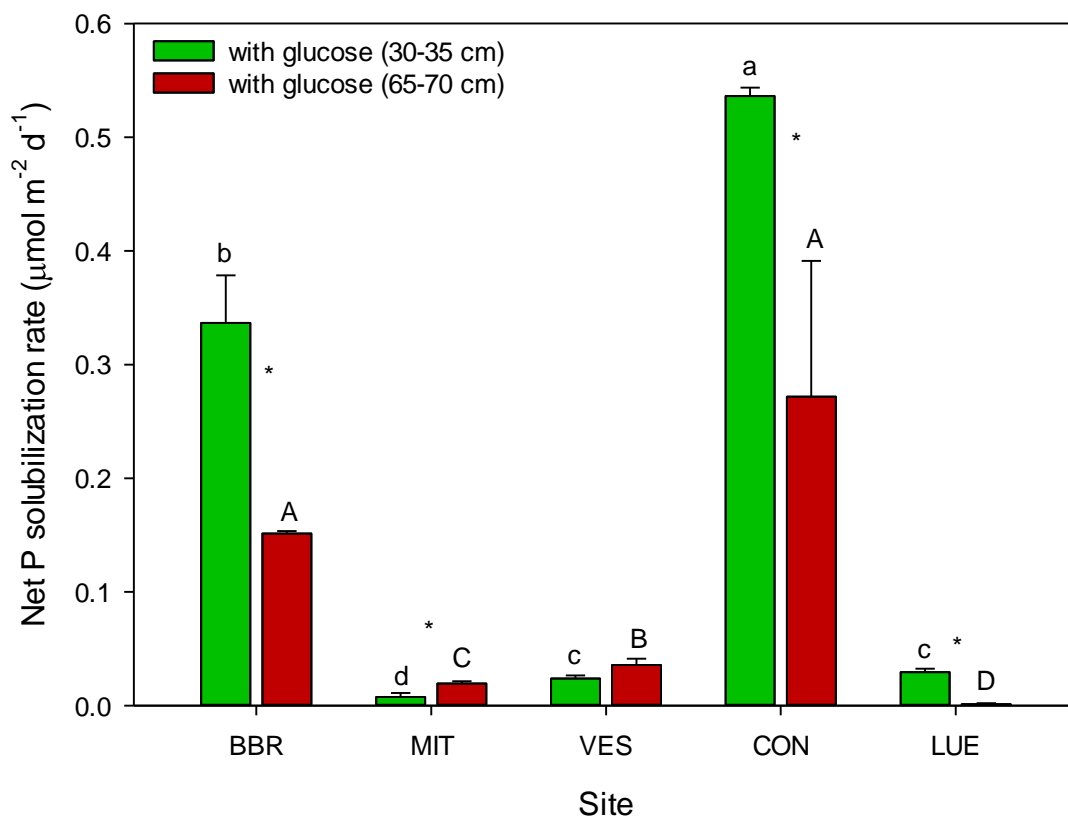


Figure 1 Net P solubilization rates for hydroxyapatite incubated with glucose in solutions extracted from different soils collected at two different depths at five forest sites. The bars show

means, and error bars indicate standard deviations ($n = 3$). Different letters indicate significant differences, tested separately for the two soil depths by one-way ANOVA, followed by post-hoc Tukey HDS ($p < 0.05$). Stars indicate significant differences between the two depths of each soil, tested by t-test followed by post-hoc Tukey HDS ($p < 0.05$).

The net P desorption from goethite was up to two orders of magnitude smaller than the net P solubilization from hydroxyapatite. The average net P desorption rates from P-loaded goethite ranged between 0.005 and 0.008 $\mu\text{mol m}^{-2} \text{d}^{-1}$ with little variability among the ten forest soil extracts (Figure 2). For the upper soil depth (30–35 cm), the only significant difference in net P desorption rates was found between the soil extracts from BBR and VES, while no significant difference was found in the other sites ($p < 0.05$).

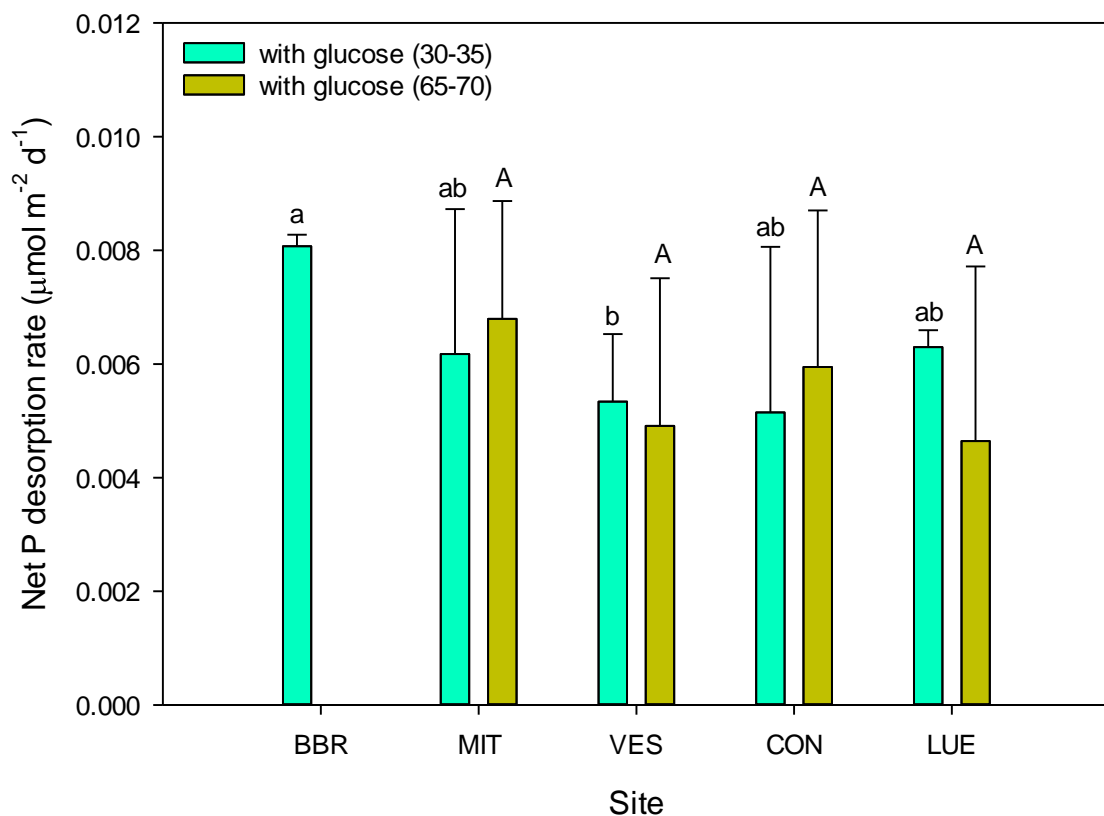


Figure 2 Net P desorption rates for P-loaded goethite incubated with glucose in solutions extracted from different soils collected at two different depths at five forest sites. Mean values and standard deviations from triplicate experiments are shown. Different letters indicate significant differences, tested separately for the two soil depths by one-way ANOVA followed by post-hoc Tukey HDS ($p < 0.05$). Note that the rates at site BBR site (65-70 cm depth) were not missing but equivalent to zero.

Comparing the P solubilization rates of this study with those obtained from soils of the Coastal Cordillera of Chile (Brucker et al., 2020) we found that the potential of microbial communities to solubilize P from apatite was slightly lower but within the same magnitude (Table 4). Also, microbial communities from acidic beech forest soils were more efficient in releasing orthophosphate from hydroxyapatite than from P-loaded goethite (Table 4). The high P solubilization rates from hydroxyapatite in comparison to P desorption rates from goethite indicate that dissolution of P is the main process contributing to P solubilization, while desorption of P plays a relatively minor role. Interestingly, the studied soils are characterized by the prevalence of P bound to Fe oxides (Prietz et al., 2016; Lang et al., 2017). Therefore, the use of goethite as a model compound that is closest to conditions found in these soils did not result in a higher ability of microbes to release P as might have been expected.

Table 4 Average net P solubilization rates from primary (hydroxyapatite) and secondary (P-loaded goethite) P-minerals. The net P solubilization rates from hydroxyapatite from five temperate forest soils (Pastore et al., 2020) were compared with those obtained from soils of the Coastal Cordillera of Chile (Brucker et al., 2020).

Incubation experiments	Rates (given values are averages across locations and considering the same specific surface area)
Net P solubilization from hydroxyapatite ($\mu\text{mol m}^{-2} \text{d}^{-1}$)*	0.14
Net P desorption from P-loaded goethite ($\mu\text{mol m}^{-2} \text{d}^{-1}$)*	0.006
Net P solubilization from hydroxyapatite ($\mu\text{mol m}^{-2} \text{d}^{-1}$)**	0.18

* Pastore et al. (2020); ** Brucker et al. (2020)

In the soil extracts incubated with P-loaded goethite we used AEMs to prevent re-adsorption of phosphate to the mineral. In addition, AEMs are often used in incubation experiments to mimic phosphate uptake by plants. To assess the total

phosphate desorption by AEMs we compared the phosphate desorption rates in the soil extracts (corrected for P mineralization) and the phosphate desorption rates in sterile water. The results showed that up to 65% of the total phosphate desorption from goethite was caused by AEMs. This implies that decreasing the phosphate concentration in solution by plant or microbial uptake enhances desorption of phosphate. Therefore, efficient depletion of the soil solution might be a key mechanism to maintain P supply under soil conditions where P becomes strongly bound to secondary minerals (see also Spohn et al., 2020).

When weathered siliceous parent materials were incubated with the respective soil extracts, we found that the net Si solubilization rate from the soil extracts incubated with the respective parent material and glucose ranged between 5.0 and 91.0 nmol m⁻² d⁻¹ (Figure 3). At 30–35 cm depth, BBR (basalt) had the highest net Si solubilization rate in comparison to the other three sites, while at 65–70 cm depth, the net Si solubilization rate in MIT (paragneiss) was significantly higher than in the other soils (+70%; P < 0.01).

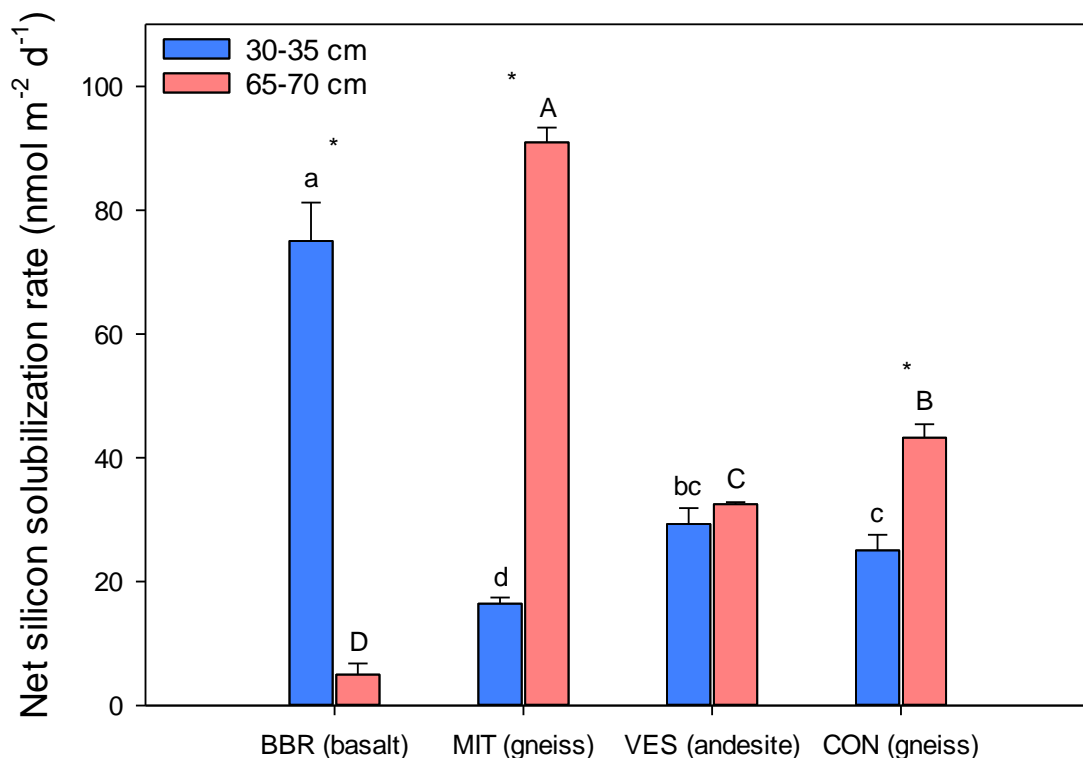


Figure 3 Net Si solubilization rates for silicate parent materials incubated with glucose in aqueous extracts obtained from the four forest soils. The rates were calculated per specific surface area and over 14 days of incubation. The samples were taken at two soil depths (30–35 and 65–70 cm). Bars show means, and error bars indicate standard deviations (n = 3). Different letters indicate significant differences tested separately for the two soil depths by one-way ANOVA followed by post-hoc Tukey HDS (P < 0.05). Stars indicate significant differences between the two depths of each soil, tested by t-test followed by post-hoc Tukey HDS (P < 0.05).

When weathered calcareous parent materials were incubated with the respective soil extracts, we found that the net Ca solubilization rate from the soil extracts incubated with the respective parent material and glucose ranged between 8.8 and 511.1 nmol m⁻² d⁻¹ (Figure 4). Dolomite showed much higher net Ca solubilization rates in comparison to limestone at both soil depths (P < 0.05).

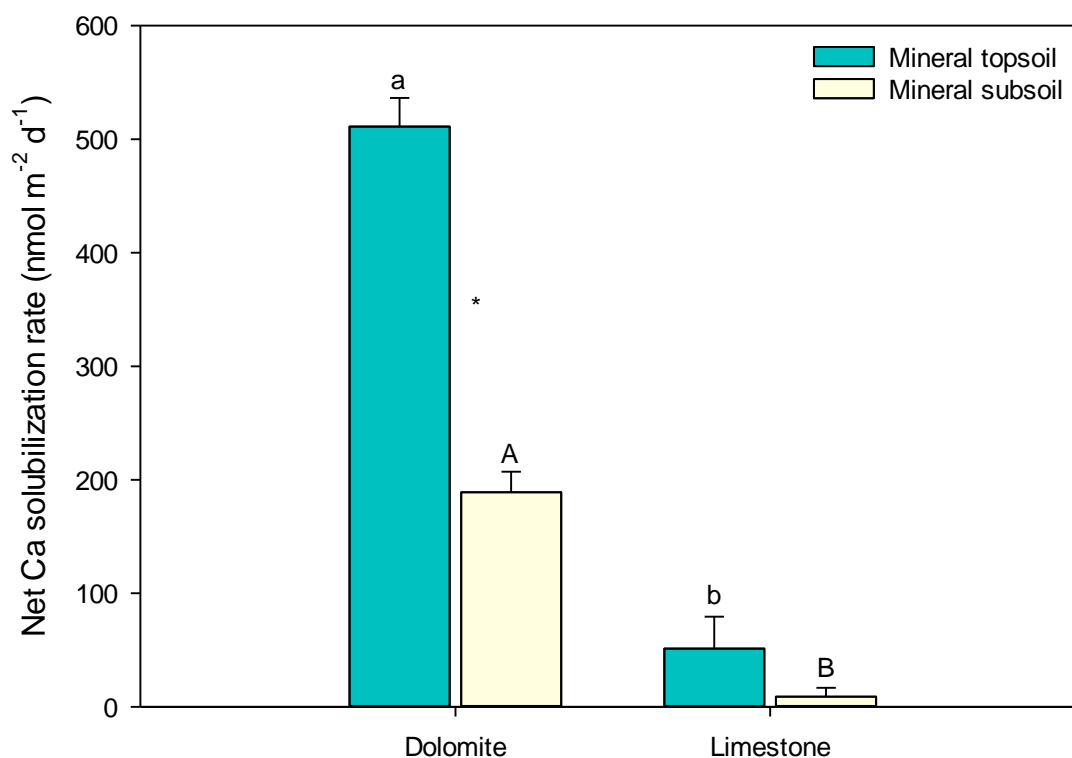


Figure 4 Net Ca solubilization rates from calcareous rocks incubated in soil extracts from two forest soils with glucose. The rates were normalized according to the specific surface area of the rocks and computed over 14 days of incubation. Soils and rocks were sampled at two different depths of two forest soils developed on dolomite (mineral topsoil: 4-9 cm and mineral subsoil: 22-37 cm) or on limestone (mineral topsoil: 11-18 cm and mineral subsoil: 42-60 cm). Bars show means and error bars indicate standard deviations (n=3). Different letters indicate significant

differences tested separately for the two soil depths by one-way ANOVA followed by post-hoc Tukey HDS ($P < 0.05$). Stars indicate significant differences between the two depths of each soil, tested by t-test followed by post-hoc Tukey HDS ($P < 0.05$).

While silicon and calcium are released for the most part from silicates and carbonates, P is mainly released from primary P-minerals (apatites) and, secondary, from P adsorbed to minerals. Our data indicate that when weathered siliceous and calcareous parent materials were incubated with the respective soil extracts no net P solubilization rates were measured. The likely reason for this is that microbes took up more phosphate than they released from the parent material or that phosphate anions quickly precipitated with metal cations. Despite this, we determined the gross P solubilization rates from (i) the P and Si content of siliceous parent materials and the Si solubilization rate but also from (ii) the P and Ca content of calcareous parent materials and the Ca solubilization rate based on stoichiometric considerations. This approach allowed us to estimate the gross release of P. When the data on gross P solubilization rates were compared between Study II and Study III, we found that significantly less P was released from carbonates than from silicates (Figure 5-a) despite the fact that the net Si solubilization rates from silicates were lower than the net Ca solubilization rates from carbonates. The likely reason for this is that while silicate minerals are affected only by hydrolysis, carbonates are affected by hydrolysis and hydration which, in turn, can have an impact on the rate at which apatite grains get exposed to the soil solution (see also Blume et al., 2016).

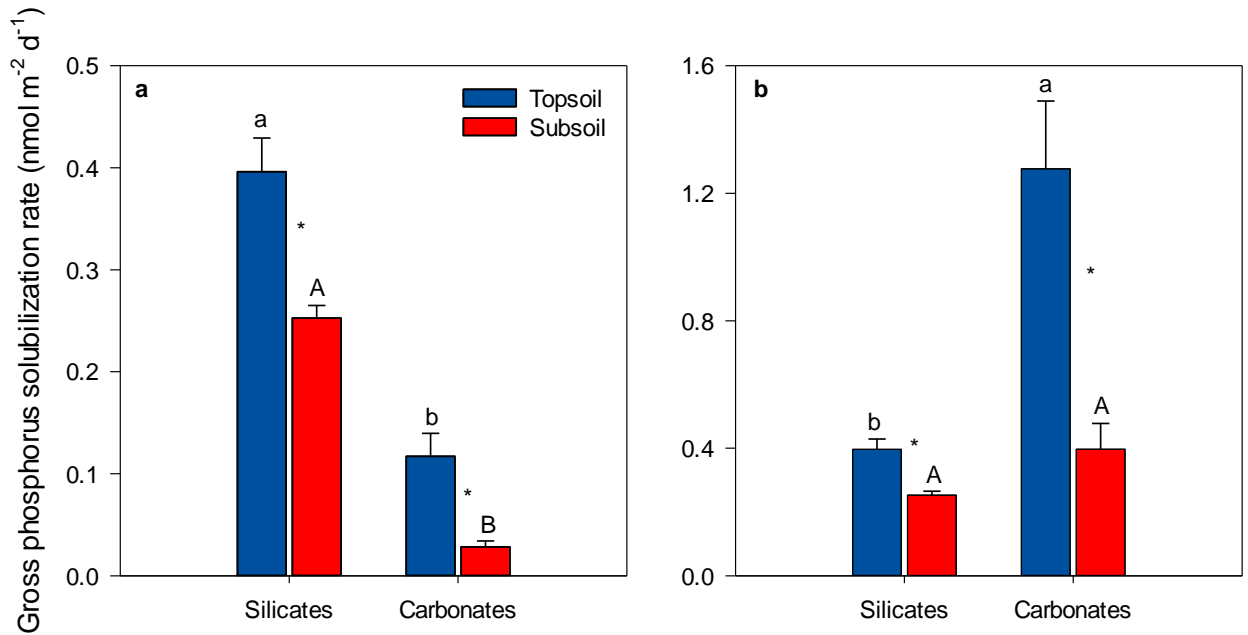


Figure 5 Stoichiometrically-derived gross P solubilization rates in two soil depth increments incubated with the respective bedrocks (silicates, n=5 and carbonates, n=2). Panel (a) shows the gross P solubilization rates based on the measured P content of the rocks, whereas panel (b) shows the weighted rates considering the same content of P. Mean values and standard deviations are shown (n=3). Uppercase and lowercase letters show significant differences tested separately for the two soil depths by one-way ANOVA. Because of the unequal sample sizes, the parametric Holm-Sidak post hoc test was chosen ($P < 0.05$). T-test was used to indicate significant differences between the two depths of each soil and represented with a star ($P < 0.05$).

However, it is important to mention that the silicates included in our study carried on average 12 times more P than carbonates (2.25 g P kg^{-1} for silicates and 0.19 g P kg^{-1} for carbonates). Therefore, to determine the effect of microbial communities on the solubilization of P under the same conditions, we considered also the case in which siliceous and calcareous rocks had the same content of P. The results reveal that the potential of microbes to solubilize P from calcareous rocks was 3.2 times higher than silicate rocks in the topsoil and 1.6 times higher in the subsoil (Figure 5-b). The reason for this lies in the different dissolution kinetics and solubility of rocks with carbonates dissolving faster than silicates (see also Gaillardet et al., 1999). Moreover, the higher gross P solubilization rates from carbonates in comparison to silicates (Figure 5-b) might be the results of a higher microbial activity, as suggested by the measured amounts of organic acids and microbial biomass (Figure 7; Table 3).

Altogether, we found that microbial P solubilization from secondary and, in particular, primary P-minerals is up to three orders of magnitude higher than microbial P solubilization from weathered parent materials. This is because silicates and carbonates undergo a stepwise weathering in the natural environment and that apatite minerals present in the crystal lattice are shielded by other minerals from biochemical weathering (White, 2003). Moreover, our results suggest that the gross P solubilization rates from siliceous parent materials, at least in the upper soil depth, were ~11 times higher at the P-rich site compared to the P-poor site. This finding supports the idea that the proportion of plant-available P derived from the bedrock decreases along the geosequence of the four soils. On the contrary, the biogeochemical dynamics of P from calcareous parent materials show that the gross P solubilization rates were on average 63.6% higher at the dolomite site (P-poor soil) compared to the limestone site (P-rich soil). Taken together, our results suggest that high rates of mineral dissolution under alkaline conditions can compensate for low mineral P content and the general assumption that “rocks having more P should also solubilize more P” might not be always true.

3.2 The role of pH on net P solubilization from primary and secondary P-minerals

The net P solubilization rates from hydroxyapatite were strongly negatively related to pH, and phosphate amounts in the incubated soil extracts gradually increased as the pH decreased over time. This suggests that acidification of the soil extracts was the main mechanism of P solubilization from hydroxyapatite. Increases of orthophosphate released from hydroxyapatite with decreasing pH, as shown here (Table 5) have been reported for other Ca orthophosphates (Illmer and Schinner, 1995; Miller et al., 2010) and in model studies (Dorozhkin, 2011). The fastest pH decrease occurred in the soil extracts from BBR and CON. After this time, the pH values continued to decrease but at a lower rate. The pH values explained 88% and 60% of the variation in net P solubilization rates from hydroxyapatite. In the soil extracts from the lower soil depth, pH explained only 55% and 72% of the variation in net P solubilization rates. On the contrary, we found a positive relationship between pH and the net P desorption rates from goethite (see Table 5) which suggests that

the release of orthophosphate from Fe oxyhydroxides did not result from acidification but is rather promoted by less acidic conditions. The reason for this is that goethite becomes increasingly positively charged due to protonation with decreasing pH (Beebout and Loeppert, 2006), which favors orthophosphate sorption, and thus, causes net removal of orthophosphate ions from the soil extracts.

Table 5 Results of simple and multiple regression analyses for the variables pH (at day 7 or day 14), low molecular weight organic acids (at day 7 and day 14), DOC (at the beginning of the incubations) and net P solubilization rates across all test sites, calculated separately for the two soil depths (30–35 and 65–70 cm). Given are the coefficients of regression (R^2 for simple regression or adjusted R^2 for multiple linear regression) as well as the p-values (highlighted in bold when statistically significant). For significant relationships, the negative (-) or positive (+) correlation was provided within parenthesis.

Incubation experiments	Depth [cm]	pH ₇	pH ₁₄	LMWOA ₇ [μmol]	LMWOA ₁₄ [μmol]	DOC (mmol l^{-1})	LMWOA ₇ [μmol] + pH ₇	LMWOA ₁₄ [μmol] + pH ₁₄
Net P solubilization rate from hydroxyapatite ($\mu\text{mol m}^{-2} \text{d}^{-1}$)	30-35	$R^2= (-)$ 0.88, p<0.001	$R^2= (-)$ 0.60, p<0.001	$R^2= (+)$ 0.88, p<0.001	$R^2= (+)$ 0.89, p<0.001	$R^2=0.11,$ $p>0.05$	adj. $R^2= (-)$ 0.87, p<0.001	adj. $R^2= (-)$ 0.76, p<0.001
	65-70	$R^2= (-)$ 0.55, p<0.01	$R^2= (-)$ 0.72, p<0.01	$R^2= (+)$ 0.78, p<0.05	$R^2= (+)$ 0.58, p<0.01	$R^2=0.05,$ $p>0.05$	adj. $R^2= (-)$ 0.55, p<0.05	adj. $R^2= (-)$ 0.55, p<0.05
Net P desorption rate from goethite ($\mu\text{mol m}^{-2} \text{d}^{-1}$)	30-35	$R^2=0.002,$ $p>0.05$	$R^2=0.18,$ $p>0.05$	$R^2=0.008,$ $p>0.05$	$R^2=0.06,$ $p>0.05$	$R^2= (+)$ 0.25, p<0.05	adj. $R^2=0.0001,$ $p>0.05$	adj. $R^2=0.14,$ $p>0.05$
	65-70	$R^2= (+)$ 0.34, p<0.05*	$R^2=0.02,$ $p>0.05$	$R^2=0.005,$ $p>0.05$	$R^2=0.01,$ $p>0.05$	$R^2=0.0001,$ $p>0.05$	adj. $R^2=0.24,$ $p>0.05$	adj. $R^2=0.0001,$ $p>0.05$

3.3 The role of organic acids on net P solubilization from primary and secondary P-minerals

The amounts of organic acids were significantly lower in the soil extracts incubated with P-loaded goethite than in the extracts incubated with hydroxyapatite, despite the fact that the soil extracts (i.e., microbial inoculum) used in both incubation experiments were from the same soils. Furthermore, whereas all four organic anions (citric, oxalic, D-gluconic and 2-keto-D-gluconic acid) were detected in the soil extracts incubated with hydroxyapatite, only two (citric and D-gluconic acid) were detected in the soil extracts incubated with P-loaded goethite. Organic acids can contribute to mineral solubilization in three ways: (i) by complexing metal cations, (ii) by ligand exchange reactions, where one molecule can “substitute” another of similar charge in the crystal lattice or (iii) by decreasing the pH of the soil extracts (Hinsinger et al., 2001; Oburger et al., 2009). Carboxyl groups of organic acids did not correlate with dissolved Fe in the incubation of P-loaded goethite. This finding suggests that the desorption of orthophosphate from goethite was partially due to direct competition between organic anions and orthophosphate for binding sites on mineral surfaces. The competitive displacement of phosphate by organic acids was stronger when soil extracts were amended with glucose. Further, the amounts of organic acids decreased over time in the incubation of P-loaded goethite. The decrease in organic acids hints at a possible downregulation by microbes to prevent acidification, and thus sorption of orthophosphate. Therefore, the lower amounts of organic acids in soil extracts with P-loaded goethite were likely the result of these two processes, i.e., competitive displacement and acid downregulation by microbes. These findings have often been disregarded in studies focusing on P desorption from Fe oxyhydroxides. We found a positive relationship between net P solubilization rates from hydroxyapatite and the amounts of organic acids. This finding suggests that dissociated organic acids formed complexes with calcium cations, and thus, promoted apatite dissolution (Smith et al., 1977). Among the tested organic anions, D-gluconic and 2-keto-D-gluconic acid were the most abundant and their production coincided significantly with high orthophosphate release from hydroxyapatite. Thus, monocarboxylic acids released by microbes may play a much larger role in P

mobilization in soil than previously thought. Also, organic acids did contribute to acidification of the solution in the incubation of hydroxyapatite. Our data show that up to 99% (on average: 71.2%) of the protons released during the incubations were derived from organic acids (Table 6). Thus, microbial production of organic acids was the likely cause of the acidification of the soil extracts during the incubation (Figure 6). On the contrary, organic acids did not contribute to acidification of the solution in the incubation of P-loaded goethite.

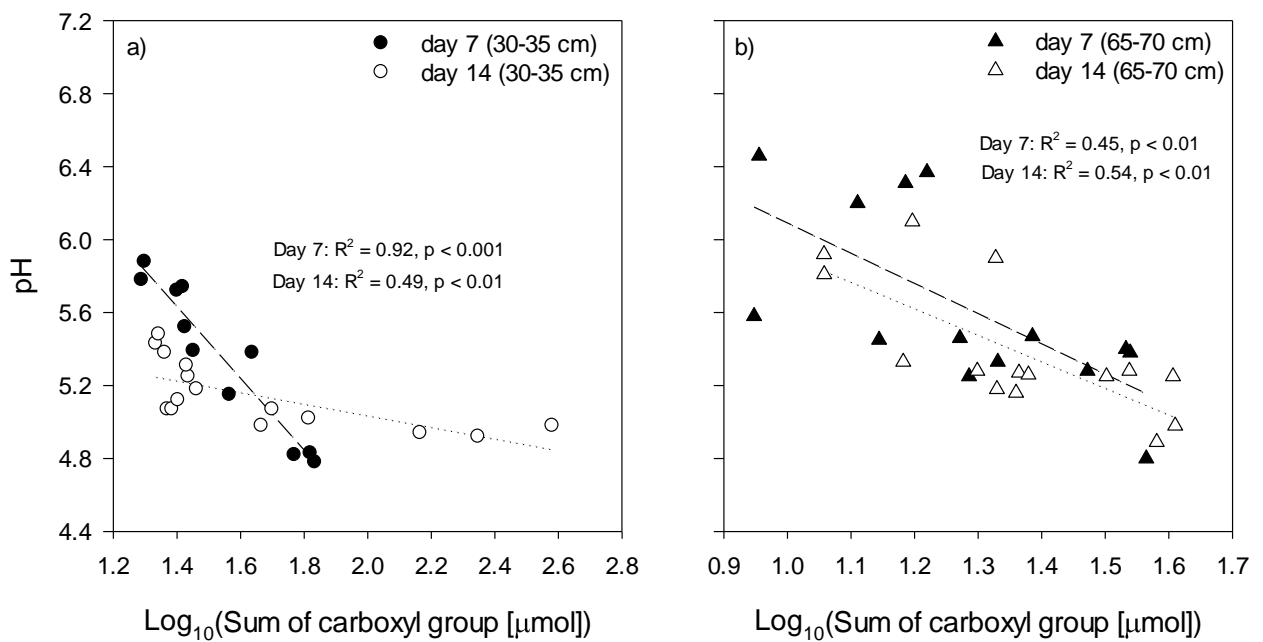


Figure 6 Relationship between the pH and the \log_{10} -transformed amounts of carboxyl groups released into solutions extracted from different soils incubated with hydroxyapatite and glucose. Two points in time are shown using respectively black and white dots (panel a) and black and white triangles (panel b). For all panels, the lines represent the best-fit regression line. Short-dashed and dotted lines depict associations after seven and fourteen days, tested separately for the two soil depths, respectively.

3.4 The influence of pH and organic acids on solubilization of weathered siliceous and calcareous parent materials

We found that the Si solubilization rates were up to 32 times higher in the biotic experiment compared to the abiotic experiment (sterile conditions) indicating that microbes exert a strong biological control over the solubilization of silicates, especially when provided with glucose. The net Si solubilization rates from siliceous

parent materials were positively related to the carboxyl groups of organic acids released by microbes. This finding suggests that organic acids effectively complexed metal cations present in the crystal lattice (i.e., Al, Fe, Ca, Mg), thereby promoting the solubilization reaction (Liu et al., 2006; Violante et al., 2010; Smits and Wallander, 2017; Lee et al., 2019). Monocarboxylic acids (D-gluconic and 2-keto-D-gluconic acid) represented up to 88% of all detected acids in soil extracts incubated with siliceous parent materials. Microbially-produced organic acids accounted for 51% of the total variability in the net Si solubilization rates in the extracts from the upper soil depth, but explained only 14% of the variation in soil extracts from the lower soil depth. Thus, at the lower soil depth, complexation by organic acids played a minor role in Si solubilization possibly as a result of a lower soil microbial activity (Vandevivere et al., 1994; Sverdrup, 2009).

High Si concentrations in the solution went along with high P concentrations. One of the reasons for this might be the competition for binding sites on mineral surfaces between Si and P. The positive relation between Si and P is in accordance with findings by other authors (Schaller et al., 2019; Homberg et al., 2020). Concentrations of Si increased steadily during the first week of incubation. During the same time interval, the pH, after an initial short increase, decreased in all soil extracts. The negative relationship between the Δ pH and the net Si solubilization rates suggests that the release of Si from silicates did result in part from acidification of the soil extract. Altogether, our results agree with Drever (1994) who found that the silicate dissolution rate depends on pH: below pH 5.0, the rate increases with decreasing pH, while at pH values above 8.0 the rate increases with increasing pH. With decreasing pH of the soil extract, there is an increase in the number of protons binding to oxygen atoms at the mineral surfaces. Protonation induced increase in reactivity of surface sites weakens the metal cations-oxygen bonds, thus promoting the dissolution of the mineral (Hinsinger, 2001; Brown et al., 2008). Considering the pK_a values of the tested organic acids, their total amounts as well as the pH values of the solutions, only 8.9% to 10.1% of protons released during the incubations were likely derived from organic acids after seven days of incubation, when the peak of solubilization occurred (Table 6). Also, no significant correlation was found between the amount of carboxyl groups of organic acids and pH. These findings suggest that

the acidification of soil extracts incubated with siliceous parent materials was promoted by the reaction that CO₂ respired by microorganisms undergoes in water to give carbonic acid (Cornelis and Delvaux, 2016; Kanakiya et al., 2017). Another complementary reason to the one above is that protons were strongly consumed by weathering of siliceous parent materials, while the release of organic acids by microbes one week after the start of the experiment was already in the waning phase, possibly due to C limitation.

Table 6 Relative contribution (%) of organic acids to the hydrogen ion concentration (H⁺) of soil extracts incubated with hydroxyapatite (Study I), siliceous parent materials (Study II) and calcareous parent materials (Study III) on the 7th day after the start of experiments.

Incubation experiments	pH (day 7)	H ⁺ concentration of soil extracts (day 7)		H ⁺ from carboxylic groups (day 7)	
Study I	5.45	3.6E-06	28.8%	5.0E-06	71.2%
Study II	4.6	2.8E-05	89.9%	2.8E-06	10.1%
Study III	8	1.0E-08	0.2%	5.3E-06	99.8%

Given values are averages across locations

Surprisingly, we found that the Ca and P solubilization rates from dolomite were significantly higher than those from limestone. This result fits well with the amounts of organic acids released by microbes in the soil extracts (dolomite > limestone). Our results agree with the findings of Pokrovsky and Schott (2001) who found that dissolution rates of dolomite are strongly promoted by the addition of organic acids. In the subsoil, the higher amounts of carboxyl groups can be related to the much higher microbial biomass C of the dolomitic soil in comparison to the limestone soil (Table 3). Citric and oxalic acid were not detected in incubations of soil extracts with

weathered calcareous parent materials, and therefore, monocarboxylic acids (D-gluconic, 2-keto-D-gluconic and lactic acid) represented 100% of the total tested acids. Gluconic acid was by far the most abundant organic acid among the ones who were tested, especially in soil extracts from the upper soil depth incubated with dolomite, and might relate to the occurrence of *Streptomyetales* which, in turn, were not found in the limestone soil (Figure 9). In this regard, Jog et al. (2014) reported that members of the genus *Streptomyces* are able to produce very high amounts of malic and gluconic acids. Due to the higher amounts of D-gluconic acid and the consequent increase of H⁺, dolomite solubilization was higher than limestone. By comparing the amounts of organic acids in the extracts incubated with calcareous soils to those found in siliceous soils we found they were significantly higher than those measured in incubations with silicates in the topsoil (+75.6%; P < 0.05), whereas no significant differences were observed in the extracts from the subsoil (Figure 7). In particular, we found that D-gluconic and 2-keto-D-gluconic acids released by microbial communities from calcareous soils were respectively 71% and 62% higher than those released from siliceous soils. One of the reasons for this may lie in the different pH of the soil extracts incubated with siliceous and calcareous parent materials which in turn can affect microbial growth and activity. Marra et al. (2015) showed that at circumneutral pH (~ pH 7.0), the production of organic acids was up to 25% greater than at pH 5.0, which was the mean pH measured in the incubation with siliceous parent materials. Our data on the activity of microbial communities in alkaline soils might closely associate with a previous finding by Tyler and Ström (1995) who found that calcicole plants, which mainly establish on calcareous soils, have also a greater capacity to release organic acids in comparison to calcifuge plants, which mainly establish on silicate soils.

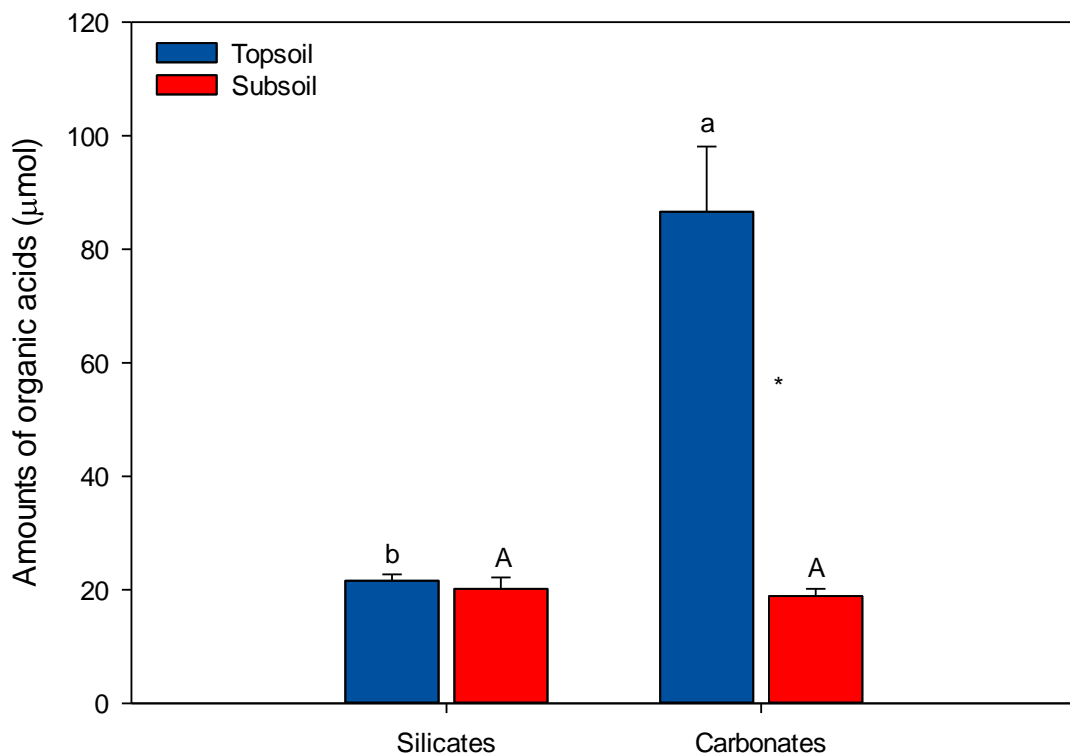


Figure 7 Total amounts of the organic acids in two soil depth increments incubated with contrasting bedrocks (silicates, n=5 and carbonates, n=2). Bars represent means, and error bars indicate standard deviations. Different uppercase and lowercase letters indicate significant differences between sites tested separately for each soil depth using one-way ANOVA. Because of the unequal sample sizes, the parametric Holm-Sidak post hoc test was chosen ($P < 0.05$). T-test was used to indicate significant differences between the two depths of each soil and represented with a star ($P < 0.05$).

3.5 Relative abundance and community composition of PSB from silicates and calcareous sites

The structure of PSB communities differed significantly between siliceous and calcareous soils (Figure 8 and Figure 9). This finding was further supported by nonmetric multi-dimensional scaling analyses (nMDS) which revealed that the PSB communities at the calcareous sites were significantly different from the PSB communities found at the silicate sites (Figure 11). Overall, PSB isolates from siliceous and calcareous soils belonged to six different phyla (Proteobacteria,

Cyanobacteria, Firmicutes, Actinobacteria, Deinococcus–Thermus and Bacteroidetes). In particular, we found that *Burkholderiales* and *Bacillales* together were by far the two most abundant bacterial orders in the siliceous soils object of this study (Figure 8). The distribution of *Burkholderiales* appeared to be strongly influenced by the mineral chemistry of the rocks, with some strains enriched in the presence of high-weatherable minerals and others enriched in the presence of less-weatherable minerals.

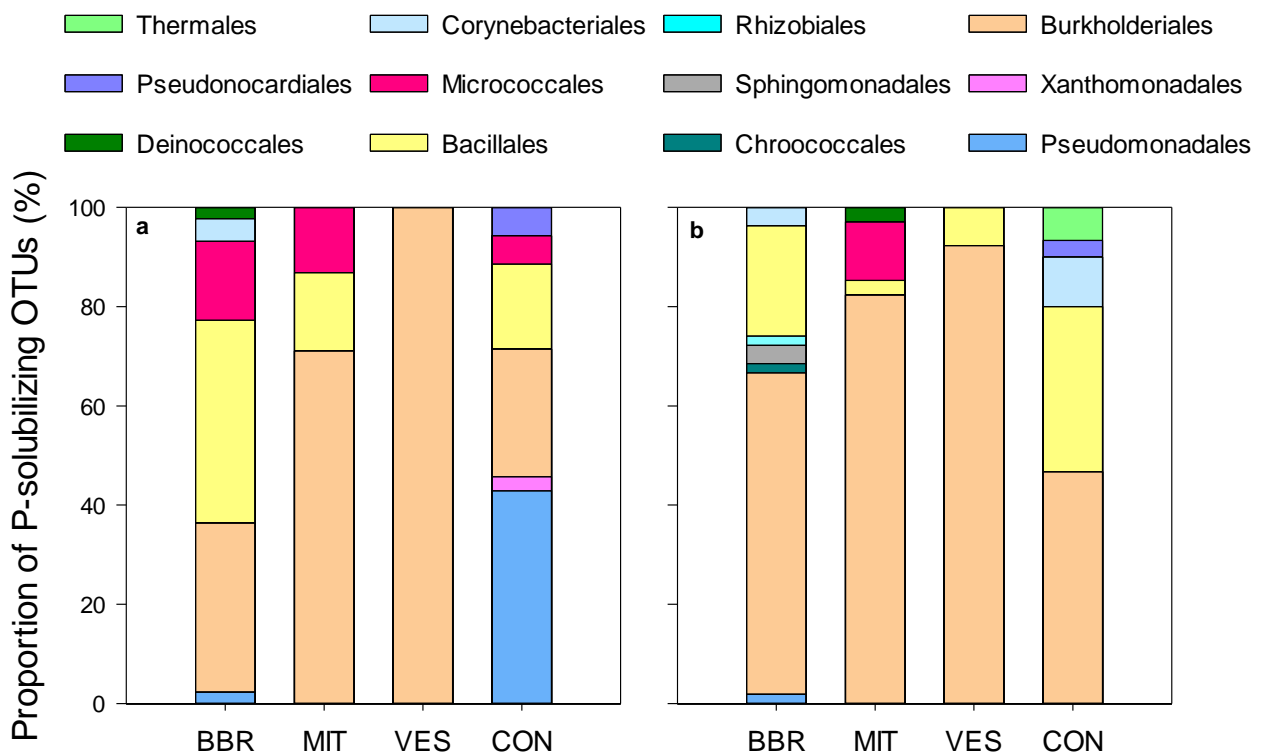


Figure 8 Relative abundance of different OTUs of P-solubilizing bacteria (PSB) from four forest soils developed on siliceous parent materials. Two panels are shown respectively for the two soil depths: (a) 30–35 cm and (b) 60–65 cm. Isolates identified as PSB were grouped into operational taxonomic units (OTU) at 98% cut-off similarity. Taxonomic classification of isolates is shown at the order level.

Bacillales appeared less affected by the mineral composition of the parent materials, and thus, showed no significant variations between sites. To this regard, several authors (Uroz et al., 2015; Nicolitch et al., 2016; Ho et al., 2017) suggested that bacterial strains, also within the same order, can have very different solubilization

strategies and the different mineral chemistry of the bedrocks might have influenced the occurrence, and likely the activity, of P-solubilizers. Notably, we found the genus *Arthrobacter* only at sites BBR and MIT. This finding is of particular interest since the studied soils are characterized by the prevalence of P bound to Fe oxyhydroxides (Prietz et al., 2016) and members of the genus *Arthrobacter* are relatively effective at mobilizing iron (Nicolitch et al., 2019).

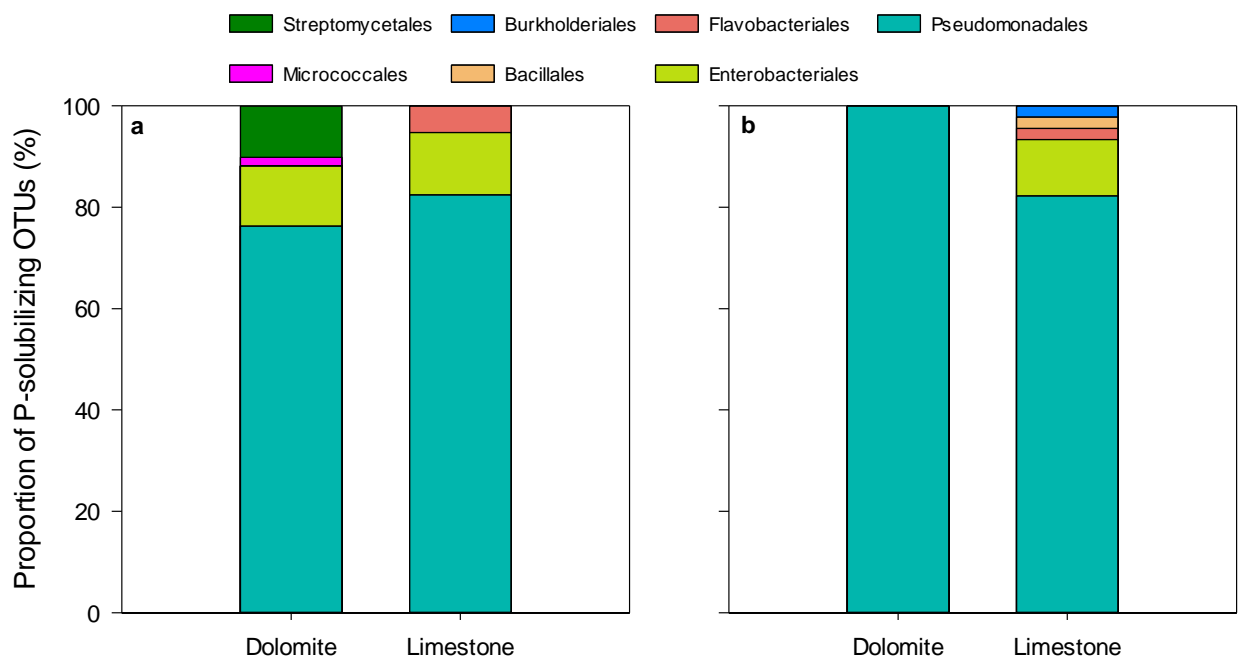


Figure 9 Relative abundance of different OTUs of P-solubilizing bacteria (PSB) from two forest soils developed on dolomite and limestone in the topsoil (a) and in the subsoil (b). Isolates identified as PSB were grouped into operational taxonomic units (OTU) at 98% cut-off similarity. Taxonomic classification of isolates is shown at the order level.

In contrast, we found that *Pseudomonadales* and *Enterobacteriales*, known to be strong P solubilizers (Rodríguez et al., 2006), dominated in calcareous soils (Figure 9). Our findings agree with Liu et al. (2015) who reported that *Pseudomonadales*, but also *Bacillales*, are the most abundant PSB strains in calcareous soils. The 16S rRNA gene sequencing revealed the presence of seven distinct isolates of *Pseudomonas* at the P-poor calcareous soil (dolomite) in comparison to the three isolates of

Pseudomonas found at the P-rich calcareous soil (limestone). Also, our data show that the genus *Pseudomonas*, which is reputed to have superior P solubilization ability among the PSB (Browne et al., 2009), was by far predominant in calcareous soils in comparison to siliceous soils, where occurred mainly at the P-poor site CON (Figure 8-a and Figure 9). Overall, this finding suggests that the higher occurrence of *Pseudomonadales* might be related to the low solubility of calcareous rocks in alkaline soils.

Interestingly, soil PSB were more abundant at P-poorest than P-richest environments, both in siliceous and calcareous soils. The reason for this might be due to a selective pressure which favors bacteria that actively mobilize inorganic P when P is scarce. On the contrary, the lower occurrence of PSB in P-rich soils might be due to a lower investment of resources by microbes into organic acids and enzymes production when nutrients are “easily” available. When the data on the relative abundance of PSB were compared between Study II and Study III, we found that they were significantly higher in calcareous than in siliceous soils ($p < 0.05$). Overall, the abundance of soil PSB at the siliceous sites ranged from 3.1% to 8.5%, whereas soil PSB ranged from 7.0% to 14.9% of all bacterial colonies at the calcareous sites (Figure 10). Previous studies pointed out that the relative abundance of PSB can constitute up to 53% of total bacterial numbers in soils (Browne et al. 2009; Zheng et al., 2019).

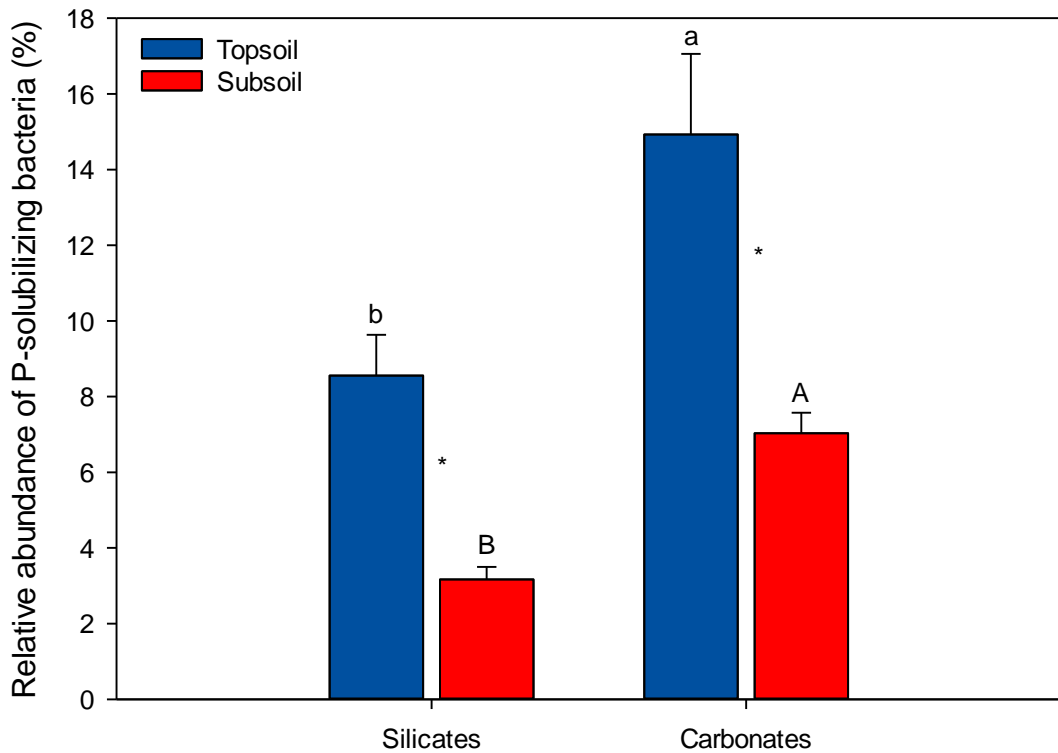


Figure 10 Relative abundance of P-solubilizing bacteria (PSB) in two soils and two soils depth increments incubated with contrasting bedrocks (silicates, n=5 and carbonates, n=2). Bars represent means, and error bars indicate standard deviations. Different uppercase and lowercase letters indicate significant differences between soils tested separately for each soil depth using one-way ANOVA. Because of the unequal sample sizes, the parametric Holm-Sidak post hoc test was chosen ($P < 0.05$). T-test was used to indicate significant differences between the two depths of each soil and represented with a star ($P < 0.05$).

Zheng et al. (2019) suggested that the abundance of PSB increases with soil pH. In addition, calcitic substrates can offer a higher affinity for bacterial attachment than silicate substrates, thereby fostering a higher bacterial growth and metabolic activity as suggested by Rodriguez-Navarro et al. (2012). Hence, calcareous soils might represent better conditions for the growth of P-solubilizers when compared to siliceous, acidic soils. The higher abundance of PSB in calcareous soils can also explain the higher gross P solubilization rates compared to siliceous soils (Figure 5-b).

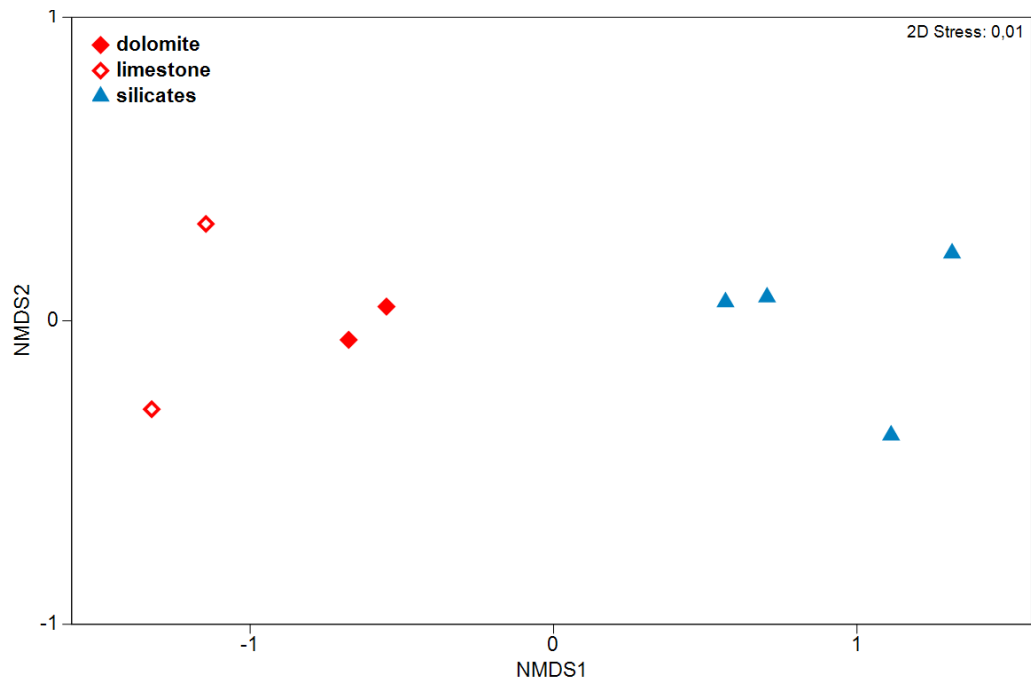


Figure 11 Nonmetric multi-dimensional scaling (nMDS) plot where each point represents the P-solubilizing bacteria (PSB) of a sample (stress = 0.01, non-metric $R^2 = 0.927$). Color and shape indicate different parent materials (blue siliceous rocks and red calcareous rocks). Manhattan distances were chosen for computing the dissimilarity between each pair of observations. Bacterial community structures differed significantly between carbonate and silicate sites ($P < 0.05$).

4. Conclusion and Outlook

This thesis evaluated the influence of microbial consortia on P, Si and Ca solubilization rates from primary and secondary P minerals and weathered parent materials in seven temperate deciduous forest soils. Most studies on P cycling have focused on processes relevant in the decomposition of P-rich organic sources in the forest floor and rhizosphere. This work studied in detail the biogeochemical processes relevant for solubilization of P in mineral soils from inorganic pools, i.e., the microbial production of metal-complexing compounds and the abundance and taxonomic diversity of P-solubilizing bacteria in relation to different soil depths and soil P stocks. The net P solubilization rates were higher from hydroxyapatite than from goethite suggesting that that dissolution of P-containing minerals is the main process contributing to P solubilization, while desorption of adsorbed P plays a relatively minor role. The microbial P solubilization from hydroxyapatite was mainly caused by acidification and the release of monocarboxylic organic acids (D-gluconic and 2-keto-D-gluconic), resulting in the dissolution of the mineral. The desorption of P from goethite was impacted negatively by acidification of soil extracts, which is why microbes possibly downregulated the production of organic acids to prevent phosphate sorption. This finding might be of critical importance for future studies focusing on P desorption from Fe oxyhydroxides. Taken together, P desorption from goethite was promoted in part by ligands competitive desorption and in part by less acidic conditions of soil extracts.

Microbes enhanced the dissolution of siliceous and calcareous parent materials by decreasing the pH of the respective soil extracts (i.e., by increasing the H⁺ concentrations of soil extracts). Acidification was caused by production of D-gluconic acid through periplasmic oxidation of glucose and likely by carbonic acid following CO₂ respired by microorganisms. Also, organic acids released by microbes promoted siliceous and calcareous solubilization rates by complexing the metal cations present in the crystal lattice of bedrocks (i.e., Al, Fe, Ca, Mg). Stoichiometrically-derived gross P solubilization rates revealed that the potential to release P from carbonates was higher than silicates when the same content of P was considered. The higher gross P solubilization rates from carbonates in comparison to silicates resulted from a higher

microbial activity, as suggested by the measured amounts of organic acids and microbial biomass. Further, our results suggest that the gross P solubilization rates from siliceous parent materials, at least in the upper soil depth, increased by a factor of ~11 from the P-poor site to the P-rich site. On the contrary, the gross P solubilization rates from calcareous parent materials increased on average by a factor of ~3 from the P-rich site to the P-poor site. Therefore, the general assumption that “rocks having more P should also solubilize more P” is not always true because high rates of mineral dissolution can compensate for low mineral P content.

The relative abundance of soil PSB was significantly higher in calcareous than siliceous soils which suggests a strong effect of soil pH on the occurrence of soil PSB. Overall, we found that the abundance of soil PSB was significantly higher from P-poor sites in comparison to P-rich sites, in both siliceous and calcareous soils. This finding is very interesting because it suggests that P availability can be a selective force driving the occurrence of bacteria with this functional trait. Among the soil PSB, *Burkholderiales* and *Bacillales* were the two most often occurring OTUs at the acidic soils, whereas *Pseudomonadales* and *Enterobacteriales* prevailed at the alkaline soils. Altogether, our results show that the activity and the taxonomic composition of PSB varied significantly across acidic and alkaline forest soils and underpinned the observed differences in silicate and carbonate solubilization rates. Moreover, we found that the abundance of soil PSB fits well with the solubilization rates of calcareous rocks but seems to have less of an effect on the solubilization rates of siliceous rocks.

In future studies, it would be interesting to investigate net P solubilization in coniferous forest stands and in a wider range of climatic zones. Also, it would be extremely interesting to evaluate to which extent bacterial and fungal communities contribute in proportion to each other to net P solubilization rates from a wider range of minerals and bedrocks. This could clarify the role they have in P solubilization and the contribution of one or the other in different ecosystems (i.e., deciduous vs. coniferous soils; acidic vs. alkaline soils).

Recent projections on climate changes suggest that temperatures might increase up to 1.5/2 °C over the next 50 years. Therefore, the idea to decrease the CO₂ concentration in the atmosphere by increasing (storing) large amounts of C in soils

received much interest. Forests represent the majority of the C that is stored in the soils of the world. However, many studies have shown that the storage of C in soils go along with a significant sequestration of large amounts of organic phosphorus. Since P is a crucial nutrient for primary producers, it is important to find alternatives that, on the one hand, help remove C from the atmosphere and, on the other, do not retain large amounts of P. One of the reasons to the enrichment of organic phosphorus with respect to C in soils is due to the sorption of organic phosphorus onto mineral surfaces which, in turn, limits P mineralization. Thus, the microbial solubilization of P from the inorganic pool, i.e., minerals and rocks, may be pivotal to support forest nutrition.

5. References

- Adeleke, R., Nwangburuka, C., Oboirien, B., 2017. Origins, roles and fate of organic acids in soils: A review. *South African Journal of Botany* 108, 393-406. <https://doi.org/10.1016/j.sajb.2016.09.002>
- Adnan, M., Shah, Z., Fahad, S., Arif, M., Alam, M., Ali Khan, I., Ahmad Mian, I., Basir, A., Ullah, H., Arshad, M., Rahman, I- U., Saud, S., Zahid Ihsan, M., Jamal, Y., Amanullah, Mohkum Hammad, H., Nasim, W., 2017. Orthophosphate-solubilizing bacteria nullify the antagonistic effect of soil calcification on bioavailability of phosphorus in alkaline soils. *Scientific Reports* 7, 16131. <https://doi.org/10.1038/s41598-017-16537-5>
- Alori, E.T., Glick, B.R., Babalola, O.O., 2017. Microbial Phosphorus Solubilization and its Potential for Use in Sustainable Agriculture. *Frontiers in Microbiology* 8, 971. <https://doi.org/10.3389/fmicb.2017.00971>
- Ahmed, A.A., Gypser, S., Freese, D., Leinweber, P., Kühn, O., 2020. Molecular level picture of the interplay between pH and phosphate binding at the goethite–water interface. *Physical Chemistry Chemical Physics*. <https://doi.org/10.1039/D0CP04698A>
- Asea, P. E. A., Kucey, R. M. N., Stewart, J. W. B., 1988. Inorganic orthophosphate solubilization by two *Penicillium* species in solution culture and soil. *Soil Biology and Biochemistry* 20(4), 459-464. [https://doi.org/10.1016/0038-0717\(88\)90058-2](https://doi.org/10.1016/0038-0717(88)90058-2)
- Atkinson, R.J., Posner, A.M., Quirk, J.P., 1967. Adsorption of potential determining ions at the ferric oxide-aqueous electrolyte interface. *J. Phys. Chem.* 71, 550–559. <https://doi.org/10.1021/j100862a014>
- Banfield, J.F., Barker, W.W., Welch, S.A., Taunton, A., 1999. Biological impact on mineral dissolution: application of the lichen model to understanding mineral weathering in the rhizosphere. *Proceedings of the National Academy of Sciences of the United States of America* 96(7), 3404-3411. <https://doi.org/10.1073/pnas.96.7.3404>
- Batterman, S., Hall, J. S., Turner, B., Hedin, L. O., Walter, J. K. L., Sheldon, P., van Breugel, M., 2018. Phosphatase activity and nitrogen fixation reflect species differences, not nutrient trading or nutrient balance, across tropical rainforest trees. *Ecology Letters* 21, 1486-1495. <https://doi.org/10.1111/ele.13129>
- Beebout, S.E.J., Loeppert, R.H., 2006. Role of organic acids in phosphate mobilization from iron oxide. *Soil Sci. Soc. Am. J.* 70 (1), 222–234. <https://doi.org/10.2136/sssaj2005.0012>
- Beneduzi, A., Moreira, F., Costa, P.B., Vargas, L.K., Lisboa, B.B., Favreto, R., Baldani, J.I., Passaglia, L.M.P., 2013. Diversity and plant growth promoting evaluation abilities of bacteria isolated from sugarcane cultivated in the south

of Brazil. *Appl. Soil Ecol.* 63, 94–104.
<https://doi.org/10.1016/j.apsoil.2012.08.010>

- Blume, H.P., Brümmer, G.W., Fleige, H., Horn, R., Kandeler, E., Kögel-Knabner, I., Kretzschmar, R., Stahr, K., Wilke, B.M., 2016. Inorganic soil components – minerals and rocks. In: Stahr, K., Springer-Verlag GmbH Berlin Heidelberg (Eds.), Scheffer/Schachtschabel Soil Science, 7-52. http://doi.org/10.1007/978-3-642-30942-7_2
- Bolan, N.S., Hedley, M.J. 1990. Dissolution of orthophosphate rocks in soils. 2. Effect of pH on the dissolution and plant availability of orthophosphate rock in soil with pH dependent charge. *Fertilizer Research* 24, 125–134. <https://doi.org/10.1007/BF01073580>
- Bononi, L., Chiramonte, J. B., Pansa, C. C., Alves Moitinho, M., Soares Melo, I., 2020. Phosphorus-solubilizing *Trichoderma* spp. from Amazon soils improve soybean plant growth. *Scientific Reports* 10, 2858. <https://doi.org/10.1038/s41598-020-59793-8>
- Brookes, P.C., Powlson, D.S., Jenkinson, D.S., 1982. Measurement of microbial biomass phosphorus in soil. *Soil Biology and Biochemistry*, 14, pp. 319-329.
- Brown, G.E., Trainor, T.P., Chaka, A.M., 2008. Geochemistry of mineral surfaces and factors affecting their chemical reactivity. In: Chemical bonding at surfaces and interfaces. Nilsson, A., Pettersson, L.G.M., Nørskov, J.K., Elsevier, 457-509. <https://doi.org/10.1016/B978-044452837-7.50008-3>
- Browne, P., Rice, O., Miller, S. H., Burke, J., Dowling, D. N., Morrissey, J. P., et al. (2009). Superior inorganic orthophosphate solubilization is linked to phylogeny within the *Pseudomonas fluorescens* complex. *Appl. Soil Ecol.* 43, 131–138. [doi: 10.1016/j.apsoil.2009.06.010](https://doi.org/10.1016/j.apsoil.2009.06.010)
- Brucker, E., Kernchen, S., Spohn, M., 2020. Release of phosphorus and silicon from minerals by soil microorganisms depends on the availability of organic carbon. *Soil Biology and Biochemistry* 143 (107737), 1–10. <https://doi.org/10.1016/j.soilbio.2020.107737>
- Chen, Y.P., Rekha, P.D., Arun, A.B., Shen, F.T., Lai, W.A., Young, C.C., 2006. Phosphate solubilizing bacteria from subtropical soil and their tricalcium phosphate solubilizing abilities. *Appl. Soil Ecol.* 34 (1), 33–41. <https://doi.org/10.1016/j.apsoil.2005.12.002>
- Chung, H., Park, M., Madhaiyan, M., Seshadri, S., Song, J., Cho, H., Sa, T., 2005. Isolation and characterization of phosphate solubilizing bacteria from the rhizosphere of crop plants of Korea. *Soil Biol. Biochem.* 37 (10), 1970–1974. <https://doi.org/10.1016/j.soilbio.2005.02.025>
- Condon, L.M., Turner, B.L., Cade-Menun, B.J., 2005. Chemistry and dynamics of soil organic phosphorus. In: Sims, J.T., Sharpley, A.N. (Eds.), *Phosphorus, Agriculture and Environment*. ASA, Madison, WI, 87–121.

- Cordell, D., Drangert, J.-O., White, S. B., 2009. The story of phosphorus: Global food security and food for thought. *Global Environmental Change* 19, 293–305. <https://doi.org/10.1016/j.gloenvcha.2008.10.009>
- Cornell, R.M., Schwertmann, U., 2003. The iron oxides: structure, properties, reactions, occurrences and uses. Wiley-VCH, 1-694. <https://doi.org/10.1002/3527602097>
- Cornelis, J. T., Delvaux, B., 2016. Soil processes drive the biological silicon feedback loop. *Functional Ecology* 30, 1298–1310. <https://doi.org/10.1111/1365-2435.12704>
- Curtin, D., Syers, J., 2001. Lime-Induced Changes in Indices of Soil Phosphate Availability. *Soil Science Society of America Journal* 65, 147-152. <https://doi.org/10.2136/sssaj2001.651147x>
- Darcy, J.L., Schmidt, S.K., Knelman, J.E., Cleveland, C.C., Castle, S.C., Nemergut, D.R., 2018. Phosphorus, not nitrogen, limits plants and microbial primary producers following glacial retreat. *Science Advances* 4, eaaq0942. <https://doi.org/10.1126/sciadv.aaq0942>
- Deelman, J. C., 2008. Low-temperature formation of dolomite and magnesite.
- Dessert, C., Dupré, B., Gaillardet, J., Francois, L.M., Allégre, C.J., 2003. Basalt weathering laws and the impact of basalt weathering on the global carbon cycle. *Chemical Geology* 202, 257–273. <https://doi.org/10.1016/j.chemgeo.2002.10.001>
- Dirnböck, T., Foldal, C., Djukic, I., Kobler, J., Haas, E., Kiese, R., Kitzler, B., 2017. Historic nitrogen deposition determines future climate change effects on nitrogen retention in temperate forests. *Climatic Change* 144 (2), 221–235. <https://doi.org/10.1007/s10584-017-2024-y>
- Dorozhkin, S.V., 2011. Calcium orthophosphates: occurrence, properties, biomineralization, pathological calcification and biomimetic applications. *Biomatter* 1:2, 121-164.
- Drever, J.I., 1994. The effect of land plants on weathering rates of silicate minerals. *Geochimica et Cosmochimica Acta* 58, 2325-2332. [https://doi.org/10.1016/0016-7037\(94\)90013-2](https://doi.org/10.1016/0016-7037(94)90013-2)
- Drever, J. I., Stillings, L.L., 1997. The role of organic acids in mineral weathering. *Colloids and Surfaces A: Physicochemical and Engineering Aspects* 120, 167-181. [https://doi.org/10.1016/S0927-7757\(96\)03720-X](https://doi.org/10.1016/S0927-7757(96)03720-X)
- Du, E., Terrer, C., Pellegrini, A., Ahlström, A., Van Lissa, C., Zhao, X., Nan, X., Wu, X., Jackson, R., 2020. Global patterns of terrestrial nitrogen and phosphorus limitation. *Nature Geoscience*. <https://doi.org/10.1038/s41561-019-0530-4>
- Egamberdieva, D., Wirth, S. J., Alqarawi, A. A., Abd_Allah, E. F., Hashem, A., 2017. Phytohormones and beneficial microbes: essential components for plants to

- balance stress and fitness. *Frontiers in Microbiology* 8, 2104. <https://doi.org/10.3389/fmicb.2017.02104>
- Elser, J. J., Bracken, M. E. S., Cleland, E. E., Gruner, D. S., Harpole, W. S., Hillebrand, H., Ngai, J. T., Seabloom, E. W., Shurin, J. B., Smith, J. E., 2007. Global analysis of nitrogen and phosphorus limitation of primary producers in freshwater, marine and terrestrial ecosystems. *Ecology Letters* 10, 1135–1142. <https://doi.org/10.1111/j.1461-0248.2007.01113.x>
- Fairbridge, R.W., Bissell, H.J., Chilingar, G.V., 1967. Developments in sedimentology. *Carbonate rocks* 9B, 1-21. [https://doi.org/10.1016/S0070-4571\(08\)71028-8](https://doi.org/10.1016/S0070-4571(08)71028-8)
- Fardeau, J. C., 1996. Dynamics of orthophosphate in soils. An isotopic outlook. *Fertilizer Research* 45, 91-100. <https://doi.org/10.1007/bf00790658>
- Filippelli, G. M., 2002. The Global Phosphorus Cycle. In: *Reviews in Mineralogy and Geochemistry* 48(1), 391-425. <https://doi.org/10.2138/rmg.2002.48.10>
- Fontaine, L., Thiffault, N., Paré, D., Fortin, J. A., Piché, Y., 2016. Phosphate-solubilizing bacteria isolated from ectomycorrhizal mycelium of *Picea glauca* are highly efficient at fluorapatite weathering. *Botany* 94, 1183-1193. <https://doi.org/10.1139/cjb-2016-0089>
- Frey, B., Rieder, S.R., Brunner, I., Plötze, M., Koetzsch, S., Lapanje, A., Brandl, H., Furrer, G., 2010. Weathering-associated bacteria from the Damma glacier forefield: physiological capabilities and impact on granite dissolution. *Appl. Environ. Microbiol.* 76(14), 4788–4796. <https://doi.org/10.1128/AEM.00657-10>
- Gaillardet, J., Dupre, B., Louvat, P., Allègre, C.J., 1999. Global silicate weathering and CO₂ consumption rates deduced from the chemistry of large rivers. *Chemical Geology* 159, 3–30. [https://doi.org/10.1016/S0009-2541\(99\)00031-5](https://doi.org/10.1016/S0009-2541(99)00031-5)
- Geelhoed, S.J., Tjisse, H., Van Riemsdijk, W.H., 1998. Competitive interaction between phosphate and citrate on goethite. *Environ. Sci. Technol.* 32, 2119–2123. <https://doi.org/10.1021/es970908y>
- Gleeson, B. D., Kennedy, N. M., Clipson, N., Melville, K., Gadd, G. M., McDermott, F. P., 2006. Characterization of bacterial community structure on a weathered pegmatitic granite. *Microbial Ecology* 51, 526-534. <http://doi.org/10.1007/s00248-006-9052-x>
- Goldstein, A.H., 1995. Recent progress in understanding the molecular genetics and biochemistry of calcium phosphate solubilization by gram negative bacteria. *Biol. Agric. Hortic.* 12, 185–193. <https://doi.org/10.1080/01448765.1995.9754736>
- Goldstein A.H., 2003. Future trends in research on microbial orthophosphate solubilization: one hundred years of insolubility. In: Velázquez E., Rodríguez-Barrueco C. (eds) *First International Meeting on Microbial Orthophosphate*

- Solubilization. *Developments in Plant and Soil Sciences*, vol 102. Springer, Dordrecht. https://doi.org/10.1007/978-1-4020-5765-6_11
- Guidry, M.W., Mackenzie, F.T., 2003. Experimental study of igneous and sedimentary apatite dissolution: control of pH, distance from equilibrium, and temperature on dissolution rates. *Geochimica et Cosmochimica Acta* 67 (16), 2949-2963. [https://doi.org/10.1016/S0016-7037\(03\)00265-5](https://doi.org/10.1016/S0016-7037(03)00265-5)
- Guntzer, F., Keller, C., Meunier, J.D., 2012. Benefits of plant silicon for crops: a review, 32. *Agronomy for Sustainable Development*, pp. 201–213. <https://doi.org/10.1007/s13593-011-0039-8>
- Haynes, R.J., Zhou, Y.-F., 2020. Silicate sorption and desorption by a Si-deficient soil – effects of pH and period of contact. *Geoderma* 365, 114204. <https://doi.org/10.1016/j.geoderma.2020.114204>
- Harley, A.D., Gilkes, R.J., 2000. Factors influencing the release of plant nutrient elements from silicate rock powders: a geochemical overview. *Nutrient Cycling in Agroecosystems* 56, 11–36. <https://doi.org/10.1023/A:1009859309453>
- He, Z., Yang, X., Yuan, K., Zhu, Z., 1994. Desorption and plant-availability of phosphate sorbed by some important minerals. *Plant and Soil* 162, 89-97. <https://doi.org/10.1007/BF01416093>
- Heuck, C., Spohn, M., 2016. Carbon, nitrogen and phosphorus net mineralization in organic horizons of temperate forest: Stoichiometry and relations to organic matter quality, *Biogeochemistry*, 131, 229-242. <https://doi.org/10.1007/s10533-016-0276-7>
- Heuck, C., Smolka, G., Whalen, E., Frey, S., Gundersen, P., Moldan, F., Fernandez, I.J., Spohn, M., 2018. Effects of long-term nitrogen addition on phosphorus cycling in organic soil horizons of temperate forests. *Biogeochemistry* 141 (2), 167–181. <https://doi.org/10.1007/s10533-018-0511-5>
- Hider, R.C., Kong, X., 2010. Chemistry and biology of siderophores. *Nat. Prod. Rep.* 27, 637-657. <https://doi.org/10.1039/B906679A>
- Hinsinger, P., 2001. Bioavailability of soil inorganic P in the rhizosphere as affected by root-induced chemical changes: a review. *Plant Soil* 237, 173–195. <https://doi.org/10.1023/A:1013351617532>
- Ho, A., Di Lonardo, D. P., Bodelier, P.L., 2017. Revisiting life strategy concepts in environmental microbial ecology. *FEMS Microbiology Ecology* 93, 1-14. <https://doi.org/10.1093/femsec/fix006>
- Hoberg, E., Marschner, P., Lieberei, R., 2005. Organic acid exudation and pH changes by *Gordonia* sp. and *Pseudomonas fluorescens* grown with P adsorbed to goethite. *Microbiol. Res.* 160 (2), 177–187. <https://doi.org/10.1016/j.micres.2005.01.003>

- Hömberg, A., Obst, M., Knorr, K.H., Kalbitz, K., Schaller, J., 2020. Increased silicon concentration in fen peat leads to a release of iron and phosphate and changes in the composition of dissolved organic matter. *Geoderma* 374, 114422. <https://doi.org/10.1016/j.geoderma.2020.114422>
- Illmer, P., Schinner, F., 1992. Solubilization of inorganic phosphates by microorganisms isolated from forest soils. *Soil Biol. Biochem.* 24 (4), 389–395. [https://doi.org/10.1016/0038-0717\(92\)90199-8](https://doi.org/10.1016/0038-0717(92)90199-8)
- Illmer, P., Schinner, F., 1995. Solubilization of inorganic calcium phosphates—Solubilization mechanisms. *Soil Biol. Biochem.* 27 (3), 257-263. [https://doi.org/10.1016/0038-0717\(94\)00190-C](https://doi.org/10.1016/0038-0717(94)00190-C)
- Jacoby, R., Peukert, M., Succurro, A., Koprivova, A., Kopriva, S., 2017. The role of soil microorganisms in plant mineral nutrition — current knowledge and future directions. *Front. Plant Sci.* 8, 1617. <https://doi.org/10.3389/fpls.2017.01617>
- Jenkinson, D. S., Brookes, P. C., Powlson, D. S., 2004. Measuring soil microbial biomass. *Soil Biology & Biochemistry* 36, 5–7. <https://doi.org/10.1016/j.soilbio.2003.10.002>
- Jog. R., Pandya M., Nareshkumar, G., Rajkumar, S., 2014. Mechanism of phosphate solubilization and antifungal activity of *Streptomyces* spp. isolated from wheat roots and rhizosphere and their application in improving plant growth. *Microbiology* 160, 778–788. <https://doi.org/10.1099/mic.0.074146-0>
- Jones, D., Smith, B. F. L., Wilson, M. J. & Goodman, B. A., 1991. Phosphate solubilizing fungi in a Scottish upland soil. *Mycological Research* 95,1090-1093. [https://doi.org/10.1016/S0953-7562\(09\)80553-4](https://doi.org/10.1016/S0953-7562(09)80553-4)
- Jones, D.L., 1998. Organic acids in the rhizosphere – a critical review. *Plant Soil* 205, 25–44. <https://doi.org/10.1023/A:1004356007312>
- Jones, D., Oburger, E., 2011. Solubilization of Phosphorus by Soil Microorganisms. From: Phosphorus in action – Biological processes in soil phosphorus cycling. *Soil Biology* 26, 169-198. https://doi.org/10.1007/978-3-642-15271-9_7
- Kanakiya, S., Adam, L., Esteban, L., Rowe, M.C., Shane, P., 2017. Dissolution and secondary mineral precipitation in basalts due to reactions with carbonic acid. *Journal of Geophysical Research: Solid Earth* 122, 4312-4327. <https://doi.org/10.1002/2017JB014019>
- Köhl, J., Kolnaar, R., Ravensberg, W. J., 2019. Mode of Action of Microbial Biological Control Agents Against Plant Diseases: Relevance Beyond Efficacy. *Frontiers in Plant Science* 10, 845. <https://doi.org/10.3389/fpls.2019.00845>
- Lang, F., Bauhus, J., Frossard, E., George, E., Kaiser, K., Kaupenjohann, M., Krüger, J., Matzner, E., Polle, A., Prietzel, J., Rennenberg, H., Wellbrock, N., 2016. Phosphorus in forest ecosystems: new insights from an ecosystem nutrition

- perspective. *J. Plant Nutr. Soil Sci.* 179 (2), 129–135. <https://doi.org/10.1002/jpln.201500541>
- Lang, F., Krüger, J., Amelung, W., Willbold, S., Frossard, E., Bünemann, E.K., Bauhus, J., Nitschke, N., Kandeler, E., Marhan, S., Schulz, S., Bergkemper, F., Schloter, M., Luster, J., Guggisberg, F., Kaiser, K., Mikutta, R., Guggenberger, G., Polle, A., Pena, R., Prietzel, J., Rodionov, A., Talkner, U., Meesenburg, H., von Wilpert, K., Hölscher, A., Dietrich, H.P., Chmara, I., 2017. Soil phosphorus supply controls P nutrition strategies of beech forest ecosystems in central Europe. *Biogeochemistry* 136 (1), 5–29. <https://doi.org/10.1007/s10533-017-0375-0>
- Leberecht, M., Tu, J., Polle, A., 2016. Acid and calcareous soils affect nitrogen nutrition and organic nitrogen uptake by beech seedlings (*Fagus sylvatica* L.) under drought, and their ectomycorrhizal community structure. *Plant and Soil* 409, 143–157. <https://doi.org/10.1007/s11104-016-2956-4>
- Lee, K.E., Adhikari, A., Kang, S.M., You, Y.H., Joo, G.J., Kim, J.O., Kim, S.J., Lee, I.-J., 2019. Isolation and characterization of the high silicate and phosphate solubilizing novel strain *Enterobacter ludwigii* GAK2 that promotes growth in rice plants. *Agronomy* 9, 144. <https://doi.org/10.3390/agronomy9030144>
- Li, L., Stanforth, R., 2000. Distinguishing Adsorption and Surface Precipitation of Phosphate on Goethite (-FeOOH). *Journal of colloid and interface science* 230, 12-21. <https://doi.org/10.1006/jcis.2000.7072>
- Liermann, L., Kalinowski, B., Brantley, S.L., Ferry, J., 2000. Role of bacterial siderophores in dissolution of hornblende. *Geochimica et Cosmochimica Acta* 64, 587-602. [https://doi.org/10.1016/S0016-7037\(99\)00288-4](https://doi.org/10.1016/S0016-7037(99)00288-4)
- Lima-Rivera, D. L., Lopez-Lima, D., Desgarennes, D., Velázquez-Rodríguez, A. S., Carrion, G., 2016. Orthophosphate solubilization by fungi with nematicidal potential. *Journal of Soil Science and Plant Nutrition* 16(2), 507-524. <https://doi.org/10.4067/S0718-95162016005000042>
- Lindsay, W.L., 1979. *Chemical Equilibria in Soils*. John Wiley and Sons, New York, pp. 1–449.
- Liu, Z., Yuan, D., Dreybrodt, W., 2005. Comparative study of dissolution rate-determining mechanisms of limestone and dolomite. *Environmental Geology* 49(2), 274–279. <https://doi.org/10.1007/s00254-005-0086-z>
- Liu, W., Xu, X., Wu, X., Yang, Q., Luo, Y., Christie, P., 2006. Decomposition of silicate minerals by *Bacillus mucilaginosus* in liquid culture. *Environmental Geochemistry and Health* 28, 133–140. <https://doi.org/10.1007/s10653-005-9022-0>
- Mair, P., Tropper, P., Harlov, D.E., Manning, C.E., 2017. The solubility of apatite in H₂O, KCl-H₂O, NaCl-H₂O at 800 °C and 1.0 GPa: implications for REE mobility in high-grade saline brines. *Chemical Geology* 470, 180-192. <https://doi.org/10.1016/j.chemgeo.2017.09.015>

- Marra, L. M., de Oliveira-Longatti, S. M., Soares, C. R., de Lima, J. M., Olivares, F. L., Moreira, F. M., 2015. Initial pH of medium affects organic acids production but do not affect phosphate solubilization. *Brazilian journal of microbiology* 46, 367–375. <https://doi.org/10.1590/S1517-838246246220131102>
- Marschner, P., Crowley, D., Rengel, Z., 2011. Rhizosphere interactions between microorganisms and plants govern iron and phosphorus acquisition along the root axis—Model and research methods. *Soil Biology and Biochemistry - Soil Biology and Biochemistry* 43, 883-894. <https://doi.org/10.1016/j.soilbio.2011.01.005>
- Masalha, J., Kosegarten, H., Elmaci, Ö., Mengel, K., 2000. The central role of microbial activity for iron acquisition in maize and sunflower. *Biol. Fertil. Soils* 30 (5–6), 433–439. <https://doi.org/10.1007/s003740050021>
- Matzanke, B. F., 2011. Iron Transport: Siderophores. In *Encyclopedia of Inorganic and Bioinorganic Chemistry*, R.A. Scott (Ed.), 1-28. <https://doi.org/10.1002/9781119951438.eibc0110>
- Margalef, O., Sardans, J., Fernández-Martínez, M., Molowny-Horas, R., Janssens, I. A., Ciais, P., Goll, D., Richter, A., Obersteiner, M., Asensio, D., Peñuelas, J., 2017. Global patterns of phosphatase activity in natural soils. *Scientific Reports* 7, 1337. <https://doi.org/10.1038/s41598-017-01418-8>
- Menge, D.N.L., Hedin, L.O., Pacala, S.W., 2012. Nitrogen and phosphorus limitation over long-term ecosystem development in terrestrial ecosystems. *PLoS ONE* 7 (8), e42045. <https://doi.org/10.1371/journal.pone.0042045>
- Miller, S.H., Browne, P., Prigent-Combaret, C., Combes-Meynet, E., Morrissey, J.P., O’Gara, F., 2010. Biochemical and genomic comparison of inorganic phosphate solubilization in *Pseudomonas* species: inorganic P-solubilization in *Pseudomonas*. *Environ. Microbiol. Rep.* 2 (3), 403–411. <https://doi.org/10.1111/j.1758-2229.2009.00105.x>
- Murphy, J., Riley, J.P., 1962. A modified single solution method for the determination of phosphate in natural waters. *Analytica Chimica Acta* 26, 678-681. [https://doi.org/10.1016/S0003-2670\(00\)88444-5](https://doi.org/10.1016/S0003-2670(00)88444-5)
- Nezat, C.A., Blum, J.D., Yanai, R.D., Park, B.B., 2008. Mineral sources of calcium and phosphorus in soils of the northeastern United States. *Soil Sci. Soc. Am. J.* 72, 1786–1794. <https://doi.org/10.2136/sssaj2007.0344>
- Newman, E.I., 1995. Phosphorus inputs to terrestrial ecosystems. *Journal of Ecology* 83, 713-726. <https://doi.org/10.2307/2261638>
- Nicolitch, O., Colin, Y. M., Turpault, P., and Uroz, S., 2016. Soil type determines the distribution of nutrient mobilizing bacterial communities in the rhizosphere of beech trees. *Soil Biology and Biochemistry* 103, 429–445. <http://doi.org/10.1016/j.soilbio.2016.09.018>

- Nicolitch, O., Feucherolles, M., Churin, J., Fauchery, L., Turpault, M.P., Uroz, S., 2019. A microcosm approach highlights the response of soil mineral weathering bacterial communities to an increase of K and Mg availability. *Scientific Reports* 9, 14403. <https://doi.org/10.1038/s41598-019-50730-y>
- Numan, M., Bashir, S., Khan, Y., Mumtaz, R., Shinwari, Z., Khan, A., Khan, A., Al-Harrasi, A., 2018. Plant growth promoting bacteria as an alternative strategy for salt tolerance in plants: a review. *Microbiological Research* 209, 21-32. <https://doi.org/10.1016/j.micres.2018.02.003>
- Oburger, E., Kirk, G., Wenzel, W., Puschenreiter, M., Jones, D., 2009. Interactive effects of organic acids in the rhizosphere. *Soil Biology and Biochemistry* 41, 449-457. <https://doi.org/10.1016/j.soilbio.2008.10.034>
- Oburger, E., Jones, D.L. Wenzel, W.W. 2011. Phosphorus saturation and pH differentially regulate the efficiency of organic acid anion-mediated P solubilization mechanisms in soil. *Plant Soil* 341, 363–382. <https://doi.org/10.1007/s11104-010-0650-5>
- Ordoñez, Y.M., Fernandez, B.R., Lara, L.S., Rodriguez, A., Uribe-Vélez, D., Sanders, I.R., 2016. Bacteria with phosphate solubilizing capacity alter mycorrhizal fungal growth both inside and outside the root and in the presence of native microbial communities. *PLoS ONE* 11 (6), 1–18. <https://doi.org/10.1371/journal.pone.0154438>
- Pavinato, P. S., Merlin, A., Rosolem, C. A., 2008. Organic compounds from plant extracts and their effect on soil phosphorus availability. *Pesquisa Agropecuária Brasileira* 43(10), 1379-1388. <https://doi.org/10.1590/S0100-204X2008001000017>
- Peñuelas, J., Poulter, B., Sardans, J., Ciais, P., Velde, M., Bopp, L., Boucher, O., Godderis, Y., Hinsinger, P., Llusia, J., Nardin, E., Vicca, S., Obersteiner, M., Janssens, I., 2013. Human-induced nitrogen–phosphorus imbalances alter ecosystems across the globe. *Nature Communications* 4, 2934. <https://doi.org/10.1038/ncomms3934>
- Penn, C., Camberato, J., 2019. A Critical Review on Soil Chemical Processes that Control How Soil pH Affects Phosphorus Availability to Plants. *Agriculture* 9, 120. <https://doi.org/10.3390/agriculture9060120>
- Pikovskaya, R. I., 1948. Mobilization of phosphorus in soil in connection with the vital activity of some microbial species. *Microbiologia* 17, 362–370.
- Pokrovsky, O.S., Schott, J., 2001. Kinetics and mechanism of dolomite dissolution in neutral to alkaline solutions revisited. *American Journal of Science* 301, 597–626. <https://doi.org/10.2475/ajs.301.7.597>
- Porder, S., Ramachandran, S., 2012. The phosphorus concentration of common rocks—a potential driver of ecosystem P status. *Plant Soil* 367, 41-55. <https://doi.org/10.1007/s11104-012-1490-2>

- Prietzl, J., Ammer, C., 2008. Montane Bergmischwälder der Bayerischen Kalkalpen: Reduktion der Schalenwildsdichte steigert nicht nur den Verjüngungserfolg, sondern auch die Bodenfruchtbarkeit. *Allgemeine Forst und Jagdzeitung* 179, 105-113.
- Prietzl, J., Klysubun, W., Werner, F., 2016. Speciation of phosphorus in temperate zone forest soils as assessed by combined wet-chemical fractionation and XANES spectroscopy. *J. Plant Nutr. Soil Sci.* 179 (2), 168–185. <https://doi.org/10.1002/jpln.201500472>
- Remy, E., Wuyts, K., Boeckx, P., Gundersen, P., Verheyen, K., 2017. Edge effects in temperate forests subjected to high nitrogen deposition. *Proceedings of the National Academy of Sciences of the United States of America* 114 (34), E7032. <https://doi.org/10.1073/pnas.1709099114>
- Rodríguez-Navarro, C., Jroundi, F., Schiro, M., Ruiz-Agudo, E., González-Muñoz, M., 2012. Influence of Substrate Mineralogy on Bacterial Mineralization of Calcium Carbonate: Implications for Stone Conservation. *Applied and environmental microbiology* 78, 4017-4029. <https://doi.org/10.1128/AEM.07044-11>
- Rodríguez, H., Fraga, R., 1999. Orthophosphate Solubilizing Bacteria and Their Role in Plant Growth Promotion. *Journal of Biotechnology Advances*, 17, 319-339. [http://dx.doi.org/10.1016/S0734-9750\(99\)00014-2](http://dx.doi.org/10.1016/S0734-9750(99)00014-2)
- Rosling, A., Midgley, M. G., Cheeke, T., Urbina, H., Fransson, P., Phillips, R. P., 2016. Phosphorus cycling in deciduous forest soil differs between stands dominated by ecto- and arbuscular mycorrhizal trees. *New Phytologist* 209, 1184–1195. <https://doi.org/10.1111/nph.13720>
- Rousk, J., Brookes, P. C., Bååth, E., 2009. Contrasting soil pH effects on fungal and bacterial growth suggest functional redundancy in carbon mineralization. *Applied and Environmental microbiology* 75, 1589–1596. <https://doi.org/10.1128/AEM.02775-08>
- Saggar, S., Hedley, J.M., White, R.E., 1990. A simplified resin membrane technique for extracting phosphorus from soil. *Fertilizer Res.* 24, 173–180. <https://doi.org/10.1007/BF01073586>
- Sandroni, V., Smith, C., 2002. Microwave digestion of sludge, soil and sediment samples for metal analysis by inductively coupled plasma–atomic emission spectrometry. *Analytica Chimica Acta* 468, 335-344. [https://doi.org/10.1016/S0003-2670\(02\)00655-4](https://doi.org/10.1016/S0003-2670(02)00655-4)
- Schaller, J., Faucherre, S., Joss, H., Obst, M., Goeckede, M., Planer-Friedrich, B., Peiffer, S., Gilfedder, B., Elberling, B., 2019. Silicon increases the phosphorus availability of arctic soils. *Scientific Reports* 9, 449. <https://doi.org/10.1038/s41598-018-37104-6>
- Sharma, S. B., Sayyed, R. Z., Trivedi, M. H., Gobi, T. A., 2013. Orthophosphate solubilizing microbes: sustainable approach for managing phosphorus

- deficiency in agricultural soils. *SpringerPlus* 2, 587, 2013. <https://doi.org/10.1186/2193-1801-2-587>
- Sinsabaugh, R. L., Lauber, C. L., Weintraub, M. N., Ahmed, B., Allison, S. D., Crenshaw, C., Contosta, A. R., Cusack, D., Frey, S., Gallo, M. E., Gartner, T. B., Hobbie, S. E., Holland, K., Keeler, B. L., Powers, J. S., Stursova, M., Takacs-Vesbach, C., Waldrop, M. P., Wallenstein, M. D., Zak, D. R., Zeglin, L. H., 2008. Stoichiometry of soil enzyme activity at global scale. *Ecology Letters* 11, 1252–1264. <https://doi.org/10.1111/j.1461-0248.2008.01245.x>
- Smith, A.N., Posner, A.M., Quirk, J.P., 1977. A model describing the kinetics of dissolution of hydroxyapatite. *J. Colloid Interface Sci.* 62, 475–494. [https://doi.org/10.1016/0021-9797\(77\)90099-6](https://doi.org/10.1016/0021-9797(77)90099-6)
- Smits, M.M., Wallander, H., 2017. Role of mycorrhizal symbiosis in mineral weathering and nutrient mining from soil parent material. *Mycorrhizal Mediation of Soil* 3, 35-46. <https://doi.org/10.1016/B978-0-12-804312-7.00003-6>
- Spohn, M., Kuzyakov, Y., 2013. Phosphorus mineralization can be driven by microbial need for carbon. *Soil Biology and Biochemistry* 61, 69-75. <https://doi.org/10.1016/j.soilbio.2013.02.013>
- Spohn, M., ZeiBig, I., Brucker, E., Widdig, M., Lacher, U., Aburto, F., 2020. Phosphorus solubilization in the rhizosphere in two saprolites with contrasting phosphorus fractions. *Geoderma* 366, 114245. <https://doi.org/10.1016/j.geoderma.2020.114245>
- Sposito, G., 1986. Distinguishing adsorption from surface precipitation; in Davis, J.A., and Hayes, K.F. (eds.), *Geochemical Processes at Mineral Surfaces*, ACS Symposium Series 323: American Chemical Society, Washington, D.C., 217–228. <https://doi.org/10.1021/bk-1987-0323.ch011>
- Sverdrup, H., Oelkers, E., Lampa, M., Belyazid, S., Kurz, D., Akselsson, C., 2019. Reviews and syntheses: Weathering of silicate minerals in soils and watersheds: Parameterization of the weathering kinetics module in the PROFILE and ForSAFE models. *Biogeosciences Discussions*, 1-58. <http://doi.org/10.5194/bg-2019-38>
- Schwertmann, U., 1991. Solubility and dissolution of iron oxides. *Plant and Soil* 130, 1–25. <https://doi.org/10.1007/BF00011851>
- Uroz, S., Kelly, L. C., Turpault, M. P., Lepleux, C., Frey-Klett, P., 2015. The mineralosphere concept: mineralogical control of the distribution and function of mineral-associated bacterial communities. *Trends in Microbiology* 23, 751–762. <http://doi.org/10.1016/j.tim.2015.10.004>
- Taylor, H. L., Kell Duivesteyn, I J., Farkas, J., Dietzel, M., Dosseto, A., 2019. Technical note: Lithium isotopes in dolostone as a palaeo-environmental proxy – an experimental approach. *Climate of the Past* 15, 635–646. <https://doi.org/10.5194/cp-15-635-2019>

- Thakur, D., Kaushal, R., Shyam, V., 2014. Orthophosphate solubilising microorganisms: role in phosphorus nutrition of crop plants-a review. *Agricultural Reviews* 35(3), 159–171, 2014. <https://doi.org/10.5958/0976-0741.2014.00903.9>
- Torrent, J., 1997. Interactions between phosphate and iron oxide. *Adv. Geocol.* 30, 321–344.
- Tunesi, S., Poggi, V., Gessa, C., 1999. Phosphate adsorption and precipitation in calcareous soils: the role of calcium ions in solution and carbonate minerals. *Nutrient Cycling in Agroecosystems* 53, 219–227. <https://doi.org/10.1023/A:1009709005147>
- Turner, B.L., Condron, L.M., Richardson, S.J., Peltzer, D.A., Allison, V.J., 2007. Soil organic phosphorus transformations during pedogenesis. *Ecosystems* 10, 1166–1181. <https://doi.org/10.1007/s10021-007-9086-z>
- Turner, B.L., Brenes-Arguedas, T., Condit, R., 2018. Pervasive phosphorus limitation of tree species but not communities in tropical forests. *Nature* 555, 367–370. <https://doi.org/10.1038/nature25789>
- Vance, E. D., Brookes, P. C., Jenkinson, D. S., 1987. An extraction method for measuring soil microbial biomass C. *Soil Biology and Biochemistry* 19, 703–707. [https://doi.org/10.1016/0038-0717\(87\)90052-6](https://doi.org/10.1016/0038-0717(87)90052-6)
- Vandevivere, P., Welch, S.A., Ullman, W.J., Kirchman, D., 1994. Enhanced dissolution of silicate minerals by bacteria at near-neutral pH. *Microbial Ecology* 27, 241-51. <http://doi.org/10.1007/BF00182408>
- Violante, A., Cozzolino, V., Perelomov, L., Caporale, A. G., Pigna, M., 2010. Mobility and bioavailability of heavy metals and metalloids in soil environments. *Journal of Soil Science and Plant Nutrition* 10, 268–292. <http://dx.doi.org/10.4067/S0718-95162010000100005>
- Wakelin, S., Warren, R.A., Harvey, P., Ryder, M., 2004. Phosphate solubilization by *Penicillium* spp. closely associated with wheat roots. *Biology and Fertility of Soils*. 40. 36-43. <https://doi.org/10.1007/s00374-004-0750-6>
- Walker, T.W., Syers, J.K., 1976. The fate of phosphorus during pedogenesis. *Geoderma* 15, 1–19. [https://doi.org/10.1016/0016-7061\(76\)90066-5](https://doi.org/10.1016/0016-7061(76)90066-5)
- Wahid, O. A. A., Mehana, T. A., 2000. Impact of orthophosphate-solubilizing fungi on the yield and phosphorus-uptake by wheat and faba bean plants. *Microbiological Research* 155(3), 221-227. [https://doi.org/10.1016/S0944-5013\(00\)80036-1](https://doi.org/10.1016/S0944-5013(00)80036-1)
- White, A. F., Brantley, S.L., 1995. Chemical weathering rates of silicate minerals. In: *Reviews in Mineralogy and Geochemistry* 31, 1-583. <https://doi.org/10.1515/9781501509650>
- White, A.F., 2003. Natural weathering rates of silicate minerals. *Treatise on Geochemistry* 5, 133-168. <https://doi.org/10.1016/B0-08-043751-6/05076-3>

- Williams, E.L., Walter, L.M., Ku, T.C.W., Baptist, K.K., Budai, J.M., Kling, G.W., 2007. Silicate weathering in temperate forest soils: insights from a field experiment. *Biogeochemistry* 82, 111–126. <https://doi.org/10.1007/s10533-006-9057-z>
- Winkelman, G. 2007. Ecology of siderophores with special reference to the fungi. *Biometals* 20, 379–392. <https://doi.org/10.1007/s10534-006-9076-1>
- Wolff-Boenisch, D., Gislason, S.R., Oelkers, E.H., 2006. The effect of crystallinity on dissolution rates and CO₂ consumption capacity of silicates. *Geochimica and Cosmochimica Acta* 70, 858–870. <https://doi.org/10.1016/j.gca.2005.10.016>
- Yang, X., Post, W.M., 2011. Phosphorus transformations as a function of pedogenesis: a synthesis of soil phosphorus data using Hedley fractionation method. *Biogeosciences* 8, 2907–2916. <https://doi.org/10.5194/bg-8-2907-2011>
- Yi, Y., Huang, W., Ge, Y., 2008. Exopolysaccharide: a novel important factor in the microbial dissolution of tricalcium phosphate. *World J. Microbiol. Biotechnol.* 24 (7), 1059–1065. <https://doi.org/10.1007/s11274-007-9575-4>
- Zhang, Y., Chen, F. S., Wu, X. Q., Luan, F. G., Zhang, L. P., Fang, X. M., Wan, S. Z., Hu, X. F., Ye, J. R., 2018. Isolation and characterization of two orthophosphate-solubilizing fungi from rhizosphere soil of moso bamboo and their functional capacities when exposed to different phosphorus sources and pH environments. *Plos One* 13(7), e0199625. <https://doi.org/10.1371/journal.pone.0199625>
- Zheng, B., Zhang, D., Wang, Y., Hao, X.J., Wadaan, M.A.M., Hozzein, W.N., Peñuelas, J., Zhu, Y.G., Yang, X.R., 2019. Responses to soil pH gradients of inorganic phosphate solubilizing bacteria community. *Scientific Reports* 9, 25. <https://doi.org/10.1038/s41598-018-37003-w>
- Zhu, F., Qu, L., Hong, X., Sun, X., 2011. Isolation and characterization of a orthophosphate solubilizing halophilic bacterium *Kushneria* sp. YCWA18 from Daqiao saltern on the coast of yellow sea of China. *Evidence-Based Complementary Alternative Medicine* 615032, 1–6. <https://doi.org/10.1155/2011/615032>

6. Manuscripts



Microbial release of apatite- and goethite-bound phosphate in acidic forest soils



Giovanni Pastore^a, Klaus Kaiser^b, Sarmite Kernchen^c, Marie Spohn^{a,*}

^a Department of Soil Biogeochemistry, Bayreuth Center of Ecology and Environmental Research (BayCEER), University of Bayreuth, Germany

^b Soil Science and Soil Protection, Martin Luther University Halle-Wittenberg, Halle (Saale), Germany

^c Atmospheric Chemistry, University of Bayreuth, Germany

ARTICLE INFO

Handling Editor: Jan Willem Van Groenigen

Keywords:

Hydroxyapatite
Phosphorus-loaded goethite
Microbial acidification
Net P solubilization
LMWOAs
Siderophores

ABSTRACT

Phosphorus (P) is an element crucial for plant nutrition. P can be bound in primary minerals such as apatites or to secondary minerals, such as metal(hydr)-oxides. Microorganisms are capable of releasing mineral-bound P, and thus, transforming it into plant-available forms. This study examined the potential of native microbial communities of five beech forest soils to release P either from hydroxyapatite or P-loaded goethite. Incubation experiments with soil extracts, either with or without glucose, were conducted. Desorption of phosphate from goethite was less effective than the solubilization of phosphate from hydroxyapatite. We found that the net P solubilization from hydroxyapatite was driven by the microbial production of low molecular weight organic acids (LMWOAs), such as D-gluconic and 2-keto-D-gluconic acids, and differed among the microbial communities extracted from the five forest soils. In contrast, the net P desorption rates from goethite did not vary significantly among the microbial communities extracted from the different soils. Microbial acidification of the solution increased the adsorption of phosphate to goethite, whereas less acidic conditions promoted progressive desorption of phosphate. Microbial communities in soil extracts incubated with P-loaded goethite down-regulated the release of organic acids, which reduced acidification. The net P solubilization rates from hydroxyapatite and the net P desorption rates from goethite were strongly increased by the addition of glucose, suggesting that microbial P mobilization from minerals is strongly carbon limited. In conclusion, the study shows that microbial communities from acidic beech forest soils are much more efficient at releasing phosphate from hydroxyapatite than from goethite.

1. Introduction

Phosphorus (P) is an essential and non-substitutable component for all living organisms (Filippelli, 2002; Ruttenberg, 2003). Soil bacteria and mycorrhizal fungi can increase availability of P by mobilizing it from organic and inorganic sources (Jacoby et al., 2017; Hallama et al., 2019). However, the specific processes underlying the release of P from mineral sources, and their contribution to forest P nutrition, are far from being well understood. Traditionally, in temperate and boreal regions, forest productivity is considered to be mostly limited by nitrogen (N), whereas tropical forests are primarily limited by P (Turner et al., 2007; Menge et al., 2012; Darcy et al., 2018). Yet, a growing number of studies have recognized that increases in atmospheric N deposition impact the biogeochemical cycle of P (Hedwall et al., 2017; Dirnböck et al., 2017; Remy et al., 2017; Heuck et al., 2018). Therefore, it is expected that temperate forests may shift from N to NP co-

limitation or even P limitation (Peñuelas et al., 2013; Jonard et al., 2014; Heuck et al., 2018).

Although total soil P concentrations can be high (~400–1200 g kg⁻¹; Rodriguez and Fraga, 1999; Borggaard et al., 2005; Rouached et al., 2010), the portion of dissolved P readily available to plants and microorganisms is often less than 0.1% of total P (Zhou et al., 1992; Zhu et al., 2011). The reason for the low availability is that phosphate either exists within poorly soluble primary minerals or becomes increasingly bound to reactive secondary phases, such as aluminium (Al) and iron (Fe) hydrous oxides, with progressing soil development (Walker and Syers, 1976). In alkaline soils, phosphate ions tend to precipitate mainly with calcium (Ca) cations (Hinsinger, 2001). Apatites, including hydroxyapatite (HAP; Ca₅(PO₄)₃OH), are the dominant P-containing primary minerals in most rocks (Nezat et al., 2008). In acidic soils, phosphate ions tend to adsorb strongly to Al and especially Fe hydroxides (Hoberg et al., 2005; Osorio and Habte, 2013).

* Corresponding author.

E-mail address: marie.spohn@uni-bayreuth.de (M. Spohn).

<https://doi.org/10.1016/j.geoderma.2020.114360>

Received 12 November 2019; Received in revised form 27 March 2020; Accepted 30 March 2020
0016-7061/ © 2020 Elsevier B.V. All rights reserved.

Goethite (α -FeO(OH)) is overall the most common secondary Fe oxyhydroxide in natural environments and is effective in forming strong monodentate- or bidentate-complexes with phosphate ions (Geelhoed et al., 1998; Cornell and Schwertmann, 2003; Antelo et al., 2005). In addition, due to its prevalence in the soil environment, goethite is commonly used in model experiments addressing basic mechanistic features of hydrous Fe oxides.

Precipitation-dissolution equilibria and adsorption-desorption onto variably charged compounds determine to which extent phosphate exists dissolved in solution (Lindsay, 1979; Pierzynski et al., 2005). Soil microorganisms can solubilize mineral-bound P by either dissolving the mineral phases or desorbing sorbed P species. The dissolution of P-bearing minerals and desorption of phosphate from minerals is driven by the release of (i) low-molecular-weight organic acids (LMWOAs), (ii) protons (H^+), (iii) siderophores and exopolysaccharides (Yi et al., 2008; Frey et al., 2010; Ordoñez et al., 2016). These substances cause release of phosphate either via complexation of metal cations (i, iii) or by acidifying the soil solution (i, ii). The effect of LMWOAs released by roots and microorganisms is partly due to the number of carboxylic groups they bear, which determines their capability to desorb phosphate from metal(hydr-)oxides (Beebout and Loeppert, 2006). Depending on their acidity and the pH of the soil solution, carboxylic groups can dissociate, thus affecting the release of phosphate by the amount of protons released into the solution (Fox and Comerford, 1990; Richardson and Simpson, 2011). Similarly, siderophores have strong affinities for divalent and trivalent metals, especially Fe. Their exudation by plant roots and microbes can cause increased solubilization of Fe oxyhydroxides and subsequently release of sorbed phosphate (Marschner et al., 2011).

Despite the increasing awareness of the role of microorganisms in plant nutrition (Chung et al., 2005; Jones and Oburger, 2011; Beneduzi et al., 2013; Sharma et al., 2013; Panhwar et al., 2014), the potential of microbial communities to release phosphate from mineral phases has not been explored with detail, so far. Laboratory incubation experiments addressing potential effects of microorganisms have mainly been performed with (a) cultured microorganisms (Hoberg et al., 2005; Schneider et al., 2010), (b) high doses of LMWOAs addition (Welch et al., 2002), and (c) initial solutions with adjusted and buffered pH values (Raulund-Rasmussen et al., 1998; He and Zhu, 1998; Welch et al., 2002). Solubilization experiments have demonstrated that microbial communities are effective in releasing phosphate from Ca-P minerals (Hinsinger, 2001). Other authors showed that fungi and bacteria have only a limited capacity to desorb sorbed phosphate from goethite (Hoberg et al., 2005) and, therefore, microbial-mediated desorption of phosphate from Fe hydrous oxides is likely less effective than the solubilization of phosphate from Ca-P minerals.

The objective of this study was to determine the potential of microbial communities in soil extracts from five temperate forest soils along a gradient of P availability to release phosphate from one typical primary mineral source, namely hydroxyapatite, and desorb phosphate bound to secondary minerals, represented by goethite (hereafter referred to as P-loaded goethite). Two soil depth increments were chosen to evaluate whether the microbial communities of different soil depths affect the solubilization of phosphate. Incubation experiments were performed with and without addition of glucose to test for possible carbon (C) and energy limitations. We hypothesized that the net microbial P solubilization from hydroxyapatite results from acidification of the soil solution due to the production of LMWOAs by microbes from different soil depths (hypothesis 1). Further, we postulated that desorption of phosphate from goethite is not promoted by acidification since increasing the positive charge on the mineral causes stronger adsorption of phosphate (hypothesis 2). In addition, we hypothesized that differences in dissolved phosphate availability affect the microbial solubilization of mineral-bound P (hypothesis 3). Finally, we assumed that amendment with glucose stimulates microbial production of LMWOAs and metal-complexing compounds, which cause increased

phosphate release from the minerals (hypothesis 4).

2. Materials and methods

2.1. Study sites and samples collection

Soil samples were collected in mid-April 2017 from five even-aged beech (*Fagus sylvatica* L.) forests in Germany. The study sites strongly differ in soil total P stocks (Lang et al., 2016), ranging from 164 to 904 g P m⁻² (see Supplementary Table S1). Two sites (Mitterfels, MIT and Conventwald, CON) are located on the German southern uplands, two (Bad Brückenau, BBR and Vessertal, VES) on the central highland region encompassing an altitudinal range from 810 to 1025 m above sea level, and one, Lüss (LUE), is located in the northern German lowlands (115 m above sea level). The sites have been intensively monitored under the ICP Forests program. We decided to focus on mineral soil because P mobilization from mineral sources is most relevant in horizons poor in organic P. In each forest stand, two different soil depths from one representative soil pit were sampled by combining material taken from five randomly selected spots per depth using a small stainless steel spatula. After being transported to the laboratory, field-moist samples were sieved (< 2 mm) and root fragments, gravel, stones, and other coarse debris were removed. Subsequently, small aliquots of each sample were air-dried for chemical analysis. The remaining soil was stored at 5 °C for further analysis.

2.2. Chemical analyses of soil samples

Soil pH of dried samples (60 °C for 24 h) was measured in deionized water using a soil-to-water ratio of 1:5 and an equilibration time of 3 h (see Supplementary Table S2). Aliquots of oven-dried samples were finely ground in a ball mill (MM400, Retsch, Germany) and the total contents of soil organic C (TOC) and total N (TN) were measured using an elemental analyzer (Vario MAX CN, Elementar, Germany). Total organic P (TOP) was quantified using the method developed by Saunders and Williams (1955) as modified by Walker and Adams (1958). Briefly, 1 g of soil was ignited at 550 °C in a muffle furnace. Phosphorus was extracted from ignited and non-ignited samples for 16 h into 0.5 M H₂SO₄ and subsequently centrifuged at 1500 × g for 15 min. The concentrations of phosphate in the 0.5 M H₂SO₄ extracts were determined by the molybdenum-blue method (Murphy and Riley, 1962), using a UV-spectrophotometer (UV-1800, Shimadzu, Japan). Total organic P was calculated as the difference between the phosphate concentrations of the ignited and non-ignited sample.

2.3. Mineral phases

Hydroxyapatite was purchased from Sigma-Aldrich (purity ≥ 95%). It had a specific surface area (SSA) of 100 m² g⁻¹, as determined by N₂ adsorption with an automatic analyzer (Gemini 2375, Micromeritics Instrument Corp., Norcross, GA, USA). Goethite (α -FeO(OH)) was produced according to the method of Atkinson et al. (1967) by neutralising 1 M FeCl₃ solution with NaOH and ageing the precipitate at 55 °C for 3 days. The product was rinsed with ultrapure water until the electrical conductivity of the rinsing solution was < 50 μ S cm⁻¹. X-ray diffraction (D5005; Bruker AXS, Germany) indicated the product to be pure and well crystalline. The specific surface area was 58 m² g⁻¹ (determined by N₂ adsorption; Autosorb iQ₂, Quantachrome, USA). Phosphate loading was done by equilibrating 20 g of goethite with 1000 ml KH₂PO₄ solution containing 1000 mg P l⁻¹ on a horizontal shaker at 60 motions min⁻¹ for 16 h at 20 °C. The suspension was centrifuged at 4500 × g for 45 min, and the supernatant decanted. The settled goethite was re-suspended in 1000 ml ultrapure water (pH 6) to remove excess phosphate, centrifuged at 4500 × g for 45 min, and then, the supernatant decanted. After rinsing, P-loaded goethite was freeze dried. Drying usually causes bonds between P and oxide surfaces to

become stronger. Goethite was prepared several weeks before use, and stored dry (after freeze drying) in the dark at room temperature. Therefore, significant aging before exposure to the soil extracts can be excluded. Aliquots of the equilibrium and rising supernatants were analysed for P by ICP-OES (Ultima 2, Horiba Jobin-Yvon, Longjumeau, France). Sorption had no detectable effect on the specific surface area of goethite.

2.4. Preparation of soil extracts for incubation experiments

Fresh homogenized soil samples were used to prepare soil extracts for incubations. Briefly, 100 g of each soil sample were placed in PE bottles and mixed with 1 l of distilled water and shaken at room temperature for 2 h using an overhead shaker. Preliminary tests showed that the filtration rates of the soil extracts were not significantly affected by the soil clay content. The extracts were filtered through cellulose filters with coarse pores that allow for passage of soil microorganisms and small organic matter particles (240 µm, Rotilabo, type 113P, Roth, Germany). When the filtration time exceeded 1 h, filtration was continued in a climatic chamber at 2 °C. After filtration, the soil extracts were immediately transferred to sterilized glass flasks.

2.5. P release from hydroxyapatite and P-loaded goethite

To determine the net microbial P release from the mineral phases, hydroxyapatite and P-loaded goethite, two different sets of incubation experiments were conducted, using soil extracts, either with or without addition of glucose following Brucker et al. (2020). The two sets of experiments were carried out in identical manner, except for the use of anion exchange membranes (AEMs) in the soil extracts incubated with P-loaded goethite in order to prevent re-adsorption of phosphate to the mineral. The AEMs were utilized following the protocol described by Saggari et al. (1990) for extracting phosphate. Briefly, AEMs (VWR Chemicals, Lutterworth, United Kingdom) were converted to the bicarbonate form by soaking in 0.5 M NaHCO₃ for 1 h. The membranes were cut into strips (3 cm × 6 cm), gently rinsed with ultrapure water, air-dried for several hours, and finally added to each flask at the beginning of the incubation. For each membrane withdrawn, a fresh one was added.

In experiment 1 and experiment 3, the total P released from the mineral phases was determined in the presence of glucose. For this purpose, 99 ml of the soil extracts and 1 ml of glucose (3.33 mM) solution were added to either 100 mg of hydroxyapatite or 1000 mg of P-loaded goethite. The large amount of goethite was necessary to ensure detectable effects. In the incubation experiments with hydroxyapatite, aliquots of 5 ml were taken 0, 6, 48, 72, 120, 168, 264, and 336 h after the beginning of the experiment. Solutions were vacuum-filtered through 0.45-µm cellulose acetate membrane filters (Sartorius Biotech, Germany) and analysed for pH and phosphate. In the experiments with P-loaded goethite, AEMs were removed from the flasks 6, 24, 48, 120, 168, and 336 h after the beginning of the experiment. The pH was determined after removing the membrane and before adding a new, fresh one. Further, we quantified the mineralization of P from dissolved organic matter by performing two control experiments (control of experiment 1 and control of experiment 3) conducted in analogy to experiment 1 and experiment 3 but without addition of hydroxyapatite or P-loaded goethite, respectively.

In experiment 2 and experiment 4, the total P released from the mineral phases was determined in absence of glucose. For this purpose, 99 ml of the soil extracts were added to either 100 mg of hydroxyapatite or 1000 mg of P-loaded goethite. As in experiments 1 and 3, we quantified the mineralization of P from dissolved organic matter by performing two additional control experiments (control of experiment 2 and control of experiment 4) in analogy to experiment 2 and experiment 4 but without addition of hydroxyapatite or P-loaded goethite.

In addition, sterile control experiments were conducted to

determine the effect of the soil extracts and the AEMs on P release. For this purpose, 99 ml of sterile water were added to either 100 mg of hydroxyapatite or 1000 mg of P-loaded goethite. The incubation flasks were kept agitated in the dark at 20 °C on a horizontal shaker for 14 days with agitation at 120 motions min⁻¹; loose covers ensured aerobic conditions. All experiments, including the sterile controls, were performed in triplicates.

The net microbial P release rates from the mineral phases, with and without addition of glucose, were calculated from experiment 1 and 3 and the respective controls, as well as from experiment 2 and 4 and the respective controls (see calculations below).

2.6. Chemical analyses of soil extracts

The original soil extracts were analysed for the initial concentrations of dissolved organic C (DOC) and dissolved organic N (DON), using a TOC/TN analyzer (multi N/C analyzer 2100A, Analytik Jena, Germany), as well as phosphate (see below). In the experiment with P-loaded goethite, the AEMs were removed from the flasks at regular intervals and extracted into 0.5 M HCl for 1 h on an automatic shaker. The concentrations of phosphate in the 0.5 M HCl extracts (in the experiment with P-loaded goethite) and in the water extracts (in the experiment with apatite and in the control experiments) were determined using the molybdenum-blue assay (Murphy and Riley, 1962) and a UV-spectrophotometer (UV-1800, Shimadzu, Japan). This assay quantifies phosphate in solution that can react with the color reagent, and therefore, is a measure of the dissolved molybdate-reactive P. The total phosphate taken up by the AEMs over each time interval was summed up to give cumulative amounts. In addition, for determination of Fe, aliquots of 10 ml were taken 0, 168, and 336 h after the beginning of the experiment, filtered through 0.45-µm cellulose acetate filters, acidified by adding 50 µl of 65% HNO₃ to prevent Fe precipitation, and then centrifuged at 1500 × g for 15 min. The resulting supernatant was analysed for Fe by ICP-OES (Vista-Pro radial, Varian, USA).

2.7. LMWOAs

The concentrations of four LMWOAs (citric, oxalic, 2-keto-D-gluconic and D-gluconic) were determined in the solution 168 and 336 h after the beginning of experiment 1 and experiment 3. We selected LMWOAs that have been shown to play significant roles in P solubilization (Illmer and Schinner, 1992; Rodriguez and Fraga, 1999). Aliquots of 0.45 µm-filtered solutions were analysed by high-performance liquid chromatography (Agilent series 1100, Agilent Technologies, Santa Clara, CA, USA) coupled to a diode-array detector (DAD) and an electrospray ionization (ESI) mass spectrometer (Agilent 6130 single quadrupole). Separation of LMWOAs was performed on a hydro-reversed-phase column (Phenomenex Synergi 4 u Hydro-RP 80A) combined with a guard column. The mobile phase was composed of 4 mM formic acid (Solvent A) and acetonitrile (Solvent B), in a gradient mode: 10 min B = 1.5%, 40 min B = 80%, 43 min B = 80% at a flow rate of 0.3 ml min⁻¹. LMWOAs were identified based on their retention times and selected ions in positive and negative ionization mode, which were *m/z* 210 for citric acid, *m/z* 212 for 2-keto-D-gluconic acid, *m/z* 219 for D-gluconic acid, and *m/z* 89 for oxalic acid. Quantification was carried out by calibration with external standards. HPLC-MS data were processed using the Agilent's Chemstation software package. All reagents used in the analytical procedures were of analytical reagent grade (p. a. ≥ 99.0%). The amounts of each LMWOA were calculated by multiplying the respective concentration (mg l⁻¹) released into the soil extracts with the exact volume (l) present in the flask at 168 and 336 h, and subsequently expressed in µmol. In addition, we calculated the concentrations of the carboxyl groups (-COOH) based on the concentrations of LMWOAs and the number of carboxyl groups of each LMWOA.

In the soil extracts incubated with P-loaded goethite, the

concentrations of six siderophores (protochelin, enterobactin, desferrioxamine B, ferricrocin, aerobactin, rhizobactin) were investigated by means of a Q-Exactive hybrid quadrupole orbitrap (Dionex Ultimate 3000, Thermo Fisher Scientific, Germany) coupled to a UHPLC-ESI-HRMS platform. Chromatographic separation was performed using a Accucore RP-MS column (150×2.1 mm with 2.6 μm) equipped with a matching guard column. The mobile phase gradient started at 95% Solvent A (HPLC grade water spiked with 0.1% formic acid) and 5% Solvent B (acetonitrile LC-MS grade spiked with 0.1% formic acid) at a flow rate of 0.25 ml min⁻¹. The composition of the mobile phase was kept constant for 0.5 min and changed to 5% solvent A and 95% solvent B within 30 min followed by an isocratic elution time of 5 min. The mass spectra were recorded in the positive ion mode. The mass range was set to *m/z* 100–1500 with auto MS/MS acquisition. LC-MS data were acquired and processed with Xcalibur 3.0 software.

2.8. Calculations and statistical analyses

For all experiments, the amount of P was calculated by multiplying the concentration of P (μmol l⁻¹) with the volume (l) of the soil extract present in the flask at each sampling time. The total P release rates in experiment 1 and 3 (hydroxyapatite or P-loaded goethite with glucose) and 2 and 4 (hydroxyapatite or P-loaded goethite without glucose) were computed using the following equation:

$$\text{Total P release rate } (\mu\text{mol d}^{-1}) = \frac{(P[\mu\text{mol}]_{\text{day}14} - P[\mu\text{mol}]_{\text{day}0})}{14 [\text{days}]} \quad (1)$$

where P[μmol] represents the amount of P at the end (day 14) and the beginning (day 0) of the experiments. To estimate the amounts of P released only from hydroxyapatite or P-loaded goethite, we considered the P released from dissolved organic matter (P mineralization, Eq. 2) from the total P release rate (Eq. 1). Therefore, P mineralization was calculated based on the data of the control experiment as follows:

$$\text{P mineralization rate } (\mu\text{mol d}^{-1}) = \frac{(P[\mu\text{mol}]_{\text{day}14} - P[\mu\text{mol}]_{\text{day}0})}{14 [\text{days}]} \quad (2)$$

Further, to determine the overall effect of the soil extracts (chemical properties of extract as well as microbial activity) on the amounts of P released from hydroxyapatite or P-loaded goethite the amount of P released in sterile water was calculated according to (Eq. 3):

$$\begin{aligned} \text{Total P release rate in sterile water } (\mu\text{mol d}^{-1}) \\ = \frac{(P[\mu\text{mol}]_{\text{day}14} - P[\mu\text{mol}]_{\text{day}0})}{14 [\text{days}]} \end{aligned} \quad (3)$$

In the experiments with P-loaded goethite, AEMs were used. The net P release rates (μmol d⁻¹, Eq. 4) from hydroxyapatite and P-loaded goethite were estimated as the difference between the respective total P release rates (Eq. 1), the corresponding P mineralization rates (Eq. 2) and the total P release rates in sterile water (Eq. 3):

$$\begin{aligned} \text{Net P release rate } (\mu\text{mol d}^{-1}) \\ = \text{total P release rate } (\mu\text{mol d}^{-1}) - \text{total P release rate in sterile} \\ \text{water } (\mu\text{mol d}^{-1}) - \text{P mineralization rate } (\mu\text{mol d}^{-1}) \end{aligned} \quad (4)$$

By subtracting the P release rates from P-loaded goethite determined in sterile water (with AEMs) from the P release rate determined in the soil extracts (with AEMs), we corrected for the P release caused by the AEMs. Finally, the net P release rates were divided by the corresponding amount of hydroxyapatite and goethite utilized, as well as by their respective specific surface areas (m² g⁻¹), to give the rate in μmol m⁻² d⁻¹.

All data sets were tested for normality (Shapiro-Wilk) as well as for equality of variance using Brown-Forsythe test. None of the data sets was normally distributed but all passed the test for homoscedasticity. When variances were not significantly different between groups,

analysis of variance (one-way ANOVA) was used to test for differences between soil chemical properties and net P solubilization and net P desorption rates. Tukey's honest significance test (Tukey's HDS) was performed as a post-hoc test following ANOVA. Differences in net P solubilization and net P desorption rates between the two soil depths of each forest site were analysed by *t*-test for related samples, followed by post-hoc Tukey HDS (*p* < 0.05). Tests for correlation analyses were carried out using the parametric Pearson's correlation coefficient. Additionally, simple and multiple linear regressions for net P solubilization and net P desorption rates (Y) and soil chemical variables (X_{*n*}) were conducted. The standard deviation (S.D.) of the mean is reported throughout the text, unless otherwise specified. All data analysis was carried out using SigmaPlot (version 13.0, Systat Software, San Jose, California, USA).

3. Results

3.1. Microbial P solubilization from hydroxyapatite

In absence of glucose, we did not observe any net P solubilization from hydroxyapatite during the incubations but rather microbial P immobilization (data not shown), as indicated by decreases in dissolved phosphate in the extracts. When glucose was added, the net P solubilization rates from hydroxyapatite ranged between 0.001 and 0.54 μmol m⁻² d⁻¹, and differed among the ten forest soil extracts (Fig. 1). The net P solubilization rates were significantly larger in the extracts of the upper soil (30–35 cm) than of the lower soil depth (65–70 cm) in three out of five cases, namely BBR (+55.1%), CON (+49.3%), and LUE (+96.1%) (*p* < 0.05, Fig. 1). In contrast, in the soil extracts from MIT and VES, the net P solubilization rates at 65–70 cm depth were either 62% or 33% higher than those at 30–35 cm depth. However, only for MIT, the difference between upper and lower soil depth was statistically significant (*p* < 0.01). The net microbial P solubilization rates from hydroxyapatite increased in the order: MIT < VES < LUE < BBR < CON for the upper soil depth. For the lower soil depth, the order was: LUE < MIT < VES < BBR < CON.

3.2. P desorption from P-loaded goethite

In absence of glucose, there was no net P desorption from P-loaded

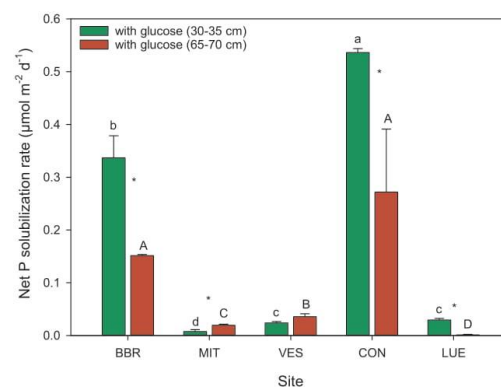


Fig. 1. Net P solubilization rates for hydroxyapatite incubated with glucose in solutions extracted from different soils collected at two different depths at five forest sites. The bars show means, and error bars indicate standard deviations (*n* = 3). Different letters indicate significant differences, tested separately for the two soil depths by one-way ANOVA, followed by post-hoc Tukey HDS (*p* < 0.05). Stars indicate significant differences between the two depths of each soil, tested by *t*-test followed by post-hoc Tukey HDS (*p* < 0.05).

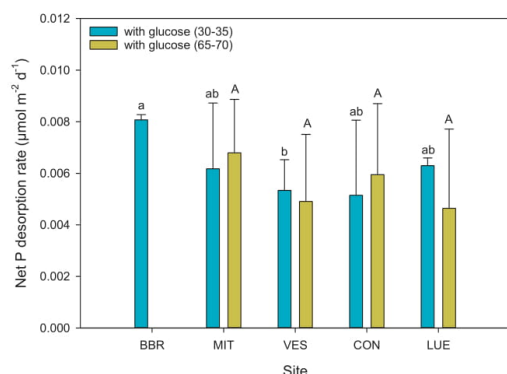


Fig. 2. Net P desorption rates for P-loaded goethite incubated with glucose in solutions extracted from different soils collected at two different depths at five forest sites. Mean values and standard deviations from triplicate experiments are shown. Different letters indicate significant differences, tested separately for the two soil depths by one-way ANOVA followed by post-hoc Tukey HSD ($p < 0.05$).

goethite during the incubations. When glucose was provided, the average net P desorption rates ranged between 0.005 and 0.008 $\mu\text{mol m}^{-2} \text{d}^{-1}$, with little variability among the ten forest soil extracts (Fig. 2). For the upper soil depth (30–35 cm), only the VES soil extract differed significantly in net P desorption rates from the extracts of the other four sites ($p < 0.05$, Fig. 2). At 65–70 cm depth, the net P desorption rates were not significantly different among the soil extracts after two weeks of incubation ($p > 0.05$). The P desorption rates in the soil extracts were on average 30% higher than the P desorption rates in sterile water.

3.3. LMWOAs in the soil extracts incubated with glucose

The amounts of LMWOAs (citric, oxalic, D-gluconic and 2-keto-D-gluconic acids) released when hydroxyapatite was incubated with glucose were larger in the extracts from the upper soil depth (30–35 cm) than in those from the lower soil depth (65–70 cm) for all soils after seven (mean: +27%) and fourteen days (from +9 to +74%; Fig. 3). The relative contribution of D-gluconic and citric acid in the soil extract from BBR at 30–35 cm depth made up 59% and 22% of the total carboxyl groups of the tested LMWOAs, respectively. Similarly, D-gluconic and citric acid in the soil extracts from 65–70 cm depth represented 66% and 17% of the total measured carboxyl groups. In contrast, during the incubations of the soil extract from CON from 30–35 cm depth, significantly greater amounts of 2-keto-D-gluconic acid were produced than of the other three LMWOAs ($p < 0.01$), thus representing 69% of total LMWOAs carboxyl groups. In contrast to the upper soil depth, D-gluconic acid was detected in significantly higher amounts than the other three LMWOAs at 65–70 cm depth (46% of the total carboxyls, $p < 0.05$). When the concentrations of the carboxyl groups of the four LMWOAs were summed up, the microbial communities in the soil extracts from BBR and CON showed a significantly larger acid production than those from the other three soil extracts ($p < 0.05$).

In the soil extracts incubated with P-loaded goethite and glucose, only two LMWOAs were detected during the two-week period (citric and D-gluconic acid; Fig. 4). Further, no siderophores were detected in this experiment. The amounts of citric acid after seven days of incubation were significantly larger for the upper soil depth than for the lower soil depth at BBR ($6.5 \mu\text{mol} \pm 0.5$ vs. $3.2 \mu\text{mol} \pm 0.2$) and VES ($6.9 \mu\text{mol} \pm 0.6$ vs. $3.7 \mu\text{mol} \pm 0.9$) ($p < 0.05$, Fig. 4a). However, after two weeks of incubation, the amount of citric acid levelled

at $\sim 4 \mu\text{mol}$, with no detectable differences among soil extracts and depths (Fig. 4a, $p > 0.05$). The amounts of D-gluconic acid detected in both soil depths after seven days of incubation were lower at site MIT than in the other soil extracts (Fig. 4b). Overall, the sum of LMWOAs produced by microbes as well as the total amounts of the carboxyl groups decreased from day seven to day fourteen in all soil extracts.

The amounts of the carboxyl groups from citric and D-gluconic acid released by microbes incubated with hydroxyapatite were significantly higher ($p < 0.01$) than the amounts measured in incubations with P-loaded goethite in all soil extracts and depths, after seven and fourteen days of incubation.

3.4. Dissolved elements in the soil extracts

The initial amounts of DOC were significantly higher in the soil extracts from 30–35 cm depth than from 65–70 cm depth, except for BBR (Table 1). Further, the DOC concentrations in the soil extracts from the upper soil depth explained 25% of the variation in the net P desorption rates from P-loaded goethite ($p < 0.05$, Table 3), whereas in the lower soil depth no relationship between DOC and P desorption rates was found. On average, the initial concentrations of DON were higher in the soil extracts from 30–35 cm depth than in those from 65–70 cm depth ($p < 0.05$). Moreover, the dissolved Fe concentrations in all soil extracts incubated with P-loaded goethite and glucose significantly increased over the two weeks period in contrast to the experiment without glucose addition. The relative increase ranged from +8% to +98% for extracts from the upper soil depth and from +38% to +98% for the extracts from the lower soil depth ($p < 0.05$, Table 2). When no glucose was added, the Fe concentrations in all soil extracts progressively decreased over time (Table 2).

3.5. Effect of carboxyl groups and acidification on net P solubilization from hydroxyapatite and P-loaded goethite

In the experiment with hydroxyapatite and glucose, pH values were inversely correlated with net microbial P solubilization rates in all soil extracts and depths (Table 3). The fastest pH decrease during the first five days of incubation occurred in the soil extracts from BBR and CON (Fig. S1). After this time, the pH values continued to decrease but at a lower rate. The pH values explained 88% and 60% of the variation in net microbial P solubilization rates from hydroxyapatite in all extracts from the upper soil depth after seven and fourteen days, respectively (Table 3). In the soil extracts from the lower soil depth, they only explained 55% and 72% of the variation in net microbial P solubilization rates. Likewise, the pH was inversely correlated with the carboxyl amounts in the soil extracts ($p < 0.01$, Fig. 5). Significant positive correlations were found between net microbial P solubilization rates and the carboxyl amounts, explaining 88% (at day seven) and 89% (at day fourteen) of the overall variation in the soil extracts from the upper soil depth but only 78% and 58% in the soil extracts from the lower soil depth (Table 3).

In the experiment with P-loaded goethite and glucose, a weak but significant positive correlation was found between pH and the net P desorption rates for soil extracts from the lower soil depth and seven days after the beginning of the experiment ($R^2 = 0.34$, $p < 0.05$). No significant relationship was found for soil extracts from the upper soil depth after either seven or fourteen days (Table 3). Furthermore, the pH did not correlate with the amount of carboxyl groups, except for one weak, positive relationship for soil extracts from 65–70 cm depth at fourteen days ($R^2 = 0.33$, $p < 0.05$). No significant correlation was found between the net P desorption rates from goethite and the amounts of carboxyl groups in the soil extracts from both soil depths.

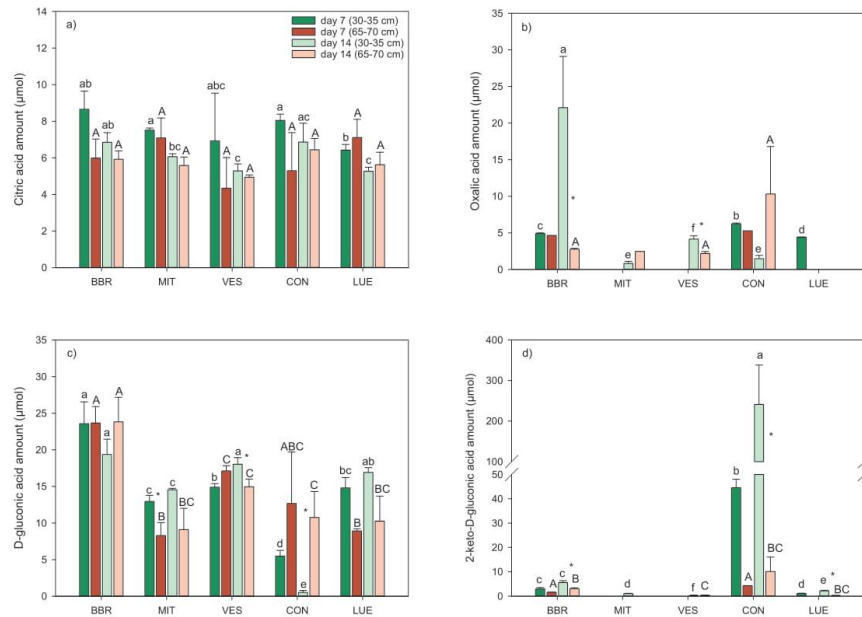


Fig. 3. Amounts of citric (a), oxalic (b), D-gluconic (c) and 2-keto-D-gluconic (d) acids, normalized to the number of carboxyl groups, in solutions extracted from different soils incubated with hydroxyapatite and glucose. Bars represent means and error bars indicate standard deviations (n = 3). Lowercase and uppercase letters indicate significant differences between soils and soil depths tested separately at day seven and day fourteen by one-way ANOVA followed by post-hoc Tukey HSD (p < 0.05). Stars indicate significant differences between two depths of one soil, tested by t-test followed by post-hoc Tukey HSD (p < 0.05). Note the different concentration scales of a), b) and c) with d).

4. Discussion

4.1. Solubilization of P from hydroxyapatite

Microbial communities from five acidic beech forest soils were more efficient in releasing phosphate from hydroxyapatite than from P-loaded goethite. This response was particularly pronounced in the soil extracts from BBR and CON where the net P solubilization rate from hydroxyapatite significantly exceeded the net P desorption rate from P-loaded goethite. This finding is of particular interest considering that the studied soils are characterized by the prevalence of P bound to Fe oxides (Prietzel et al., 2016; Lang et al., 2017).

The net P solubilization rates from hydroxyapatite were strongly negatively related to pH (Table 3), and the phosphate amounts in the incubated soil extracts gradually increased as the pH decreased over

time (Fig. S1). This suggests that the acidification of the soil extracts was the main mechanism of P solubilization from hydroxyapatite. Our results are in agreement with several previous studies reporting that the amount of phosphate released from Ca phosphates and the pH of the soil extract were inversely correlated (Whitelaw et al., 1999; Chen et al., 2006; Miller et al., 2010; Castagno et al., 2011; Brucker et al., 2020). In addition, we found a positive relationship between net microbial P solubilization rates and the concentration of LMWOAs (Table 3), similar to Brucker et al. (2020). One possible explanation for this is that dissociated LMWOAs form complexes with Ca²⁺, and thus, cause dissolution of apatite (Smith et al., 1977). However, LMWOAs can also contribute to acidification of the solution (Menezes-Blackburn et al., 2016). In the present study, pH and carboxyl groups in the soil solutions were inversely correlated (Fig. 5). Based on the pK_A values of LMWOAs (between 3.13 and 6.40 for citric acid; between 1.25 and 4.15

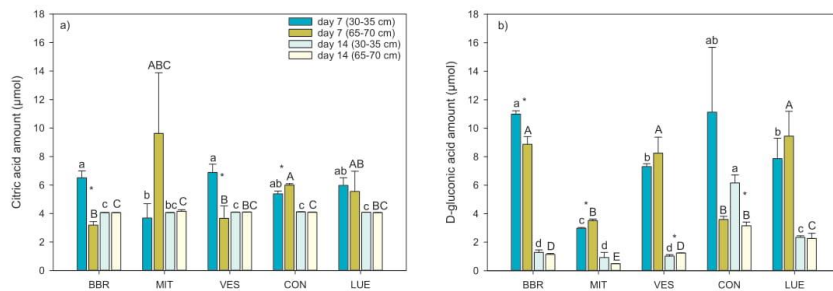


Fig. 4. Amounts of citric (a), and D-gluconic (b) acids, normalized to the number of carboxyl groups, in solutions extracted from different soils incubated with P-loaded goethite and glucose. Bars represent means and error bars indicate standard deviations (n = 3). Lowercase and uppercase letters show significant differences between soils and soil depths tested separately at day seven and day fourteen by one-way ANOVA followed by post-hoc Tukey HSD (p < 0.05). Stars indicate significant differences between two depths of one soil tested by t-test followed by post-hoc Tukey HSD (p < 0.05).

Table 1

Concentrations of dissolved phosphate, dissolved organic carbon (DOC), and dissolved organic nitrogen (DON) in the solutions extracted from the soil samples, representing the conditions at the beginning of the incubation experiments. Mean values \pm standard deviations ($n = 3$) are shown together with the respective DOC:DON ratio.

Site	Soil depth [cm]	Dissolved phosphate [$\mu\text{mol l}^{-1}$]	Dissolved organic carbon (DOC) [mmol l^{-1}]	Dissolved organic nitrogen (DON) [mmol l^{-1}]	DOC:DON ratio
BBR	30–35	0.18 (\pm 0.03)	5.89 (\pm 0.92)	0.07 (\pm 0.01)	89: 1
	65–70	0.18 (\pm 0.04)	9.65 (\pm 2.24)	0.04 (\pm 0.01)	215: 1
MIT	30–35	0.16 (\pm 0.01)	3.87 (\pm 0.65)	0.03 (\pm 0.00)	140: 1
	65–70	0.15 (\pm 0.01)	2.35 (\pm 0.47)	0.03 (\pm 0.00)	88: 1
VES	30–35	0.13 (\pm 0.02)	4.69 (\pm 0.76)	0.03 (\pm 0.01)	151: 1
	65–70	0.11 (\pm 0.01)	3.14 (\pm 0.66)	0.03 (\pm 0.01)	110: 1
CON	30–35	0.09 (\pm 0.01)	3.37 (\pm 0.85)	0.04 (\pm 0.01)	80: 1
	65–70	0.08 (\pm 0.02)	1.33 (\pm 0.29)	0.02 (\pm 0.00)	55: 1
LUE	30–35	0.04 (\pm 0.02)	4.97 (\pm 0.93)	0.03 (\pm 0.00)	155: 1
	65–70	0.03 (\pm 0.02)	3.16 (\pm 0.49)	0.02 (\pm 0.00)	204: 1

Table 2

Concentrations of dissolved Fe released from P-loaded goethite in the incubation solutions. Two incubation experiments were conducted, with and without addition of glucose. Mean values \pm standard deviations ($n = 3$) are shown. Lowercase and uppercase letters indicate significant differences, tested separately at each point in time and for the two soil depths ($p < 0.05$).

Site	Soil depth [cm]	Experiment 3 (with glucose)			Experiment 4 (without glucose)		
		Dissolved Fe [mmol l^{-1}]					
		Day 0	Day 7	Day 14	Day 0	Day 7	Day 14
BBR	30–35	0.013 (\pm 0.00) ^b	0.006 (\pm 0.00) ^a	0.001 (\pm 0.00) ^b	0.008 (\pm 0.006) ^a	0.001 (\pm 0.00) ^{ab}	0.001 (\pm 0.00) ^{ab}
	65–70	0.016 (\pm 0.00) ^A	0.013 (\pm 0.00) ^A	0.019 (\pm 0.00) ^A	0.01 (\pm 0.002) ^A	0.003 (\pm 0.00) ^A	0.001 (\pm 0.00) ^A
MIT	30–35	0.023 (\pm 0.01) ^{ab}	0.022 (\pm 0.01) ^a	0.017 (\pm 0.00) ^a	0.008 (\pm 0.004) ^a	0.001 (\pm 0.00) ^a	0.001 (\pm 0.00) ^a
	65–70	0.029 (\pm 0.02) ^{AB}	0.026 (\pm 0.01) ^A	0.023 (\pm 0.01) ^A	0.007 (\pm 0.001) ^A	0.001 (\pm 0.00) ^A	0.000 (\pm 0.00) ^A
VES	30–35	0.009 (\pm 0.00) ^c	0.016 (\pm 0.01) ^a	0.02 (\pm 0.01) ^a	0.015 (\pm 0.007) ^a	0.001 (\pm 0.00) ^a	0.001 (\pm 0.00) ^b
	65–70	0.01 (\pm 0.00) ^{AB}	0.02 (\pm 0.01) ^A	0.026 (\pm 0.02) ^A	0.012 (\pm 0.006) ^A	0.002 (\pm 0.00) ^A	0.001 (\pm 0.00) ^A
CON	30–35	0.04 (\pm 0.01) ^a	0.019 (\pm 0.01) ^a	0.02 (\pm 0.01) ^a	0.015 (\pm 0.011) ^a	0.001 (\pm 0.00) ^a	0.000 (\pm 0.00) ^{ab}
	65–70	0.008 (\pm 0.00) ^B	0.02 (\pm 0.01) ^A	0.07 (\pm 0.04) ^A	0.001 (\pm 0.00) ^B	0.000 (\pm 0.00) ^A	0.001 (\pm 0.00) ^A
LUE	30–35	0.009 (\pm 0.00) ^c	0.017 (\pm 0.01) ^a	0.011 (\pm 0.00) ^a	0.008 (\pm 0.004) ^a	0.000 (\pm 0.00) ^B	0.001 (\pm 0.00) ^{ab}
	65–70	0.01 (\pm 0.00) ^{AB}	0.012 (\pm 0.00) ^A	0.023 (\pm 0.01) ^A	0.001 (\pm 0.00) ^B	0.000 (\pm 0.00) ^A	0.002 (\pm 0.00) ^A

for oxalic acid; 3.41 for gluconic acid; 2.66 for 2-ketogluconic acid), the concentration of LMWOAs, and the pH values of the solution, we estimated that up to 99% of the protons released during the incubations were derived from LMWOAs. Thus, microbial production of LMWOAs was the likely cause of the acidification of the soil solution during the incubation.

4.2. Ecological implications of the microbial solubilization of P from hydroxyapatite

Most research on P release from mineral phases has focused on single microorganisms cultured in isolation, but little is known about how microbial communities affect the release of P from minerals. Incubation of the soil extracts from BBR (highest P availability) and CON (relatively low P availability) from both soil depths resulted in significantly higher net P solubilization rates from hydroxyapatite than in the other three soil extracts (MIT, VES, and LUE). The reason for this is likely the different microbial communities among the tested soils as well as the biochemical processes they perform since the concentration of microbial biomass C did not vary much among soils and soil depths (Table S2). This is in accordance with studies showing that the occurrence of P-solubilizing bacteria significantly differs among soils (Browne et al., 2009). Further, comparing the P solubilization rates of this study with those obtained from soils of the Coastal Cordillera of Chile (Brucker et al., 2020) we found that the potential of microbial communities to solubilize P from apatite was in the same magnitude.

Since most of the P in the soil of LUE is present in organic forms (Lang et al., 2017), the microbial community at LUE is likely little adapted to solubilize P from hydroxyapatite, in contrast to the microbial community in the soil in BBR that contains a large proportion of Ca phosphates. Bergkemper et al. (2016) found at LUE a 10-fold higher

abundance of fungal sequences than at BBR. Thus, the much lower net P solubilization rates in the soil extracts from LUE (lowest P availability) than in those from BBR (highest P availability) might indicate that the fungi-dominated microbial community present at LUE has a low potential to solubilize P.

4.3. Desorption of P-loaded to goethite

The net P desorption from goethite was up to two orders of magnitude smaller than the net P solubilization from hydroxyapatite. The positive relationship between pH and the net P release rates (Table 3) suggests that desorption of phosphate from goethite did not result from acidification but was rather promoted by less acidic conditions. The reason for this is that goethite becomes increasingly positively charged due to protonation with decreasing pH (Beebout and Loeppert, 2006), which favors phosphate sorption, and thus, causes net removal of phosphate from the soil extracts. Since protons were consumed by protonation of goethite, the pH did not correlate well with the amount of carboxyl groups. Some studies on ferric phosphates (Whitelaw et al., 1999; Xu et al., 2004) suggested that the phosphate desorption by LMWOAs is due to complexation of Fe with their carboxyl and hydroxyl groups. However, the lack of a significant correlation between carboxyl groups and dissolved Fe in the incubation of P-loaded goethite suggests that the desorption of phosphate from goethite by LMWOAs was partially due to direct competition between organic anions and phosphate for binding sites on the mineral surfaces (e.g. Jones and Brassington, 1998; Guppy et al., 2005). Further evidence for the relevance of this mechanism arises from the observation that when glucose was not supplied, a significant decline in the Fe concentration as well as in the phosphate concentration in the soil solution occurred (Table 2). The decline in Fe, but especially in the phosphate concentrations when no

Table 3
Results of simple and multiple regression analyses for the variables soil P_{tot}, soil P_{org}, pH (at day 7 or day 14), low molecular weight organic acids (at day 7 and day 14), DOC (at the beginning of the incubations), sand and clay content, and net P solubilization and desorption rates across all test sites, calculated separately for the two soil depths (30–35 and 65–70 cm). Given are the coefficients of regression (R² for simple regression or adjusted R² for multiple linear regression) as well as the p-values (highlighted in bold when statistically significant). For significant relationships, the negative (–) or positive (+) correlation was provided within parenthesis.

Depth [cm]	Soil P _{tot} [mg kg ⁻¹]	Soil P _{org} [mg kg ⁻¹]	pH ₇	pH ₁₄	LMWAO ₇ [μmol]	LMWAO ₁₄ [μmol]	DOC [mmol l ⁻¹]	LMWAO ₇ [μmol] + pH ₇		LMWAO ₁₄ [μmol] + pH ₁₄		LMWAO ₇ [μmol] + pH ₇ + Sand [%] + Clay [%]		LMWAO ₁₄ [μmol] + pH ₁₄ + Sand [%] + Clay [%]	
								R ²	p	R ²	p	R ²	p	R ²	p
Net P solubilization rate from hydroxyapatite [μmol m ⁻² d ⁻¹]	30–35	R ² = 0.11, p > 0.05	R ² = 0.07, p > 0.05	R ² = 0.88, p < 0.001	R ² = 0.60, p < 0.001	R ² = (+) 0.88, p < 0.001	R ² = (+) 0.89, p < 0.001	R ² = 0.11, p > 0.05	adj. R ² = 0.87, p < 0.001	adj. R ² = 0.76, p < 0.001	adj. R ² = (+) 0.96, p < 0.001	adj. R ² = (+) 0.87, p < 0.001	adj. R ² = (+) 0.87, p < 0.001	adj. R ² = (+) 0.87, p < 0.001	adj. R ² = (+) 0.87, p < 0.001
	65–70	R ² = 0.07, p > 0.05	R ² = 0.1, p > 0.05	R ² = 0.55, p < 0.01	R ² = 0.72, p < 0.01	R ² = (+) 0.78, p < 0.05	R ² = (+) 0.58, p < 0.05	R ² = 0.05, p > 0.05	adj. R ² = 0.55, p < 0.05	adj. R ² = 0.55, p < 0.05	adj. R ² = (+) 0.63, p < 0.05	adj. R ² = (+) 0.48, p < 0.05	adj. R ² = (+) 0.48, p < 0.05	adj. R ² = (+) 0.48, p < 0.05	adj. R ² = (+) 0.48, p < 0.05
Net P desorption rate from goethite [μmol m ⁻² d ⁻¹]	30–35	R ² = 0.07, p > 0.05	R ² = 0.08, p > 0.05	R ² = 0.02, p > 0.05	R ² = 0.18, p > 0.05	R ² = 0.008, p > 0.05	R ² = 0.06, p > 0.05	R ² = (+) 0.25, p > 0.05	adj. R ² = 0.0001, p > 0.05	adj. R ² = 0.14, p > 0.05	adj. R ² = 0.0001, p > 0.05	adj. R ² = 0.26, p > 0.05	adj. R ² = 0.26, p > 0.05	adj. R ² = 0.26, p > 0.05	adj. R ² = 0.26, p > 0.05
	65–70	R ² = 0.18, p > 0.05	R ² = 0.47, p < 0.05	R ² = (+) 0.34, p < 0.05	R ² = 0.02, p > 0.05	R ² = 0.005, p > 0.05	R ² = 0.01, p > 0.05	R ² = 0.24, p > 0.05	adj. R ² = 0.24, p > 0.05	adj. R ² = 0.0001, p > 0.05	adj. R ² = 0.27, p > 0.05	adj. R ² = 0.0001, p > 0.05	adj. R ² = 0.0001, p > 0.05	adj. R ² = 0.0001, p > 0.05	adj. R ² = 0.0001, p > 0.05

^aDetermined in soils, not in solutions.
^{**}y = 0.0189x – 0.0679.

glucose was provided, supports the idea that desorption of phosphate from goethite is due to competitive displacement of phosphate by organic anions that are only produced when C is available in larger amounts.

In the experiment with P-loaded goethite, we used AEMs that mimic phosphate uptake by plants (Turrión et al., 1997; Qian and Schoenau, 2002; Schefe et al., 2008). The bicarbonate-loaded AEMs had no significant effects on the pH of the soil solutions but might play a role in the adsorption of LMWOAs. However, phosphate has a stronger affinity to adsorb to charged surfaces such as the membranes than most LMWOAs. Thus, we exclude that adsorption of LMWOAs might have significantly influenced (i.e. decreased) the adsorption of phosphate on the AEMs in this specific case (Affif et al., 1995; Cooperband et al., 1999). We corrected for the strong AEM-induced desorption of phosphate from goethite using the experiment conducted with AEMs and P-loaded goethite under sterile conditions (Eq. 4). The comparison of the phosphate desorption rates in the soil extracts (corrected for P mineralization) and the phosphate desorption rates in sterile water showed that 60–65% of the total phosphate desorption was caused by AEMs. These results indicate that decreasing the phosphate concentration in solution by plant or microbial uptake enhances desorption of phosphate, according to the Le Chatelier's principle. Therefore, efficient depletion of the soil solution might be a valuable mechanism for plants and microorganisms to maintain P supply under soil conditions where P becomes strongly bound to secondary minerals (Spohn et al., 2020). With regard to this, despite being less soluble than short range-ordered ferrihydrite, goethite is still prone to dissolution and release of sorbed phosphate by siderophores and organic acids, and thus should have shown at least some response to microbial exudates. However, no siderophores were detected in our experiment, and therefore, we assume that the microbial communities did not produce them. Probable reasons for this are: (i) their production occurs only under Fe-deficient growth conditions, which was not the case in our experiment or (ii) the energetic cost of siderophores production was too high. The decrease in organic acids from day seven to day fourteen suggests that microbes were C-limited in our experiment, which supports point (ii). Masalha et al. (2000) suggested that siderophores play an important role especially in calcareous soils, and therefore their contribution to Fe dissolution in acidic soils might be overrated.

4.4. Production of LMWOAs

We observed much higher concentrations of LMWOAs in the soil extracts from BBR and CON than in the extracts from the other forest soils (MIT, VES and LUE). In previous studies (Chen et al., 2006; Oburger et al., 2011), citrate was shown to be most capable to solubilize P among all tested organic anions. In our incubations with glucose added, D-gluconic and 2-keto-D-gluconic acid were the most abundant LMWOAs and their production significantly coincided with high phosphate release from hydroxyapatite. Citric acid contributed little to the acidification of the solution, and thus, to the solubilization of P. This suggests that monocarboxylic acids released by microbial consortia may play a much larger role in P mobilization in soil than previously thought. Periplasmic oxidation of glucose is probably the most cost-efficient microbial pathway to produce large amounts of LMWOAs (Goldstein, 1995). Similarly, Brucker et al. (2020) found that 2-keto-D-gluconic acid, but also oxalic acid, were the most abundant LMWOAs secreted by microbial communities from a humid site in the Coastal Cordillera of Chile. 2-keto-D-gluconic acid is typically produced by Pseudomonads which have a high ability to solubilize P in soils (Goldstein, 2007).

The concentrations of LMWOAs were significantly lower in the soil extracts incubated with P-loaded goethite than in the extracts incubated with hydroxyapatite. Possible reasons for this are: (i) sorption of LMWOAs to goethite and (ii) downregulation of LMWOAs production by microbial communities to prevent acidification, and thus, strong

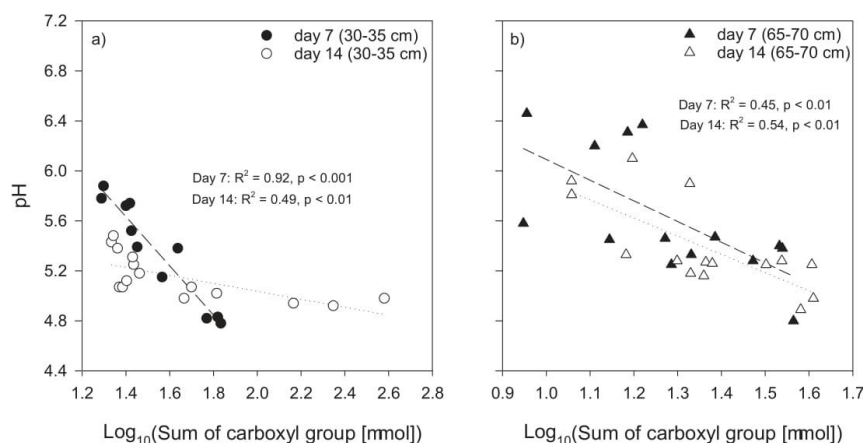


Fig. 5. Relationship between the pH and the log₁₀-transformed amounts of carboxyl groups released into solutions extracted from different soils incubated with hydroxyapatite and glucose. Two points in time are shown using respectively black and white dots (panel a) and black and white triangles (panel b). For all panels, the lines represent the best-fit regression line. Short-dashed and dotted lines depict associations after seven and fourteen days, tested separately for the two soil depths, respectively.

sorption to phosphate ions. Srinivasan and Mahadevan (2010) noted that the microbial-mediated metabolization of LMWOAs could contribute to the pH increase. Thus, the decrease (consumption) of LMWOAs over time could have partially slowed down the acidification of the soil extracts incubated with goethite. This effect has often been disregarded in studies on microbial mineral weathering (Jones, 1998; Geelhoed et al., 1998; Hoberg et al., 2005; Beebout and Loeppert, 2006).

5. Conclusions

We found that microbial communities from acidic beech forest soils are much more efficient at releasing phosphate from hydroxyapatite than from goethite. The microbial P solubilization from hydroxyapatite was mainly caused by acidification and the production of LMWOAs, resulting in the dissolution of the mineral. When incubated with glucose, soil microorganisms produced large amounts of LMWOAs, predominantly monocarboxylic acids (D-gluconic and 2-keto-D-gluconic acids) rather than di- or tri-carboxylic acids. The concentrations of LMWOAs in the soil extracts incubated with P-loaded goethite decreased over time. This decrease in LMWOAs hints at a possible downregulation of LMWOA production by microbes, which likely prevented acidification, and thus sorption of phosphate. Thus, microbial release of phosphate from goethite is not caused by acidification but likely by ligand competitive desorption. Overall, microbial communities in acid forest soils seem well capable to mobilize phosphate from primary mineral phases, such as apatites, but less effective in desorbing phosphate sorbed to secondary hydrous oxide phases, such as goethite. Future research needs to address microbial P solubilization from complex mixes of minerals and from weathered bedrock. In addition, the relationship between the soil microbial community composition and P solubilization warrants detailed investigation.

Funding

This research was funded by the German Research Foundation (DFG) as part of projects SP 1389/4-2 and KA 1673/9-2 of the priority program SPP1685 “Ecosystem nutrition: Forest strategies for limited phosphorus resources”.

Acknowledgements

The authors gratefully acknowledge the assistance of Dr. Ulrike Lacher for help with the mass spectrometry. We thank members of the BayCEER Laboratory for Analytical Chemistry for the chemical analyses and Ms. Karin Söllner and Ms. Renate Krauß for assistance provided in the laboratory. Special thanks to Mr. Uwe Hell for help in sample collection. Christian Treptow and Alexandra Boritzki assisted in the preparation and characterization of the P-loaded goethite at the Soil Science and Soil Protection Laboratory of Martin Luther University Halle-Wittenberg.

References

- Afif, E., Barrón, V., Torrent, J., 1995. Organic matter delays but does not prevent phosphate sorption by Cerrado soils from Brazil. *Soil Sci. Soc. Am. J.* 59, 207–211. <https://doi.org/10.1097/00010694-199503000-00008>.
- Antelo, J., Avena, M., Fiol, S., López, R., Arce, F., 2005. Effects of pH and ionic strength on the adsorption of phosphate and arsenate at the goethite–water interface. *J. Colloid Interface Sci.* 285 (2), 476–486. <https://doi.org/10.1016/j.jcis.2004.12.032>.
- Atkinson, R.J., Posner, A.S., Quirk, J.P., 1967. Adsorption of potential determining ions at the ferric oxide-aqueous electrolyte interface. *J. Phys. Chem.* 71, 550–559. <https://doi.org/10.1021/j100862a014>.
- Beebout, S.E.J., Loeppert, R.H., 2006. Role of organic acids in phosphate mobilization from iron oxide. *Soil Sci. Soc. Am. J.* 70 (1), 222–234. <https://doi.org/10.2136/sssaj2005.0012>.
- Beneduzi, A., Moreira, F., Costa, P.B., Vargas, L.K., Lisboa, B.B., Favreto, R., Baldani, J.I., Passaglia, L.M.P., 2013. Diversity and plant growth promoting evaluation abilities of bacteria isolated from sugarcane cultivated in the south of Brazil. *Appl. Soil Ecol.* 63, 94–104. <https://doi.org/10.1016/j.apsoil.2012.08.010>.
- Bergkemper, F., Schöler, A., Engel, M., Lang, F., Krüger, J., Schloter, M., Schulz, S., 2016. Phosphorus depletion in forest soils shapes bacterial communities towards phosphorus recycling systems. *Environ. Microbiol.* 18 (6), 1988–2000. <https://doi.org/10.1111/1462-2920.13188>.
- Borggaard, O.K., Raben-Lange, B., Gimsing, A.L., Strobel, B.W., 2005. Influence of humic substances on phosphate adsorption by aluminium and iron oxides. *Geoderma* 127 (3–4), 270–279. <https://doi.org/10.1016/j.geoderma.2004.12.011>.
- Browne, P., Rice, O., Miller, S., Burke, J., Dowling, D., Morrissey, J., O’Gara, F., 2009. Superior inorganic phosphate solubilization is linked to phylogeny within the *Pseudomonas fluorescens* complex. *Appl. Soil Ecol.* 43, 131–138. <https://doi.org/10.1016/j.apsoil.2009.06.010>.
- Brucker, E., Kernchen, S., Spohn, M., 2020. Release of phosphorus and silicon from minerals by soil microorganisms depends on the availability of organic carbon. *Soil Biol. Biochem.* 143 (107737), 1–10. <https://doi.org/10.1016/j.soilbio.2020.107737>.
- Castagno, L.N., Estrella, M.J., Sannazzaro, A.I., Grassano, A.E., Ruiz, O.A., 2011. Phosphate-solubilization mechanism and in vitro plant growth promotion activity mediated by *Pantoea eucalypti* isolated from *Lotus tenuis* rhizosphere in the Salado river basin (Argentina): phosphate-solubilization and plant growth promotion. *J. Appl. Microbiol.* 110 (5), 1151–1165. <https://doi.org/10.1111/j.1365-2672.2011>.

- 04968.x.
- Chen, Y.P., Rekha, P.D., Arun, A.B., Shen, F.T., Lai, W.A., Young, C.C., 2006. Phosphate solubilizing bacteria from subtropical soil and their tricalcium phosphate solubilizing abilities. *Appl. Soil Ecol.* 34 (1), 33–41. <https://doi.org/10.1016/j.apsoil.2005.12.002>.
- Chung, H., Park, M., Madhaiyan, M., Seshadri, S., Song, J., Cho, H., Sa, T., 2005. Isolation and characterization of phosphate solubilizing bacteria from the rhizosphere of crop plants of Korea. *Soil Biol. Biochem.* 37 (10), 1970–1974. <https://doi.org/10.1016/j.soilbio.2005.02.025>.
- Cooperband, L.R., Gale, P.M., Comerford, N.B., 1999. Refinement of the anion exchange membrane method for soluble phosphorus measurement. *Soil Sci. Soc. Am. J.* 63, 58–64. doi: 10.2136/sssaj1999.03615995006300010010x.
- Cornell, R.M., Schwertmann, U., 2003. The iron oxides: structure, properties, reactions, occurrences and uses. Wiley-VCH, 1-694. doi: 10.1002/3527602097.
- Darcy, J.L., Schmidt, S.K., Knelman, J.E., Cleveland, C.C., Castle, S.C., Nemerger, D.R., 2018. Phosphorus, not nitrogen, limits plants and microbial primary producers following glacial retreat. *Sci. Adv.* 4, eaaq0942. <https://doi.org/10.1126/sciadv.aaq0942>.
- Dirnböck, T., Földal, C., Djukic, I., Kobler, J., Haas, E., Kiese, R., Kitzler, B., 2017. Historic nitrogen deposition determines future climate change effects on nitrogen retention in temperate forests. *Clim. Change* 144 (2), 221–235. <https://doi.org/10.1007/s10584-017-2024-y>.
- Filippelli, G.M., 2002. The global phosphorus cycle. *Rev. Mineral. Geochem.* 48, 391–425. <https://doi.org/10.2113/GSELEMENTS.4.2.89>.
- Fox, T.R., Comerford, N.B., 1990. Low-molecular-weight organic acids in selected forest soils of the southeastern USA. *Soil Sci. Soc. Am. J.* 54, 1139–1144. <https://doi.org/10.2136/sssaj1990.03615995005400040051x>.
- Frey, B., Rieder, S.R., Brunner, I., Plötze, M., Koetzsch, S., Lapanje, A., Brandl, H., Furrer, G., 2010. Weathering-associated bacteria from the Damma glacier forefield: physiological capabilities and impact on granite dissolution. *Appl. Environ. Microbiol.* 76 (14), 4788–4796. <https://doi.org/10.1128/AEM.00657-10>.
- Geelhoed, S.J., Tjisse, H., Van Riemsdijk, W.H., 1998. Competitive interaction between phosphate and citrate on goethite. *Environ. Sci. Technol.* 32, 2119–2123. <https://doi.org/10.1021/es970908y>.
- Goldstein, A.H., 1995. Recent progress in understanding the molecular genetics and biochemistry of calcium phosphate solubilization by gram negative bacteria. *Biol. Agric. Hortic.* 12, 185–193. <https://doi.org/10.1080/01448765.1995.9754736>.
- Goldstein, A.H., 2007. Future trends in research on microbial phosphate solubilization: one hundred years of insolubility. In: *First International Meeting on Microbial Phosphate Solubilization*. Springer, Dordrecht, pp. 91–96.
- Guppy, C.N., Menzies, N.W., Moody, P.W., Blamey, F.P.C., 2005. Competitive sorption reactions between phosphorus and organic matter in soil: a review. *Soil Res.* 43 (2), 189–202. <https://doi.org/10.1071/SR04049>.
- Hallama, M., Pekrun, C., Lambers, H., Kandler, E., 2019. Hidden miners – the roles of crop roots and soil microorganisms in phosphorus cycling through agroecosystems. *Plant Soil* 434, 7–45. <https://doi.org/10.1007/s11104-018-3810-7>.
- He, Z., Zhu, J., 1998. Microbial utilization and transformation of phosphate adsorbed by variable charge minerals. *Soil Biol. Biochem.* 30 (7), 917–923. [https://doi.org/10.1016/S0038-0717\(97\)00188-0](https://doi.org/10.1016/S0038-0717(97)00188-0).
- Hedwall, P.O., Bergh, J., Brunet, J., 2017. Phosphorus and nitrogen co-limitation of forest ground vegetation under elevated anthropogenic nitrogen deposition. *Oecologia* 185 (2), 317–326. <https://doi.org/10.1007/s00442-017-3945-x>.
- Heuck, C., Smolka, G., Whalen, E., Frey, S., Gundersen, P., Moldan, F., Fernandez, I.J., Spohn, M., 2018. Effects of long-term nitrogen addition on phosphorus cycling in organic soil horizons of temperate forests. *Biogeochemistry* 141 (2), 167–181. <https://doi.org/10.1007/s10533-018-0511-5>.
- Hinsinger, P., 2001. Bioavailability of soil inorganic P in the rhizosphere as affected by root-induced chemical changes: a review. *Plant Soil* 237, 173–195. <https://doi.org/10.1023/A:1013351617532>.
- Hoberg, E., Marschner, P., Lieberei, R., 2005. Organic acid exudation and pH changes by *Gordonia* sp. and *Pseudomonas fluorescens* grown with P adsorbed to goethite. *Microbiol. Res.* 160 (2), 177–187. <https://doi.org/10.1016/j.micres.2005.01.003>.
- Illmer, P., Schinner, F., 1992. Solubilization of inorganic phosphates by microorganisms isolated from forest soils. *Soil Biol. Biochem.* 24 (4), 389–395. [https://doi.org/10.1016/0038-0717\(92\)90199-8](https://doi.org/10.1016/0038-0717(92)90199-8).
- Jacoby, R., Peukert, M., Succurro, A., Koprivova, A., Kopriva, S., 2017. The role of soil microorganisms in plant mineral nutrition – current knowledge and future directions. *Front. Plant Sci.* 8, 1617. <https://doi.org/10.3389/fpls.2017.01617>.
- Jonard, M., Fürst, A., Verstraeten, A., Thimonier, A., Timmermann, V., Potočić, N., Waldner, P., Benham, S., Hansen, K., Merilä, P., Ponette, Q., de la Cruz, A., Roskams, P., Nicolas, M., Croisé, L., Ingerslev, M., Matteucci, G., Decinti, B., Bascietto, M., Rautio, P., 2014. Tree mineral nutrition is deteriorating in Europe. *Glob. Change Biol.* 21, 418–430. <https://doi.org/10.1111/gcb.12657>.
- Jones, D.L., 1998. Organic acids in the rhizosphere – a critical review. *Plant Soil* 205, 25–44. <https://doi.org/10.1023/A:1004356007312>.
- Jones, D.L., Brassington, D.S., 1998. Sorption of organic acids in acid soils and its implications in the rhizosphere. *Eur. J. Soil Sci.* 49, 447–455. <https://doi.org/10.1046/j.1365-2389.1998.4930447.x>.
- Jones, D.L., Oburger, E., 2011. Solubilization of phosphorus by soil microorganisms. In: Bünenmann, E., Oberson, A., Frossard, E., (Eds.), *Phosphorus in Action* 26, 169–198. doi: 10.1007/978-3-642-15271-9_7.
- Lang, F., Bauhus, J., Frossard, E., George, E., Kaiser, K., Kaupenjohann, M., Krüger, J., Matzner, E., Polle, A., Priezel, J., Rennenberg, H., Wellbrock, N., 2016. Phosphorus in forest ecosystems: new insights from an ecosystem nutrition perspective. *J. Plant Nutr. Soil Sci.* 179 (2), 129–135. <https://doi.org/10.1002/jpln.201500541>.
- Lang, F., Krüger, J., Amelung, W., Willbold, S., Frossard, E., Bünenmann, E.K., Bauhus, J., Nitschke, N., Kandler, E., Marhan, S., Schulz, S., Bergkemper, F., Schlöter, M., Luster, J., Guggisberg, F., Kaiser, K., Mikutta, R., Guggenberger, G., Polle, A., Pena, R., Priezel, J., Rodionov, A., Talkner, U., Meesenburg, H., von Wilpert, K., Hölscher, A., Dietrich, H.P., Chmara, I., 2017. Soil phosphorus supply controls P nutrition strategies of beech forest ecosystems in central Europe. *Biogeochemistry* 136 (1), 5–29. <https://doi.org/10.1007/s10533-017-0375-0>.
- Lindsay, W.L., 1979. *Chemical Equilibria in Soils*. John Wiley and Sons, New York, pp. 1–449.
- Marschner, P., Crowley, D., Rengel, Z., 2011. Rhizosphere interactions between microorganisms and plants govern iron and phosphorus acquisition along the root axis – model and research methods. *Soil Biol. Biochem.* 43, 883–894. <https://doi.org/10.1016/j.soilbio.2011.01.005>.
- Masalha, J., Kosegarten, H., Elmaci, Ö., Mengel, K., 2000. The central role of microbial activity for iron acquisition in maize and sunflower. *Biol. Fertil. Soils* 30 (5–6), 433–439. <https://doi.org/10.1007/s003740050021>.
- Menezes-Blackburn, D., Paredes, C., Zhang, H., Giles, C.D., Darch, T., Stutter, M., George, T.S., Shand, C., Lumsdon, D., Cooper, P., Wendler, R., Brown, L., Blackwell, M.S., Wearing, C., Haygarth, P.M., 2016. Organic acid regulation of chemical-microbial phosphorus transformations in soils. *Environ. Sci. Technol.* 50, 11521–11531. <https://doi.org/10.1021/acs.est.6b03017>.
- Menge, D.N.L., Hedin, L.O., Pacala, S.W., 2012. Nitrogen and phosphorus limitation over long-term ecosystem development in terrestrial ecosystems. *PLoS ONE* 7 (8), e42045. <https://doi.org/10.1371/journal.pone.0042045>.
- Miller, S.H., Browne, P., Prigent-Combaret, C., Combes-Meynet, E., Morrissey, J.P., O’Gara, F., 2010. Biochemical and genomic comparison of inorganic phosphate solubilization in *Pseudomonas* species: inorganic P-solubilization in *Pseudomonas*. *Environ. Microbiol. Rep.* 2 (3), 403–411. <https://doi.org/10.1111/j.1758-2229.2009.00105.x>.
- Murphy, J., Riley, J.P., 1962. A modified single solution method for the determination of phosphate in natural waters. *Anal. Chim. Acta* 26, 678–681. [https://doi.org/10.1016/S0003-2670\(00\)88444-5](https://doi.org/10.1016/S0003-2670(00)88444-5).
- Nezat, C.A., Blum, J.D., Yanai, R.D., Park, B.B., 2008. Mineral sources of calcium and phosphorus in soils of the northeastern United States. *Soil Sci. Soc. Am. J.* 72, 1786–1794. <https://doi.org/10.2136/sssaj2007.0344>.
- Oburger, E., Jones, D.L., Wenzel, W.W., 2011. Phosphorus saturation and pH differentially regulate the efficiency of organic acid anion-mediated P solubilization mechanisms in soil. *Plant Soil* 341 (1–2), 363–382. <https://doi.org/10.1007/s11104-010-0650-5>.
- Ordoñez, Y.M., Fernandez, B.R., Lara, L.S., Rodriguez, A., Uribe-Vélez, D., Sanders, I.R., 2016. Bacteria with phosphate solubilizing capacity alter mycorrhizal fungal growth both inside and outside the root and in the presence of native microbial communities. *PLoS ONE* 11 (6), 1–18. <https://doi.org/10.1371/journal.pone.0154438>.
- Osoorio, N.W., Habte, M., 2013. Phosphate desorption from the surface of soil mineral particles by a phosphate-solubilizing fungus. *Biol. Fertil. Soils* 49 (4), 481–486. <https://doi.org/10.1007/s00374-012-0763-5>.
- Panhwar, Q.A., Naher, U.A., Jusop, S., Othman, R., Latif, M.A., Ismail, M.R., 2014. Biochemical and molecular characterization of potential phosphate-solubilizing bacteria in acid sulfate soils and their beneficial effects on rice growth. *PLoS ONE* 9 (10), e97241. <https://doi.org/10.1371/journal.pone.0097241>.
- Pierzynski, G.M., McDowell, R.W., Sims, J.T., 2005. Chemistry, cycling, and potential movement of inorganic phosphorus in soils. In: Sims, J.T., Sharpley, A.N., Westermann, D.T., (Eds.), *Phosphorus: Agriculture and the Environment* 46, 53–86. doi: 10.2134/agronmonogr46.c3.
- Peñuelas, J., Poulter, B., Sardans, J., Ciais, P., Velde, M., Bopp, L., Boucher, O., Godderis, Y., Hinsinger, P., Llusia, J., Nardin, E., Vicca, S., Obersteiner, M., Janssens, I., 2013. Human-induced nitrogen-phosphorus imbalances alter ecosystems across the globe. *Nat. Commun.* 4, 2934. <https://doi.org/10.1038/ncomms3934>.
- Priezel, J., Klysbun, W., Werner, F., 2016. Speciation of phosphorus in temperate zone forest soils as assessed by combined wet-chemical fractionation and XANES spectroscopy. *J. Plant Nutr. Soil Sci.* 179 (2), 168–185. <https://doi.org/10.1002/jpln.201500472>.
- Qian, P., Schoenau, J.J., 2002. Practical applications of ion exchange resins in agricultural and environmental soil research. *Can. J. Soil Sci.* 82 (1), 9–21. <https://doi.org/10.4141/2000-091>.
- Raulund-Rasmussen, K., Borggaard, O.K., Hansen, H.C.B., Olsson, M., 1998. Effect of natural organic soil solutes on weathering rates of soil minerals. *Eur. J. Soil Sci.* 49, 397–406. <https://doi.org/10.1046/j.1365-2389.1998.4930397.x>.
- Remy, E., Wuyts, K., Boeckx, P., Gundersen, P., Verheyen, K., 2017. Edge effects in temperate forests subjected to high nitrogen deposition. *Proc. Natl. Acad. Sci. U.S.A.* 114 (34), E7032. <https://doi.org/10.1073/pnas.1709099114>.
- Richardson, A.E., Simpson, R.J., 2011. Soil microorganisms mediating phosphorus availability. Update on microbial phosphorus. *Plant Physiol.* 156 (3), 989–996. <https://doi.org/10.1104/pp.111.175448>.
- Rodríguez, H., Fraga, R., 1999. Phosphate solubilizing bacteria and their role in plant growth promotion. *J. Biotechnol. Adv.* 17, 319–339. [https://doi.org/10.1016/S0734-9750\(99\)00014-2](https://doi.org/10.1016/S0734-9750(99)00014-2).
- Rouached, H., Arpat, A.B., Poirier, Y., 2010. Regulation of phosphate starvation responses in plants: signaling players and cross-talks. *Molecular Plant* 3 (2), 288–299. <https://doi.org/10.1093/mp/ssp120>.
- Ruttenberg, K.C., 2003. The global phosphorus cycle. *Treatise on Geochemistry* 8, 585–643. <https://doi.org/10.1016/B0-08-043751-6/08153-6>.
- Saggar, S., Hedley, J.M., White, R.E., 1990. A simplified resin membrane technique for extracting phosphorus from soil. *Fertilizer Res.* 24, 173–180. <https://doi.org/10.1007/BF01073586>.
- Saunders, W.M.H., Williams, E.G., 1955. Observations on the determination of total organic phosphorus in soils. *J. Soil Sci.* 6, 254–267. <https://doi.org/10.1111/j.1365->

- 2389.1955.tb00849.x.
- Scheffe, C., Watt, M., Slattery, W.J., Mele, P., 2008. Organic anions in the rhizosphere of Al-tolerant and Al-sensitive wheat lines grown in an acid soil in controlled and field conditions. *Aust. J. Soil Res.* 46 (3), 257–264. <https://doi.org/10.1071/SR07139>.
- Schneider, K.D., Van Straaten, P., Mira De Orduña, R., Glasauer, S., Trevors, J., Fallow, D., Smith, P.S., 2010. Comparing phosphorus mobilization strategies using *Aspergillus niger* for the mineral dissolution of three phosphate rocks. *J. Appl. Microbiol.* 108 (1), 366–374. <https://doi.org/10.1111/j.1365-2672.2009.04489.x>.
- Sharma, S., Riyaz, S., Mrugesh, T., Alagiri, T., 2013. Phosphate solubilizing microbes: sustainable approach for managing phosphorus deficiency in agricultural soils. *Springer Plus* 2, 587. <https://doi.org/10.1186/2193-1801-2-587>.
- Smith, A.N., Posner, A.M., Quirk, J.P., 1977. A model describing the kinetics of dissolution of hydroxyapatite. *J. Colloid Interface Sci.* 62, 475–494. [https://doi.org/10.1016/0021-9797\(77\)90099-6](https://doi.org/10.1016/0021-9797(77)90099-6).
- Spohn, M., Zeißig, I., Brucker, E., Widdig, M., Lacher, U., Aburto, F., 2020. Phosphorus solubilization in the rhizosphere in two saporolites with contrasting phosphorus fractions. *Geoderma* 366, 114245. <https://doi.org/10.1016/j.geoderma.2020.114245>.
- Srinivasan, K., Mahadevan, R., 2010. Characterization of proton production and consumption associated with microbial metabolism. *BMC Biotech.* 10 (2), 1–10. <https://doi.org/10.1186/1472-6750-10-2>.
- Turner, B.L., Condon, L.M., Richardson, S.J., Peltzer, D.A., Allison, V.J., 2007. Soil organic phosphorus transformations during pedogenesis. *Ecosystems* 10, 1166–1181. <https://doi.org/10.1007/s10021-007-9086-z>.
- Turrión, M.B., Gallardo L., J., Hernández, M., 1997. Nutrient availability in forest soils as measured with anion-exchange membranes. *Geomicrobiol. J.*, 14, 51–64. doi: 10.1080/01490459709378033.
- Walker, T.W., Adams, A.F.R., 1958. Studies on soil organic matter: influence of phosphorus content of parent materials on accumulations of carbon, nitrogen, sulphur and organic phosphorus in grassland soils. *Soil Sci.* 85, 307–318.
- Walker, T.W., Syers, J.K., 1976. The fate of phosphorus during pedogenesis. *Geoderma* 15, 1–19. [https://doi.org/10.1016/0016-7061\(76\)90066-5](https://doi.org/10.1016/0016-7061(76)90066-5).
- Welch, S.A., Taunton, A.E., Banfield, J.F., 2002. Effect of microorganisms and microbial metabolites on apatite dissolution. *Geomicrobiol. J.* 19 (3), 343–367. <https://doi.org/10.1080/01490450290098414>.
- Whitelaw, M.A., Harden, T.J., Helyar, K.R., 1999. Phosphate solubilisation in solution culture by the soil fungus *Penicillium radicum*. *Soil Biol. Biochem.* 31 (5), 655–665. [https://doi.org/10.1016/S0038-0717\(98\)00130-8](https://doi.org/10.1016/S0038-0717(98)00130-8).
- Xu, R.K., Zhu, Y.G., Chittleborough, D., 2004. Phosphorus release from phosphate rock and iron phosphate by low-molecular-weight organic acids. *J. Environ. Sci.* 16, 5–8.
- Yi, Y., Huang, W., Ge, Y., 2008. Exopolysaccharide: a novel important factor in the microbial dissolution of tricalcium phosphate. *World J. Microbiol. Biotechnol.* 24 (7), 1059–1065. <https://doi.org/10.1007/s11274-007-9575-4>.
- Zhou, K., Binkley, D., Doxtader, K.G., 1992. A new method for estimating gross phosphorus mineralization and immobilization rates in soils. *Plant Soil* 147, 243–250. <https://doi.org/10.1007/BF00029076>.
- Zhu, F., Qu, L., Hong, X., Sun, X., 2011. Isolation and characterization of a phosphate solubilizing halophilic bacterium *Kushneria* sp. YCWA18 from Daqiao saltern on the coast of yellow sea of China. *Evid.-Based Complement Altern. Med.* 615032, 1–6. <https://doi.org/10.1155/2011/615032>.



Microbial solubilization of silicon and phosphorus from bedrock in relation to abundance of phosphorus-solubilizing bacteria in temperate forest soils

Giovanni Pastore^a, Sarmite Kernchen^b, Marie Spohn^{a,c,*}

^a Department of Soil Biogeochemistry, Bayreuth Center of Ecology and Environmental Research (BayCEER), University of Bayreuth, Germany

^b Atmospheric Chemistry, University of Bayreuth, Germany

^c Biogeochemistry of Forest Soils, Swedish University of Agricultural Sciences, Uppsala, Sweden

ARTICLE INFO

Keywords:

Biogenic rock weathering
Silicate weathering
P-solubilizing bacteria
Phosphorus solubilization
Silicon solubilization
Organic acids

ABSTRACT

Biogeochemical weathering of bedrock is the most important input of silicon (Si) and phosphorus (P) to forest ecosystems. While soil microbes, and in particular P-solubilizing bacteria (PSB), are known to accelerate the solubilization of Si and P from silicate rocks, our understanding of the mechanisms driving biogenic weathering are still limited. To fill this gap, incubation experiments with weathered parent materials (i.e. basalt, andesite and paragneiss) of four soils and water extracts of the four soils, differing in P stocks, were conducted. We found that the net Si solubilization rate ranged from 5.0 (± 1.8) to 91.0 (± 2.4) nmol m⁻² d⁻¹ across all examined soils. The silicate dissolution rates were negatively related to the decrease in pH (Δ pH) and positively related to the amounts of organic acids released by microbes. We found that the gross P solubilization rates from the parent materials were ~11 times higher at the P-rich site (BBR) compared to the P-poor site (CON). In addition, we determined the abundance and the taxonomic composition of PSB communities in the four soils. The abundance of PSB ranged from 2% at the P-rich site to 22.1% at the P-poor site, indicating that a selective pressure exists in P-poor soils towards a higher abundance of P-solubilizers. Yet, despite the relative high abundance of PSB, the gross P solubilization rates were low in the soils derived from P-poor parent material. The genus *Pseudomonas* was found only in the PSB community at the P-poor site. *Burkholderiales* and *Bacillales* together were by far the two most abundant orders among the PSB communities in all soils and depths. In conclusion, this study shows that PSB are more abundant in P-poor soil than in P-rich soil, while the weathering rate seems to be mostly dependent on the bedrock.

1. Introduction

Phosphorus (P) plays a significant role for a broad array of cellular processes of all organisms (Malhotra et al., 2018). However, only a very limited proportion of P in soils is directly available to plants and microbes (Zhu et al., 2011). Therefore, P is a key factor that limits plant growth in many areas of the world (Ågren et al., 2012). Microorganisms are known to play a major role in the dissolution of minerals (Banfield et al., 1999; Vorhies and Gaines, 2009). Various studies have shown that P-solubilizing bacteria (PSB) can constitute up to 53% of total bacterial numbers and can convert insoluble forms of P to accessible ones (Browne et al., 2009). Among them, bacterial strains of the genus *Pseudomonas*, *Burkholderia*, *Erwinia*, *Enterobacter* and *Klebsiella* have been reported to be efficient P solubilizers (Chung et al., 2005; Oteino

et al., 2015; Lee et al., 2019).

P mobilization from organic matter (i.e. P mineralization) has been comprehensively explored in many studies (Zou et al., 1992; Achat et al., 2010; Spohn and Kuzyakov, 2013; Bünemann, 2015). In contrast, microbial P solubilization from silicate parent materials is not fully understood yet. The term P solubilization refers to desorption of adsorbed P as well as dissolution of P-containing minerals (Hinsinger, 2001; Penn and Camberato, 2019). In soils, P largely derives from apatites dissolution, while other nutrients become mostly available from silicate weathering (Harley and Gilkes, 2000). Although much knowledge has been gained over the past decades, the processes involved in biogenic weathering and the role of soil microbial communities are not yet fully understood (White and Brantley, 2003; Brucker et al., 2020). Bacteria and fungi are capable to secrete different compounds (e.g., organic

* Corresponding author. Department of Soil Biogeochemistry, Bayreuth Center of Ecology and Environmental Research (BayCEER), University of Bayreuth, Germany.

E-mail address: marie.spohn@slu.se (M. Spohn).

<https://doi.org/10.1016/j.soilbio.2020.108050>

Received 12 May 2020; Received in revised form 13 October 2020; Accepted 15 October 2020

Available online 16 October 2020

0038-0717/© 2020 Elsevier Ltd. All rights reserved.

acids; siderophores) that may affect the solubilization of P and other nutrients from rocks in three principal ways: (i) through binding (complexation) of carboxylic (-COOH) and hydroxyl (-OH) groups to metal cations (Al, Fe, Ca), (ii) through exchange of organic compounds and sorbed P (ligand exchange) and (iii) by acidification of the soil solution which causes dissolution since the dissolution of silicates and apatites is largely dependent on pH (Lindsay, 1979; Kpombrekou and Tabatabai, 1994; Welch et al., 2002; Oburger et al., 2011; Wang et al., 2016).

Primary P-rich minerals such as apatites, $\text{Ca}_5(\text{PO}_4)_3(\text{OH}, \text{F}, \text{Cl})$, are present as small inclusions in nearly all silicates. Silicates compose more than 90 percent of Earth's crust and are found as major constituents of most igneous, sedimentary and metamorphic rocks (for a review see White and Brantley, 1995). Igneous rocks contain on average a higher proportion of apatite than metamorphic and sedimentary rocks (Syers et al., 1967; Bacon and Brown, 1992; Nezat et al., 2007; Mehmood et al., 2018). Thus, one would expect a higher release of P from rocks having a higher content of apatite-P. The crystallographic arrangement of silicate minerals is centered around the silicon-oxygen tetrahedron group (SiO_4^{4-}). Silica tetrahedra contains void spaces that are occupied by various metal cations to maintain electrical neutrality (Huang and Wang, 2005). Contrary to P, silicon (Si) is not considered essential for plant growth, although several studies have proven its favorable effects on growth and disease resistance in many crops (Ma, 2004; Guntzer et al., 2012; Duboc et al., 2019). In soils, the content of bioavailable Si varies from 0.003 to 0.45 g Si kg^{-1} (Liang et al., 2015), whereas bioavailable P varies from 0.02 to 0.1 g P kg^{-1} (Yang and Post, 2011). Biogenic silicate weathering can be caused by the same mechanisms as apatite weathering (Uroz et al., 2009; Brucker et al., 2020). In addition, the Si concentration in soil is affected by Si sorption/desorption (Haynes and Zhou, 2020). However, the extent to which microorganisms, and in particular PSB, impact the solubilization rate of silicate minerals is far from being completely understood.

The rates of silicate solubilization by microbial consortia differ depending on the type of parent material and soil properties (Vandevivere et al., 1994; Rogers and Bennett, 2004). Some authors (Gleeson et al., 2006; Uroz et al., 2015) suggested that rocks and soils influence the composition of the microbial communities according to their mineralogy, nutrient content and weatherability. For example, Nicolitch et al. (2016) showed that PSB were significantly more abundant in nutrient-poor than in nutrient-rich soils, but this analysis was limited to the rhizosphere and no rates of P and Si solubilization were determined. To the best of our knowledge, only one study investigated the relationship between the P solubilization rates from weathered bedrocks and the PSB communities together, so far (Spohn et al., 2020). The authors found that P solubilization was higher in moderately-weathered than in strongly-weathered saprolite and that the abundance of PSB was increased in the strongly-weathered saprolite (Spohn et al., 2020).

The principal aim of this study was to examine microbial solubilization of Si and P from different silicate parent materials (i.e. basalt, andesite and paragneiss) in four beech forest soils differing in total P stocks. A second objective was to explore the relationship between the abundance and the community composition of soil PSB and the Si and P solubilization rates. We hypothesized that (i) the rates of biogenic Si and P solubilization from weathered silicate parent materials are correlated with the concentrations of organic acids and protons released by microorganisms; (ii) the rates of microbial P solubilization from silicate parent materials increase with decreasing crystallinity of the parent material since silicates with a high content of Si (paragneiss) tend to weather more slowly than silicates having less Si (basalt, andesite) and (iii) the abundance of PSB increases with decreasing P stocks of the soils. To test these hypotheses, we performed an experiment in which we determined the solubilization of Si and P from four silicate parent materials incubated with soil extracts. Two depth increments were chosen to gain a more complete insight into microbial Si and P solubilization. In each soil extract incubated with the corresponding parent material, the

amounts of organic acids and the pH were recorded at different time points during the incubation. In addition, we determined the abundance and the taxonomy of soil PSB based on a physiological assay in combination with 16s rRNA gene sequencing.

2. Materials and methods

2.1. Study sites and sample collection

Soil samples and weathered silicate parent materials were collected in April 2017 from four even-aged beech (*Fagus sylvatica* L.) forests in Germany (Table 1). Two sites (Mitterfels, MIT and Conventwald, CON) are located on the German southern uplands and two (Bad Brückenau, BBR and Vessertal, VES) on the central uplands encompassing an altitudinal range from 810 to 1025 m above sea level. The mean annual temperatures (MAT) in the four studied sites vary from 4.5 °C at MIT to 6.8 °C at CON, whereas the mean annual precipitations (MAP) vary from 1031 mm at BBR to 1749 mm at CON. The soils of the four study sites are classified as Cambisols (WRB 2015) as described in Lang et al. (2017). The pH of the studied soils ranged from 4.5 to 5.1. The soil texture is shown in Table S2. In each forest stand, the mineral soil was sampled at two depths (30–35 cm and 65–70 cm) from one representative soil pit by combining material taken from five randomly selected spots per depth using small stainless steel spatulas. Silicate parent materials were collected from each soil depth and placed into plastic bags. After being transported to the laboratory, field-moist soil samples were sieved (<2 mm) and root fragments as well as other coarse debris were removed. Subsequently, small aliquots of each soil sample were air-dried for chemical analysis. The remaining soil was stored at (i) 5 °C for the incubation experiments or (ii) frozen at -20 °C for the microbial analysis.

2.2. Sample preparation

Parent materials were crushed using a jaw crusher (Pulverisette, Fritsch, Germany). Each crushed sample was initially sieved through a 0.63 mm sieve. The resulting size fraction was further sieved through a 0.2 mm sieve. The material that did not pass the latter was used for the incubation experiments (0.2–0.63 mm size fraction). The specific surface area (SSA) of each crushed rock was determined by N_2 adsorption on a micromeritics automatic analyzer (Gemini 2375, Shimadzu, Japan). The adsorption isotherms were evaluated for adsorbent surface area with the BET (Brunauer-Emmet-Teller) model by the instrument software (StarDriver v2.03). The soil extracts used for the incubation experiments were prepared as previously described (Pastore et al., 2020). Briefly, 100 g of each soil sample was placed in a polyethylene (PE) bottle, mixed with 1 l of distilled water and shaken at room temperature for 2 h using an overhead shaker. The extracts were filtered through cellulose filters with a particle retention range of 5–8 μm and pores such as to enable the passage of soil microorganisms and small particles of organic matter.

2.3. Chemical analyses of silicate parent material samples

In order to analyze the contents of total P (P_{tot}) and total Si (Si_{tot}) from the parent materials, crushed subsamples were digested using a combination of nitric acid (65% HNO_3), hydrofluoric acid (40% HF), and hydrochloric acid (37% HCl) according to Sandroni and Smith (2002) by ICP-OES (Vista-Pro radial, Varian). The specific absorption of radiation for Si and P was 253 nm and 190 nm, respectively. The reference material used for the analysis consisted of borosilicate glass (SiO_2 53.98%, LGC, SPS-SW2 surface water 2 for Si and SPS-WW2 waste water 2 for P).

2.4. Weathering of silicate parent materials

To determine the net Si and P solubilization rates from silicate parent

Table 1

Basic characteristics and description of the four forest soils and their parent materials at Bad Brückenau (BBR), Mitterfels (MIT), Vessertal (VES) and Conventwald (CON).

Site	Soil depth [cm]	C [g kg ⁻¹]	N [g kg ⁻¹]	P [g kg ⁻¹]	Microbial biomass C [mg kg ⁻¹]	Microbial biomass P [mg kg ⁻¹]	Specific surface area (SSA) of ground parent material [m ² g ⁻¹]	Total P of parent material [g kg ⁻¹]	Total Si of parent material [g kg ⁻¹]
BBR	30–35	42.0	3.2	2.5	170.4	2.0	16.7	3.05	190
	65–70	26.2	1.9	2.0	112.6	1.0	28.1	3.1	183
MIT	30–35	31.4	1.7	0.9	215.7	3.9	3.7	2.1	311
	65–70	26.8	1.4	0.9	140.8	3.3	5.7	1.8	278
VES	30–35	37.7	2.3	1.0	110.6	6.1	10.9	2.6	267
	65–70	12.8	0.8	0.9	102.9	7.8	10.9	2.7	263
CON	30–35	45.7	2.0	0.6	183.9	0.8	3.5	2.05	348
	65–70	7.7	0.6	0.4	126.6	1.2	6.1	0.6	274

Adapted from Lang et al., 2017.)

materials, three incubation experiments were conducted using soil extracts following Brucker et al. (2020) and Pastore et al. (2020). In experiment 1, the total Si and P mobilization rates from parent material were determined. For this purpose, 1 g of each parent material was incubated with 99 ml of the respective soil extract and 1 ml of glucose (3.33 mM). In addition, we performed a control experiment in analogy to experiment 1, but without addition of silicate parent material in order to quantify the mineralization of P from dissolved organic matter, which allowed us to correct the results of experiment 1 for P release from organic matter. Further, sterile control incubations were conducted to determine the effect of the soil extracts on Si and P solubilization. For this purpose, 99 ml of sterile soil solution and 1 ml of glucose (3.33 mM) were added to 1 g of each parent material. All experiments were performed in triplicate. Each incubation flask was loosely covered with aluminium foils which allowed the passage of air and continuously agitated at 20 °C for 14 days on a horizontal shaker.

2.5. Chemical analyses of soil extracts incubated with parent material

In each soil extract, dissolved Si was measured at 0, 7 and 14 days after the beginning of the experiment. Briefly, aliquots of 10 ml were taken and filtered through 0.45-µm cellulose acetate filters. The filtrates were acidified by adding 50 µl of 65% HNO₃ to prevent Si precipitation and then centrifuged at 1500×g for 15 min. The resulting supernatant was analysed for Si by ICP-OES (Vista-Pro radial, Varian, USA). In parallel, the amounts of phosphate released from the parent material in the soil extracts were also quantified. At defined time intervals (0, 2, 3, 5, 7, 11, and 14 days after the beginning of the experiment), 5 ml were taken from the flasks and vacuum filtered using 0.45 µm cellulose acetate filters. The resulting filtrates were analysed for pH and phosphate. The latter was determined according to the molybdenum-blue assay (Murphy and Riley, 1962) and measured with an Infinite M200 Pro microplate reader (Tecan, Switzerland).

2.6. Abundance of P-solubilizing bacteria

The relative abundance of P-solubilizing bacteria (PSB) was assessed by suspending 0.5 g of fresh soil in 49.5 ml of sterile water and shaking for 1 h. Serial dilutions (10⁻², 10⁻³) from each soil suspension were tested to identify the appropriate cell density. Subsequently, from each suspension, an aliquot of 100 µl was aseptically spread on Pikovskaya's agar medium (PVK) and the plates were incubated at 20 °C for 10 days. The PVK medium was composed of: 10 g glucose; 5 g hydroxyapatite; 0.5 g yeast extract; 0.5 g ammonium sulphate; 0.2 g potassium chloride; 0.2 g sodium chloride; 0.1 g magnesium sulphate; 0.002 g ferrous

sulphate; 0.002 g manganese sulphate and 15 g agar-agar in 1 l of distilled water (Pikovskaya, 1948). The pH of the solution was adjusted to 7.0. One-hundred colony-forming units (CFUs) from each soil sample were screened. If a bacterial colony dissolves hydroxyapatite, a halo (clear zone) becomes visible in the otherwise milky medium. In this case, the colony was considered to be formed by a PSB. The relative abundance of PSB was calculated by dividing the number of colonies formed by PSB by the total number of colonies and multiplying by 100.

2.7. Amplification and sequencing analysis of P-solubilizing bacteria (16S rRNA gene)

Bacterial colonies identified as PSB were collected from the PVK agar plates using sterile toothpicks and aseptically transferred into buffer solutions for DNA extraction. Detailed procedure describing amplification of 16S rRNA genes, quality trimming and annotation was provided previously by Widdig et al. (2019). Briefly, genomic DNA of bacterial colonies was extracted using the NucleoMag® Tissue kit on a KingFisher platform (Thermo Fisher Scientific, Massachusetts, USA) and diluted 100-fold with nuclease free water according to the manufacturer's instructions. The 16S fragment covering variable regions V5-V8 were amplified using primers 799F and 1391R as recommended in Beckers et al. (2016). PCR products were purified using the NucleoMag® 96 PCR cleanup kit. PCR products were sequenced (Sanger sequencing, GATC Biotech) using primer 799F.

2.8. Sequencing data analysis

Sequence data were processed using Geneious v. 11 (Biomatters Ltd., New Zealand). The sequences were searched for PCR primer sequences (799F and 1391R) and for low quality bases, which were excluded from sequence database searches. Sequence similarity searches were conducted against the nr/nt nucleotide database at NCBI as well as the NCBI RefSeq Loci 16S database. Sequences were aligned using MAFFT software (v. 7.388; Katoh and Standley, 2013). Sequences with a 98% cut-off similarity were clustered into operational taxonomic units (OTUs) and the name of the lowest common rank in the nomenclature hierarchy was chosen. The OTU classification method is a commonly used approach to estimate microbial diversity and demonstrated to be ecologically consistent across habitats (Schmidt et al., 2014; Mysara et al., 2017). Only the non-redundant top hits were selected for taxonomic annotation. For this purpose, each sequence was compared with all other sequences and sequences sharing identity above 98% identity were assigned to one taxon. OTUs assignment was done using the NCBI database, considering that eleven species of the genus *Burkholderia* have

been transferred to the genus *Paraburkholderia* and three species of the genera *Burkholderia* have been transferred to the new genus *Caballeronia* gen. nov. which represents a distinctive clade in phylogenetic trees (Dobritsa and Samadpour, 2016). Major phylogenetic changes were detected at the order and genus levels. Based on their partial 16S rRNA gene sequence, a phylogenetic tree for each of the two most abundant genera (*Burkholderia* sp. and *Peanibacillus* sp.) was constructed, using *Ralstonia pickettii* (AY741342) and *Brevibacillus brevis* (AB271756) as outgroups, respectively. Phylogenetic trees were reconstructed and edited in MEGAX (v. 10.1.5) based on the neighbor-joining method with 1000 bootstrap replicates. The maximum composite likelihood method was the chosen distance method. The partial 16S rRNA gene sequences were deposited in GenBank (<https://www.ncbi.nlm.nih.gov/genbank/>) under the accession numbers MN727301-MN727311 and MN728272-MN728288.

2.9. Soil microbial biomass

Soil microbial biomass C (MBC) and P (MBP) were determined using the chloroform fumigation-extraction method (Brookes et al., 1982; Vance et al., 1987). Briefly, 10 g of fresh soil were split into two equal parts, of which 5 g were fumigated at room temperature for 24 h with ethanol-free CHCl_3 . Organic C was extracted from the fumigated and non-fumigated samples using 0.5 M K_2SO_4 with a soil: solution ratio of 1:5 and measured by a TOC/TN analyzer (Multi N/C 2100S, Analytik Jena, Germany). Dissolved P was extracted from the fumigated and non-fumigated samples using a solution of 0.025 M HCl and 0.03 M NH_4F (Bray-1 extractant) with a 1:10 soil to solution ratio (Bray and Kurtz, 1945) and determined using the molybdenum-blue assay (Murphy and Riley, 1962). Microbial biomass C and P were calculated as the difference between extractable C and P in the fumigated and non-fumigated soil samples using a conversion factor of 2.22 for MBC (Joergensen et al., 1996) and 2.5 for MBP (Brookes et al., 1982; Jen-

$$\text{Gross P solubilization rate (nmol d}^{-1}\text{)} = \frac{(\text{Net Si solubilization rate [nmol d}^{-1}\text{]} * \text{P content [g kg}^{-1}\text{]})}{\text{Si content [g kg}^{-1}\text{]}} \quad (3)$$

kinson et al., 2004).

2.10. Organic acids

The amounts of four organic acids (citric, oxalic, 2-keto-D-gluconic and D-gluconic) were determined in filtered samples from the soil extracts on day 7 and 14 after the beginning of the experiment. All filtrates were examined by means of high-performance liquid chromatography (Agilent series 1100, USA) coupled to a diode array HPLC detector (DAD) and a mass spectrometry (Agilent 6130 single quadrupole). Separation of the organic acids was carried out on a hydro-reversed-phase column (Phenomenex Synergi 4 u Hydro-RP 80A) combined with a guard column. Organic acids were identified based on their retention times and selected ions in negative ionization mode. Quantification was performed according to the external standard calibration method. HPLC-MS data were processed using the Agilent's Chemstation software package (v. 3.3.1). The amounts of each organic acid were calculated by multiplying the corresponding concentration (mg l^{-1}) in the soil extracts by the volume (l) present in the flask at the time of sampling and subsequently expressed in μmol . In addition, the concentration of the carboxylic groups was calculated from the concentrations of organic acids and the respective number of carboxyl groups they contain.

2.11. Calculation and statistics

The amounts of Si and P in the incubated soil extracts were calculated by multiplying the element concentration (nmol l^{-1}) by the volume (l) of the soil extract at the time of sampling. The total Si mobilization rates were computed according to the following equation (Eq. (1)):

$$\text{Total Si mobilization rate (nmol d}^{-1}\text{)} = \frac{(\text{Si[nmol]}_{\text{day14}} - \text{Si[nmol]}_{\text{day0}})}{14 [\text{days}]} \quad (1)$$

Where Si[nmol] represents the amount of Si at the end (day 14) and the beginning (day 0) of the experiment. Additionally, to determine the chemical effects of the soil extracts on the amounts of Si released from the silicate parent material, the amounts of Si released in the sterile control were also calculated. The net Si solubilization rate (nmol d^{-1} , Eq. (2)) from each silicate parent material was estimated as the difference between the total Si mobilization rate and the release rate determined in the sterile experiment:

$$\begin{aligned} \text{Net Si solubilization rate (nmol d}^{-1}\text{)} &= \text{total Si mobilization rate (nmol d}^{-1}\text{)} \\ &- \text{Si release rate in sterile control (nmol d}^{-1}\text{)} \end{aligned} \quad (2)$$

We consider this a net rate since we cannot exclude microbial immobilization (i.e., uptake) of Si. The net Si solubilization rates were divided by the corresponding amount of silicate parent material utilized as well as by the respective specific surface area ($\text{m}^2 \text{g}^{-1}$) of the ground parent material to result in a final rate expressed as $\text{nmol m}^{-2} \text{d}^{-1}$. Also, we estimated the solubilization of P from silicate parent materials based on the Si and P content of the parent materials and the Si solubilization rates using the equation below (Eq. (3)):

We consider this a gross rate because microbial immobilization (i.e., uptake) of P is not taken into account here and the net P solubilization is likely smaller due to microbial P immobilization. The gross P solubilization rates were divided by the corresponding amount of silicate parent material utilized as well as by the respective surface area ($\text{m}^2 \text{g}^{-1}$) to result in a final rate expressed as $\text{nmol m}^{-2} \text{d}^{-1}$. To check if variables were normally distributed, the Shapiro-Wilk test was performed ($P > 0.05$). Further, all data sets were tested for equality of variance using Levene's test. When variances were not significantly different between groups, analysis of variance (one-way ANOVA) was applied to test for differences between soil chemical properties, net Si solubilization rates and gross P solubilization rates. Differences in net Si solubilization rates and the relative abundance of PSB between the two soil depths of each soil were analysed by *t*-test followed by post-hoc Tukey HSD ($P < 0.05$). The non-parametric Kruskal-Wallis H test was used with a pairwise Wilcoxon test when variances were unequal. Relations between net Si solubilization rates and chemical properties of the soil extracts were assessed by Spearman rank correlations. Additionally, linear regressions for net Si solubilization and the variables pH and carboxyl groups (-COOH) determined in the soil extracts were conducted. All statistical analysis was performed using SigmaPlot (version 13.0, Systat Software, San Jose, California, USA).

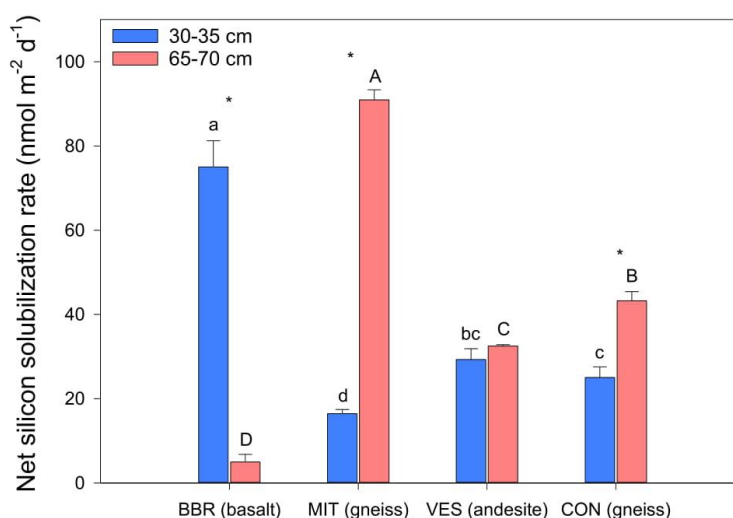


Fig. 1. Net Si solubilization rates for silicate parent materials incubated with glucose in aqueous extracts obtained from the four forest soils. The rates were calculated per specific surface area and over 14 days of incubation. The samples were taken at two soil depths (30–35 and 65–70 cm). Bars show means, and error bars indicate standard deviations ($n = 3$). Different letters indicate significant differences tested separately for the two soil depths by one-way ANOVA followed by post-hoc Tukey HDS ($P < 0.05$). Stars indicate significant differences between the two depths of each soil, tested by t -test followed by post-hoc Tukey HDS ($P < 0.05$).

3. Results

3.1. Net Si solubilization from silicate parent material

The concentrations of dissolved Si ranged between 2.9 and 13.0 mg l⁻¹ after two weeks of incubation of the soil with weathered parent materials and glucose. The concentrations of dissolved Si from weathered parent materials and autoclaved soil solution (sterile control) were equal on average to 0.4 mg l⁻¹. The Si concentrations were up to 32 times higher in the biotic experiment compared to the abiotic experiment, indicating that microbes strongly enhance silicate dissolution. Rates of Si solubilization normalized to the surface area of silicates differed significantly among the four soils and the two soil depth increments (Fig. 1). The net Si solubilization rate from the soil extracts incubated with the respective parent material and glucose ranged between 5.0 (± 1.8) and 91.0 (± 2.4) nmol m⁻² d⁻¹. At 30–35 cm depth, BBR (basalt) had the highest net Si solubilization rate in comparison to the other three sites, whereas MIT (paragneiss) had the lowest ($P < 0.05$). At 65–70 cm depth, the net Si solubilization rate in MIT was significantly higher than in the other soils (+70%; $P < 0.01$). We found that the Si concentrations increased during the first week of incubation, while the pH showed a twofold trend: it increased in the first 3 days and then decreased from day 4 to day 6 (Fig. S1). After day 7 no substantial changes in pH were recorded at all sites. At site MIT, the soil extracts from 65 to 70 cm depths showed the highest pH decline compared to the extracts from the other soils (Figs. S1–b). Further, linear regression analysis pointed out that the Si content of the parent material at 30–35 cm depth was negatively related with the Si solubilization rate ($R^2 = 0.63$, $P < 0.001$), whereas at 65–70 cm depth, a positive relationship was observed ($R^2 = 0.93$, $P < 0.001$).

3.2. P solubilization from silicate parent material

We did not measure net P solubilization but rather P immobilization, as indicated by a steady decline in the concentration of phosphate over the two-week period (data not shown). The likely reason for this is that microorganisms took up more P than they released from the parent material. However, we determined the gross P solubilization rates from the P and Si content of the parent materials and the Si solubilization rate based on stoichiometric considerations. This approach allowed us to estimate the gross release of P. Gross P solubilization ranged from 0.1

Table 2

P solubilization from four weathered parent materials at two different soil depths (30–35 and 60–65 cm). The stoichiometrically-derived gross P solubilization rates were determined according to the measured Si and P content of the respective weathered parent material and the amount of Si that was released over the course of 14 days. Mean values and standard deviations (\pm SD, in parentheses) are shown ($n = 3$). Uppercase and lowercase letters show significant differences tested separately for the two soil depths by one-way ANOVA, followed by post-hoc Tukey HDS ($P < 0.05$).

Site	Parent material	Soil depth [cm]	Gross P solubilization rate [nmol m ⁻² d ⁻¹] ^a
BBR	Basalt	30–35	1.1 (± 0.1) ^a
		65–70	0.1 (± 0.03) ^b
MIT	Paragneiss	30–35	0.1 (± 0.01) ^d
		65–70	0.5 (± 0.01) ^A
VES	Trachyandesite	30–35	0.3 (± 0.02) ^b
		65–70	0.3 (± 0.07) ^A
CON	Paragneiss	30–35	0.1 (± 0.01) ^f
		65–70	0.1 (± 0.00) ^b

^a Computed per g of parent material.

nmol m⁻² d⁻¹ (± 0.00) to 1.1 nmol m⁻² d⁻¹ (± 0.1). Overall, the gross P solubilization rates were significantly higher at the P-rich site (BBR) compared to the P-poor site (CON) in the upper soil depth (Table 2).

3.3. Organic acids in soil extracts

We found that the amounts of organic acids from BBR and VES were significantly larger than those measured at sites MIT and CON ($P < 0.05$). Further, our data show that monocarboxylic acids (D-gluconic and 2-keto-D-gluconic acid) represented together up to 88% of all detected acids. At site BBR, 2-keto-D-gluconic acid was found in higher amounts, whereas in the other three soil extracts D-gluconic acid was predominant (Fig. 2). We found that the sum of the four organic acids decreased significantly from day 7 to day 14 in all soil extracts (Fig. 2, P

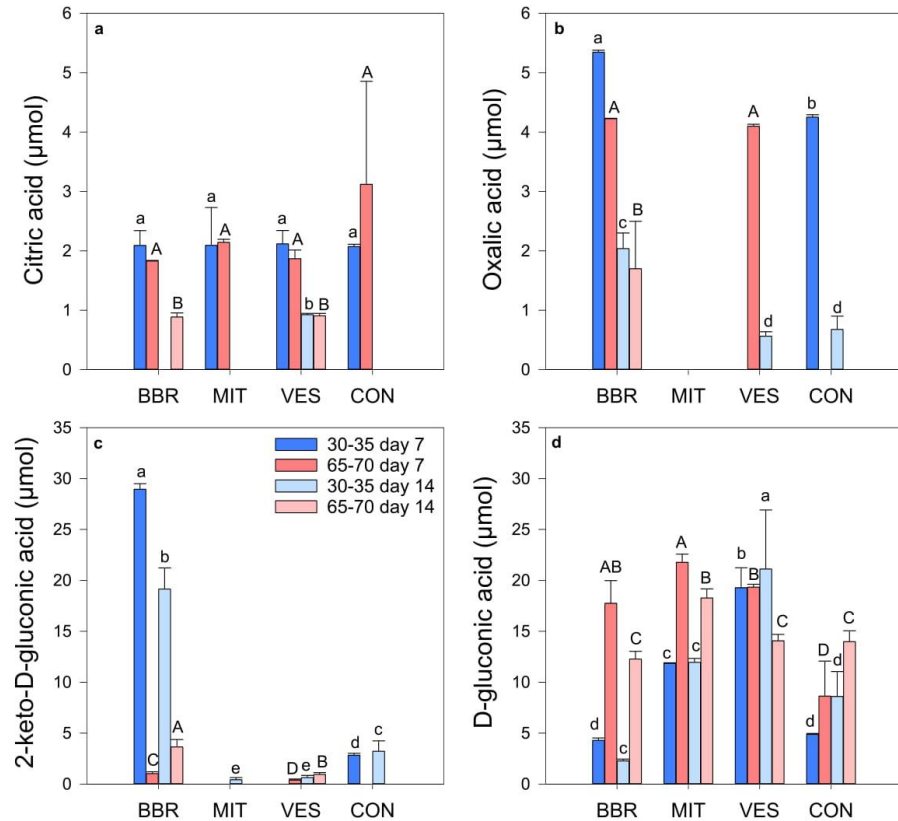


Fig. 2. Amounts of citric (a), oxalic (b), 2-keto-D-gluconic (c), and D-gluconic (d) acids measured at day 7 and 14 of the incubation experiment conducted with soil extracts from two different soil depths (30–35 and 65–70 cm). Bars represent means and error bars indicate standard deviations ($n = 3$). Different lowercase and uppercase letters show significant differences between soils and soil depths tested separately for day 7 and day 14 by one-way ANOVA followed by post-hoc Tukey HSD ($P < 0.05$). Stars indicate significant differences between two depths of one soil, tested by t -test followed by post-hoc Tukey HSD ($P < 0.05$).

Table 3

Relationships between the net Si solubilization rates (Si_{sol}) and the changes in pH (ΔpH) and the mean concentrations of carboxyl groups ($-\text{COOH}$) determined in the soil extracts over 14 days and calculated separately for the two soil depths (30–35 cm and 65–70 cm).

Mineral soil depth [cm]	Linear equation	Coefficient of determination (R^2) and p-value
30–35	$\text{Si}_{\text{sol}} = -3.0792x + (16.209 * \Delta\text{pH})$	0.43, $P < 0.05$
30–35	$\text{Si}_{\text{sol}} = 0.5979x - (3.1603 * \text{COOH})$	0.51, $P < 0.05$
65–70	$\text{Si}_{\text{sol}} = -5.7113x + (34.086 * \Delta\text{pH})$	0.73, $P < 0.05$
65–70	$\text{Si}_{\text{sol}} = 0.3093x + (4.7554 * \text{COOH})$	0.14, $P < 0.05$

< 0.05), except at site CON. Citric acid was detected only during the first week of incubation in MIT and CON, but not thereafter (Fig. 2-a). The amounts of carboxyl groups in the soil extracts were not significantly correlated with pH ($P > 0.05$). Also, we found that the amounts of carboxyl groups measured in the soil extracts at 30–35 cm depth explained 51% of the variation in the net Si solubilization, while at 65–70 cm depth they explained only 14% of the overall variability (Table 3).

3.4. Relative abundance and community composition of PSB

The relative abundance of PSB ranged from 2.0% to 22.1% of all bacterial colonies from all soils and soil depth increments (Fig. 3). Overall, we found that the relative abundance of PSB was significantly higher in CON (at both soil depths) than in any other soil ($P < 0.001$). At 65–70 cm depth, the abundance of PSB was significantly larger at site BBR than at MIT and VES. In total, 333 PSB colonies were identified by 16S rRNA gene sequence analysis. The sequenced PSB belonged to five phyla (Proteobacteria, Cyanobacteria, Firmicutes, Actinobacteria, Deinococcus-Thermus) and seven different classes (α -Proteobacteria,

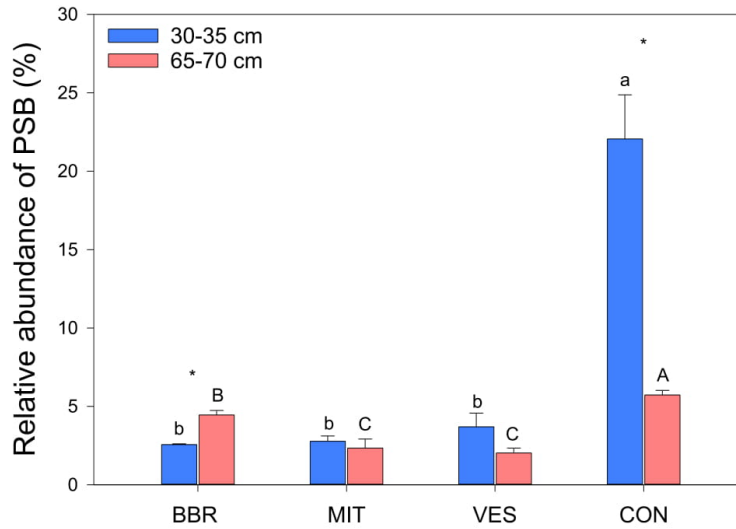


Fig. 3. Relative abundance of P-solubilizing bacteria (PSB) in the four forest soils at two different depths (30–35 and 65–70 cm). Bars represent means and error bars indicate standard deviations ($n = 3$). Different uppercase and lowercase letters indicate significant differences between sites tested separately for each soil depth using one-way ANOVA followed by post-hoc Tukey HSD ($p < 0.05$). Stars indicate significant differences between the two depths of each soil, tested by t -test followed by post-hoc Tukey HSD ($P < 0.05$).

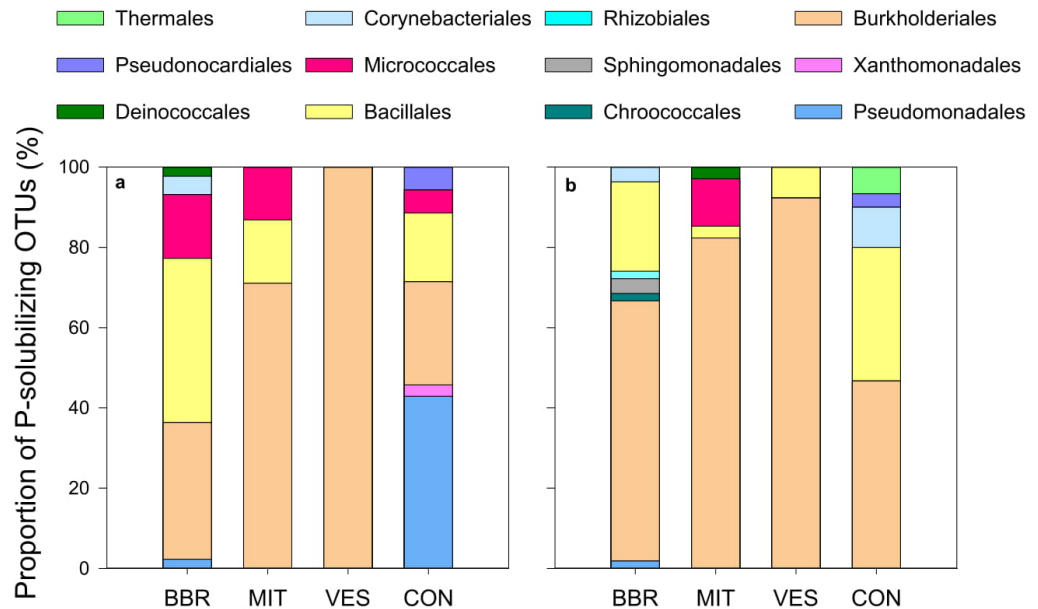


Fig. 4. Relative abundance of different OTUs of P-solubilizing bacteria (PSB) from four forest soils in 30–35 cm (a) and 60–65 cm (b) soil depth. Isolates identified as PSB were grouped into operational taxonomic units (OTU) at 98% cut-off similarity. Taxonomic classification of isolates is shown at the order level.

β -Proteobacteria, γ -Proteobacteria, Cyanophyceae, Bacilli, Actinobacteria, Deinococci). At 30–35 cm depth, *Bacillales* dominated at the site BBR and *Pseudomonadales* at site CON. *Burkholderiales* was the dominant order in MIT and VES (Fig. 4-a). At 65–70 cm depth, *Burkholderiales* were found to be the dominant order at all sites (Fig. 4-b). For comparative purposes with other studies, the relative abundance of

different OTUs of PSB is shown also at the genus level in the supplementary material (Fig. S2). We found that *Caballeronia* sp., *Collimonas* sp., *Paraburkholderia* sp. and *Paenibacillus* sp. were present in all soils, while *Herbaspirillum* sp. and *Variovorax* sp. were found in all soils except MIT and CON, respectively. Among all sequenced PSB colonies, 51 different OTUs were obtained as defined by clustering of the 16S rRNA

gene similarity. Of these, *Paenibacillus* (17 OTUs), *Burkholderia* (11 OTUs), and *Pseudomonas* (6 OTUs) were the most abundant across all sites. Since *Paenibacillus* sp. and *Burkholderia* sp. made up together at least 70% of all P-solubilizing OTUs across all sites, we further explored the species composition for the two genera. A significant genetic diversity existed within the same OTU species from the four tested soils. Overall, at site BBR we found the highest genetic diversity, while the lowest was found at site VES. The mineral composition of the bedrock had a strong effect on the distribution of *Burkholderia* species, but not on the distribution of *Paenibacillus* species (Figs. S3–S4).

4. Discussion

4.1. Factors controlling the weathering of silicate parent materials

Here we found that the Si solubilization rates were 7–32 times higher in the biotic experiment compared to the abiotic experiment (sterile conditions) indicating that microbes exert a strong biological control over the dissolution of silicates, especially when provided with an easily accessible C source. High Si concentrations in the solution went along with high P concentrations. The reason for this can be that Si and P compete for binding sites on mineral surfaces, as suggested by other authors who showed that with high concentrations of Si more P was dissolved in peat and permafrost soils (Schaller et al., 2019; Hömberg et al., 2020). We found a significant positive relationship between the carboxyl groups of the organic acids and the net Si solubilization rates (Table 3), in accordance with Hömberg et al. (2020). Organic acids accounted for 51% of the total variability in the net Si solubilization rates in the extracts from the upper soil depth. These findings suggest that organic acids effectively complexed metal cations present in the crystal lattice (i.e. Al, Fe, Ca, Mg) or served as silicon substituents (ligand exchange), thereby promoting the solubilization reaction (Liu et al., 2006; Violante et al., 2010; Smits and Wallander, 2017; Lee et al., 2019). Our results are in agreement with several previous studies reporting that the formation of stable complexes of metal ions and organic ligands results in an increase in dissolved Si in the soil solution (Welch and Ullman, 1993; Vandevivere et al., 1994; Blume et al., 2016). Dissolution rates depend on the amounts of functional groups (-COOH) that can react with mineral surfaces as well as on the strength of the bond that is established between the ligand (mono-, di- and tri-carboxylic acids) and the metal ion. The net Si solubilization rates from basalt (BBR) were up to three times higher than the net Si solubilization rates from paragneiss and andesite in the soil extracts from the upper soil depth (Fig. 1). As shown in Table S1, we found that the amounts of carboxyl groups at site BBR were 1.6–3.7 times higher than the amounts of carboxyl groups in the other soil extracts after seven days of incubation. Oxalic and 2-keto-D-gluconic acids made up together 84% of the total carboxyl groups measured in the soil extract from BBR (Fig. 2). Therefore, the higher dissolution of basalt compared to the other parent materials likely resulted from the higher amounts of carboxyl functional groups released by microbes in the soil BBR, especially mono- and di-carboxylic acids (Goldstein, 1995).

In the soil extracts from the lower soil depth, organic acids explained only 14% of the variation in the net Si solubilization rates, whereas the change in pH accounted for 73% of the total variability. Thus, in the lower soil depth, complexation by organic acids played only a marginal role for the Si solubilization rates possibly as a result of a lower soil microbial activity, as also described previously (Vandevivere et al., 1994; Sverdrup, 2009). The negative relationship between the decrease in pH (Δ pH) and the net Si solubilization rates suggests that the release of Si from silicates resulted from acidification of the soil extract. Our results agree with Drever (1994) who found that silicate dissolution rate

depends on pH: below pH 4–5, the rate increases with decreasing pH, in the circumneutral region the rate is pH-independent, and at pH values above 8 the rate increases with increasing pH. The decrease in pH (Δ pH) was particularly pronounced in the soil extracts from MIT and CON (paragneiss) where the pH significantly decreased during the incubation in comparison to the pH of the soil extracts from BBR (basalt) and VES (andesite). With decreasing pH of the soil extract there was an increase in the number of protons capable to binding to oxygen atoms at the mineral surfaces. Protonation induced increase in reactivity of surface sites weakens the metal cations-oxygen bonds, thus favoring dissolution of the mineral (Hinsinger, 2001; Brown et al., 2008). Taken together our findings confirm the first hypothesis that the dissolution of silicates in these acid soil extracts is primarily controlled by a decrease in pH and the release of organic acids by microbes (Harley and Gilkes, 2000; Cama and Ganor, 2006). In addition, this study shows how the general mechanisms of silicates dissolution are impacted by the different organic acids released by microbes from different soils and soil depths.

4.2. Organic acids

We found that the amounts of organic acids released by microbial communities in our study were fairly low compared to other solubilization experiments (Frey et al., 2010; Li et al., 2016) which we relate to the initial acidic conditions of our soil extracts. Marra et al. (2015) showed that the pH of the soil solution significantly affects the growth as well as the biochemical processes that microbes perform and, therefore, the total amounts of acids they produce. Marra et al. (2015) showed that at a relatively high pH (~pH 7.0), the production of organic acids was up to 25% greater than at pH 5.0, which was the mean pH measured in our experiments. The organic acid concentrations decreased over time indicating that microbes may have quickly faced conditions of low C availability. In addition, the increase in pH in the soil extracts during the first 3 days of incubation suggests the metabolization (decomposition) of organic acids by organisms at the early stages of the experiment (Jones et al., 2003; Sauer et al., 2008). Most of the pH variation in the soil extracts took place in the first days of incubation (Fig. S1). Therefore, it is plausible that the production of organic acids must have been high during this phase, in particular after glucose addition, to then decline thereafter. Therefore, the relatively low detection of organic acids at day seven of the incubation might be the result of previous intense microbial utilization of organic acids, similarly to what was documented by Menezes-Blackburn et al. (2016) who found that nearly all organic acids were degraded by soil microbes within 24 h of incubation.

Considering the pK_a values of the four tested organic acids, their total amounts as well as the pH values of the solutions, only 8.9%–10.1% of protons released during the incubations were likely derived from organic acids after 7 days of incubation, when the peak of solubilization occurred. Therefore, the production of organic acids by microbes did not contribute significantly to the acidification of the soil extracts from day 7 to day 14. We assume that the acidification of the soil extracts was mainly due to carbonic acid production based on CO_2 respired by the microorganisms (Cornelis and Delvaux, 2016; Kanakiya et al., 2017).

4.3. The role of parent material in P nutrition strategies

Our results suggest that the gross P solubilization rates from parent materials in the upper soil depth were ~11 times higher at the P-rich site (BBR) compared to the P-poor site (CON) (Table 2). This finding supports the idea that the proportion of plant-available P derived from the bedrock, as opposed to that derived from the soil organic matter, decreases along the geosequence of the four soils from BBR to CON (Lang et al., 2017). As hypothesized by Lang et al. (2016), plant and microbes

at sites rich in mineral-bound P introduce P from primary minerals into the P cycle (acquiring systems). In contrast, ecosystems poor in mineral-bound P recycle P between soils and plants more efficiently (recycling systems). Overall, the gross P solubilization rates calculated for basalt (BBR) and andesite (VES) point out at a higher release of P from these weathered rocks than for paragneiss (MIT, CON) (Table 2). Similarly, some authors indicated that basalts have a larger weathering rate than other major continental silicate rocks (Dessert et al., 2003; Wolff-Boenisch et al., 2006). Taken together, our findings partially confirm the second hypothesis that in the upper soil depth, the rates of microbial gross P solubilization increased with decreasing crystallinity of the weathered bedrock (paragneiss < andesite < basalt).

4.4. Abundance and activity of PSB

We found that the abundance of PSB in the four mineral soils ranged from 2% at VES to 22.1% at CON (Fig. 3) which is in accordance with previous studies reporting that the relative abundance of PSB ranges from 0.5% to 53% in soils (Kucey, 1983; Chen et al., 2006; Browne et al., 2009; Azziz et al., 2012; Widdig et al., 2019). The higher relative abundance of PSB in P-poor environments such as CON might be the result of a selective pressure which favors organisms that actively mobilize inorganic P when P is scarce. The lower occurrence of PSB in nutrient-rich soils might be related to a lower microbial investment in the processes of P solubilization when nutrients are easily available. This finding is in accordance with other authors who found that the abundance of PSB is higher in P-poor environments than in P-rich environments (Mander et al., 2012; Nicolitch et al., 2016; Widdig et al., 2019; Spohn et al., 2020). The higher abundance of PSB at the P-poor site (CON) fits well with the high P release rates from hydroxyapatite at this site (Pastore et al., 2020), indicating that the abundance of PSB is related to the capacity of the microbial community to release P from apatite. On the contrary, despite the higher abundance of PSB at the P-poor site (CON) the gross P solubilization rates from the parent material at this site (paragneiss) were relatively low. This apparent incongruence was likely due to the fact that all structurally complex silicates undergo a stepwise weathering in the natural environment and that apatites are shielded by other minerals from biochemical weathering (White, 2003).

4.5. Diversity of PSB communities

We found that *Burkholderiales* and *Bacillales* together were by far the two most abundant bacterial orders in all soils and depths (Fig. 4). Results from the BLASTn analysis showed a high intraspecific diversity within *Burkholderiales* and *Bacillales*, especially at sites BBR and CON. *Burkholderiales* and *Bacillales* are adapted to live in C and N-rich environments (Fierer et al., 2007; Mandic-Mulec et al., 2015). We observed that the distribution of *Burkholderiales* seems highly influenced by the mineral chemistry of the rocks, with some members enriched in the presence of high-weatherable minerals and others enriched in the presence of less-weatherable minerals. *Bacillales* appeared less affected by the mineral composition of the rocks, and thus showed no significant variations between the different parent materials (Fig. S4). This finding fits with the recent view that members within the same bacterial order might be adapted to different functional strategies (Ho et al., 2017). Notably, we found the genus *Arthrobacter* only at sites BBR and MIT. This finding is of particular interest since the studied soils are characterized by the prevalence of P bound to Fe oxyhydroxides (Prietz et al., 2016) and members of the genus *Arthrobacter* are relatively effective at mobilizing iron (Nicolitch et al., 2019). Our data show that the genus *Pseudomonas*, which is reputed to have superior P solubilization ability among the PSB (Gulati et al., 2008; Browne et al., 2009), was only found at the P-poor site CON, suggesting the existence of a selective advantage for bacteria with this functional trait under P-poor conditions. As detailed in Fig. S2, *Pseudomonas* predominated in the upper soil depth. Some authors (Sutra et al., 2000; Qessaoui et al., 2019) showed that

members of the genus *Pseudomonas* represent typically root-associated microorganisms and might have positive effects on plant yields.

Soil PSB are known to also solubilize Si (Kang et al., 2017; Adhikari et al., 2020). We found that the highest release of Si occurred at site BBR and coincided with a significant prevalence of *Bacillales* which represented alone 41% of all PSB OTUs in this soil. Olsson-Francis et al. (2015) found that *Bacillales* solubilized up to 32.8% more Si from basalt than other bacterial groups. Surprisingly, in the lower soil depth, the highest Si solubilization rates were measured at site MIT where *Burkholderiales* represented ~80% of all PSB OTUs. Previous studies showed that the members of the genus *Burkholderia* exhibit stronger mineral weathering effectiveness compared to members of the genera *Bacillus* and *Paenibacillus* (Collignon et al., 2011; Lepleux et al., 2012; Wang et al., 2014; Nicolitch et al., 2019). Therefore, the high release of Si from paragneiss at site MIT might be due to the higher occurrence of *Burkholderia alpina* that likely acidified the soil extract. Our findings are partially in accordance with Bist et al. (2020) who showed that *Bacillus* and *Pseudomonas* in addition to *Sphingobacterium* have the capacity to strongly solubilize Si.

5. Conclusions

Taken together, we found that Si solubilization was increased by microbial activity. Si solubilization was negatively related to the observed decrease in pH (proton-promoted dissolution) and positively related to organic acids released by microbes (ligand-promoted dissolution). The four measured organic acids did not contribute significantly to the acidification of the soil extracts. Thus, the acidification was likely due to carbonic acid production based on CO₂ respired by microorganisms. Stoichiometrically-derived gross P solubilization rates in the upper soil depth were much higher at the P-rich site (BBR) compared to the P-poor site (CON). However, at site CON we found a significantly higher abundance of PSB compared to other soils. This finding might be related to a higher microbial investment in the processes of P solubilization in the P-poor soil, suggesting that P availability is a selective force driving the occurrence of bacteria with this functional trait. Overall, *Burkholderiales* and *Bacillales* were the two most widely occurring PSB OTUs across the four mineral soils and the genus *Pseudomonas*, reputed to have superior P solubilization ability among the PSB, was only found at the P-poor site. In conclusion, this study shows that the activity and the taxonomic composition of PSB varied significantly across the four forest soils and underpinned the observed differences in Si solubilization rates.

Declaration of competing interest

The authors declare that they have no known competing financial interests or personal relationships that could have appeared to influence the work reported in this paper.

Acknowledgements

This research was funded by the German Research Foundation (DFG) as part of the project SP 1389/4-2 of the priority program "Ecosystem nutrition: Forest strategies for limited phosphorus resources". The authors gratefully acknowledge the assistance of Alfons Weig, Michaela Hochholzer and Andrea Kirpal of the Keylab for Genomics and Bioinformatics for sequencing the bacterial colonies. We thank Baoli Zhu and Dheeraj Kanaparthi for assistance with the phylogenetic trees. Further, we thank Eduardo Vazquez, Meike Widdig and Alexander Guhr for their helpful comments on a previous version of the manuscript. We also thank members of the Laboratory for Analytical Chemistry (BayCEER) for the chemical analyses. Further, we thank Karin Söllner, Renate Krauß and Ralf Mertel for assistance provided in the laboratory. Thanks to Uwe Hell for help in sample collection and handling of the silicate parent materials.

Appendix A. Supplementary data

Supplementary data to this article can be found online at <https://doi.org/10.1016/j.soilbio.2020.108050>.

References

- Achat, D.L., Bakker, M.R., Zeller, B., Pellerin, S., Bienaimé, S., Morel, C., 2010. Long-term organic phosphorus mineralization in spodosols under forests and its relation to carbon and nitrogen mineralization. *Soil Biology & Biochemistry* 42, 1479–1490. <https://doi.org/10.1016/j.soilbio.2010.05.020>.
- Adhikari, A., Lee, K.E., Khan, M.A., Kang, S.M., Adhikari, B., Imran, M., Jan, M., Kim, K.M., Lee, I.J., 2020. Effect of silicate and phosphate solubilizing rhizobacterium *Enterobacter ludwigii* GAK2 on *Oryza sativa* L. under cadmium stress. *Journal of Microbiology and Biotechnology* 30, 118–126. <https://doi.org/10.4014/jmb.1906.06010>.
- Ågren, G.L., Wetterstedt, J.Å.M., Billberger, M.F.K., 2012. Nutrient limitation on terrestrial plant growth – modeling the interaction between nitrogen and phosphorus. *New Phytologist* 194, 953–960. <https://doi.org/10.1111/j.1469-8137.2012.04116.x>.
- Azziz, G., Bajsa, N., Haghjoui, T., Taulé, C., Valverde, A., Igual, J., Arias, A., 2012. Abundance, diversity and prospecting of culturable phosphate solubilizing bacteria on soils under crop–pasture rotations in a no-tillage regime in Uruguay. *Applied Soil Ecology* 61, 320–326. <https://doi.org/10.1016/j.apsoil.2011.10.004>.
- Bacon, C.R., 1992. Partially melted granodiorite and related rocks ejected from crater lake caldera, Oregon. In: Brown, Chappell (Eds.), *The Second Hutton Symposium on the Origin of Granites and Related Rocks*, 83. Transactions of the Royal Society of Edinburgh: Earth Sciences, pp. 27–47. <https://doi.org/10.1017/S0263593300007732>.
- Banfield, J.F., Barker, W.W., Welch, S.A., Taunton, A., 1999. Biological impact on mineral dissolution: application of the lichen model to understanding mineral weathering in the rhizosphere. *Proceedings of the National Academy of Sciences of the United States of America* 96, 3404–3411. <https://doi.org/10.1073/pnas.96.7.3404>.
- Beckers, B., Op De Beeck, M., Thijs, S., Truyens, S., Weyens, N., Boerjan, W., Vangronsveld, J., 2016. Performance of 16s rDNA primer pairs in the study of rhizosphere and endosphere bacterial microbiomes in metabarcoding studies. *Frontiers in Microbiology* 7, 650. <https://doi.org/10.3389/fmicb.2016.00650>.
- Bist, V., Niranjana, A., Ranjan, M., Lehri, A., Seem, K., Srivastava, S., 2020. Silicon-solubilizing media and its implication for characterization of bacteria to mitigate biotic stress. *Frontiers of Plant Science* 11, 28. <https://doi.org/10.3389/fpls.2020.00028>.
- Blume, H.P., Brümmer, G.W., Fleige, H., Horn, R., Kandeler, E., Kögel-Knabner, I., Kretzschmar, R., Stahr, K., Wilke, B.M., 2016. Inorganic soil components – minerals and rocks. In: Stahr, K. (Ed.), *Scheffer/Schachtschabel Soil Science*. Springer-Verlag GmbH Berlin Heidelberg, pp. 7–52. https://doi.org/10.1007/978-3-642-30942-7_2.
- Bray, R.H., Kurtz, L.T., 1945. Determination of total, organic, and available forms of phosphorus in soils. *Soil Science* 59, 39–45. <https://doi.org/10.1097/00010694-194501000-00006>.
- Brookes, P.C., Powlson, D.S., Jenkinson, D.S., 1982. Measurement of microbial biomass phosphorus in soil. *Soil Biology & Biochemistry* 14, 319–329. [https://doi.org/10.1016/0038-0717\(82\)90001-3](https://doi.org/10.1016/0038-0717(82)90001-3).
- Browne, P., Rice, O., Miller, S.H., Burke, J., Dowling, D.N., Morrissey, J.P., O’Gara, F., 2009. Superior inorganic phosphate solubilization is linked to phylogeny within the *Pseudomonas fluorescens* complex. *Applied Soil Ecology* 43, 131–138. <https://doi.org/10.1016/j.apsoil.2009.06.010>.
- Brucker, E., Sarmite, K., Spohn, M., 2020. Release of phosphorus and silicon from minerals by soil microorganisms depends on the availability of organic carbon. *Soil Biology & Biochemistry* 143, 107737. <https://doi.org/10.1016/j.soilbio.2020.107737>.
- Bünemann, E.K., 2015. Assessment of gross and net mineralization rates of soil organic phosphorus - a review. *Soil Biology and Biochemistry* 89, 82–98. <https://doi.org/10.1016/j.soilbio.2015.06.026>.
- Cama, J., Ganor, J., 2006. The effects of organic acids on the dissolution of silicate minerals: a case study of oxalate catalysis of kaolinite dissolution. *Geochimica et Cosmochimica Acta* 70, 2191–2209. <https://doi.org/10.1016/j.gca.2006.01.028>.
- Chen, Y.P., Rekha, P.D., Arun, A.B., Shen, F.T., Lai, W.-A., Young, C.C., 2006. Phosphate solubilizing bacteria from subtropical soil and their tricalcium phosphate solubilizing abilities. *Applied Soil Ecology* 34, 33–41. <https://doi.org/10.1016/j.apsoil.2005.12.002>.
- Chung, H., Park, M., Madhayan, M., Seshadri, S., Song, J., Cho, H., Sa, T., 2005. Isolation and characterization of phosphate solubilizing bacteria from the rhizosphere of crop plants of Korea. *Soil Biology & Biochemistry* 37, 1970–1974. <https://doi.org/10.1016/j.soilbio.2005.02.025>.
- Collignon, C., Uroz, S., Turpault, M., Frey-Klett, P., 2011. Seasons differently impact the structure of mineral weathering bacterial communities in beech and spruce stands. *Soil Biology & Biochemistry* 43, 2012. <https://doi.org/10.1016/j.soilbio.2011.05.008>, 2022.
- Cornelis, J.T., Delvaux, B., 2016. Soil processes drive the biological silicon feedback loop. *Functional Ecology* 30, 1298–1310. <https://doi.org/10.1111/1365-2435.12704>.
- Dessert, C., Dupré, B., Gaillardet, J., Francois, L.M., Allègre, C.J., 2003. Basalt weathering laws and the impact of basalt weathering on the global carbon cycle. *Chemical Geology* 202, 257–273. <https://doi.org/10.1016/j.chemgeo.2002.10.001>.
- Dobritsa, A.P., Samadpour, M., 2016. Transfer of eleven species of the genus *Burkholderia* to the genus *Paraburkholderia* and proposal of *Caballeronia* gen. nov. to accommodate twelve species of the genera *Burkholderia* and *Paraburkholderia*. *International Journal of Systematic and Evolutionary Microbiology* 66, 2836–2846. <https://doi.org/10.1099/ijsem.0.001065>.
- Duboc, O., Robbe, A., Santner, J., Folegnani, G., Gallais, P., Lecanuet, C., Zehetner, F., Nagl, P., Wenzel, W., 2019. Silicon availability from chemically diverse fertilizers and secondary raw materials. *Environmental Science and Technology* 53, 5359–5368. <https://doi.org/10.1021/acs.est.8b06597>.
- Drever, J.I., 1994. The effect of land plants on weathering rates of silicate minerals. *Geochimica et Cosmochimica Acta* 58, 2325–2332. [https://doi.org/10.1016/0016-7037\(94\)90013-2](https://doi.org/10.1016/0016-7037(94)90013-2).
- Fierer, N., Bradford, M.A., Jackson, R.B., 2007. Toward an ecological classification of soil bacteria. *Ecology* 88, 1354–1364. <https://doi.org/10.1890/05-1839>.
- Frey, B., Rieder, S.R., Brunner, L., Plötze, M., Koetsch, S., Lapanje, A., Brandl, H., Furrer, G., 2010. Weathering-associated bacteria from the damma glacier forefield: physiological capabilities and impact on granite dissolution. *Applied and Environmental Microbiology* 76, 4788–4796. <https://doi.org/10.1128/AEM.00657-10>.
- Gleeson, B.D., Kennedy, N.M., Clipson, N., Melville, K., Gadd, G.M., McDermott, F.P., 2006. Characterization of bacterial community structure on a weathered pegmatitic granite. *Microbial Ecology* 51, 526–534. <https://doi.org/10.1007/s00248-006-9052-x>.
- Goldstein, A.H., 1995. Recent progress in understanding the molecular genetics and biochemistry of calcium phosphate solubilization by gram negative bacteria. *Biological Agriculture and Horticulture* 12, 185–193. <https://doi.org/10.1080/01448765.1995.9754736>.
- Guntzer, F., Keller, C., Meunier, J.D., 2012. Benefits of plant silicon for crops: a review, 32. *Agronomy for Sustainable Development*, pp. 201–213. <https://doi.org/10.1007/s13593-011-0039-8>.
- Gulati, A., Rahi, P., Vyas, P., 2008. Characterization of phosphate-solubilizing fluorescent pseudomonads from the rhizosphere of sea buckthorn growing in the cold deserts of Himalayas. *Current Microbiology* 56, 73–79. <https://doi.org/10.1007/s00284-007-9042-3>.
- Haynes, R.J., Zhou, Y.-F., 2020. Silicate sorption and desorption by a Si-deficient soil – effects of pH and period of contact. *Geoderma* 365, 114204. <https://doi.org/10.1016/j.geoderma.2020.114204>.
- Harley, A.D., Gilkes, R.J., 2000. Factors influencing the release of plant nutrient elements from silicate rock powders: a geochemical overview. *Nutrient Cycling in Agroecosystems* 56, 11–36. <https://doi.org/10.1023/A:1009859309453>.
- Hinsinger, P., 2001. Bioavailability of soil inorganic P in the rhizosphere as affected by root-induced chemical changes: a review. *Plant and Soil* 237, 173–195. <https://doi.org/10.1023/A:1013351617532>.
- Ho, A., Di Lonardo, D.P., Bodelier, P.L., 2017. Revisiting life strategy concepts in environmental microbial ecology. *FEMS Microbiology Ecology* 93, 1–14. <https://doi.org/10.1093/femsec/fix006>.
- Hömberg, A., Obst, M., Knorr, K.H., Kalbitz, K., Schaller, J., 2020. Increased silicon concentration in fen peat leads to a release of iron and phosphate and changes in the composition of dissolved organic matter. *Geoderma* 374, 114422. <https://doi.org/10.1016/j.geoderma.2020.114422>.
- Huang, P.M., Wang, M.K., 2005. Minerals, primary. *Encyclopedia of Soils in the Environment*, pp. 500–510. <https://doi.org/10.1016/B0-12-348530-4/00464-1>.
- Jenkinson, D.S., Brookes, P.C., Powlson, D.S., 2004. Measuring soil microbial biomass. *Soil Biology & Biochemistry* 36, 5–7. <https://doi.org/10.1016/j.soilbio.2003.10.002>.
- Jones, L.D., Dennis, P.G., Owen, A.G., Van Hees, P.A.W., 2003. Organic acids behavior in soils—misconceptions and knowledge gaps. *Plant and Soil* 248, 31–41. <https://doi.org/10.1023/A:1022304332313>.
- Kang, S.M., Waqas, M., Shahzad, R., You, Y.H., Asaf, S., Khan, M.A., Lee, K.E., Joo, G.J., Kim, S.J., Lee, I.J., 2017. Isolation and characterization of a novel silicate-solubilizing bacterial strain *Burkholderia eburnea* CS4-2 that promotes growth of japonica rice (*Oryza sativa* L. cv. Dongjin). *Soil Science and Plant Nutrition* 63, 233–241. <https://doi.org/10.1080/00380768.2017.1314829>.
- Kanakiya, S., Adam, L., Esteban, L., Rowe, M.C., Shane, P., 2017. Dissolution and secondary mineral precipitation in basalts due to reactions with carbonic acid. *Journal of Geophysical Research: Solid Earth* 122, 4312–4327. <https://doi.org/10.1002/2017JB014019>.
- Katoh, K., Standley, D.M., 2013. MAFFT multiple sequence alignment software version 7: improvements in performance and usability. *Molecular Biology and Evolution* 30, 772–780. <https://doi.org/10.1093/molbev/mst010>.
- Kpombekou, K., Tabatabai, M.A., 1994. Effect of organic acids on release of phosphorus from phosphate rocks. *Soil Science* 158, 442–453. <https://doi.org/10.1097/00010694-199415860-00006>.
- Kucey, R.M.N., 1983. Phosphate-solubilizing bacteria and fungi in various cultivated and virgin Alberta soils. *Canadian Journal of Soil Science* 63, 671–678. <https://doi.org/10.1414/cjss83-068>.
- Lang, F., Bauhus, J., Frossard, E., George, E., Kaiser, K., Kaupenjohann, M., Krüger, J., Matzner, E., Polle, A., Prietzel, J., Rennenberg, H., Wellbrock, N., 2016. Phosphorus in forest ecosystems: new insights from an ecosystem nutrition perspective. *Journal of Plant Nutrition and Soil Science* 179, 129–135. <https://doi.org/10.1002/jpln.201500541>.
- Lang, F., Krüger, J., Amelung, W., Willbold, S., Frossard, E., Bünemann, E.K., Bauhus, J., Nitschke, N., Kandler, E., Marhan, S., Schulz, S., Bergkemper, F., Schlotter, M., Luster, J., Guggisberg, F., Kaiser, K., Mikutta, R., Guggenberger, G., Polle, A., Pena, R., Prietzel, J., Rodionov, A., Talkner, U., Meessenburg, H., von Wilpert, K., Höscher, A., Dietrich, H.P., Chmara, I., 2017. Soil phosphorus supply controls P

- nutrition strategies of beech forest ecosystems in Central Europe. *Biogeochemistry* 136, 5–29. <https://doi.org/10.1007/s10533-017-0375-0>.
- Lee, K.E., Adhikari, A., Kang, S.M., You, Y.H., Joo, G.J., Kim, J.O., Kim, S.J., Lee, I.-J., 2019. Isolation and characterization of the high silicate and phosphate solubilizing novel strain *Enterobacter ludwigii* GAK2 that promotes growth in rice plants. *Agronomy* 9, 144. <https://doi.org/10.3390/agronomy9030144>.
- Lepieux, C., Turpault, M.P., Oger, P., Frey-Klett, P., Uroz, S., 2012. Correlation of the abundance of betaproteobacteria on mineral surfaces with mineral weathering in forest soils. *Applied and Environmental Microbiology* 78, 7114–7119. <https://doi.org/10.1128/AEM.00996-12>.
- Liang, Y., Nikolic, M., Belanger, R., Gong, G., Song, A., 2015. In: Liang, Y., Nikolic, M., Belanger, R., Gong, G., Song, A. (Eds.), *Silicon Biogeochemistry and Bioavailability in Soil. Silicon in Agriculture*. Springer, Dordrecht, the Netherlands, pp. 45–68.
- Li, Z., Bai, T., Dai, L., Wang, F., Tao, J., Meng, S., Hu, Y., Wang, S., Hu, S., 2016. A study of organic acid production in contrasts between two phosphate solubilizing fungi: *Penicillium oxalicum* and *Aspergillus niger*. *Scientific Reports* 6, 25313. <https://doi.org/10.1038/srep25313>.
- Lindsay, W.L., 1979. *Chemical Equilibria in Soils*. John Wiley and Sons, New York, pp. 1–449.
- Liu, W., Xu, X., Wu, X., Yang, Q., Luo, Y., Christie, P., 2006. Decomposition of silicate minerals by *Bacillus mucilaginosus* in liquid culture. *Environmental Geochemistry and Health* 28, 133–140. <https://doi.org/10.1007/s10653-005-9022-0>.
- Ma, J.F., 2004. Role of silicon in enhancing the resistance of plants to biotic and abiotic stresses. *Soil Science and Plant Nutrition* 50, 11–18. <https://doi.org/10.1080/00380768.2004.10408447>.
- Malhotra, H., Vandana, Sharma S., Pandey, R., 2018. Phosphorus nutrition: plant growth in response to deficiency and excess. In: Hasanuzzaman, M., Fujita, M., Oki, H., Nahar, K., Hawrylak-Nowak, B. (Eds.), *Plant Nutrients and Abiotic Stress Tolerance*. Springer, Singapore. https://doi.org/10.1007/978-981-10-9044-8_7.
- Mander, C., Wakelin, S., Young, S., Condon, L., O'Callaghan, M., 2012. Incidence and diversity of phosphate-solubilising bacteria are linked to phosphorus status in grassland soils. *Soil Biology & Biochemistry* 44, 93–101. <https://doi.org/10.1016/j.soilbio.2011.09.009>.
- Mandic-Mulec, I., Stefanic, P., van Elsas, J.D., 2015. Ecology of *bacillaceae*. *Microbiology Spectrum* 3, 1–24. <https://doi.org/10.1128/microbiolspec.TBS-0017-2013>.
- Marra, L.M., de Oliveira-Longatti, S.M., Soares, C.R., de Lima, J.M., Olivares, F.L., Moreira, F.M., 2015. Initial pH of medium affects organic acids production but do not affect phosphate solubilization. *Brazilian Journal of Microbiology* 46, 367–375. <https://doi.org/10.1590/S1517-838246246220131102>.
- Mehmood, A., Akhtar, M., Imran Baloch, M., Rukh, S., 2018. Soil apatite loss rate across different parent materials. *Geoderma* 310, 218–229. <https://doi.org/10.1016/j.geoderma.2017.09.036>.
- Menezes-Blackburn, D., Paredes, C., Zhang, H., Giles, C.D., Darch, T., Stutter, M., George, T.S., Shand, C., Lumsdon, D., Cooper, P., Wendler, R., Brown, L., Blackwell, M., Wearing, C., Haygarth, P.M., 2016. Organic acids regulation of chemical-microbial phosphorus transformations in soils. *Environmental Science and Technology* 50, 11521–11531. <https://doi.org/10.1021/acs.est.6b03017>.
- Mysara, M., Vandamme, P., Props, R., Kerckhof, F.M., Leys, N., Boon, N., Raes, J., Monstieus, P., 2017. Reconciliation between operational taxonomic units and species boundaries. *FEMS Microbiology Ecology* 93, fix029.
- Murphy, J., Riley, J.P., 1962. A modified single solution method for the determination of phosphate in natural waters. *Analytica Chimica Acta* 26, 678–681. [https://doi.org/10.1016/S0003-2670\(00\)88444-5](https://doi.org/10.1016/S0003-2670(00)88444-5).
- Nezat, C., Blum, J., Yanai, R., Hamburg, S., 2007. A sequential extraction to determine the distribution of apatite in granitoid soil mineral pools with application to weathering at the Hubbard Brook Experimental Forest, NH, USA. *Applied Geochemistry* 22, 2406–2421. <https://doi.org/10.1016/j.apgeochem.2007.06.012>.
- Nicolitch, O., Colin, Y.M., Turpault, P., Uroz, S., 2016. Soil type determines the distribution of nutrient mobilizing bacterial communities in the rhizosphere of beech trees. *Soil Biology & Biochemistry* 103, 429–445. <https://doi.org/10.1016/j.soilbio.2016.09.018>.
- Nicolitch, O., Feucherolles, M., Churin, J., Fauchery, L., Turpault, M.P., Uroz, S., 2019. A microcosm approach highlights the response of soil mineral weathering bacterial communities to an increase of K and Mg availability. *Scientific Reports* 9, 14403. <https://doi.org/10.1038/s41598-019-50730-y>.
- Oburger, E., Jones, D.L., Wenzel, W.W., 2011. Phosphorus saturation and pH differentially regulate the efficiency of organic acid anion-mediated P solubilization mechanisms in soil. *Plant and Soil* 341, 363–382. <https://doi.org/10.1007/s11104-010-0650-5>.
- Olsson-Francis, K., Boardman, C., Pearson, V., Schofield, P., Oliver, A., Summers, S., 2015. A culture-independent and culture-dependent study of the bacterial community from the bedrock soil interface. *Advances in Microbiology* 5, 842–857. <https://doi.org/10.4236/aim.2015.513089>.
- Oteino, N., Lally, R.D., Kivanuka, S., Lloyd, A., Ryan, D., Germaine, K.J., Dowling, D.N., 2015. Plant growth promotion induced by phosphate solubilizing endophytic *Pseudomonas* isolates. *Frontiers in Microbiology* 6, 745. <https://doi.org/10.3389/fmicb.2015.00745>.
- Pastore, G., Kaiser, K., Kernchen, S., Spohn, M., 2020. Microbial release of apatite- and goethite-bound phosphate in acidic forest soils. *Geoderma* 370, 114360. <https://doi.org/10.1016/j.geoderma.2020.114360>.
- Penn, J.C., Camberato, J., 2019. A critical review on soil chemical processes that control how soil pH affects phosphorus availability to plants. *Agriculture* 9 (6), 120. <https://doi.org/10.3390/agriculture9060120>.
- Pikovskaya, R.I., 1948. Mobilization of phosphorus in soil in connection with the vital activity of some microbial species. *Microbiologia* 17, 362–370.
- Prietz, J., Klysubun, W., Werner, F., 2016. Speciation of phosphorus in temperate zone forest soils as assessed by combined wet-chemical fractionation and XANES spectroscopy. *Journal of Plant Nutrition and Soil Science* 179, 168–185. <https://doi.org/10.1002/jpln.201500472>.
- Qessoui, R., Bouharrou, R., Furze, J.N., El Aalaoui, M., Akroud, H., Amarraque, A., Van Vaerenbergh, J., Tahzima, R., Mayad, E.H., Chebli, B., 2019. Applications of new rhizobacteria *Pseudomonas* isolates in agroecology via fundamental processes complementing plant growth. *Scientific Reports* 9, 12832. <https://doi.org/10.1038/s41598-019-49216-8>.
- Rogers, J., Bennett, P., 2004. Mineral stimulation of subsurface microorganisms: release of limiting nutrients from silicates. *Chemical Geology* 203, 91–108. <https://doi.org/10.1016/j.chemgeo.2003.09.001>.
- Sandroni, V., Smith, C., 2002. Microwave digestion of sludge, soil and sediment samples for metal analysis by inductively coupled plasma-atomic emission spectrometry. *Analytica Chimica Acta* 468, 335–344. [https://doi.org/10.1016/S0003-2670\(02\)00655-4](https://doi.org/10.1016/S0003-2670(02)00655-4).
- Sauer, M., Porro, D., Mattanovich, D., Branduardi, P., 2008. Microbial production of organic acids: expanding the markets. *Trends in Biotechnology* 26, 100–108. <https://doi.org/10.1016/j.tibtech.2007.11.006>.
- Schaller, J., Faucher, S., Joss, H., Obst, M., Goedecke, M., Planer-Friedrich, B., Peiffer, S., Gilfedder, B., Elberling, B., 2019. Silicon increases the phosphorus availability of arctic soils. *Scientific Reports* 9, 449. <https://doi.org/10.1038/s41598-018-37104-6>.
- Schmidt, T., Rodrigues, J., von Mering, C., 2014. Ecological consistency of SSU rRNA-based operational taxonomic units at a global scale. *PLoS Computational Biology* 10, e1003594. <https://doi.org/10.1371/journal.pcbi.1003594>.
- Smits, M.M., Wallander, H., 2017. Role of mycorrhizal symbiosis in mineral weathering and nutrient mining from soil parent material. *Mycorrhizal Mediation of Soil* 3, 35–46. <https://doi.org/10.1016/B978-0-12-804312-7.00003-6>.
- Spohn, M., Kuzyakov, Y., 2013. Phosphorus mineralization can be driven by microbial need for carbon. *Soil Biology & Biochemistry* 61, 69–75. <https://doi.org/10.1016/j.soilbio.2013.02.013>.
- Spohn, M., Zeißig, I., Brucker, E., Widdig, M., Lacher, U., Aburto, F., 2020. Phosphorus solubilization in the rhizosphere in two saprolites with contrasting phosphorus fractions. *Geoderma* 366, 114245. <https://doi.org/10.1016/j.geoderma.2020.114245>.
- Syers, J.K., Williams, J.D.H., Campbell, A.S., Walker, T.W., 1967. The significance of apatite inclusions in soil phosphorus studies. *Soil Science Society of America Journal* 31, 752–756. <https://doi.org/10.2136/sssaj1967.03615995003100060016x>.
- Sutra, L., Risede, J., Gardan, L., 2000. Isolation of fluorescent *Pseudomonas* from the rhizosphere of banana plants antagonistic towards root necrotizing fungi. *Letters in Applied Microbiology* 4, 289–293. <https://doi.org/10.1046/j.1472-765x.2000.00816.x>.
- Sverdrup, H., 2009. Chemical weathering of soil minerals and the role of biological processes. *Fungal Biology Reviews* 23, 94–100. <https://doi.org/10.1016/j.fbr.2009.12.001>.
- Uroz, S., Kelly, L.C., Turpault, M.P., Lepieux, C., Frey-Klett, P., 2015. The mineralosphere concept: mineralogical control of the distribution and function of mineral-associated bacterial communities. *Trends in Microbiology* 23, 751–762. <https://doi.org/10.1016/j.tim.2015.10.004>.
- Uroz, S., Calvaruso, C., Turpault, M.P., Frey-Klett, P., 2009. Mineral weathering by bacteria: ecology, actors and mechanisms. *Trends in Microbiology* 17, 378–387. <https://doi.org/10.1016/j.tim.2009.05.004>.
- Vance, E.D., Brookes, P.C., Jenkinson, D.S., 1987. An extraction method for measuring soil microbial biomass C. *Soil Biology & Biochemistry* 19, 703–707. [https://doi.org/10.1016/0038-0717\(87\)90052-6](https://doi.org/10.1016/0038-0717(87)90052-6).
- Vandevivere, P., Welch, S.A., Ullman, W.J., Kirchner, D., 1994. Enhanced dissolution of silicate minerals by bacteria at near-neutral pH. *Microbial Ecology* 27, 241–251. <https://doi.org/10.1007/BF00182408>.
- Violante, A., Cozzolino, V., Perelomov, L., Caporale, A.G., Pigna, M., 2010. Mobility and bioavailability of heavy metals and metalloids in soil environments. *Journal of Soil Science and Plant Nutrition* 10, 268–292. <https://doi.org/10.4067/S0718-95162010000100005>.
- Vorhies, J., Gaines, R., 2009. Microbial dissolution of clay minerals as a source of iron and silica in marine sediments. *Nature Geoscience* 2, 221–225. <https://doi.org/10.1038/ngeo441>.
- Wang, Q., Wang, R.R., He, L.Y., Lu, J.J., 2014. Changes in weathering effectiveness and community of culturable mineral-weathering bacteria along a soil profile. *Biology and Fertility of Soils* 50, 1025–1034. <https://doi.org/10.1007/s00374-014-0924-9>.
- Wang, D., Xie, Y., Jaisi, D., Jin, Y., 2016. Effects of low-molecular-weight organic acids on the dissolution of hydroxyapatite nanoparticles. *Environmental Sciences: Nano* 3, 768–779. <https://doi.org/10.1039/C6EN00085A>.
- Welch, S.A., Ullman, W.J., 1993. The effect of organic acids on plagioclase dissolution rates and stoichiometry. *Geochimica et Cosmochimica Acta* 57, 2725–2736. [https://doi.org/10.1016/0016-7037\(93\)90386-B](https://doi.org/10.1016/0016-7037(93)90386-B).
- Welch, S.A., Taunton, A.E., Banfield, J.F., 2002. Effect of microorganisms and microbial metabolites on apatite dissolution. *Geomicrobiology Journal* 19, 343–367. <https://doi.org/10.1080/01490450209098414>.
- White, A.F., Brantley, S.L., 1995. Chemical weathering rates of silicate minerals. In: *Reviews in Mineralogy and Geochemistry*, 31, pp. 1–583. <https://doi.org/10.1515/9781501509650>.
- White, A.F., Brantley, S.L., 2003. The effect of time on the weathering of silicate minerals: why do weathering rates differ in the laboratory and field? *Chemical Geology* 202, 479–506. <https://doi.org/10.1016/j.chemgeo.2003.03.001>.
- White, A.F., 2003. Natural weathering rates of silicate minerals. *Treatise on Geochemistry* 5, 133–168. <https://doi.org/10.1016/B0-08-043751-6/05076-3>.

- Widdig, M., Schleuss, P.M., Weig, A.R., Guhr, A., Biederman, L.A., Borer, E.T., Crawley, M.J., Kirkman, K.P., Seabloom, E.W., Wragg, P.D., Spohn, M., 2019. Nitrogen and phosphorus additions alter the abundance of phosphorus-solubilizing bacteria and phosphatase activity in grassland soils. *Frontiers in Environmental Science* 7, 185. <https://doi.org/10.3389/fenvs.2019.00185>.
- Wolff-Boenisch, D., Gislason, S.R., Oelkers, E.H., 2006. The effect of crystallinity on dissolution rates and CO₂ consumption capacity of silicates. *Geochimica and Cosmochimica Acta* 70, 858–870. <https://doi.org/10.1016/j.gca.2005.10.016>.
- Yang, X., Post, W.M., 2011. Phosphorus transformations as a function of pedogenesis: a synthesis of soil phosphorus data using Hedley fractionation method. *Biogeosciences* 8, 2907–2916. <https://doi.org/10.5194/bg-8-2907-2011>.
- Zhu, F., Qu, L., Hong, X., Sun, X., 2011. Isolation and characterization of a phosphate solubilizing halophilic bacterium *Kushneria* sp. YCWA18 from Daqiao saltern on the coast of yellow sea of China. *Evidence-based Complementary and Alternative Medicine* 615032, 1–6. <https://doi.org/10.1155/2011/615032>.
- Zou, X., Binkley, D., Doxtader, K.G., 1992. A new method for estimating gross P mineralization and microbial P immobilization rates in soils. *Plant and Soil* 147, 243–250. <https://doi.org/10.1007/BF00029076>.



Weathering of calcareous bedrocks is strongly affected by the activity of soil microorganisms

Giovanni Pastore^a, Alfons R. Weig^b, Eduardo Vazquez^a, Marie Spohn^{a,c,*}

^a Department of Soil Biogeochemistry, Bayreuth Center of Ecology and Environmental Research (BayCEER), University of Bayreuth, Germany

^b KeyLab for Genomics and Bioinformatics, University of Bayreuth, Germany

^c Biogeochemistry of Forest Soils, Swedish University of Agricultural Sciences, Uppsala, Sweden

ARTICLE INFO

Handling Editor: Ingrid Kögel-Knabner

Keywords:

Calcareous soils
Phosphate-solubilizing bacteria
Dolomite
Limestone
Phosphate solubilization
Phosphate adsorption

ABSTRACT

Phosphorus (P) availability in calcareous forest soils is commonly low compared to siliceous soils. The main reason for this is that phosphate ions tend to precipitate with calcium (Ca). Weathering of calcareous rocks and the potential of microorganisms to dissolve calcareous parent material is not fully understood. Therefore, we examined microbial carbonate dissolution and the abundance of phosphorus-solubilizing bacteria in temperate forest soils with contrasting calcareous parent materials. We incubated soil extracts with weathered parent materials (i.e., dolomite and limestone) from two calcareous forest soils differing in P content and determined the rates of P and Ca solubilization. In addition, we determined the abundance of phosphorus-solubilizing bacteria (PSB). We found that the net Ca solubilization rate ranged from 8.8 to 511.1 nmol m⁻² d⁻¹ across both soils and depths. Calcium dissolution rates were negatively related to pH and positively related to the concentration of organic acids. The gross P solubilization rates were on average 63.6% higher from dolomite (P-poor soil) than from limestone (P-rich soil). The abundance of soil PSB ranged from 3.8 % at the limestone site (P-rich soil) to 24.4 % at the dolomite site (P-poor soil). The higher abundance of PSB in the soil derived from dolomite is in line with the high Ca and P solubilization rates at this site, indicating that PSB abundance is related to rock weathering rates from calcareous soils. Pseudomonadales and Enterobacteriales were by far the two most abundant bacterial orders in the PSB community of both soils and soil depths. In conclusion, this study shows, first, that weathering of calcareous bedrocks is strongly affected by the activity of soil microorganisms, and second, that there is likely a selective pressure in P-poor soils towards a higher abundance of PSB.

1. Introduction

Weathering of bedrock is the result of physico-chemical and biological processes that render nutrients available for uptake by organisms (Arvin et al., 2017; Finlay et al., 2019; Zaharescu et al., 2019; Wan et al., 2019). Phosphorus (P) is an essential nutrient and occurs in soils as phosphate ion. Once dissolved in the soil solution, P can be taken up by organisms (Ruttenberg, 2003). The dissolved P concentrations in the soil liquid phase is generally very low (Plante, 2007). The reason for this is that phosphate ions become quickly unavailable through (i) adsorption to soil colloids and (ii) precipitation with cations, depending on the pH conditions of the soil (Lindsay, 1979; Hinsinger, 2001). In alkaline and calcareous soils, P availability is mainly reduced by precipitation of phosphate with calcium (Ca) and magnesium (Mg) ions (Dreybrodt et al., 1996; Kaufmann and Dreybrodt, 2007).

Carbonates constitute up to 15% of the sedimentary rock of the Earth's crust (Fairbridge et al., 1967) and occur in various climatic zones mainly in form of the minerals calcite [CaCO₃] and dolomite [CaMg(CO₃)₂] (Bisutti et al., 2004). Younger carbonates are predominantly limestones (rich in calcite) that when exposed to acidic environments release Ca and carbon dioxide (CO₂). Dolomites react with acids more slowly than limestones and, therefore, their dissolution occurs at a lower rate (Liu et al., 2005). One reason for this is that dolomite may contain significant amounts of detrital silicate minerals which are scantily soluble in water (Taylor et al., 2019). Both limestones and dolomites may contain high P concentrations, ranging from 1.5 to 2.8 g kg⁻¹ due to the apatite minerals they contain (Porder and Ramachandran, 2013). Apatites belong to the group of Ca-phosphates whose solubility increases in the presence of protons (H⁺) in aqueous solutions (Hinsinger, 2001; Bengtsson and Sjöberg, 2009). While the abiotic dissolution of

* Corresponding author at: Biogeochemistry of Forest Soils, Swedish University of Agricultural Sciences, Uppsala, Sweden.
E-mail address: marie.spohn@slu.se (M. Spohn).

<https://doi.org/10.1016/j.geoderma.2021.115408>

Received 9 December 2020; Received in revised form 17 July 2021; Accepted 19 August 2021

Available online 6 September 2021

0167-0661/© 2021 The Authors. Published by Elsevier B.V. This is an open access article under the CC BY license (<http://creativecommons.org/licenses/by/4.0/>).

carbonates has been intensively studied, less is known about the biological contribution to this process.

Soil microorganisms can accelerate the weathering of carbonate rocks and apatite minerals (Banfield et al., 1999; Napieralski et al., 2020). Weathering of carbonates leads to solubilization of Ca, while weathering of apatite leads to solubilization of P. In addition, soil microorganisms can increase the desorption of P and Ca, which is also referred to as solubilization (Hinsinger, 2001). Bacteria with a high capacity to solubilize P are known as P-solubilizing bacteria (PSB). The mechanisms used by soil PSB to convert insoluble P forms into available P forms are acidification and production of chelating compounds (Goldstein, 1995). Microbes can release organic acids and siderophores which can chelate Ca and Mg cations bound to phosphate through their hydroxyl and carboxyl groups, which prevents the cations from precipitating with phosphate (Khan et al., 2009). Organic acids can also contribute to the acidification of the soil solution or can serve as selective ligands (ligand exchange) with elements of similar charge in the crystal lattice (Rodríguez and Fraga, 1999). To the best of our knowledge, only one study investigated the ability and the role of soil PSB collected from calcareous soils in the solubilization of tricalcium phosphate (Liu et al., 2015), and it is currently unknown to what extent microorganisms affect the Ca and P solubilization of calcareous parent materials in temperate forest soils. Thus, the principal aim of this study was to determine Ca and P solubilization rates of two alkaline soils developed on different calcareous parent materials. For this purpose, we incubated weathered limestone and dolomite from two temperate beech forest soils with water extracts of the soils and determined the Ca and P solubilization rate. Organic acids and the pH were quantified at different time points during the incubation. A second objective was to determine to which extent the abundance and the taxonomy of PSB from calcareous forest soils is related to the Ca and P solubilization rates from calcareous parent materials. In this regard, the abundance and the taxonomy of soil PSB was assessed by using a physiological assay in combination with 16S rRNA gene sequencing. First, we hypothesized that the Ca and P solubilization rates from limestone are higher than those from dolomite. Second, we hypothesized that the release of organic acids by microbes is positively correlated with the amounts of Ca released from both calcareous rocks. Third, we hypothesized that the relative abundance of PSB is higher in soils developed on dolomite than on limestone because the relative low P content in dolomite favors bacteria that can mobilize P.

2. Materials and methods

2.1. Study sites and sampling

Soils and weathered calcareous parent materials were sampled in September 2018 from two temperate forest ecosystems (*Fagus sylvatica* L., *Picea abies* L. H. Karst. and *Pseudotsuga menziesii* Mirb. Franco) in Germany. The Tuttingen site developed on limestone and is located in

proximity to the Swabian Alps (47°59' N, 8°45' E), whereas the site Mangfallgebirge developed on dolomite and is part of the central Bavarian Alps (47°39' N, 11°56' E). The composition of the two parent materials is described in Prietzel et al. (2021). The sites are located at 820 and 1190 m above sea level and differ in terms of precipitation and tree species composition (Table 1). The soils of the two study sites are classified as Leptosol as described in Christophel et al. (2013) and Prietzel et al. (2016). Some important chemical characteristics of the mineral soil horizons of the two forest soils are shown in Table 2. One profile was excavated at each site, and two different genetic horizons; the AC horizon and the weathered C horizon, were sampled in each profile. The samples were taken in 4–9 and 22–37 cm depth at the dolomitic site and in 11–18 and 42–60 cm depth at the limestone site. In addition, weathered calcareous parent materials were collected from each soil horizon. The pH of the studied soils ranged from 7.2 to 8.6 (Table 2). Field-moist samples were sieved in the laboratory (<2 mm) and all organic debris was removed. From each soil sample one aliquot was air-dried for chemical analyses, another aliquot was stored at 5 °C for the incubation experiments and a third one was frozen at –20 °C for microbial analysis.

2.2. Preparation and characteristics of calcareous parent materials

Weathered calcareous parent materials were crushed using a jaw crusher (Pulverisette, Fritsch, Germany). Each crushed sample was initially sieved through a 0.63 mm sieve. The resulting size fraction was further sieved through a 0.2 mm sieve. The material that did not pass the latter was used for the incubation experiments (0.2–0.63 mm size fraction). The specific surface area (SSA) of each crushed weathered parent material was determined by N₂ adsorption on a micromeritics automatic analyzer (Gemini 2375, Shimadzu, Japan). The adsorption isotherms were evaluated for adsorbent surface area with the BET (Brunauer-Emmet-Teller) model by the instrument software (StarDriver v2.03). In order to analyze the contents of total Ca (TCa) and total P (TP) from parent materials, 100 mg of crushed subsamples were digested using a combination of 2 ml nitric acid (65% HNO₃) and 5 ml hydrochloric acid

Table 2
Chemical characteristics of the mineral soil horizons of the two forest soils at Mangfallgebirge (dolomite) and Tuttingen (limestone).

Site	Soil depth [cm]	Soil pH [H ₂ O]	Total C [g kg ⁻¹]	Total N [g kg ⁻¹]*	Total P [g kg ⁻¹]	Microbial biomass C [mg g ⁻¹]
Dolomite	4–9	7.3	92.2	6.2	0.6	2.6
	22–37	7.6	48.5	2	0.3	1.4
Limestone	11–18	7.2	46.5	3.8	1	2.9
	42–60	8.6	39.5	–	0.7	0.1

* missing values were below the detection limit (0.5 g kg⁻¹).

Table 1

Basic characteristics of the two forest soils and their weathered calcareous parent material at Mangfallgebirge (dolomite) and Tuttingen (limestone). Abbreviations: SSA (specific surface area), TP (total phosphorus) and TCa (total calcium).

Site	Forest type	Stand age [yr.]	Elevation [m a. s. l.]	MAT [°C]	MAP [mm]	Soil type [WRB 2007]	Soil depth [cm] ^a	SSA of parent material [m ² g ⁻¹]	TP of parent material [mg kg ⁻¹]	TCa of parent material [g kg ⁻¹]
Triassic Dolomite	<i>Fagus sylvatica</i> , <i>Picea abies</i> , <i>Pseudotsuga menziesii</i>	120	1190	5.5	1863	Haplic Leptosol	4–9	3.8	53.1	210
Jurassic Limestone	<i>Fagus sylvatica</i>	90	820	6.6	855	Rendzic Leptosol	22–37	2.0	43.6	218
							11–18	5.1	382	379
							42–60	3.5	264	387

^a The sampling depths refers to the same genetic horizon (AC and C horizon) in both soils.

(37% HCl) brought to a final volume of 40 ml by adding distilled water. Each sample was digested in three replicates and Ca and P contents were determined by inductively coupled plasma optical emission spectroscopy ICP-OES (Vista-Pro radial, Varian). The specific absorption of radiation for Ca and P was 356 nm and 190 nm, respectively. The reference material used for the analysis consisted of spectrapure standards surface water type 2 for Ca (SPS-SW2) and spectrapure standards waste water type 2 for P (SPS-WW2) (LGC Standards, France).

2.3. Soil chemical analyses

Soil pH of dried samples (60 °C for 24 h) was measured by a SenTix gel electrode (WTW, Xylem Analytics, Germany) in a suspension with deionized water at a ratio of 1:5 (w/v) after an equilibration time of 3 h (Table 2). Sub aliquots of oven dried samples were finely grounded in a ball mill (MM400, Retsch, Germany) and the total soil carbon (TC) and nitrogen (TN) concentrations were determined using a CN elemental analyzer (Vario MAX, Elementar, Germany). Total soil phosphorus (TP) concentrations of dried samples were measured using inductively coupled plasma optical emission spectroscopy (ICP-OES, Vista-Pro radial, Varian) after pressure digestion in concentrated nitric acid.

2.4. Soil microbial biomass

Soil microbial biomass C and N were determined using the chloroform fumigation-extraction method (Brookes et al., 1982; Vance et al., 1987). Briefly, 10 g of fresh soil were split into two equal parts, of which 5 g were fumigated in a desiccator at room temperature for 24 h with ethanol-free CHCl_3 and the other 5 g were used as controls (hereafter referred to as non-fumigated samples). For microbial C and N, fumigated and non-fumigated samples were extracted in 0.5 M K_2SO_4 with a ratio (w/v) of 1:5 (Joergensen, 1996). The C and N contents in the soil extracts were determined with a CN analyzer (multi N/C 2100, Analytik Jena). Soil microbial biomass C and N were calculated as the difference of C and N concentrations in fumigated and non-fumigated samples. Both concentrations were then corrected by a factor of 2.22 (Jenkinson et al., 2004).

2.5. Incubation experiments

To determine the net Ca and P solubilization rates from the weathered calcareous parent materials, incubation experiments were conducted using soil extracts following Brucker et al. (2020) and Pastore et al. (2020a; Pastore et al. 2020b). For this purpose, a soil extract from one soil was incubated with weathered bedrock of the same soil horizon. The soil extracts used for the incubations were prepared as follows: 100 g of each soil sample were placed in PE bottles and mixed with 1 L of distilled water and shaken at room temperature for 2 h using an overhead shaker. The extracts were then filtered through cellulose filters with coarse pores that allow for passage of soil microorganisms and small organic matter particles (Rotilabo, type 113P, Roth, Germany). To determine the Ca and P solubilization rates from calcareous parent materials, three incubation experiments were conducted, all once with and once without the addition of glucose. Glucose was added to soil extracts to provide microbes with a readily available carbon (C) source since it was observed in previous experiments (Pastore et al., 2020a; Pastore et al., 2020b) that the rate of microbial P solubilization is very small, and can only be determined in incubation experiments if microbial activity is stimulated. The glucose addition reflects the situation in the rhizosphere, where a large flux of sugars enters the soil. In experiment 1, the total Ca and P mobilization rates from parent material were determined. For this purpose, 1 g of each parent material was incubated with 99 ml of the respective soil extract and with/without 1 ml of glucose solution (3.33 mM). In experiment 2, we quantified the mobilization of P from the dissolved organic matter in order to determine organic P mineralization, either with or without the addition of glucose.

This experiment was conducted in the same way as experiment 1 but without parent material, thus the only source of P was organic P. Third, sterile control incubations were conducted to determine the chemical effect of the sterile soil extracts on Ca and P solubilization. All experiments were performed in triplicates. The incubation flasks were loosely covered with aluminium foils and continuously agitated at 20 °C for fourteen days on a horizontal shaker.

2.6. Chemical analyses of soil extracts incubated with parent material

In each soil extract, dissolved Ca was measured 0, 3, 7, and 14 days after the beginning of the experiment. Aliquots of 6 ml were taken and filtered through cellulose acetate filters of 0.45- μm pore size (Sartorius Biotech, Germany). The filtrates were acidified by adding 30 μl of 65% HNO_3 to prevent Ca precipitation and then centrifuged at $1500 \times g$ for 15 min. The resulting supernatant was analysed for Ca by ICP-OES (Vista-Pro radial, Varian, USA). In parallel, the amounts of phosphate released from parent materials were also quantified. At defined time intervals (0, 3, 7, 10, and 14 days after the beginning of the experiment), 10 ml were taken from the flasks and vacuum filtered using 0.45 μm cellulose acetate filters. The resulting filtrates were analysed for pH and phosphate concentration. The latter was determined according to the molybdenum-blue assay (Murphy and Riley, 1962) and measured with an Infinite M200 Pro microplate reader (Tecan, Switzerland).

2.7. Organic acids

Organic acids (citric, oxalic, 2-keto-D-gluconic, D-gluconic and lactic) were determined in filtered samples from soil extracts incubated with the respective parent material and glucose on day 7 and 14 after the beginning of the experiment. We chose acids that have been identified as the major organic acids relevant in P solubilization (Rodríguez and Fraga, 1999). All filtrates were examined by means of high-performance liquid chromatography (Agilent series 1200, Germany) coupled to a diode array HPLC detector (DAD). Chromatographic separation of the organic acids was performed with a RezexTM ROA-Organic Acid H⁺ (8%), LC column (300 \times 7.8 mm; Phenomenex) equipped with a matching guard column. Organic acids were identified based on their retention times. The solvent used to separate organic acids consisted of 4 mmol phosphoric acid aqueous solution at a flow rate of 0.8 ml min⁻¹. Quantification was performed according to the external standard calibration method. HPLC-MS data were processed using the Agilent Chemstation software package. The amounts of each organic acid were calculated by multiplying the respective concentration (mg l⁻¹) in the soil extracts by the volume (l) present in the flask at the time of sampling, and subsequently expressed in μmol . The concentrations of the carboxyl groups were determined from the concentrations of organic acids and the respective number of carboxyl groups of each acid (mono-, di- and tri-carboxylic).

2.8. Abundance of PSB

The relative abundance of culturable PSB was assessed by suspending 0.5 g of fresh soil in 49.5 ml of sterile water and shaking for 1 h. Serial dilutions (10^{-3} , 10^{-4}) from each soil suspension were tested to identify the appropriate cell density. Subsequently, from each suspension, an aliquot of 100 μl was spread on Piskovskaya's agar medium (PVK, Piskovskaya, 1948) and the plates were incubated at ~ 20 °C for 7 days. The PVK medium was composed of: 10 g glucose; 5 g hydroxyapatite; 0.5 g yeast extract; 0.5 g ammonium sulphate; 0.2 g potassium chloride; 0.2 g sodium chloride; 0.1 g magnesium sulphate; 0.002 g ferrous sulphate; 0.002 g manganese sulphate and 15 g agar-agar in 1 L distilled water. The pH of the medium was adjusted to 7.0. If a bacterial colony dissolves hydroxyapatite present in the medium, a halo (clear zone) becomes visible in the otherwise milky medium. When bacterial colonies produced halos with a diameter larger than 1 mm, the relative

isolate was classified as “strong” PSB. When the halos had a diameter lower than 1 mm, the relative isolate was classified as “weak” PSB. The relative abundance of culturable PSB was calculated as the percentage of colonies that were formed by PSB of the total number of bacterial colonies.

2.9. Amplification and sequencing of PSB (16S rRNA gene)

Bacterial colonies identified as PSB were collected using sterile toothpicks and aseptically transferred into buffer solutions for sequencing analysis as described in Widdig et al. (2019). Sequence similarity searches of high-quality regions larger than 514 bp were conducted against NCBI’s nucleotide database (Nucleotide [Internet]. Bethesda (MD): National Library of Medicine (US), National Center for Biotechnology Information, available from: <https://www.ncbi.nlm.nih.gov/nucleotide/>) and against the 16S section of NCBI’s RefSeq Targeted Loci Project (RefSeq Targeted Loci Project [Internet]. Bethesda (MD): National Library of Medicine (US), National Center for Biotechnology Information, available from: <https://www.ncbi.nlm.nih.gov/efseq/targetedloci/>) (max e-value 1e-10). Sequence data were processed using Geneious v. 11 (Biomatters Ltd., New Zealand) and aligned using MAFFT software (v. 7.388; see also Katoh and Standley, 2013). The best 20 hits were selected. Sequences with a 98% cut-off similarity were clustered into operational taxonomic units (OTUs). To this end, the name of the lowest common rank in the taxonomy was chosen. Only the non-redundant top hits were selected for taxonomic annotation. For this purpose, each 16S sequence was compared with all other sequences and sequences sharing identity above 98% identity were assigned to one taxon. Major phylogenetic changes were detected at the order and genus levels by means of ANOVA with a false discovery rate correction test (FDR, $p < 0.05$). The partial 16S rRNA gene sequences were deposited in GenBank (<https://www.ncbi.nlm.nih.gov/genbank/>) under the accession numbers MT955367-MT955590. The abundance matrix of the 16S sequence types was uploaded in PRIMER 7 (PRIMER-E Ltd., United Kingdom), standardized and cumulated at the genus level. A resemblance matrix (Manhattan distance) was calculated from the abundance matrix of bacterial fragments before nonmetric multi-dimensional scaling (nMDS) was performed (using a stress test = 0.01). Subsequently, analyses of similarities (ANOSIM) based on the number of OTU grouped by taxon were conducted using 999 permutations to determine whether the P-solubilizing bacterial communities were significantly different among the tested soils.

$$\text{GrossPsolubilizationrate}(\text{nmold}^{-1}) = \frac{\text{NetCasolubilizationrate}[\text{nmold}^{-1}] * \text{Pcontent}[\text{gKg}^{-1}]}{\text{Cacontent}[\text{gKg}^{-1}]} \quad (3)$$

and against the 16S section of NCBI’s RefSeq Targeted Loci Project (RefSeq Targeted Loci Project [Internet]. Bethesda (MD): National Library of Medicine (US), National Center for Biotechnology Information, available from: <https://www.ncbi.nlm.nih.gov/efseq/targetedloci/>) (max e-value 1e-10). Sequence data were processed using Geneious v. 11 (Biomatters Ltd., New Zealand) and aligned using MAFFT software (v. 7.388; see also Katoh and Standley, 2013). The best 20 hits were selected. Sequences with a 98% cut-off similarity were clustered into operational taxonomic units (OTUs). To this end, the name of the lowest common rank in the taxonomy was chosen. Only the non-redundant top hits were selected for taxonomic annotation. For this purpose, each 16S sequence was compared with all other sequences and sequences sharing identity above 98% identity were assigned to one taxon. Major phylogenetic changes were detected at the order and genus levels by means of ANOVA with a false discovery rate correction test (FDR, $p < 0.05$). The partial 16S rRNA gene sequences were deposited in GenBank (<https://www.ncbi.nlm.nih.gov/genbank/>) under the accession numbers MT955367-MT955590. The abundance matrix of the 16S sequence types was uploaded in PRIMER 7 (PRIMER-E Ltd., United Kingdom), standardized and cumulated at the genus level. A resemblance matrix (Manhattan distance) was calculated from the abundance matrix of bacterial fragments before nonmetric multi-dimensional scaling (nMDS) was performed (using a stress test = 0.01). Subsequently, analyses of similarities (ANOSIM) based on the number of OTU grouped by taxon were conducted using 999 permutations to determine whether the P-solubilizing bacterial communities were significantly different among the tested soils.

2.10. Data analyses and statistics

The amounts of Ca and P in the incubated soil extracts were calculated by multiplying the element concentration (nmol l^{-1}) with the volume (l) of the soil extract at the time of sampling. The total Ca mobilization rates represent the change in the amounts of Ca from the parent material in the solution over fourteen days (biotic + abiotic) and were computed according to the following equation (Eq. (1)).

$$\text{TotalCamobilizationrate}(\text{nmold}^{-1}) = \frac{(\text{Ca}[\text{nmol}]_{\text{day14}} - \text{Ca}[\text{nmol}]_{\text{day0}})}{14[\text{days}]} \quad (1)$$

where Ca[nmol] represents the amount of Ca at the end (day 14) and the beginning (day 0) of the experiment. The net Ca solubilization rate (nmol d^{-1}) from calcareous parent materials was estimated as the

difference between the total Ca mobilization rate (biotic + abiotic) and the release rate determined in the sterile control experiment as follows:

$$\text{NetCasolubilizationrate}(\text{nmold}^{-1}) = \text{totalCamobilizationrate}(\text{nmold}^{-1}) - \text{Careleaseratefromsterilecontrol}(\text{nmold}^{-1}) \quad (2)$$

We consider this a net rate because we did not correct for microbial Ca uptake. The net Ca solubilization rates were divided by the corresponding amount of calcareous parent material utilized as well as by the respective surface area of the weathered parent material ($\text{m}^2 \text{g}^{-1}$) to result in a final rate expressed as $\text{nmol m}^{-2} \text{d}^{-1}$.

In addition, we determined the gross P solubilization rates, i.e., the total amount of P released from calcareous parent materials, based on the Ca and P content of the parent materials and the net Ca solubilization rates, as follows:

The gross P solubilization rates were divided by the corresponding amount of calcareous parent material as well as by the respective surface area of the weathered parent material ($\text{m}^2 \text{g}^{-1}$) to result in a rate expressed as $\text{nmol m}^{-2} \text{d}^{-1}$. Both the net Ca and the gross P solubilization rates ($\text{nmol m}^{-2} \text{d}^{-1}$) are given per unit area of parent material ($\text{m}^2 \text{g}^{-1}$). P is generally solubilized when P-containing calcareous rock weathers and the gross solubilization rates of Ca and P during weathering reflect the Ca:P ratio of the rock (Hartnam et al., 2014). Here we followed Gardner (1990) who suggested to use the export of dissolved Si as a weathering index to estimate the rate of P release due to chemical weathering by means of the P:Si loss ratio in saprolite.

To check if variables were normally distributed, the Shapiro-Wilk test was performed ($p > 0.05$). Further, all data sets were tested for equality of variance using Levene’s test. When variances were not significantly different between groups, analysis of variance (one-way ANOVA) was used to test for differences between soil properties and net Ca solubilization rates. Differences in Ca and P solubilization rates between the two soil depths were analyzed by *t*-test followed by post-hoc Tukey HDS ($p < 0.05$). For unequal numbers of observation with equal variance, the parametric Holm-Sidak post hoc test was used (siliceous vs. calcareous parent materials). Linear regression analysis was used to test for a relationship between the amounts of Ca and P in solution. Tests for correlations were made using Spearman correlation analysis. All statistical analysis was performed using SigmaPlot (version 13.0, Systat Software, San Jose, California, USA).

3. Results

3.1. Net Ca solubilization from weathered calcareous parent material

The amounts of dissolved Ca increased during the two-week period only in the experiment with the addition of glucose, but not in the experiment without addition of glucose, as shown in Table S1. Moreover, we found that the dissolved Ca concentrations were up to 79.4% higher in the biotic experiment compared to the abiotic experiment (sterile conditions). Rates of Ca solubilization normalized to the surface area of the weathered calcareous parent material differed significantly among the two soils and the two soil horizons (Fig. 1). The net Ca solubilization rate from the two different parent materials incubated in soil water extracts and glucose ranged between $8.8 (\pm 7.7)$ and $511.1 (\pm 25.4) \text{ nmol m}^{-2} \text{d}^{-1}$ over the two-week period. Dolomite showed

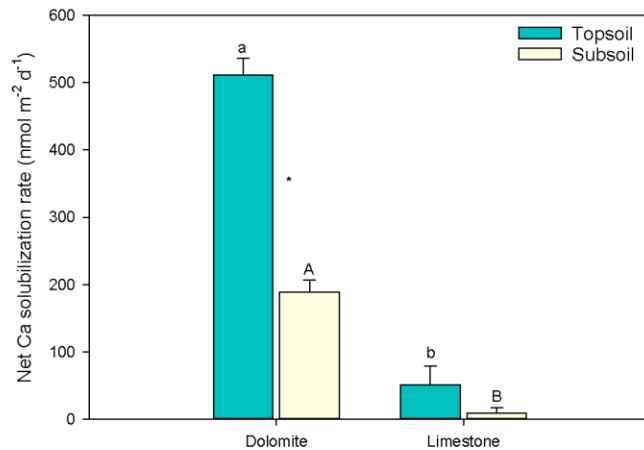


Fig. 1. Net Ca solubilization rates from calcareous rocks incubated in soil extracts from two forest soils with glucose. The rates were normalized according to the specific surface area of the rocks and computed over 14 days of incubation. Soils and rocks were sampled at two different depths of two forest soils developed on dolomite (topsoil: 4–9 cm and subsoil: 22–37 cm) or on limestone (topsoil: 11–18 cm and subsoil: 42–60 cm). Bars show means and error bars indicate standard deviations ($n = 3$). Different letters indicate significant differences tested separately for the two soil depths by one-way ANOVA followed by post-hoc Tukey HDS ($p < 0.05$). Stars indicate significant differences between the two depths of each soil, tested by *t*-test followed by post-hoc Tukey HDS ($p < 0.05$).

higher net Ca solubilization rates in comparison to limestone (Fig. 1, $p < 0.05$). At the dolomite site, the net Ca solubilization rates in the upper soil horizon were significantly higher than in the lower soil horizon (+63%; $p < 0.001$), while no statistically significant difference in the net Ca solubilization rates was observed between the upper and the lower soil horizon in incubations with limestone (Fig. 1). At the dolomite site, the extracts from the topsoil showed the highest pH decrease (from 7.8 to 6.9), in particular during the first three days of the incubation. The pH in the extracts from the subsoil at both sites decreased much less and, after three days, a slight increase in pH was registered (Table 5). The amounts of Ca were negatively related to the amounts of P in solution, with the best-fitting, linear model for the dolomite soil (topsoil $R^2 = 0.87$; subsoil $R^2 = 0.40$, $p < 0.05$).

3.2. Gross P solubilization from weathered calcareous parent material

During the incubation experiments, we did not observe any net P solubilization but rather P immobilization, as indicated by a steady decline in the concentration of phosphate over the two-week period (Table S2). However, we determined the gross P solubilization rates from the P and Ca content of the parent materials and the net Ca solubilization rate. Gross P solubilization normalized to the surface area of the weathered calcareous parent material ranged from $0.01 \text{ nmol m}^{-2} \text{ d}^{-1}$ (± 0.00) to $0.17 \text{ nmol m}^{-2} \text{ d}^{-1}$ (± 0.01) (Table 3). Overall, the gross P solubilization rates were significantly higher from dolomite compared to limestone. Moreover, we found that the P concentrations were 12.7% to

Table 3

Gross P solubilization from two calcareous parent materials in two soil horizons determined according to the Ca and P contents of the respective rocks and the Ca solubilization rate computed over 14 days. Mean values and standard deviations (S.D., in parentheses) are shown ($n = 3$). Uppercase and lowercase letters show significant differences tested separately for the two soil depths by one-way ANOVA, followed by post-hoc Tukey HDS ($p < 0.05$).

Site	Soil depth [cm]	Gross P solubilization rate [$\text{nmol m}^{-2} \text{ d}^{-1}$]*
Dolomite	Topsoil (4–9)	0.17 (± 0.01) ^a
	Subsoil (22–37)	0.05 (± 0.00) ^A
Limestone	Topsoil (11–18)	0.07 (± 0.04) ^b
	Subsoil (42–60)	0.01 (± 0.00) ^B

*Computed per g of parent material.

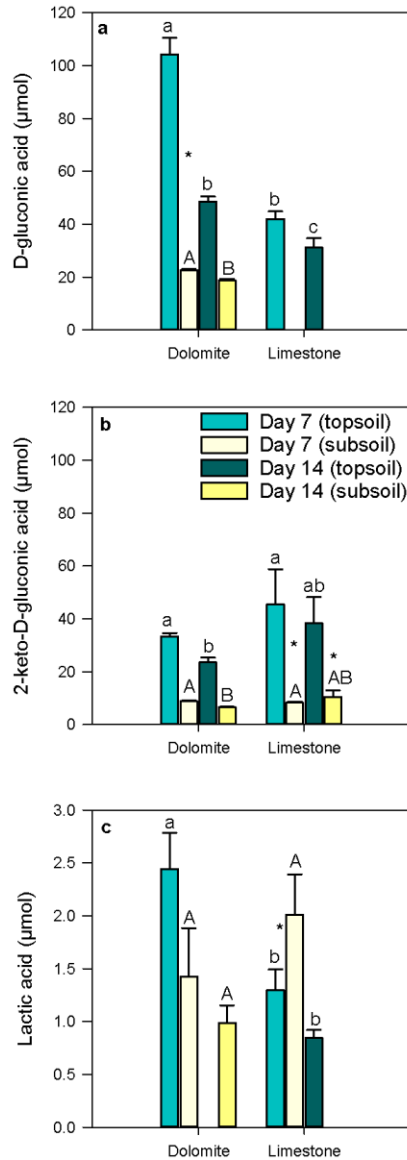
63.4% higher in the biotic experiment compared to the abiotic experiment (sterile conditions).

3.3. Organic acids in soil extracts

Citric and oxalic acids were not detected after 7 and 14 days of incubation, and thus monocarboxylic acids (D-gluconic, 2-keto-D-gluconic and lactic acid) represented 100% of all tested acids at these times. We found that the total amounts of the three measured organic acids were higher in solution with dolomite than with limestone ($p < 0.05$) (Fig. 2). 2-keto-D-gluconic acid prevailed at the limestone soil, whereas D-gluconic and lactic acid dominated at the dolomite soil (Fig. 2). Overall, organic acids decreased significantly from day 7 to day 14 in all soil extracts ($p < 0.05$) (Fig. 2). The sum of organic acids (D-gluconic, 2-keto-D-gluconic and lactic acid) released by microbes was 2.6 to 7.7 times larger in the soil extracts from the topsoil compared to the subsoil at both sites after 14 days of incubation. The amounts of carboxyl groups detected in the extracts from the topsoil after 14 days of incubation had a significant negative relationship with pH ($R^2 = 0.87$ for the dolomite soil and $R^2 = 0.81$ for the limestone soil, $p < 0.05$), whereas in the extracts from the subsoil, the negative relationship between the carboxyl groups and pH occurred only at the dolomite soil ($R^2 = 0.86$, $p < 0.05$).

3.4. Abundance and taxonomic composition of PSB

The relative abundance of culturable PSB ranged from 3.8 % to 24.4 % of all colony-forming bacteria isolated from the two soils and horizons (Fig. 3). Overall, we found that the relative abundance of culturable PSB was significantly higher at the dolomite soil in comparison to the limestone soil for both soil horizons (Fig. 3). Based on the diameter of the halo, by which we discriminated strong versus weak PSB, we found that the dolomite soil harbored on average 28.1% more strong P-solubilizers than the limestone soil in the upper soil horizon (data not shown). In total, 224 PSB colonies were identified by 16S rRNA gene sequence analysis. The sequenced PSB belonged to four phyla (Proteobacteria, Bacteroidetes, Firmicutes and Actinobacteria). Pseudomonadales dominated in both soils and depths, representing almost 80% of all isolates, whereas Enterobacteriales were the second most abundant order and represented, on average, 10% of all PSB OTUs (Fig. 4). Among all sequenced PSB colonies, 32 different OTUs were obtained by



(caption on next column)

Fig. 2. Amounts of D-gluconic (a), 2-keto-D-gluconic (b), and lactic acid (c) calculated based on the concentrations and the volumes of the solutions at day 7 and 14 of the incubation experiment conducted with soil extracts from two forest soils developed on dolomite (topsoil: 4–9 cm and subsoil: 22–37 cm) and limestone (topsoil: 11–18 cm and subsoil: 42–60 cm). Bars represent means and error bars indicate standard deviations ($n = 3$). Different lowercase and uppercase letters show significant differences between soils and soil depths tested separately for day 7 and day 14 by one-way ANOVA followed by post-hoc Tukey HSD ($p < 0.05$). Stars indicate significant differences between two depths of one soil, tested by *t*-test followed by post-hoc Tukey HSD ($p < 0.05$). Citric and oxalic acids were also investigated but no amounts were detected after 7 and 14 days of incubation. Note the different scales of the y axes.

clustering of the 16S rRNA gene similarity. We found that *Serratia* sp. and *Pseudomonas* sp. were present in all soils. The 16S rRNA gene sequencing revealed seven distinct isolates of *Pseudomonas* at the dolomite soil and only three at the limestone soil. *Erwinia* sp., *Arthrobacter* sp. and *Streptomyces* sp. were found only at the dolomite soil, whereas *Ewingella* sp., *Flavobacterium* sp., *Rahnella* sp. and *Paenibacillus* sp. were found only at the limestone soil. Nonmetric multidimensional scaling (nMDS) analysis revealed that the PSB community at the limestone site was significantly different from the PSB community at the dolomite site ($p < 0.05$).

4. Discussion

4.1. Solubilization of Ca from weathered calcareous rocks

We found that the Ca and P solubilization rates from dolomite were significantly higher than those from limestone (Fig. 1; Table 3), in contrast to our first hypothesis. The most likely reason for this is that the sum of organic acids, as well as the total amounts of carboxyl groups, were significantly higher in the incubation with dolomite than with limestone, in particular during the first week of the incubation when most dissolution of the parent rock occurred (Table 4). Our results agree with Pokrovsky and Schott (2001) who found that dissolution rates of dolomite are strongly promoted by the addition of organic acids. Organic acids can affect solubilization rates of calcareous rock in three ways: (i) by complexation of cations, such as Ca and Mg, (ii) by ligand exchange reactions or (iii) by decreasing the pH of the soil extracts (Hinsinger, 2001; Oburger et al., 2009). Gluconic acid was by far the most abundant organic acid among the ones that were determined, especially in the soil extracts from the topsoil of the dolomite soil, which might be related to the occurrence of Streptomycetales in the dolomite but not in the limestone soil (Fig. 4). Members of the genus *Streptomyces* are able to produce very high amounts of malic and gluconic acids (Jog et al., 2014). Further, the high concentrations of D-gluconic and 2-keto-D-gluconic acids are likely related to the high abundance of *Pseudomonas* and other gram-negative bacteria in both soils (Goldstein, 2007).

In the topsoil, the pH of the soil extracts incubated with dolomite decreased by 1 unit up to a minimum of pH 6.9 during the first week of the experiment (Table 5) probably due to the high amounts of D-gluconic acid released by microbes. Up to 66.64% of the total concentrations of H^+ present in these alkaline soil extracts were probably derived from D-gluconic acid, according to its concentration as well as its pK_a . On the contrary, the pH of the soil extracts incubated with limestone in the topsoil did not decrease significantly during the two-week period with values consistently between 7.9 and 8.1 (Table 5). Thus, pH-mediated solubilization, due to the higher amounts of D-gluconic acid and the related decrease in pH, likely caused the different solubilization rates of the two calcareous parent materials in the upper soil horizon (dolomite \gg limestone).

In the lower soil horizon, the higher Ca solubilization rates from dolomite than from limestone can be explained also by the higher amount of carboxyl groups present in the soil extracts (on average ~ 3.6 times higher in the incubations with dolomite than with limestone)

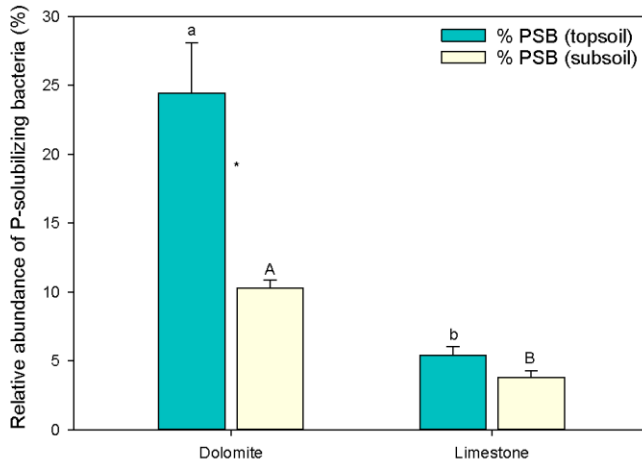


Fig. 3. Relative abundance of culturable P-solubilizing bacteria (PSB) from two forest soils developed on dolomite (topsoil: 4–9 cm and subsoil: 22–37 cm) and limestone (topsoil: 11–18 cm and subsoil: 42–60 cm). Bars represent means and error bars indicate standard deviations ($n = 3$). Different uppercase and lowercase letters indicate significant differences between sites tested separately for each soil depth using one-way ANOVA followed by post-hoc Tukey HSD ($p < 0.05$). Stars indicate significant differences between the two depths of each soil, tested by *t*-test followed by post-hoc Tukey HSD ($p < 0.05$).

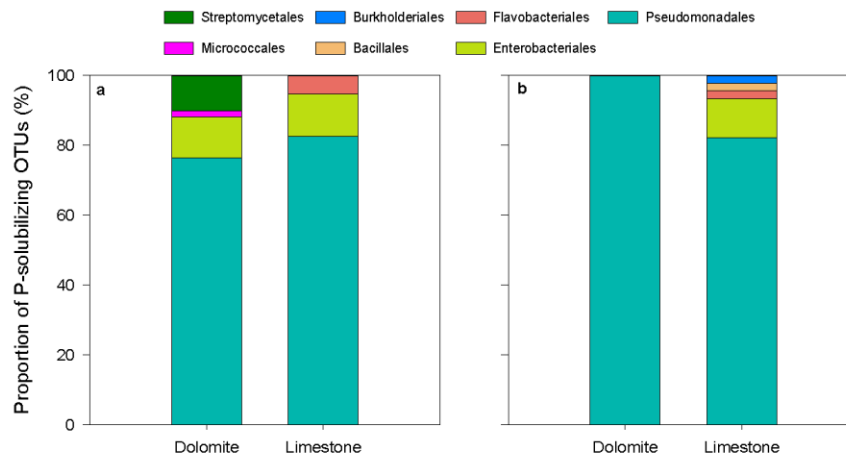


Fig. 4. Relative abundance of different OTUs of P-solubilizing bacteria (PSB) from two forest soils developed on dolomite and limestone in the topsoil (a) and in the subsoil (b). Isolates identified as PSB were grouped into operational taxonomic units (OTU) at 98% cut-off similarity. Taxonomic classification of isolates is shown at the order level.

which, in turn, can likely be related to the higher microbial biomass of the dolomitic soil in comparison to the limestone soil (Table 2). Despite this, in the lower soil horizon, the pH of the soil extracts incubated with dolomite and limestone remained relatively stable (Table 5). This is likely related to the lower microbial biomass in the subsoil in comparison to the topsoil which likely resulted in a smaller rate of proton release.

It is worth mentioning that in this study we worked under laboratory conditions with relatively high temperatures and high organic C availability. This allowed us to determine Ca solubilization by microorganisms from weathered bedrock. However, it has to be taken into account

that temperature in soils tends to be lower than in our incubation experiments. Further, the C availability was high at the beginning of the incubation, which reflects rhizosphere conditions but does not represent conditions in root-free soil. In addition, it needs to be taken into account that the incubation experiment was conducted on a shaker, which is common practice when determining net and gross P mobilization rates (Bünemann, 2015), but likely causes higher solubilization rates than *in situ*.

Comparing the amounts of organic acids in the extracts incubated with calcareous soils to a previous study on siliceous soils (Pastore et al., 2020b) we found they were significantly higher than those measured in

Table 4

Sum of carboxyl groups released by microbes in soil extracts incubated with two different calcareous parent materials (dolomite and limestone). Values are shown for day 7 and day 14 of the incubation.

Site	Soil depth [cm]	Sum of carboxyl groups [μmol]*	
		Day 7	Day 14
Dolomite	Topsoil (4–9)	140.1	48.1
	Subsoil (22–37)	32.9	26.2
Limestone	Topsoil (11–18)	88.3	70.1
	Subsoil (42–60)	9.6	6.9

* Computed for the three measured organic acids.

the incubations with silicates in the topsoil (+75.6%; $p < 0.05$), whereas no significant differences were observed in the extracts from the subsoil (Fig. S1). In particular, we found that the concentrations of D-gluconic and 2-keto-D-gluconic acids in the incubation experiment with the calcareous soils were 71% and 62%, respectively, higher than in the incubation experiment with siliceous soils. The higher concentrations of organic acids in the calcareous soils are likely related to a higher soil microbial biomass (see Table 2) in the calcareous than in the siliceous soils (Pastore et al., 2020b). Our data on the activity of microbial communities in alkaline soils is in accordance with a previous finding by Tyler and Ström (1995) who found that calcicole plants, which mainly establish on calcareous soils, release more organic acids in comparison to calcifuge plants, which mainly establish on silicate soils. However, to date, the evidence for a higher release of organic acids in alkaline soils compared to siliceous soils is still very limited (see also Syers et al., 1967; López-Bucio et al., 2000). Altogether, our study suggests that the Ca solubilisation rate from the two calcareous rocks was strongly affected by pH and the organic acid concentration which, in turn, likely resulted from a difference in microbial biomass between the two soils.

4.2. Solubilization of P from weathered calcareous rocks

The stoichiometrically-derived gross P solubilization rates from dolomite were significantly higher than the ones from limestone although the latter carried almost 6.7 times more P than dolomite (Table 1). The reason for this is the higher Ca solubilization rates from dolomite. Calcium is released from carbonates, while P is mainly released from primary P-minerals (apatites) and, secondary, from P adsorbed to minerals. The assumption made here is that Ca and P are solubilized in the same proportion as they are found in the weathered bedrock. In the long-term, the ratio of gross Ca to gross P solubilization during weathering must reflect the ratio of Ca:P in the rock. However, for the short-term, this assumption might have led to an overestimation of P solubilization as the solubility of apatite is low compared to carbonates (see also Guidry and Mackenzie, 2003; Mair et al., 2017) and apatite is not homogeneously distributed in calcareous rock. However, it could also be that P was preferentially solubilized by microorganisms, as observed in a recent study on solubilisation of P from siliceous saprolite (Spohn et al., 2020).

Table 5

pH values of the soil extracts incubated with two calcareous parent materials in the experiment with and without addition of glucose.

Site	Soil depth [cm]	Experiment with glucose				Experiment without glucose			
		pH				pH			
		DAY 0	DAY 3	DAY 7	DAY 14	DAY 0	DAY 3	DAY 7	DAY 14
Dolomite	4–9	7.8 (± 0.11)	6.9 (± 0.17)	7.8 (± 0.07)	8.1 (± 0.05)	7.9 (± 0.01)	7.9 (± 0.03)	8.0 (± 0.05)	8.2 (± 0.06)
	22–37	7.9 (± 0.04)	7.9 (± 0.07)	8.1 (± 0.09)	8.3 (± 0.05)	7.9 (± 0.11)	8.0 (± 0.06)	8.1 (± 0.07)	8.2 (± 0.08)
	11–18	8.0 (± 0.01)	7.9 (± 0.02)	8.1 (± 0.03)	8.1 (± 0.05)	7.9 (± 0.08)	7.9 (± 0.01)	8.1 (± 0.01)	8.0 (± 0.08)
Limestone	42–60	8.0 (± 0.01)	7.9 (± 0.03)	8.0 (± 0.03)	8.1 (± 0.06)	7.8 (± 0.05)	7.9 (± 0.04)	8.0 (± 0.01)	8.0 (± 0.06)

When the data on gross P solubilization rates were compared to those obtained from a previous study (Pastore et al., 2020b) we found that significantly less P was released from carbonates than from silicates (Fig. S3a) despite the fact that the net Si solubilization rates from silicates were lower than the net Ca solubilization rates from carbonates. The reason for this is that silicates carried on average 12 times more P than the carbonates (2.25 g P kg⁻¹ in silicates and 0.19 g P kg⁻¹ in carbonates). Thus, to determine the effect of soil extracts on gross P solubilization under the same conditions, we recalculated the P release assuming that the carbonates would have the same P content as silicates. The results show that the “potential” of microbes to solubilize P from calcareous rocks was 3.2 times higher than silicate rocks in the topsoil (Fig. S3b; $p < 0.05$) and ~ 1.6 times higher in the subsoil. Taken together, our results suggest that high rates of mineral dissolution can compensate for low mineral P content.

4.3. Abundance of PSB

The higher abundance of PSB in the soil derived from dolomite fits well with the high Ca and P solubilization rates at this site, indicating that the abundance of PSB is related to mobilization of Ca and P from the weathered calcareous parent materials. We found that the relative abundance of culturable PSB in the two mineral soils ranged from 3.8% in the limestone soil to 24.4% in the dolomite soil (Fig. 3). Previous studies pointed out that the relative abundance of PSB can constitute up to 53% of total number of culturable bacteria in soils (Browne et al., 2009; Zheng et al., 2019). The higher relative abundance of PSB at the dolomite site (P-poor soil) in comparison to the limestone site (P-rich soil) may be due to environmental pressures favoring organisms that can strongly mobilize P when P is limiting (Nicolitch et al., 2016; Spohn et al., 2020). On the contrary, the lower occurrence of PSB in the soil derived from limestone might be due to a lower microbial investment into organic acids when P is easily available (Jones et al., 2009; Forstner et al., 2019). This would also explain why the dolomite soil harbored stronger P-solubilizers in comparison to the limestone soil. We found that Pseudomonadales and Enterobacteriales, known to be strong P solubilizers (Rodríguez et al., 2007; Nassal et al., 2018), dominated in both soils and depths (Fig. 4). Also, our findings agree with Liu et al. (2015) who reported that Pseudomonadales and Bacillales are the most abundant PSB strains in calcareous soils.

We found that the relative abundance of culturable PSB was significantly higher in calcareous than in siliceous soils studied previously (see Pastore et al., 2020b; Fig. S2; $p < 0.05$). This is in accordance with Zheng et al. (2019) who reported that the abundance of PSB increases with soil pH. In addition, Rodríguez-Navarro et al. (2012) found that calcitic substrates offer a higher affinity for bacterial attachment than silicate substrates, thereby fostering a higher bacterial growth and metabolic activity. The higher relative abundance of PSB can also explain the higher gross P solubilization rates in calcareous soils in comparison to siliceous soils in both soil depths (Fig. S3b). Further, nonmetric multi-dimensional scaling analyses (nMDS) revealed that the PSB communities at the calcareous soils were significantly different from the PSB communities found at the siliceous soils studied in Pastore

et al. (2020b; Fig. S5, $p < 0.05$). Bacillales and Burkholderiales dominated in siliceous soils, whereas Pseudomonadales, and to a much lesser extent Enterobacteriales, were the dominant orders in calcareous soils. Our data show that the genus *Pseudomonas*, which is reputed to have superior P solubilization ability among PSB (Goldstein, 1995; Browne et al., 2009), was by far predominant in calcareous soils in comparison to siliceous soils where it only occurred at the P-poor site. This finding suggests that the higher occurrence of Pseudomonadales might be related to the low P availability in alkaline soils. Taken together, this study suggests that the dolomite site (P-poor soil) had a higher relative abundance of PSB in comparison to the limestone site (P-rich soil) which indicates that there is likely a selective pressure in P-poor soils towards a higher abundance of PSB.

5. Conclusions

We found that the weathering of calcareous rocks was strongly affected by the activity of soil microorganisms. Soil microorganisms incubated with weathered calcareous bedrocks produced large amounts of monocarboxylic acids (mainly D-gluconic acid and, to a lesser extent, 2-keto-D-gluconic acid). Di- and tri-carboxylic acids were not found among the organic acids tested. The higher microbial P solubilization from dolomite in comparison to limestone was mainly caused by the high relative abundance of PSB in the dolomite soil in comparison to the limestone soil. Overall, Pseudomonadales and Enterobacteriales were the two most widely occurring PSB OTUs across the two mineral soils. The higher occurrence of Pseudomonadales, which are reputed to strongly solubilize P compared to other bacteria, might be related to the low solubility of calcareous rocks in alkaline soils. In conclusion, this study shows that the rates of Ca solubilization from weathered calcareous parent materials are related to the activity of soil microorganisms.

Declaration of Competing Interest

The authors declare that they have no known competing financial interests or personal relationships that could have appeared to influence the work reported in this paper.

Acknowledgements

This research was funded by the German Research Foundation (DFG) as part of the project SP 1389/4-2 of the priority program "Ecosystem nutrition: Forest strategies for limited phosphorus resources". We are particularly obliged to Jörg Prietzel of Technische Universität München (TUM) for having provided us with the soil samples and calcareous parent materials. We are grateful to Michaela Hochholzer and Andrea Kirpal of the KeyLab for Genomics and Bioinformatics for the molecular biology part. We thank Katerina Diakova for her helpful comments on a previous version of the manuscript. The authors gratefully acknowledge Uwe Hell, Karin Söllner, Renate Krauß and Anita Gößner for assistance provided in the laboratory. Finally, we thank members of the Laboratory for Analytical Chemistry (BayCEER) for the chemical analyses.

Appendix A. Supplementary data

Supplementary data to this article can be found online at <https://doi.org/10.1016/j.geoderma.2021.115408>.

References

- Arvin, L.J., Riebe, C.S., Aciego, S.M., Blakowski, M.A., 2017. Global patterns of dust and bedrock nutrient supply to montane ecosystems. *Am. Assoc. Adv. Sci.* 3, eao1588. <https://doi.org/10.1126/sciadv.aao1588>.
- Banfield, J.F., Barker, W.W., Welch, S.A., Taunton, A., 1999. Biological impact on mineral dissolution: application of the lichen model to understanding mineral weathering in the rhizosphere. *PNAS* 96 (7), 3404–3411. <https://doi.org/10.1073/pnas.96.7.3404>.
- Bengtsson, A., Sjöberg, S., 2009. Surface complexation and proton-promoted dissolution in aqueous apatite systems. *Pure Appl. Chem.* 81 (9), 1569–1584. <https://doi.org/10.1039/B9AC00068G>.
- Bisutti, I., Hille, J., Raesler, M., 2004. Determination of total organic carbon - an overview of current methods. *Trends Anal. Chem.* 23 (10–11), 716–726. <https://doi.org/10.1016/j.trac.2004.09.003>.
- Brookes, P.C., Powlson, D.S., Jenkinson, D.S., 1982. Measurement of microbial biomass phosphorus in soil. *Soil Biol. Biochem.* 14 (4), 319–329. [https://doi.org/10.1016/0038-0717\(82\)90001-3](https://doi.org/10.1016/0038-0717(82)90001-3).
- Browne, P., Rice, O., Miller, S.H., Burke, J., Dowling, D.N., Morrissey, J.P., O'Gara, F., 2009. Superior inorganic phosphate solubilization is linked to phylogeny within the *Pseudomonas fluorescens* complex. *Appl. Soil Ecol.* 43, 131–138. <https://doi.org/10.1016/j.apsoil.2009.06.010>.
- Brucker, E., Kerchen, S., Spohn, M., 2020. Release of phosphorus and silicon from minerals by soil microorganisms depends on the availability of organic carbon. *Soil Biol. Biochem.* 143, 107737. <https://doi.org/10.1016/j.soilbio.2020.107737>.
- Bünermann, E.K., 2015. Assessment of gross and net mineralization rates of soil organic phosphorus—a review. *Soil Biol. Biochem.* 89, 82–98. <https://doi.org/10.1016/j.soilbio.2015.06.026>.
- Christophel, D., Spengler, S., Schmidt, B., Ewald, J., Prietzel, J., 2013. Customary close-to-nature forest management has considerably decreased organic carbon and nitrogen stocks in soils of the Bavarian Limestone Alps. *For. Ecol. Manage.* 305, 167–176. <https://doi.org/10.1016/j.foreco.2013.05.054>.
- Dreybrodt, W., Lauekner, J., Zaihua, L., Svensson, U., Buhmann, D., 1996. The kinetics of the reaction $\text{CO}_2 + \text{H}_2\text{O} \rightarrow \text{H}^+ + \text{HCO}_3^-$ as one of the rate limiting steps for the dissolution of calcite in the system $\text{H}_2\text{O}-\text{CO}_2-\text{CaCO}_3$. *Geochim. Cosmochim. Acta* 60 (18), 3375–3381. [https://doi.org/10.1016/0016-7037\(96\)00181-0](https://doi.org/10.1016/0016-7037(96)00181-0).
- Fairbridge, R.W., Bissel, H.J., Chilingar, G.V., 1967. Developments in sedimentology. *Carbonate Rocks* 9B, 1–21. [https://doi.org/10.1016/S0070-4571\(08\)71028-8](https://doi.org/10.1016/S0070-4571(08)71028-8).
- Firley, R., Mahmood, S., Rosenstock, H., Bolou Bi, E., Köhler, S., Fahad, Z., Rosling, A., Wallander, H., Belyazid, S., Bishop, K., Lian, B., 2019. Biological weathering and its consequences at different spatial levels – from nanoscale to global scale. *Biogeosci. Discuss.* 1–43. <https://doi.org/10.5194/bg-2019-41>.
- Forstner, S.J., Wechsberger, V., Stecher, S., Müller, S., Keilinger, K.M., Wanek, W., Schleppl, P., Gundersen, P., Tatzber, M., Gerzabek, M.H., Zechmeister-Boltenstern, S., 2019. Resistant soil microbial communities show signs of increasing phosphorus limitation in two temperate forests after long-term nitrogen addition. *Front. Forests Global Change* 2. <https://doi.org/10.3389/fgc.2019.0007310.3389/fige.2019.00073.s00110.3389/fige.2019.00073.s00210.3389/fige.2019.00073.s00310.3389/fige.2019.00073.s00410.3389/fige.2019.00073.s00510.3389/fige.2019.00073.s006>.
- Gardner, L.R., 1990. The role of rock weathering in the phosphorus budget of terrestrial watersheds. *Biogeochemistry* 11 (2), 97–110.
- Goldstein, A.H., 1995. Recent progress in understanding the molecular genetics and biochemistry of calcium phosphate solubilization by gram negative bacteria. *Biol. Agric. Hort.* 12 (2), 185–193. <https://doi.org/10.1080/01448765.1995.9754736>.
- Goldstein, A.H., 2007. In: *Developments in Plant and Soil Sciences: First International Meeting on Microbial Phosphate Solubilization*. Springer Netherlands, Dordrecht, pp. 91–96.
- Gaidy, M.W., Mackenzie, E.T., 2003. Experimental study of igneous and sedimentary apatite dissolution: control of pH, distance from equilibrium, and temperature on dissolution rates. *Geochim. Cosmochim. Acta* 67 (16), 2949–2963. [https://doi.org/10.1016/S0016-7037\(03\)0265-5](https://doi.org/10.1016/S0016-7037(03)0265-5).
- Hartmann, J., Moosdorf, N., Lauerwald, R., Hinderer, M., West, A.J., 2014. Global chemical weathering and associated P-release - the role of lithology, temperature and soil properties. *Chem. Geol.* 363, 145–163. <https://doi.org/10.1016/j.chemgeo.2013.10.025>.
- Hinsinger, P., 2001. Bioavailability of soil inorganic P in the rhizosphere as affected by root induced chemical changes: a review. *Plant Soil* 237, 173–195. <https://doi.org/10.1023/A:1013351617532>.
- Jenkinson, D.S., Brookes, P.C., Powlson, D.S., 2004. Measuring soil microbial biomass. *Soil Biol. Biochem.* 36, 5–7. <https://doi.org/10.1016/j.soilbio.2003.10.002>.
- Jog, R., Pandya, M., Nareshkumar, G., Rajkumar, S., 2014. Mechanism of phosphate solubilization and antifungal activity of *Streptomyces* spp. isolated from wheat roots and rhizosphere and their application in improving plant growth. *Microbiology* 160, 778–788. <https://doi.org/10.1099/mic.0.074146-0>.
- Jones, D.L., Nguyen, C., Firley, R.D., 2009. Carbon flow in the rhizosphere: carbon trading at the soil-root interface. *Plant Soil* 321 (1–2), 5–33. <https://doi.org/10.1007/s11104-009-9925-0>.
- Joergensen, R.G., 1996. The fumigation-extraction method to estimate soil microbial biomass: calibration of the K_{EC} value. *Soil Biol. Biochem.* 28 (1), 25–31. [https://doi.org/10.1016/0038-0717\(95\)00102-6](https://doi.org/10.1016/0038-0717(95)00102-6).
- Kaufmann, G., Dreybrodt, W., 2007. Calcite dissolution kinetics in the system $\text{CaCO}_3-\text{H}_2\text{O}-\text{CO}_2$ at high undersaturation. *Geochim. Cosmochim. Acta* 71 (6), 1398–1410. <https://doi.org/10.1016/j.gca.2006.10.024>.

- Katoh, K., Standley, D.M., 2013. MAFFT multiple sequence alignment software version 7: improvements in performance and usability. *Mol. Biol. Evol.* 30 (4), 772–780. <https://doi.org/10.1093/molbev/mst010>.
- Khan, A.A., Jilani, G., Akhtar, M.S., Naqvi, S.M.S., Rasheed, M., 2009. Phosphorus Solubilizing Bacteria: occurrence, mechanisms and their role in crop production. *J. Agric. Biol. Sci.* 1, 48–58.
- Lindsay, W.L., 1979. *Chemical Equilibria in Soils*. John Wiley and Sons, New York, pp. 1–449.
- Liu, Z., Yuan, D., Dreybrodt, W., 2005. Comparative study of dissolution rate-determining mechanisms of limestone and dolomite. *Environ. Geol.* 49 (2), 274–279. <https://doi.org/10.1007/s00254-005-0086-z>.
- Liu, Z., Li, Y.C., Zhang, S., Fu, Y., Fan, X., Patel, J.S., Zhang, M., 2015. Characterization of phosphate-solubilizing bacteria isolated from calcareous soils. *Appl. Soil Ecol.* 96, 217–224. <https://doi.org/10.1016/j.apsoil.2015.08.003>.
- López-Bucio, J., Nieto-Jacobo, M.F., Ramirez-Rodriguez, V., Herrera-Estrella, L., 2000. Organic acid metabolism in plants: From adaptive physiology to transgenic varieties for cultivation in extreme soils. *Plant Sci.* 160 (1), 1–13. [https://doi.org/10.1016/S0168-9452\(00\)00347-2](https://doi.org/10.1016/S0168-9452(00)00347-2).
- Mair, P., Tropper, P., Harlov, D.E., Manning, C.E., 2017. The solubility of apatite in H₂O, KCl-H₂O, NaCl-H₂O at 800 °C and 1.0 GPa: implications for REE mobility in high-grade mafic veins. *Chem. Geol.* 470, 180–192. <https://doi.org/10.1016/j.chemgeo.2017.09.015>.
- Murphy, J., Riley, J.P., 1962. A modified single solution method for the determination of phosphate in natural waters. *Anal. Chim. Acta* 26, 678–681. [https://doi.org/10.1016/S0003-2670\(00\)88444-5](https://doi.org/10.1016/S0003-2670(00)88444-5).
- Napietalski, S., Buss, H., Brantley, S., Lee, S., Xu, H., Roden, E., 2020. Microbial chemolithotrophy mediates oxidative weathering of granitic bedrock. *Proc. Natl. Acad. Sci. U. S. A.* 116 (52), 26394–26401. <https://doi.org/10.1073/pnas.1909970117>.
- Nassal, D., Spohn, M., Hübner, N., Jacquiod, S., Smalla, K., Marhan, S., Kandeler, E., 2018. Effects of phosphorus-mobilizing bacteria on tomato growth and soil microbial activity. *Plant Soil* 427 (1–2), 17–37. <https://doi.org/10.1007/s11104-017-3528-y>.
- Nicolitch, O., Colin, Y.M., Turpault, P., Uroz, S., 2016. Soil type determines the distribution of nutrient mobilizing bacterial communities in the rhizosphere of beech trees. *Soil Biol. Biochem.* 103, 429–445. <https://doi.org/10.1016/j.soilbio.2016.09.018>.
- Oburger, E., Kirk, G.J.D., Wenzel, W.W., Puschenreiter, M., Jones, D.L., 2009. Interactive effects of organic acids in the rhizosphere. *Soil Biol. Biochem.* 41 (3), 449–457. <https://doi.org/10.1016/j.soilbio.2008.10.034>.
- Pastore, G., Kaiser, K., Kernechen, S., Spohn, M., 2020a. Microbial release of apatite- and goethite-bound phosphate in acidic forest soils. *Geoderma* 370, 114360. <https://doi.org/10.1016/j.geoderma.2020.114360>.
- Pastore, G., Kernechen, S., Spohn, M., 2020b. Microbial solubilization of silicon and phosphorus from bedrock in relation to abundance of phosphorus-solubilizing bacteria in temperate forest soils. *Soil Biol. Biochem.* 151, 108050. <https://doi.org/10.1016/j.soilbio.2020.108050>.
- Pikovskaya, R.I., 1948. Mobilization of phosphorus in soil in connection with the vital activity of some microbial species. *Mikrobiologiya* 17, 362–370.
- Plante, Alain F., 2007. In: *Soil Microbiology, Ecology and Biochemistry*. Elsevier, pp. 389–432. <https://doi.org/10.1016/B978-0-08-047514-1.50019-6>.
- Pokrovsky, O.S., Schott, J., 2001. Kinetics and mechanism of dolomite dissolution in neutral to alkaline solutions revisited. *Am. J. Sci.* 301, 597–626. <https://doi.org/10.2475/ajsc.301.7.597>.
- Porder, S., Ramachandran, S., 2013. The phosphorus concentration of common rocks—a potential driver of ecosystem P status. *Plant Soil* 367 (1–2), 41–55. <https://doi.org/10.1007/s11104-012-1490-2>.
- Prietzel, J., Zimmermann, L., Schubert, A., Christophel, D., 2016. Organic matter losses in German Alps forest soils since the 1970s most likely caused by warming. *Nat. Geosci.* 9 (7), 543–548. <https://doi.org/10.1038/ngeo2732>.
- Prietzel, J., Kljnsbun, W., Hurtarte, L.C.C., 2021. The fate of calcium in temperate forest soils: a Ca K-edge XANES study. *Biogeochemistry* 152 (2–3), 195–222. <https://doi.org/10.1007/s10533-020-00748-6>.
- Rodríguez, H., Fraga, R., 1999. Phosphate solubilizing bacteria and their role in plant growth promotion. *Biotechnol. Adv.* 17 (4–5), 319–339. [https://doi.org/10.1016/S0734-9750\(99\)00014-2](https://doi.org/10.1016/S0734-9750(99)00014-2).
- Rodríguez, H., Fraga, R., Gonzalez, T., Bashan, Y., 2007. In: *First International Meeting on Microbial Phosphate Solubilization*. Springer Netherlands, Dordrecht, pp. 15–21. https://doi.org/10.1007/978-1-4020-5765-6_2.
- Rodríguez-Navarro, C., Jroundi, F., Schiro, M., Ruiz-Agudo, E., González-Muñoz, M.T., 2012. Influence of substrate mineralogy on bacterial mineralization of calcium carbonate: implications for stone conservation. *Appl. Environ. Microbiol.* 78 (11), 4017–4029. <https://doi.org/10.1128/AEM.07044-11>.
- Ruttenberg, K.C., 2003. The global phosphorus cycle. *Treatise Geochem.* 8, 585–643. <https://doi.org/10.1016/B0-08-043751-6/08153-6>.
- Spohn, M., Zeißig, I., Brucker, E., Widdig, M., Lacher, U., Aburto, F., 2020. Phosphorus solubilization in the rhizosphere in two saproclites with contrasting phosphorus fractions. *Geoderma* 366, 114245. <https://doi.org/10.1016/j.geoderma.2020.114245>.
- Syers, J.K., Birnie, A.C., Mitchell, B.D., 1967. The calcium oxalate content of some lichens growing on limestone. *Lichenologist* 3 (3), 409–414. <https://doi.org/10.1017/S0024282967000416>.
- Tyler, G., Ström, L., 1995. Differing organic-acid exudation pattern explains calcifuge and acidifuge behavior of plants. *Ann. Bot.* 75, 75–78. [https://doi.org/10.1016/S0305-7364\(05\)80011-3](https://doi.org/10.1016/S0305-7364(05)80011-3).
- Taylor, Holly L., Duivestijn, Isaac J. Kell, Farkas, Juraj, Dietzel, Martin, Dosseto, Anthony, 2019. Technical note: lithium isotopes in dolostone as a palaeo-environmental proxy – an experimental approach. *Clim. Past* 15 (2), 635–646. <https://doi.org/10.5194/cp-15-635-2019>.
- Vance, E.D., Brookes, P.C., Jenkinson, D.S., 1987. An extraction method for measuring soil microbial biomass C. *Soil Biol. Biochem.* 19 (6), 703–707. [https://doi.org/10.1016/0038-0717\(87\)90052-6](https://doi.org/10.1016/0038-0717(87)90052-6).
- Wan, J., Tokunaga, T.K., Williams, K.H., Dong, W., Brown, W., Henderson, A.N., Newman, A.W., Hubbard, S.S., 2019. Predicting sedimentary bedrock subsurface weathering fronts and weathering rates. *Sci. Rep.* 9, 17198. <https://doi.org/10.1038/s41598-019-53205-2>.
- Widdig, M., Schläuss, P.M., Weig, A.R., Guhr, A., Biederman, L.A., Borer, E.T., Crawley, M.J., Kirkman, K.P., Seabloom, E.W., Wrang, P.D., Spohn, M., 2019. Nitrogen and phosphorus additions alter the abundance of phosphorus-solubilizing bacteria and phosphatase activity in grassland soils. *Front. Environ. Sci.* 7, 185. <https://doi.org/10.3389/fenvs.2019.00185>.
- Zaharescu, D.G., Burghesa, C.I., Dontsova, K., Presler, J.K., Hunt, E.A., Domaniuk, K.J., Amistadi, M.R., Sandhaus, S., Munoz, E.N., Gaddis, E.E., Gale, M., Vaquerá-Ibarra, M.O., Palacios-Mendez, M.A., Castrejón-Martínez, R., Roldán-Nicolau, E. C., Li, K., Maier, R.M., Reinhard, C.T., Chorover, J., 2019. Ecosystem-bedrock interaction changes nutrient compartmentalization during early oxidative weathering. *Sci. Rep.* 9, 15006. <https://doi.org/10.1038/s41598-019-51274-x>.
- Zheng, B., Zhang, D., Wang, Y., Hao, X.J., Wadaan, M.A.M., Hozzein, W.M., Peñúñas, J., Zhu, Y.G., Yang, X.R., 2019. Responses to soil pH gradients of inorganic phosphate solubilizing bacteria community. *Sci. Rep.* 9, 25. <https://doi.org/10.1038/s41598-018-37003-w>.

Contributions to the included manuscripts

The contribution [%] of each author was weighted with regard to the following points:

a: concept and experimental design; b: field and laboratory work; c: data evolution and statistical analysis
d: discussion and interpretation of results; e: manuscript preparation

Manuscript	Author	a	b	c	d	e
1. Microbial release of apatite- and goethite-bound phosphate in acidic forest soils. <i>Geoderma</i> , 370 (114360).	Giovanni Pastore	50	90	70	65	75
	Klaus Kaiser	0	0	5	15	10
	Sarmite Kernchen	0	10	5	0	0
	Marie Spohn	50	0	20	20	15
2. Microbial solubilization of silicon and phosphorus from bedrock in relation to abundance of phosphorus-solubilizing bacteria in temperate forest soils. <i>Soil Biology and Biochemistry</i> , 151 (108050).	Giovanni Pastore	50	80	70	70	80
	Sarmite Kernchen	0	20	5	0	0
	Marie Spohn	50	0	25	30	20
3. Weathering of calcareous bedrocks is strongly affected by the activity of soil microorganisms. <i>Geoderma</i> , 405 (115408).	Giovanni Pastore	50	80	65	65	70
	Alfons R. Weig	0	20	10	0	0
	Eduardo Vazquez	0	0	5	15	10
	Marie Spohn	50	0	20	20	20

Acknowledgments

This PhD thesis is the output of the effort and support of many people to whom I am extremely grateful. I thank my supervisor Professor Marie Spohn. Your advices were of great help during these (almost) 4 years. I am grateful for your attention in guiding my way through this unpredictable PhD journey. I am also profoundly grateful to the hard work of my co-authors and their contribution to the articles presented in this thesis. My thanks go, with no particular order, to Klaus Kaiser, Sarmite Kernchen, Alfons R. Weig and Eduardo Vazquez. I am delighted to have worked with you. My sincere gratitude goes to all the colleagues of the Department of Soil Ecology and Biochemistry at BayCEER for having supported and encouraged my daily activities, especially when things were not right. Thanks to Karin Söllner, Renate Krauß, Uwe Hell, Anita Gößner and Ralf Mertel for the opportunity of working together in the lab and in the field. Your patience and remarkable experience have helped me to successfully complete this research project. I want to thank Ingeborg Vogler who demonstrated to be a great person during my time in Bayreuth. Special thanks to all the people that shared with me the space in the office B.1: Emanuel, Christine, Andrea, Harold. More in general thanks to all the colleagues and friends that, in a way or another, shared their time at BayCEER with me: Mai-Van, Alex, Per, Pablo, Christian, Felix, Corinna, Meike, Katerina, Christina, Steve, Humay, Robert, Cynthia. I am sure to have probably forgotten someone here, but I thank you all for your support. Thanks for having provided me with a friendly and inspiring environment to work. Wish you all the best. My sincere thanks to all staff members of the Laboratory for Analytical Chemistry and the members of the Keylab for Genomics and Bioinformatics for their active participation in part of the analyses presented in this thesis. Vielen Dank! All the people listed here have contributed, in many ways, to my growth, both professionally and personally. I would need more than an entire acknowledgement section to thank you for everything you have done for me during these 4 years.

I extend also my sincerest thanks to Professor Egbert Matzner for his numerous hints during the first two years of my PhD and to Professor Eva Lehndorff for her attitude and patience in making me keep a small space in the office during the last months at BayCEER and during the “Covid-19 crisis” which caused unprecedented disruption of lives and work.

This 4-year PhD journey would not have been possible without the financial support of the German Research Foundation (DFG) as part of the project SP 1389/4-2 of the priority program “Ecosystem nutrition: Forest strategies for limited phosphorus resources”. I am sincerely grateful for your support. Luckily, I have also **the privilege of having a lovely family** and friends who had a fundamental role in getting me through the PhD project successfully. I thank my family for the encouragement they have shown me over the years and to all my friends for the joyous moments spent together. In this sense, I express my gratitude to Emanuel, Eduardo, Manuel, Felicia, Vero, Bene, Lucas, Saul, Andreas and Andrei for being important part of my life in Bayreuth. Very special thanks go to Bessel’s family for their warm welcome and goodness. There was no way not to love Bayreuth without the warm welcome of the International Office at the University Campus and, in particular, the priceless help I received from Susan Lausmann, who from my first day helped me navigate the troubled waters of the German bureaucracy. Last, but not least, I want to thank all the friends I have met in my travels and stays around the world and who have always encouraged and supported me, even from distance (thanks Skype!). I cannot fail to mention my friends in Italy with whom I have shared many joys during this long journey.

This work is dedicated to my beloved son, Daniel. You have made me stronger, better and more fulfilled than I could have ever imagined. I love you to the moon and back.

Publications

- Giovanni Pastore, Klaus Kaiser, Sarmite Kernchen and Marie Spohn (2020): Microbial release of apatite- and goethite-bound orthophosphate in acidic forest soils. *Geoderma*, 370 (114360).
<https://doi.org/10.1016/j.geoderma.2020.114360>
- Giovanni Pastore, Sarmite Kernchen and Marie Spohn (2020): Microbial solubilization of silicon and phosphorus from bedrock in relation to abundance of phosphorus-solubilizing bacteria in temperate forest soils. *Soil Biology and Biochemistry*, 151 (108050).
<https://doi.org/10.1016/j.soilbio.2020.108050>
- Giovanni Pastore, Alfons R. Weig, Eduardo Vazquez and Marie Spohn (2022): Weathering of calcareous bedrocks is strongly affected by the activity of soil microorganisms. *Geoderma*, 405 (115408).
<https://doi.org/10.1016/j.geoderma.2021.115408>

Additional publication(s):

- Antonios Michas, Giovanni Pastore, Akane Chiba, Martin Grafe, Simon Clausing, Andrea Polle, Micheal Schloter, Marie Spohn and Stefanie Schulz (2021): Phosphorus Availability Alters the effect of tree girdling on the diversity of phosphorus solubilizing soil bacterial communities in temperate beech forests. *Frontiers in Forests and Global Change*, 4 (696983).
<https://doi.org/10.3389/ffgc.2021.696983>

Versicherungen und Erklärungen (Declarations)

(§ 8 Satz 2 Nr. 3 PromO Fakultät)

Hiermit versichere ich eidesstattlich, dass ich die Arbeit selbständig verfasst und keine anderen als die von mir angegebenen Quellen und Hilfsmittel benutzt habe (vgl. Art. 64 Abs. 1 Satz 6 BayHSchG).

(§ 8 Satz 2 Nr. 3 PromO Fakultät)

Hiermit erkläre ich, dass ich die Dissertation nicht bereits zur Erlangung eines akademischen Grades eingereicht habe und dass ich nicht bereits diese oder eine gleichartige Doktorprüfung endgültig nicht bestanden habe.

(§ 8 Satz 2 Nr. 4 PromO Fakultät)

Hiermit erkläre ich, dass ich Hilfe von gewerblichen Promotionsberatern bzw. –vermittlern oder ähnlichen Dienstleistern weder bisher in Anspruch genommen habe noch künftig in Anspruch nehmen werde.

(§ 8 Satz 2 Nr. 7 PromO Fakultät)

Hiermit erkläre ich mein Einverständnis, dass die elektronische Fassung der Dissertation unter Wahrung meiner Urheberrechte und des Datenschutzes einer gesonderten Überprüfung unterzogen werden kann.

(§ 8 Satz 2 Nr. 8 PromO Fakultät)

Hiermit erkläre ich mein Einverständnis, dass bei Verdacht wissenschaftlichen Fehlverhaltens Ermittlungen durch universitätsinterne Organe der wissenschaftlichen Selbstkontrolle stattfinden können.

.....

Ort, Datum, Unterschrift

